Alma Mater Studiorum - Università di Bologna

DOTTORATO DI RICERCA IN

TECNOLOGIE INNOVATIVE E USO SOSTENIBILE DELLE RISORSE DI PESCA E BIOLOGICHE DEL MEDITERRANEO (FISHMED-PHD)

Ciclo 35

Settore Concorsuale: 05/E1 - BIOCHIMICA GENERALE

Settore Scientifico Disciplinare: BIO/10 - BIOCHIMICA

RELATIONSHIP BETWEEN PHENOTYPE AND ENVIRONMENT IN MARINE CALCIFYING ORGANISMS: EXPLORING GROWTH AND SHELL PROPERTIES OF DIFFERENT MOLLUSKS SPECIES IN PAST AND MODERN SCENARIO

Presentata da: Alessandro Cheli

Coordinatore Dottorato

Stefano Goffredo

Supervisore

Jacobus Adrianus Kaandorp

Co-supervisore

Giuseppe Falini

Esame finale anno 2023

Abstract

Coastal ecosystems represent an inestimable source of biodiversity, being among the most productive areas on the planet. Despite the great ecological and economic value of those environments, many threats endanger the species living in this ecosystem, like the rapid warming and the sea acidification, among many other. Benthic calcifying organisms (e.g. mollusks, corals and echinoderms) in particular, are among the most exposed to those hazards. These organisms use calcium carbonate as a structural and protective material through the biomineralization process, biologically controlled by the organism, but nevertheless, strongly influenced by the environmental surroundings. Evaluating how a changing environment can influence the process of biomineralization is critical to understand how those species of great ecological and economic importance will face the ongoing climate change.

This thesis investigates the mechanism of biomineralization in different mollusks' species of the Adriatic Sea, providing detailed descriptions of shells skeletal, biometric and growth parameters. Applying a multidisciplinary and multi-scale research approach, the influence of external environmental factors on the process of shell formation has been investigated. To achieve this purpose analysis were conducted both on current populations and on fossil remain, which allows to investigate ecological responses to past climate transitions. Mollusks' shells in fact are one of the best tools to understand climate change in the past, present and future, since they record the environmental conditions prevailed during their life, reflected on the geochemical properties, microstructure and growth of the shell. This approach allowed to overcome the time scale limit imposed by field and laboratory survey, and better understand species long term adaptive response to changing environment, a crucial issue to define proper conservation and management strategies.

Furthermore, the investigation of fossil record of mollusks assemblages offered the opportunity to evaluate the long-term biotic response to anthropogenic stressors in the north Adriatic Sea.

Index

Chapter 1. General introduction

Biomineralization is a dynamic physiological process that lead to the formation of well-organized mineralized structure by a living organism (Dauphin, 2016; Lowenstam & Weiner, 1989b). Under strict biological control, organisms selectively extract specific elements from the surrounding environment and incorporates them into functional structures (Ren et al., 2011). The obtained biominerals are composite materials formed both from a mineral phase and an organic matrix with a specific hierarchical structure. The high level of control over the composition, structure, size, and morphology of biominerals results in complex materials with unique properties that strongly contrast with those of geological minerals and often surpass those of synthetic analogues (Lowenstam & Weiner, 1989). Biomineralization is a widespread phenomenon that involves 55 phyla from all five kingdoms in the biosphere, from bacteria and archea to eucaryotic organisms, including protists, chlorophyll plants, algae, fungi and metazoans (Knoll, 2003). More than 60 distinct types of biominerals can be found in nature, with a wide range of functions like tissues support, UV protection, shelter against predation, nutrition, reproduction, gravity, light or magnetic field perceptions, storage of mineral ions (Weiner & Dove, 2003a). A distinction is often made between biologically induced versus biologically controlled biomineralization. The former generally refers to side-products of metabolism that are dependent on environmental conditions and often not significantly different to the inorganic minerals themselves, whereas the latter are products of specialized, genetically controlled metabolic processes and are generally distinct from their inorganic counterparts (Dhami et al., 2013; Lowenstam, 1981; Lowenstam & Weiner, 1989b; Marin et al., 2012a; Perry et al., 2007; Schneidermann & Harris, 1985; Weiner & Dove, 2003b).

The most abundant biogenic minerals found in nature are calcium carbonate structures, produced by marine and freshwaters organisms like mollusks, corals, sea urchins, sponges, and crustaceans for structural, protective and mechanical functions (Lowenstam & Weiner, 1989b). $CaCO_3$ stuctures also forms gravity sensors in marine and land animals and is part of the photosensory organ in brittlestars (Aizenberg et al., 2001; Lowenstam & Weiner, 1989b).

Calcium carbonate is present in nature in six different structural forms, three anhydrous crystalline polymorphs referred to as calcite, aragonite, vaterite, and three hydrated forms: amorphous calcium carbonate (ACC), calcium carbonate monohydrate, and calcium carbonate hexahydrate. Calcite and aragonite are the most common form of $CaCO_3$ crystals in nature because are more stable than the other polymorphs (Jamieson, 2004). Vaterite is rare in nature because of is low stability in solution where spontaneously becomes calcite or aragonite (Ren et al., 2011). The other three crystalline forms are monohydrate $CaCO_3$, produced by a limited number of organisms, hexahydrate $CaCO_3$, which is not present in the biological world and ACC. This latter is particularly important, since it is often used by organisms either as an integral constituent of a biomineral or as a precursor phase to calcite or aragonite, as observed in some mollusk larva (Addadi et al., 2003; Beniash et al., 1999; Weiner et al., 2009; Weiss et al., 2002). Organisms have the ability to genetically control which polymorph to precipitate (Weiner & Dove, 2003a).

Because of their persistence in the fossil record, biominerals provide a major archive of the evolutionary history of life and environments on Earth, thus representing a precious reservoir of information about the past (Addadi & Weiner, 2014; Epstein & Lowenstam, 1953).

The mineralization of mollusk's shell

Mollusks are considered model organisms to study biomineralization since they produce many different shell types, are easily accessible, and have a rich and well documented fossil record. They also produce the highest diversity of biominerals of any animal group, both in terms of the mineral type deposited and the function of the materials themselves (Lowenstam & Weiner, 1989b).

Among the wide range of calcium carbonate morphologies produced by mollusks (e.g. pearls, epithelial spicules, scales and plates, and others) the shell, that supports those soft-bodied organisms and protects them from predation and desiccation, is the principal and most known.

The mollusk shell is typically an organo-mineral composite, where the mineral phase represents the dominant fraction, associated to a minor organic part called shell organic matrix, accounting for 0.1–5% of the shell weight and composed of proteins, polysaccharides, and lipids (Furuhashi et al., 2009). The adjunction of organic components to a mineralized structure enhances the mechanical properties to the whole biomineral (Marin et al., 2012a). The mollusk shell represents an ideal example of a biologically-controlled mineralization (Lowenstam & Weiner, 1989b; Mann, 1993), and fulfils the criteria defined for this type of biogenic product: its synthesis requires a specialized macromolecular machinery; furthermore, the formed minerals are produced in a closed system, not in direct contact with the environment; in addition, the mineral synthesis is an active process; the formed minerals exhibit shapes, different from that of their chemically-produced counterpart; finally, all the steps of the mineral synthesis are mediated by the shell matrix (Marin et al., 2012b). In spite of being a minor component, the shell matrix plays a critical role in crystal nucleation events and crystal growth (Kong et al., 2009; Marin et al., 2012a; Suzuki et al., 2009; Zhang et al., 2006). The exact mix of these proteins with calcium carbonate crystals significantly influences the particular shell microstructure (Clark, 2020).

A common trait between the huge amount of different architecture and pattern found in mollusk shell is that they all are composed of multiple layers (generally two to five) of calcium carbonate polymorphs, and an organic external layer, the periostracum. Those layers can have different microstructure, on the base of the arrangement of singles calcium carbonate nanometric units. These arrangements are classified on the base of their morphology, and include prismatic, spherulitic, crossed-lamellar, homogenous, and nacreous forms (Carter & Clark, 1985; Chateigner et al., 2000, among others). The association of two or more mineralized layers with different microstructures and different carbonate polymorphs within a shell, results in a biomaterial with improved mechanical properties which combines toughness and flexibility.

Furthermore, the presence of interfaces between layers of different textures prevents the propagation of fractures throughout the whole thickness of the shell. Hierarchy in biomineralization largely explains how complex shapes and amazing optical or mechanical properties can emerge from a coarse material— calcium carbonate—which is abundant at the surface of the Earth, but which never exhibits such remarkable properties when precipitated without any control of a biological system (Marin et al., 2012a).

Biomineralization and climate change

Rising temperatures and ocean acidification are predicted to severely impact coastal ecosystem and their services in the next century. Calcifying macroinvertebrates such as mollusks, corals and echinoderms rely on calcium carbonate exoskeletons for structural support and mechanical strength (Addadi & Weiner, 2014) and are considered among the most exposed to those hazard (Cooley & Doney, 2009; Harley, 2011). Morphology, mineralogy and chemistry of biologically formed $CaCO_3$ skeletons are largely dependent on both biology and environmental surroundings, with structural proteins and enzymes that act as keys to controlling internal conditions and that respond to external environmental parameters (Falini et al., 1996).

Changes in the calcium carbonate saturation state, with a subsequent decrease in the concentration of available carbonate ions in seawater and higher dissolution rates of $CaCO_3$ (especially its more soluble polymorph aragonite), as well as high magnesium calcite are expected results of ocean acidification trends (Morse et al., 2006; Zeebe, 2012). These will result in a general decrease in the production and accumulation of marine biogenic carbonates, less favourable conditions for biogenic calcification and severe impacts on marine calcifiers and marine biogenic processes, with different calcareous organisms being affected in different ways. Moreover, temperature rise is expected to accompany current ocean acidification with severe impacts already documented for several marine areas (Barnes & Peck, 2008; Schofield et al., 2010). Beside ocean acidification and warming, other environmental factors, such as solar radiation, salinity, oxygen and food availability, all can influence energy expenditure in marine organisms, especially in temperate seas, where marine organisms show marked seasonal patterns in growth, reproduction and abundance (Fitzer et al., 2014; Gazeau et al., 2013; Kroeker et al., 2010; Mancuso et al., 2019a; Pfister et al., 2016; Thomsen & Melzner, 2010; Waldbusser et al., 2013).

Quantifying the effect of near future climate change on marine calcifying organisms requires long-term multi-generational studies for assessing their adaptability to changing environmental conditions (S. Watson, 2012). While laboratory studies enable the isolation of a specific stressor, field studies are necessary to widely understand the effects of stressors in a natural and more complex system. Nevertheless, the time required to detect long-term population dynamics can be prohibitive (Hofmann et al., 2010; Pfister et al., 2016). In this light, well-resolved, fossil-rich sedimentary successions record ecological responses to past climatic shifts, far beyond the limited timescales of direct ecological monitoring, typically restricted to the most recent decades (e.g., (Dillon et al., 2020; Kidwell, 2015; Tomašových et al., 2020a). As major calcareous organisms with an extensive fossil record, marine calcifying organisms can be considered valuable recorders of past environmental change in marine habitats (Bemis et al., 1998; Chauvaud et al., 2005; Lutz & Rhoads, 1980; Schöne & Gillikin, 2013; Vihtakari et al., 2017). In particular, mollusk shells archive historical data due to their seasonal deposition of carbonate material, retaining high-resolution temporal records of the ambient physical and chemical conditions during growth (Klein et al., 1996; Purroy et al., 2018; Schöne et al., 2003).

Research objectives

The objective of this Thesis was to investigate the effect of environment on the biomineralization process of mollusk species of ecological and economical relevance in the Adriatic Sea. Analysis were conducted both on current populations and on fossil ones, which allow to investigate long-term ecological dynamics with respect to past climate transitions.

The main project described in this thesis aimed to investigate the biomineralization dynamics of different populations of the bivalve *Chamelea gallina* (Linnaeus, 1758) in the Northern Adriatic Sea, along a temporal gradient of 8,000 years.

C. gallina is a valuable economic species in the Mediterranean Sea, expected to be severely impacted by numerous anthropogenic stressors that threaten the biological and economic sustainability of its fishery. It seems to be particularly sensitive to environmental changes, showing shell morphology variations in response to environmental change (Gizzi, Caccia, Simoncini, Mancuso, Reggi, Fermani, Brizi, Fantazzini, Stagioni, Falini, et al., 2016a; Mancuso et al., 2019b; Ramon & Richardson, 1992; Romanelli et al., 2009). Previous studies have mainly focused on population dynamics, shell growth and composition of this species in the present-day

Mediterranean and along latitudinal gradients (Mancuso et al., 2019b and reference therein). In contrast, there are no information about shell variations in relation to climate-driven environmental change along temporal gradients. Here, the overall biomineralization process (including biometry, skeletal parameters, microstructure characterization and calcification) of *C. gallina* shells were investigated comparing fossil remains from the middle Holocene with modern specimens retrieved in the same area (Po Adriatic system).

Four shoreface-related *C. gallina* horizons have being evaluated: two from the present-day Adriatic setting and two from the Middle Holocene, when regional sea temperatures were higher than today, thus representing a possible analogue for the near-future global warming.

The investigation of the fossil record has also been used for a second project aimed to evaluate the status of north Adriatic coastal ecosystem in response to anthropogenic stresses. Preserving adaptive capacities of coastal ecosystems in the Anthropocene requires an understanding of their natural variability prior to modern times. Ecological studies provide a relatively short record by which to measure ecosystem changes and disentangling present-day natural factors from anthropogenic forcing is often a challenging, if not impossible, task. Geohistorical data, including the youngest fossil record, are thus needed to understand the status and variability of marine ecosystems prior to major phases of human impact. The Adriatic Sea is being affected by multiple anthropogenic stressors and has already been highly impacted by human activities. Habitat loss and degradation, pollution, eutrophication, overfishing, and invasive species are major causes of changes in the Adriatic coastal ecosystems, with many of these pressures operating for decades or centuries.

In this study, aimed at providing a deeper historical perspective, we compared mid-late Holocene assemblages preserved in the subsurface stratigraphic record of the Po coastal plain (Northern Italy) with surficial assemblages that accumulated along the Po Delta and Emilia Romagna coastline during the Anthropocene. Specifically, we evaluated changes in the composition of mollusk assemblages between the present-day fluvial influenced coastal shoreface and delta front settings with sustained sedimentary inputs (hereafter referred to as “nearshore”) and their mid-late Holocene counterparts representing a time interval when anthropogenic pressure were notably less significant (between ~6 and 0.5 kyr cal BP i.e., prior to the early modern period). This study contributes to the area of near-time Conservation Palaeobiology that provides the framework against which to evaluate extant biotic dynamics.

A further line of research here presented focuses on shells growth and properties of *Mytilus galloprovincialis* from the North-western coasts of the Adriatic Sea, a bivalve mollusk with high ecological and economical relevance. The shell has a fundamental role in the protection of the organism, and it has been demonstrated that the mechanical and structural properties can be influenced by various environmental factors (Bergström & Lindegarth, 2016a; Kroeker et al., 2017; Telesca et al., 2018a). Despite structural, physical and mechanical properties of mussel shells change during the ontogenesis the effect of environmental and anthropogenic stresses on the organism at different life stages is poorly investigated. The conducted analysis aimed to provide a detailed description of how shell feature changes during the growth of the organism, evaluating both the mechanical properties and the biometrical, compositional and structural features of shell along different stages of life, i.e. juvenile and adult.

References

Addadi, L., Raz, S., & Weiner, S. (2003). Taking advantage of disorder: Amorphous calcium carbonate and its roles in biomineralization. *Advanced Materials*, *15*(12), 959–970. https://doi.org/10.1002/ADMA.200300381

Addadi, L., & Weiner, S. (2014). Biomineralization: mineral formation by organisms. *Physica Scripta*, *89*(9), 098003. https://doi.org/10.1088/0031-8949/89/9/098003

Aizenberg, J., Tkachenko, A., Weiner, S., Addadi, L., & Hendler, G. (2001). Calcitic microlenses as part of the photoreceptor system in brittlestars. *Nature 2001 412:6849*, *412*(6849), 819–822. https://doi.org/10.1038/35090573

Amorosi, A., Barbieri, G., Bruno, L., Campo, B., Drexler, T., Hong, W., & Fielding, C. (2019). Three-fold nature of coastal progradation during the Holocene eustatic highstand, Po Plain, Italy–close correspondence of stratal character with distribution patterns. *Sedimentology*, *66*.

Amorosi, A., Barbieri, G., Bruno, L., Campo, B., Drexler, T. M., Hong, W., Rossi, V., Sammartino, I., Scarponi, D., Vaiani, S. C., & Bohacs, K. M. (2019). Three-fold nature of coastal progradation during the Holocene eustatic highstand, Po Plain, Italy – close correspondence of stratal character with distribution patterns. *Sedimentology*, *66*(7), 3029–3052. https://doi.org/10.1111/sed.12621

Amorosi, A., Bruno, L., Campo, B., Morelli, A., Rossi, V., Scarponi, D., Hong, W., Bohacs, K. M., & Drexler, T. M. (2017). Global sea-level control on local parasequence architecture from the Holocene record of the Po Plain, Italy. *Marine and Petroleum Geology*, *87*, 99–111. https://doi.org/10.1016/j.marpetgeo.2017.01.020

Amorosi, A., Colalongo, M., Fusco, F., Pasini, G., & Fiorini, F. (1999a). Glacio-eustatic control of continental-shallow marine cyclicity from late quaternary deposits of the southeastern Po Plain, northern Italy. *Quat Res*, *52*.

Amorosi, A., Colalongo, M. L., Fiorini, F., Fusco, F., Pasini, G., Vaiani, S. C., & Sarti, G. (2004). Palaeogeographic and palaeoclimatic evolution of the Po Plain from 150-ky core records. *Global and Planetary Change*, *40*(1–2), 55–78. https://doi.org/10.1016/S0921-8181(03)00098-5

Amorosi, A., Colalongo, M. L., Fusco, F., Pasini, G., & Fiorini, F. (1999b). Glacio-eustatic control of continental-shallow marine cyclicity from late quaternary deposits of the southeastern Po Plain, northern Italy. *Quaternary Research*, *52*(1), 1–13. https://doi.org/10.1006/qres.1999.2049

Anagnostou, E., Sherrell, R. M., Gagnon, A., LaVigne, M., Field, M. P., & McDonough, W. F. (2011). Seawater nutrient and carbonate ion concentrations recorded as P/Ca, Ba/Ca, and U/Ca in the deep-sea coral Desmophyllum dianthus. *Geochimica et Cosmochimica Acta*, *75*(9), 2529–2543.

Andrisoa, A., Lartaud, F., Rodellas, V., Neveu, I., & Stieglitz, T. C. (2019). Enhanced Growth Rates of the Mediterranean Mussel in a Coastal Lagoon Driven by Groundwater Inflow . In *Frontiers in Marine Science* (Vol. 6).

Azzarone, M., Pellegrini, C., Barbieri, G., Rossi, V., Gamberi, F., Trincardi, F., Scarponi, D., Barbieri, G., & Rossi, V. (2020). Linking benthic fauna and seismic facies to improve stratigraphic reconstructions: the case of the Mid-Adriatic Deep since the late glacial period (Central Adriatic Sea). *Bollettino Della Società Paleontologica Italiana*, *59*(1), 9–23. https://doi.org/10.4435/BSPI.2020.03

Bajt, O., Ramšak, A., Milun, V., Andral, B., Romanelli, G., Scarpato, A., Mitrić, M., Kupusović, T., Kljajić, Z., Angelidis, M., Çullaj, A., & Galgani, F. (2019a). Assessing chemical contamination in the coastal waters of the Adriatic Sea using active mussel biomonitoring with Mytilus galloprovincialis. *Marine Pollution Bulletin*, *141*, 283–298. https://doi.org/10.1016/J.MARPOLBUL.2019.02.007

Bajt, O., Ramšak, A., Milun, V., Andral, B., Romanelli, G., Scarpato, A., Mitrić, M., Kupusović, T., Kljajić, Z., Angelidis, M., Çullaj, A., & Galgani, F. (2019b). Assessing chemical contamination in the coastal waters of the Adriatic Sea using active mussel biomonitoring with Mytilus galloprovincialis. *Marine Pollution Bulletin*, *141*, 283–298. https://doi.org/10.1016/J.MARPOLBUL.2019.02.007

Barnes, D. K. A., & Peck, L. S. (2008). Vulnerability of Antarctic shelf biodiversity to predicted regional warming. *Climate Research*, *37*(2–3), 149–163. https://doi.org/10.3354/CR00760

Beer, N. A., Wing, S. R., & Hu, Y. (2011). Physical versus biological control of element incorporation into biogenic carbonate: an in situ experiment in a New Zealand fjord. *Marine Ecology Progress Series*, *433*, 289–301.

Bemis, B. E., Spero, H. J., Bijma, J., & Lea, D. W. (1998). Reevaluation of the oxygen isotopic composition of planktonic foraminifera: Experimental results and revised paleotemperature equations. *Paleoceanography*, *13*(2), 150–160. https://doi.org/10.1029/98PA00070

Beniash, E., Addadi, L., & Weiner, S. (1999). Cellular control over spicule formation in sea urchin embryos: A structural approach. *Journal of Structural Biology*, *125*(1), 50–62. https://doi.org/10.1006/JSBI.1998.4081

Bergström, P., & Lindegarth, M. (2016a). Environmental influence on mussel (Mytilus edulis) growth – A quantile regression approach. *Estuar. Coast. Shelf Sci.*, *171*, 123–132. https://doi.org/10.1016/j.ecss.2016.01.040

Bergström, P., & Lindegarth, M. (2016b). Environmental influence on mussel (Mytilus edulis) growth - A quantile regression approach. *Estuarine, Coastal and Shelf Science*, *171*, 123–132. https://doi.org/10.1016/J.ECSS.2016.01.040

Bertness, M. D., & Grosholz, E. (1985). Population dynamics of the ribbed mussel, Geukensia demissa: the costs and benefits of an aggregated distribution. *Oecologia*, *67*(2), 192–204.

Beyer, J., Green, N. W., Brooks, S., Allan, I. J., Ruus, A., Gomes, T., Bråte, I. L. N., & Schøyen, M. (2017). Blue mussels (Mytilus edulis spp.) as sentinel organisms in coastal pollution monitoring: A review. *Marine Environmental Research*, *130*, 338–365. https://doi.org/https://doi.org/10.1016/j.marenvres.2017.07.024

Brando, V. E., Braga, F., Zaggia, L., Giardino, C., Brando, V. E., Braga, F., Zaggia, L., Giardino, C., Bresciani, M., Matta, E., Bellafiore, D., Ferrarin, C., Maicu, F., Benetazzo, A., Bonaldo, D., Falcieri, F. M., Coluccelli, A., Russo, A., & Carniel, S. (2015). High-resolution satellite turbidity and sea surface temperature observations of river plume interactions during a significant flood event BLASCO-Blending Laboratory And Satellite techniques for detecting CyanObacteria View project HAZADR View project High-resolution satellite turbidity and sea surface temperature observations of river plume interactions during a significant flood event. *Ocean Sci*, *11*, 1–11. https://doi.org/10.5194/os-11-909-2015

Bråte, I. L. N., Hurley, R., Iversen, K., Beyer, J., Thomas, K. V., Steindal, C. C., Green, N. W., Olsen, M., & Lusher, A. (2018). Mytilus spp. as sentinels for monitoring microplastic pollution in Norwegian coastal waters: A qualitative and quantitative study. *Environmental Pollution*, *243*, 383–393. https://doi.org/10.1016/J.ENVPOL.2018.08.077

Bruckschen, P., Bruhn, F., Meijer, J., Stephan, A., & Veizer, J. (1995). Diagenetic alteration of calcitic fossil shells: Proton microprobe (PIXE) as a trace element tool. *Nuclear Inst. and Methods in Physics Research, B*, *104*(1–4), 427–431. https://doi.org/10.1016/0168-583X(95)00424-6

Bruno, L., Amorosi, A., Severi, P., & Costagli, B. (2017). Late Quaternary aggradation rates and stratigraphic architecture of the southern Po Plain, Italy. *Basin Research*, *29*(2), 234–248. https://doi.org/10.1111/bre.12174

Bruno, L., Campo, B., Di Martino, A., Hong, W., & Amorosi, A. (2019). Peat layer accumulation and post-burial deformation during the mid-late Holocene in the Po coastal plain (Northern Italy). *Basin Research*, *31*(3), 621–639. https://doi.org/10.1111/bre.12339

Busse, C., Homs, J. L., Gustafsson, D., Palmert, F., Sjödin, B., Moverare, J. J., Simonsson, K., & Leidermark, D. (2016). A finite element study of the effect of crystal orientation and misalignment on the crack driving force in a single-crystal superalloy. *Proceedings of the ASME Turbo Expo: Turbomachinery Technical Conference and Exposition*, 1–8. https://doi.org/10.1115/GT2016-56305

Carter, J. G., & Clark, G. R. (1985). Classification and Phylogenetic Significance of Molluscan Shell Microstructure. *Series in Geology, Notes for Short Course*, *13*, 50–71. https://doi.org/10.1017/S0271164800001093

Chateigner, D., Hedegaard, C., & Wenk, H. R. (2000). Mollusc shell microstructures and crystallographic textures. *Journal of Structural Geology*, *22*(11–12), 1723–1735. https://doi.org/10.1016/S0191-8141(00)00088-2

Chauvaud, L., Lorrain, A., Dunbar, R. B., Paulet, Y.-M., rard Thouzeau, G., ric Jean, F., Guarini, J.-M., Mucciarone, D., Lorrain, A., Dunbar, R. B., Paulet, Y., Thouzeau, G., Jean, F., Guarini, J., & Mucciarone, D. (2005). Shell of the Great Scallop Pecten maximus as a high-frequency archive of paleoenvironmental changes. *Geochemistry, Geophysics, Geosystems*, *6*(8). https://doi.org/10.1029/2004GC000890

Cheli, A., Mancuso, A., Azzarone, M., Fermani, S., Kaandorp, J., Marin, F., Montroni, D., Polishchuk, I., Prada, F., Stagioni, M., Valdré, G., Pokroy, B., Falini, G., Goffredo, S., & Scarponi, D. (2021a). Climate variation during the Holocene influenced the skeletal properties of Chamelea gallina shells in the North Adriatic Sea (Italy). *PLOS ONE*, *16*(3), e0247590. https://doi.org/10.1371/JOURNAL.PONE.0247590

Cheli, A., Mancuso, A., Azzarone, M., Fermani, S., Kaandorp, J., Marin, F., Montroni, D., Polishchuk, I., Prada, F., Stagioni, M., Valdré, G., Pokroy, B., Falini, G., Goffredo, S., &

Scarponi, D. (2021b). Climate variation during the Holocene influenced the skeletal properties of Chamelea gallina shells in the North Adriatic Sea (Italy). *PLOS ONE*, *16*(3), e0247590. https://doi.org/10.1371/JOURNAL.PONE.0247590

Clark, M. S. (2020). Molecular mechanisms of biomineralization in marine invertebrates. *Journal of Experimental Biology*, *223*(11). https://doi.org/10.1242/JEB.206961

Clarke, A. (1993a). Temperature and Extinction in the Sea: A Physiologist's View. *Paleobiology*, *19*(4), 499–518.

Clarke, A. (1993b). Temperature and extinction in the sea: a physiologist's view. *Paleobiology*, *19*, 499–518.

Coll, M., Piroddi, C., Steenbeek, J., Kaschner, K., Lasram, F. B. R., Aguzzi, J., Ballesteros, E., Bianchi, C. N., Corbera, J., Dailianis, T., Danovaro, R., Estrada, M., Froglia, C., Galil, B. S., Gasol, J. M., Gertwage, R., Gil, J., Guilhaumon, F., Kesner-Reyes, K., … Voultsiadou, E. (2010). The Biodiversity of the Mediterranean Sea: Estimates, Patterns, and Threats. *PLOS ONE*, *5*(8), e11842. https://doi.org/10.1371/JOURNAL.PONE.0011842

Conte, M. H., Sicre, M. A., Rühlemann, C., Weber, J. C., Schulte, S., Schulz-Bull, D., & Blanz, T. (2006). Global temperature calibration of the alkenone unsaturation index (U 37k) in surface waters and comparison with surface sediments. *Geochemistry, Geophysics, Geosystems*, *7*(2). https://doi.org/10.1029/2005GC001054

Cooley, S. R., & Doney, S. C. (2009). Anticipating ocean acidification's economic consequences for commercial fisheries. *Environmental Research Letters*, *4*(2). https://doi.org/10.1088/1748-9326/4/2/024007

Copernicus Marine Environment Monitoring Service. (n.d.). *Global Ocean OSTIA Sea Surface Temperature and Sea Ice Analysis — European Environment Agency*. https://www.eea.europa.eu/data-and-maps/data/external/global-ocean-ostia-sea-surface

Correggiari, A., Cattaneo, A., & Trincardi, F. (2005a). The modern Po Delta system: Lobe switching and asymmetric prodelta growth. *Marine Geology*, *222–223*(1–4), 49–74. https://doi.org/10.1016/j.margeo.2005.06.039

Correggiari, A., Cattaneo, A., & Trincardi, F. (2005b). The modern Po Delta system: Lobe switching and asymmetric prodelta growth. *Marine Geology*, *222–223*(1–4), 49–74. https://doi.org/10.1016/J.MARGEO.2005.06.039

Crane, R. L., & Denny, M. W. (2022). Bivalves maintain repair when faced with chronically repeated mechanical stress. *Journal of Experimental Biology*, *225*(10), jeb243813. https://doi.org/10.1242/jeb.243813

Currey, J. D., & Taylor, J. D. (1974). The mechanical behaviour of some molluscan hard tissues. *Journal of Zoology*, *173*(3), 395–406. https://doi.org/10.1111/j.1469-7998.1974.tb04122.x

Cusack, M., Huerta, A. P., & EIMF. (2012). Brachiopods recording seawater temperature-A matter of class or maturation? *Chemical Geology*, *334*, 139–143. https://doi.org/10.1016/j.chemgeo.2012.10.021

Dalgi, G., Okumuş, I., & Karaycel, S. (2010). The effect of fishing on growth of the clam Chamelea gallina (Bivalvia: Veneridae) from the Turkish Black Sea coast. *Journal of the*

Marine Biological Association of the United Kingdom, *90*(2), 261–265. https://doi.org/10.1017/S0025315409000939

Dauphin, Y. (2016). Biomineralization. *Encyclopedia of Inorganic and Bioinorganic Chemistry*, 1–15. https://doi.org/10.1002/9781119951438.EIBC0017.PUB2

Davis, B. A. S., Brewer, S., Stevenson, A. C., Guiot, J., Allen, J., Almqvist-Jacobson, H., Ammann, B., Andreev, A. A., Argant, J., Atanassova, J., Balwierz, Z., Barnosky, C. D., Bartley, D. D., De Beaulieu, J. L., Beckett, S. C., Behre, K. E., Bennett, K. D., Berglund, B. E. B., Beug, H. J., … Zernitskaya, V. P. (2003). The temperature of Europe during the Holocene reconstructed from pollen data. *Quaternary Science Reviews*, *22*(15–17), 1701–1716. https://doi.org/10.1016/S0277-3791(03)00173-2

Degobbis, D., Gilmartin, M., & Revelante, N. (1986). An annotated nitrogen budget calculation for the northern Adriatic Sea. *Marine Chemistry*, *20*(2), 159–177. https://doi.org/10.1016/0304-4203(86)90037-X

Deng, Z., & Li, L. (2021). Intrinsic Mechanical Properties of Individual Biogenic Mineral Units in Biomineralized Skeletons. *ACS Biomaterials Science and Engineering*. https://doi.org/10.1021/acsbiomaterials.0c01587

Denny, M. W., & Gaylord, B. (2010). Marine ecomechanics. *Annu Rev Mar Sci*, *2*, 89–114.

Dhami, N. K., Reddy, M. S., & Mukherjee, M. S. (2013). Biomineralization of calcium carbonates and their engineered applications: A review. *Frontiers in Microbiology*, *4*(OCT), 314. https://doi.org/10.3389/FMICB.2013.00314/BIBTEX

Dillon, E. M., Lafferty, K. D., McCauley, D. J., Bradley, D., Norris, R. D., Caselle, J. E., DiRenzo, G. v., Gardner, J. P. A., & O’Dea, A. (2020). Dermal denticle assemblages in coral reef sediments correlate with conventional shark surveys. *Methods in Ecology and Evolution*, *11*(3), 362–375. https://doi.org/10.1111/2041-210X.13346

DP Häder, H. K. R. S. R. W. (2007). Effects of solar UV radiation on aquatic ecosystems and interactions with climate change. *Photochem. Photobiol. Sci.*, *6*, 267–285.

Dunca, E., Schöne, B. R., & Mutvei, H. (2005). Mutvei’s solution: An ideal agent for resolving microgrowth structures of biogenic carbonates. *Palaeogeogr. Palaeoclimatol. Palaeoecol.*, *228*(1–2), 149–166. https://doi.org/10.1016/j.palaeo.2005.03.050

E Arneri, G. G. R. P. B. A. (1995). Age and growth of Chamelea gallina (Bivalvia: Veneridae) in the Central Adriatic Sea obtained by thin sections. *Rapp. Comm. Int. Mer Médit*, *34*, 17.

Ellis, J., Cummings, V., Hewitt, J., Thrush, S., & Norkko, A. (2002). Determining effects of suspended sediment on condition of a suspension feeding bivalve (*Atrina zelandica*): Results of a survey, a laboratory experiment and a field transplant experiment. *Journal of Experimental Marine Biology and Ecology*, *267*(2), 147–174. https://doi.org/10.1016/S0022-0981(01)00355-0

Epstein, S., & Lowenstam, H. A. (1953). Temperature-Shell-Growth Relations of Recent and Interglacial Pleistocene Shoal-Water Biota from Bermuda. *The Journal of Geology*, *61*(5), 424–438. https://doi.org/10.1086/626110

Eyster, L. S., & Morse, M. P. (1984). Early shell formation during molluscan embryogenesis, with new studies on the surf clam, Spisula solidissima. *Integrative and Comparative Biology*, *24*(4), 871–882. https://doi.org/10.1093/icb/24.4.871

Falini, G., Albeck, S., Weiner, S., & Addadi, L. (1996). Control of aragonite or calcite polymorphism by mollusk shell macromolecules. *Science*, *271*(5245), 67–69. https://doi.org/10.1126/SCIENCE.271.5245.67

Falini, G., Fermani, S., & Goffredo, S. (2015). Coral biomineralization: A focus on intra-skeletal organic matrix and calcification. In *Seminars in Cell and Developmental Biology* (Vol. 46, pp. 17–26). Academic Press. https://doi.org/10.1016/j.semcdb.2015.09.005

FAO. (2020). The State of World Fisheries and Aquaculture. *Sustainability in Action*. https://doi.org/10.4060/ca9229en

Fermani, S., Džakula, B. N., Reggi, M., Falini, G., & Kralj, D. (2017). Effects of magnesium and temperature control on aragonite crystal aggregation and morphology. *CrystEngComm*, *19*(18), 2451–2455.

Fitzer, S. C., Cusack, M., Phoenix, V. R., & Kamenos, N. A. (2014). Ocean acidification reduces the crystallographic control in juvenile mussel shells. *Journal of Structural Biology*, *188*(1), 39–45. https://doi.org/10.1016/J.JSB.2014.08.007

Fitzer, S. C., Vittert, L., Bowman, A., Kamenos, N. A., Phoenix, V. R., & Cusack, M. (2015). Ocean acidification and temperature increase impact mussel shell shape and thickness: Problematic for protection? *Ecology and Evolution*, *5*(21), 4875–4884. https://doi.org/10.1002/ECE3.1756

Flessa, K. W., Cutler, A. H., & Meldahl, K. H. (1993). Time and Taphonomy: Quantitative Estimates of Time-Averaging and Stratigraphic Disorder in a Shallow Marine Habitat. In *Paleobiology* (Vol. 19, Issue 2).

Fox, D. L., & Coe, W. R. (1943). Biology of the California sea-mussel (Mytilus californianus). II. Nutrition, metabolism, growth and calcium deposition. *Journal of Experimental Zoology*, *93*(2), 205–249. https://doi.org/10.1002/JEZ.1400930204

Frank Kenneth McKinney. (2007). *The Northern Adriatic Ecosystem: Deep Time in a Shallow Sea* . Columbia University Press.

Frascari, F., Spagnoli, F., Marcaccio, M., & Giordano, P. (2006). Anomalous Po River flood event effects on sediments and the water column of the northwestern Adriatic Sea. *Climate Research*, *31*(2–3), 151–165. https://doi.org/10.3354/cr031151

Furuhashi, T., Schwarzinger, C., Miksik, I., Smrz, M., & Beran, A. (2009). Molluscan shell evolution with review of shell calcification hypothesis. *Comparative Biochemistry and Physiology Part B: Biochemistry and Molecular Biology*, *154*(3), 351–371. https://doi.org/10.1016/J.CBPB.2009.07.011

Gaspar, M. B., Pereira, A. M., Vasconcelos, P., & Monteiro, C. C. (2004). Age and growth of Chamelea gallina from the Algarve coast (southern Portugal): Influence of seawater temperature and gametogenic cycle on growth rate. *Journal of Molluscan Studies*, *70*(4), 371–377. https://doi.org/10.1093/MOLLUS/70.4.371

Gazeau, F., Parker, L. M., Comeau, S., Gattuso, J. P., O’Connor, W. A., Martin, S., Pörtner, H. O., & Ross, P. M. (2013). Impacts of ocean acidification on marine shelled molluscs. *Marine Biology*, *160*(8), 2207–2245. https://doi.org/10.1007/S00227-013-2219-3

Gibson, R. N. , M. B. and R. J. A. Atkinson. (2002). Impact of changes in flow of freshwater on estuarine and open coastal habitats and the associated organisms. *Oceanography and Marine Biology: An Annual Review 40*, 233–309. https://doi.org/10.1201/9780203180594.ch5

Gilbert, S. F. (2001). Ecological developmental biology: Developmental biology meets the real world. *Developmental Biology*, *233*(1), 1–12. https://doi.org/10.1006/dbio.2001.0210

Gizzi, F., Caccia, M. G., Simoncini, G. A., Mancuso, A., Reggi, M., Fermani, S., Brizi, L., Fantazzini, P., Stagioni, M., & Falini, G. (2016). Shell properties of commercial clam Chamelea gallina are influenced by temperature and solar radiation along a wide latitudinal gradient. *Scientific Reports*, *6*(1), 1–12.

Gizzi, F., Caccia, M. G., Simoncini, G. A., Mancuso, A., Reggi, M., Fermani, S., Brizi, L., Fantazzini, P., Stagioni, M., Falini, G., Piccinetti, C., & Goffredo, S. (2016a). Shell properties of commercial clam Chamelea gallina are influenced by temperature and solar radiation along a wide latitudinal gradient. *Scientific Reports 2016 6:1*, *6*(1), 1–12. https://doi.org/10.1038/srep36420

Gizzi, F., Caccia, M. G., Simoncini, G. A., Mancuso, A., Reggi, M., Fermani, S., Brizi, L., Fantazzini, P., Stagioni, M., Falini, G., Piccinetti, C., & Goffredo, S. (2016b). Shell properties of commercial clam *Chamelea gallina* are influenced by temperature and solar radiation along a wide latitudinal gradient. *Scientific Reports*, *6*(1), 36420. https://doi.org/10.1038/srep36420

Gizzi, F., Caccia, M. G., Simoncini, G. A., Mancuso, A., Reggi, M., Fermani, S., Brizi, L., Fantazzini, P., Stagioni, M., Falini, G., Piccinetti, C., & Goffredo, S. (2016c). Shell properties of commercial clam Chamelea gallina are influenced by temperature and solar radiation along a wide latitudinal gradient. *Scientific Reports*, *6*. https://doi.org/10.1038/SREP36420

Goldberg, E. (1975). The mussel watch-a first step in global marine monitoring. *Mar. Pollut. Bull.*, *6*(7), 111.

Gosling, E. (2015). *Marine bivalve molluscs*. John Wiley & Sons.

Grazioli, E., Guerranti, C., Pastorino, P., Esposito, G., Bianco, E., Simonetti, E., Rainis, S., Renzi, M., & Terlizzi, A. (2022). Review of the Scientific Literature on Biology, Ecology, and Aspects Related to the Fishing Sector of the Striped Venus (Chamelea gallina) in Northern Adriatic Sea. *Journal of Marine Science and Engineering*, *10*(9), 1328. https://doi.org/10.3390/JMSE10091328/S1

Grienke, U., Silke, J., & Tasdemir, D. (2014). Bioactive compounds from marine mussels and their effects on human health. *Food Chemistry*, *142*, 48–60. https://doi.org/10.1016/J.FOODCHEM.2013.07.027

Hahn, S., Rodolfo-Metalpa, R., Griesshaber, E., Schmahl, W. W., Buhl, D., Hall-Spencer, J. M., Baggini, C., Fehr, K. T., & Immenhauser, A. (2012). Marine bivalve shell geochemistry and ultrastructure from modern low pH environments: Environmental effect versus experimental bias. *Biogeosciences, 9*(5), 1897–1914. https://doi.org/10.5194/BG-9-1897-2012

Hall-Spencer, J. M., & Harvey, B. P. (2019a). Ocean acidification impacts on coastal ecosystem services due to habitat degradation. *Emerging Topics in Life Sciences, 3*(2), 197–206. https://doi.org/10.1042/etls20180117

Hall-Spencer, J. M., & Harvey, B. P. (2019b). Ocean acidification impacts on coastal ecosystem services due to habitat degradation. *Emerging Topics in Life Sciences, 3*(2), 197–206. https://doi.org/10.1042/ETLS20180117

Harley, C. D. G. (2011). Climate change, keystone predation, and biodiversity loss. *Science, 334*(6059), 1124–1127. https://doi.org/10.1126/SCIENCE.1210199

Heilmayer, O., Brey, T., & Portner, H. O. (2004). Growth efficiency and temperature in scallops: a comparative analysis of species adapted to different temperatures. *Functional Ecology, 18*(5), 641–647. https://doi.org/10.1111/j.0269-8463.2004.00905.x

Hofmann, G. E., Barry, J. P., Edmunds, P. J., Gates, R. D., Hutchins, D. A., Klinger, T., & Sewell, M. A. (2010). The effect of Ocean acidification on calcifying organisms in marine ecosystems: An organism-to-ecosystem perspective. *Annual Review of Ecology, Evolution, and Systematics, 41*, 127–147. https://doi.org/10.1146/ANNUREV.ECOLSYS.110308.120227

Hofmann, G. E., Smith, J. E., Johnson, K. S., Send, U., Levin, L. A., Micheli, F., Paytan, A., Price, N. N., Peterson, B., Takeshita, Y., Matson, P. G., de Crook, E., Kroeker, K. J., Gambi, M. C., Rivest, E. B., Frieder, C. A., Yu, P. C., & Martz, T. R. (2011). High-frequency dynamics of ocean pH: A multi-ecosystem comparison. *PLoS ONE, 6*(12). https://doi.org/10.1371/JOURNAL.PONE.0028983

Huang, W., Restrepo, D., Jung, J. Y., Su, F. Y., Liu, Z., Ritchie, R. O., McKittrick, J., Zavattieri, P., & Kisailus, D. (2019). Multiscale Toughening Mechanisms in Biological Materials and Bioinspired Designs. *Advanced Materials, 31*, 1901561. https://doi.org/10.1002/adma.201901561

Jalali, B., Sicre, M.-A., Bassetti, M.-A., & Kallel, N. (2016). Holocene climate variability in the North-Western Mediterranean Sea (Gulf of Lions). *Climate of the Past, 12*(1), 91–101. https://doi.org/10.5194/cp-12-91-2016

Jamieson, J. C. (2004). Phase Equilibrium in the System Calcite-Aragonite. *The Journal of Chemical Physics, 21*(8), 1385. https://doi.org/10.1063/1.1699228

Jansen, J. M., Pronker, A. E., Kube, S., Sokolowski, A., Sola, J. C., Marquiegui, M. A., Schiedek, D., Wendelaar Bonga, S., Wolowicz, M., & Hummel, H. (2007). Geographic and seasonal patterns and limits on the adaptive response to temperature of *European Mytilus* spp. and *Macoma balthica* populations. *Oecologia, 154*(1), 23–34. https://doi.org/10.1007/s00442-007-0808-x

Kidwell, S. M. (2015). Biology in the Anthropocene: Challenges and insights from young fossil records. *Proceedings of the National Academy of Sciences, 112*(16), 4922–4929. https://doi.org/10.1073/PNAS.1403660112

Kidwell, S. M., & Behrensmeyer, A. K. (1993). Taphonomic approaches to time resolution in fossil assemblages: Introduction. *Short Courses in Paleontology, 6,* 1–8. https://doi.org/10.1017/s2475263000001021

Kjerfve, B., & Magill, K. E. (1989). Geographic and hydrodynamic characteristics of shallow coastal lagoons. *Marine Geology, 88*(3–4), 187–199. https://doi.org/10.1016/0025-3227(89)90097-2

Klein, R. T., Lohmann, K. C., & Thayer, C. W. (1996). SrCa and 13C12C ratios in skeletal calcite of Mytilus trossulus: Covariation with metabolic rate, salinity, and carbon isotopic composition of seawater. *Geochimica et Cosmochimica Acta, 60*(21), 4207–4221. https://doi.org/10.1016/S0016-7037(96)00232-3

Knoll, A. H. (2003). Biomineralization and Evolutionary History. *Reviews in Mineralogy and Geochemistry, 54*(1), 329–356. https://doi.org/10.2113/0540329

Kong, Y., Jing, G., Yan, Z., Li, C., Gong, N., Zhu, F., Li, D., Zhang, Y., Zheng, G., Wang, H., Xie, L., & Zhang, R. (2009). Cloning and characterization of Prisilkin-39, a novel matrix protein serving a dual role in the prismatic layer formation from the oyster Pinctada fucata. *Journal of Biological Chemistry, 284*(16), 10841–10854. https://doi.org/10.1074/JBC.M808357200

Kowalewski, M., Wittmer, J. M., Dexter, T. A., Amorosi, A., & Scarponi, D. (2015). Differential responses of marine communities to natural and anthropogenic changes. *Proceedings of the Royal Society B: Biological Sciences*, *282*(1803), 20142990. https://doi.org/10.1098/rspb.2014.2990

Kroeker, K. J., Kordas, R. L., Crim, R. N., & Singh, G. G. (2010). Meta-analysis reveals negative yet variable effects of ocean acidification on marine organisms. *Ecology Letters*, *13*(11), 1419–1434. https://doi.org/10.1111/J.1461-0248.2010.01518.X

Kroeker, K. J., Kordas, R. L., & Harley, C. D. G. (2017). Embracing interactions in ocean acidification research: Confronting multiple stressor scenarios and context dependence. *Biology Letters*, *13*(3). https://doi.org/10.1098/RSBL.2016.0802

Kroeker, K. J., Sanford, E., Rose, J. M., Blanchette, C. A., Chan, F., Chavez, F. P., Gaylord, B., Helmuth, B., Hill, T. M., Hofmann, G. E., McManus, M. A., Menge, B. A., Nielsen, K. J., Raimondi, P. T., Russell, A. D., & Washburn, L. (2016a). Interacting environmental mosaics drive geographic variation in mussel performance and predation vulnerability. *Ecology Letters*, *19*(7), 771–779. https://doi.org/10.1111/ELE.12613

Kroeker, K. J., Sanford, E., Rose, J. M., Blanchette, C. A., Chan, F., Chavez, F. P., Gaylord, B., Helmuth, B., Hill, T. M., Hofmann, G. E., McManus, M. A., Menge, B. A., Nielsen, K. J., Raimondi, P. T., Russell, A. D., & Washburn, L. (2016b). Interacting environmental mosaics drive geographic variation in mussel performance and predation vulnerability. *Ecology Letters*, *19*(7), 771–779. https://doi.org/10.1111/ELE.12613

Lemasson, A., & Knights, M. (2021). Differential responses in anti-predation traits of the native oyster Ostrea edulis and invasive Magallana gigas to ocean acidification and warming. *Marine Ecology Progress Series, 665,* 87–102.

Leonard, G. H., Bertness, M. D., & Yund, P. O. (1999). Crab predation, waterborne cues, and inducible defenses in the blue mussel, Mytilus edulis. *Ecology, 80*(1), 1–14.

Li, H. X., Ma, L. S., Lin, L., Ni, Z. X., Xu, X. R., Shi, H. H., Yan, Y., Zheng, G. M., & Rittschof, D. (2018). Microplastics in oysters Saccostrea cucullata along the Pearl River Estuary, China. *Environmental Pollution*, *236*, 619–625. https://doi.org/10.1016/j.envpol.2018.01.083

Lippmann, F. (1973). *Sedimentary carbonate minerals*. Springer Verlag.

Loo, L. O., & Rosenberg, R. (1989). Bivalve suspension-feeding dynamics and benthic-pelagic coupling in an eutrophicated marine bay. *Journal of Experimental Marine Biology and Ecology*, *130*(3), 253–276. https://doi.org/10.1016/0022-0981(89)90167-6

Loosanoff, V. L. (1962). *Effects of turbidity on some larval and adult bivalves*.

Lorens, R. B., & Bender, M. L. (1980). The impact of solution chemistry on Mytilus edulis calcite and aragonite. *Geochimica et Cosmochimica Acta*, *44*(9), 1265–1278.

Lorrain, A., Paulet, Y.-M., Chauvaud, L., Dunbar, R., Mucciarone, D., & Fontugne, M. (2004). δ13C variation in scallop shells: increasing metabolic carbon contribution with body size? *Geochimica et Cosmochimica Acta*, *68*(17), 3509–3519.

Lowenstam, H. A. (1954). Factors affecting the aragonite: calcite ratios in carbonate-secreting marine organisms. *The Journal of Geology*, *62*(3), 284–322.

Lowenstam, H. A. (1981). Minerals Formed by Organisms. *Science*, *211*(4487), 1126–1131. https://doi.org/10.1126/SCIENCE.7008198

Lowenstam, H. A., & Weiner, S. (1989a). *On biomineralization*. Oxford University Press on Demand.

Lowenstam, H. A., & Weiner, S. (1989b). *On Biomineralization* (Oxford University Press on Demand, Ed.). https://books.google.it/books?hl=it&lr=&id=16znCwAAQBAJ&oi=fnd&pg=PR7&dq=Lowenstam,+H.+A.%3B+Weiner,+S.,+On+Biomineralization.+New+York,+1989.+&ots=7xDD6oWe1E&sig=L8GoWmGPA1zzMypvdlcDo8sJI4I&redir_esc=y#v=onepage&q=Lowenstam%2C%20H.%20A.%3B%20Weiner%2C%20S.%2C%20On%20Biomineralization.%20New%20York%2C%201989.&f=false

Lowenstam Heinz Adolf, & Weiner Stephen. (1989). On Biomineralization. In *On Biomineralization*. Oxford University Press.

Lutz, R. A., & Rhoads, D. C. (1980). *Growth patterns within the molluscan shell: an overview*. 750.

Lynton S. Land. (1967). Diagenesis of Skeletal Carbonates. *SEPM Journal of Sedimentary Research*, *Vol. 37*(3), 914–930. https://doi.org/10.1306/74d717d5-2b21-11d7-8648000102c1865d

M Ramón, C. R. (1992). Age determination and shell growth of Chamelea gallina (Bivalvia: Veneridae) in the western Mediterranean. *Mar. Ecol. Prog. Ser.*, *89*, 15–23.

Mackenzie, C. L., Ormondroyd, G. A., Curling, S. F., Ball, R. J., Whiteley, N. M., & Malham, S. K. (2014a). Ocean Warming, More than Acidification, Reduces Shell Strength in a Commercial Shellfish Species during Food Limitation. *PLOS ONE, 9*(1), e86764. https://doi.org/10.1371/JOURNAL.PONE.0086764

Mackenzie, C. L., Ormondroyd, G. A., Curling, S. F., Ball, R. J., Whiteley, N. M., & Malham, S. K. (2014b). Ocean Warming, More than Acidification, Reduces Shell Strength in a Commercial Shellfish Species during Food Limitation. *PLOS ONE*, *9*(1), e86764.

Magnabosco, G., Giuri, D., Di Bisceglie, A. P., Scarpino, F., Fermani, S., Tomasini, C., & Falini, G. (2021). New material perspective for waste seashells by covalent functionalization. *ACS Sustainable Chemistry and Engineering*, *9*(18), 6203–6208. https://doi.org/10.1021/acssuschemeng.1c01306

Mancuso, A., Stagioni, M., Prada, F., Scarponi, D., Piccinetti, C., & Goffredo, S. (2019a). Environmental influence on calcification of the bivalve Chamelea gallina along a latitudinal gradient in the Adriatic Sea. *Scientific Reports*, *9*(1), 11198. https://doi.org/10.1038/S41598-019-47538-1

Mancuso, A., Stagioni, M., Prada, F., Scarponi, D., Piccinetti, C., & Goffredo, S. (2019b). Environmental influence on calcification of the bivalve *Chamelea gallina* along a latitudinal gradient in the Adriatic Sea. *Scientific Reports*, *9*(1), 11198. https://doi.org/10.1038/s41598-019-47538-1

Mancuso, A., Stagioni, M., Prada, F., Scarponi, D., Piccinetti, C., & Goffredo, S. (2019c). Environmental influence on calcification of the bivalve Chamelea gallina along a latitudinal gradient in the Adriatic Sea. *Scientific Reports*, *9*(1), 11198. https://doi.org/10.1038/s41598-019-47538-1

Mancuso, A., Stagioni, M., Prada, F., Scarponi, D., Piccinetti, C., & Goffredo, S. (2019d). Environmental influence on calcification of the bivalve Chamelea gallina along a latitudinal gradient in the Adriatic Sea. *Scientific Reports*, *9*(1), 11198. https://doi.org/10.1038/s41598-019-47538-1

Mann, S. (1993). Molecular tectonics in biomineralization and biomimetic materials chemistry. *Nature 1993 365:6446*, *365*(6446), 499–505. https://doi.org/10.1038/365499a0

Marchetti, R., Provini, A., & Crosa, G. (1989). Nutrient load carried by the River Po into the Adriatic Sea, 1968–1987. *Marine Pollution Bulletin*, *20*(4), 168–172. https://doi.org/10.1016/0025-326X(89)90487-6

Marin, F., le Roy, N., & Marie, B. (2012a). The formation and mineralization of mollusk shell. *Frontiers in Bioscience*, *4*, 1099.

Marin, F., le Roy, N., & Marie, B. (2012b). The formation and mineralization of mollusk shell. *Frontiers in Bioscience*, *4*, 1099.

Marsden, I. (2004). Effects of reduced salinity and seston availability on growth of the New Zealand little-neck clam *Austrovenus stutchburyi*. *Marine Ecology Progress Series*, *266*, 157–171. https://doi.org/10.3354/meps266157

Marszalek, D. S. (1982a). The role of heavy skeletons in vertical movements of non-motile zooplankton. *Marine Behaviour and Physiology*, *8*(4), 295–303. https://doi.org/10.1080/10236248209387026

Marszalek, D. S. (1982b). The role of heavy skeletons in vertical movements of non-motile zooplankton. *Marine & Freshwater Behaviour & Phy*, *8*(4), 295–303.

Martinez, M., Mangano, M. C., Maricchiolo, G., Genovese, L., Mazzola, A., & Sarà, G. (2018). Measuring the effects of temperature rise on Mediterranean shellfish aquaculture. *Ecological Indicators*, *88*, 71–78. https://doi.org/10.1016/j.ecolind.2018.01.002

Maselli, V., & Trincardi, F. (2013). Man made deltas. *Scientific Reports*, *3*(1), 1–7. https://doi.org/10.1038/srep01926

Monari, M., Serrazanetti, G. P., Foschi, J., Matozzo, V., Marin, M. G., & Cattani, O. (2007). Effects of salinity on the clam Chamelea gallina haemocytes. Part II: Superoxide dismutase response. *Marine Biology*, *151*(3), 1059–1068. https://doi.org/10.1007/S00227-006-0544-5/METRICS

Montroni, D. (2020). *Hierarchically organized chitin-based matrices*. University of Bologna.

Morello, E. B., Froglia, C., Atkinson, R. J. A., & Moore, P. G. (2005). Hydraulic dredge discards of the clam (Chamelea gallina) fishery in the western Adriatic Sea, Italy. *Fisheries Research*, *76*(3), 430–444. https://doi.org/10.1016/J.FISHRES.2005.07.002

Morse, J. W., Andersson, A. J., & Mackenzie, F. T. (2006). Initial responses of carbonate-rich shelf sediments to rising atmospheric pCO2 and “ocean acidification”: Role of high Mg-calcites. *Geochimica et Cosmochimica Acta*, *70*(23), 5814–5830. https://doi.org/10.1016/J.GCA.2006.08.017

Muñoz-Moya, E., García-Herrera, C. M., Lagos, N. A., Abarca-Ortega, A. F., Checa, A. G., & Harper, E. M. (2022). Evaluation of remodeling and geometry on the biomechanical properties of nacreous bivalve shells. *Scientific Reports*, *12*(1), 1–11.

Myrand, B., Tremblay, R., & Sévigny, J. M. (2002a). Selection against blue mussels (Mytilus edulis L.) homozygotes under various stressful conditions. *Journal of Heredity*, *93*(4), 238–248. https://doi.org/10.1093/jhered/93.4.238

Myrand, B., Tremblay, R., & Sévigny, J.-M. (2002b). Selection against blue mussels (*Mytilus edulis* L.) homozygotes under various stressful conditions. *The Journal of Heredity*. https://doi.org/DOI 10.1093/jhered/93.4.238

Nagarajan, R., Lea, S. E. G., & Goss-Custard, J. D. (2006). Seasonal variations in mussel, Mytilus edulis L. shell thickness and strength and their ecological implications. *Journal of Experimental Marine Biology and Ecology*, *339*(2), 241–250.

Nash, M. C., Opdyke, B. N., Troitzsch, U., Russell, B. D., Adey, W. H., Kato, A., Diaz-Pulido, G., Brent, C., Gardner, M., Prichard, J., & Kline, D. I. (2012). Dolomite-rich coralline algae in reefs resist dissolution in acidified conditions. *Nature Climate Change 2012 3:3*, *3*(3), 268–272. https://doi.org/10.1038/nclimate1760

Nawrot, R., Scarponi, D., Azzarone, M., Dexter, T. A., Kusnerik, K. M., Wittmer, J. M., Amorosi, A., & Kowalewski, M. (2018). Stratigraphic signatures of mass extinctions: ecological and sedimentary determinants. *Proceedings of the Royal Society B: Biological Sciences*, *285*(1886), 20181191. https://doi.org/10.1098/rspb.2018.1191

Niu, Y.-Q., Liu, J.-H., Aymonier, C., Fermani, S., Kralj, D., Falini, G., & Zhou, C.-H. (2022). Calcium carbonate: controlled synthesis, surface functionalization, and nanostructured materials. *Chemical Society Reviews*, *51*, 7883–7943.

Nudelman, F., Shimoni, E., Klein, E., Rousseau, M., Bourrat, X., Lopez, E., Addadi, L., & Weiner, S. (2008). Forming nacreous layer of the shells of the bivalves Atrina rigida and Pinctada margaritifera: An environmental- and cryo-scanning electron microscopy study. *Journal of Structural Biology*, *162*, 290–300. https://doi.org/10.1016/j.jsb.2008.01.008

Olson, I. C., Kozdon, R., Valley, J. W., & Gilbert, P. U. P. A. (2012). Mollusk shell nacre ultrastructure correlates with environmental temperature and pressure. *Journal of the American Chemical Society*, *134*(17), 7351–7358. https://doi.org/10.1021/ja210808s

Orban, E., di Lena, G., Nevigato, T., Casini, I., Caproni, R., Santaroni, G., & Giulini, G. (2007). Nutritional and commercial quality of the striped venus clam, Chamelea gallina, from the Adriatic sea. *Food Chemistry*, *101*(3), 1063–1070. https://doi.org/10.1016/J.FOODCHEM.2006.03.005

P Moura, M. G. C. M. (2009). Age determination and growth rate of a Callista chione population from the southwestern coast of Portugal. Aquat. *Biol.*, *5*, 97–106.

Palmer, A. R. (1981). Do carbonate skeletons limit the rate of body growth? *Nature*, *292*(5819), 150–152.

Palmer, A. R. (1983). Relative cost of producing skeletal organic matrix versus calcification: evidence from marine gastropods. *Marine Biology*, *75*(2), 287–292.

Parsons, K. E. (1997). Contrasting patterns of heritable geographic variation in shell morphology and growth potential in the marine gastropod Bembicium vittatum: evidence from field experiments. *Evolution*, *51*(3), 784–796.

Pauly, M., Kamenos, N. A., Donohue, P., & LeDrew, E. (2015). Coralline algal Mg-O bond strength as a marine pCO2 proxy. *Geology*, *43*(3), 267–270. https://doi.org/10.1130/G36386.1

Pavicic, J., Raspor, B., & Martincic, D. (1993). Quantitative determination of metallothionein-like proteins in mussels. Methodological approach and field evaluation. *Marine Biology*, *115*, 435–444. https://doi.org/10.1038/164914a0

Penney, R. W., Hart, M. J., & Templeman, N. D. (2007). Shell Strength and Appearance in Cultured Blue Mussels Mytilus edulis, M. trossulus, and M. edulis × M. trossulus Hybrids. *North American Journal of Aquaculture*, *69*(3), 281–295. https://doi.org/10.1577/A06-044.1

Pérez-Huerta, A., Coronado, I., & Hegna, T. A. (2018). Understanding biomineralization in the fossil record. In *Earth-Science Reviews* (Vol. 179, pp. 95–122). Elsevier B.V. https://doi.org/10.1016/j.earscirev.2018.02.015

Perry, R. S., Mcloughlin, N., Lynne, B. Y., Sephton, M. A., Oliver, J. D., Perry, C. C., Campbell, K., Engel, M. H., Farmer, J. D., Brasier, M. D., & Staley, J. T. (2007). Defining biominerals and organominerals: Direct and indirect indicators of life. *Sedimentary Geology*, *201*(1–2), 157–179. https://doi.org/10.1016/J.SEDGEO.2007.05.014

Pfister, C. A., Roy, K., Wootton, J. T., McCoy, S. J., Paine, R. T., Suchanek, T. H., & Sanford, E. (2016). Historical baselines and the future of shell calcification for a foundation species in a changing ocean. *Proceedings of the Royal Society B: Biological Sciences*, *283*(1832). https://doi.org/10.1098/RSPB.2016.0392

Pokroy, B., Fitch, A. N., Marin, F., Kapon, M., Adir, N., & Zolotoyabko, E. (2006a). Anisotropic lattice distortions in biogenic calcite induced by intra-crystalline organic molecules. *Journal of Structural Biology*, *155*(1), 96–103. https://doi.org/10.1016/j.jsb.2006.03.008

Pokroy, B., Fitch, A. N., Marin, F., Kapon, M., Adir, N., & Zolotoyabko, E. (2006b). Anisotropic lattice distortions in biogenic calcite induced by intra-crystalline organic molecules. *Journal of Structural Biology*, *155*(1), 96–103. https://doi.org/10.1016/J.JSB.2006.03.008

Pokroy, B., Fitch, A. N., & Zolotoyabko, E. (2007). Structure of biogenic aragonite (CaCO3). *Crystal Growth and Design*, *7*(9), 1580–1583. https://doi.org/10.1021/cg060842v

Poulain, P. M. (2001). Adriatic Sea surface circulation as derived from drifter data between 1990 and 1999. *Journal of Marine Systems*, *29*(1–4), 3–32. https://doi.org/10.1016/S0924-7963(01)00007-0

Proćków, M., Proćków, J., Błażej, P., & Mackiewicz, P. (2018). The influence of habitat preferences on shell morphology in ecophenotypes of Trochulus hispidus complex. *Science of The Total Environment*, *630*, 1036–1043. https://doi.org/https://doi.org/10.1016/j.scitotenv.2018.02.311

Purroy, A., Milano, S., Schöne, B. R., Thébault, J., & Peharda, M. (2018). Drivers of shell growth of the bivalve, Callista chione (L. 1758) – Combined environmental and biological factors. *Mar. Environ. Res.*, *134*, 138–149. https://doi.org/10.1016/j.marenvres.2018.01.011

Rahman, M. A., & Shinjo, R. (2011). *Biocalcification of Corals and their Response to Global Climate Change*.

Ramon, M., & Richardson, C. A. (1992). Age determination and shell growth of Chamelea gallina (Bivalvia: Veneridae) in the western Mediterranean. *Marine Ecology Progress Series*, *89*(1), 15–23. https://doi.org/10.3354/meps089015

Ramsey, C. B., & Lee, S. (2013). Recent and Planned Developments of the Program OxCal. *Radiocarbon*, *55*(2), 720–730. https://doi.org/10.1017/s0033822200057878

Rasband, W. S. (n.d.). *ImageJ, U. S. National Institutes of Health, Bethesda, Maryland, USA, https://imagej.nih.gov/ij/, 1997-2018.*

Reimer, P. J., Bard, E., Bayliss, A., Beck, J. W., Blackwell, P. G., Ramsey, C. B., Buck, C. E., Cheng, H., Edwards, R. L., Friedrich, M., Grootes, P. M., Guilderson, T. P., Haflidason, H., Hajdas, I., Hatté, C., Heaton, T. J., Hoffmann, D. L., Hogg, A. G., Hughen, K. A., … van der Plicht, J. (2013). IntCal13 and Marine13 Radiocarbon Age Calibration Curves 0–50,000 Years cal BP. *Radiocarbon*, *55*(4), 1869–1887. https://doi.org/10.2458/azu_js_rc.55.16947

Ren, D., Feng, Q., & Bourrat, X. (2011). Effects of additives and templates on calcium carbonate mineralization in vitro. *Micron*, *42*(3), 228–245. https://doi.org/10.1016/J.MICRON.2010.09.005

Ries, J. B., Cohen, A. L., & McCorkle, D. C. (2009a). Marine calcifiers exhibit mixed responses to CO2-induced ocean acidification. *Geology*, *37*(12), 1131–1134. https://doi.org/10.1130/G30210A.1

Ries, J. B., Cohen, A. L., & McCorkle, D. C. (2009b). Marine calcifiers exhibit mixed responses to CO2-induced ocean acidification. *Geology*, *37*(12), 1131–1134. https://doi.org/10.1130/G30210A.1

Romanelli, M., Cordisco, A. C., & Giovanardi, O. (2009). The long-term decline of the *Chamelea gallina* L. (Bivalvia: Veneridae) clam fishery in the Adriatic Sea: is a synthesis possible? *Acta Adriatica*, *50*(2), 171–205.

RStudio Team. (2020). *RStudio: Integrated Development for R. RStudio*. RStudio, PBC.

Russo, A., Rabitti, S., & Bastianini, M. (2002). Decadal Climatic Anomalies in the Northern Adriatic Sea Inferred from a New Oceanographic Data Set. *Mar. Ecol.*, *23*(SUPPL. 1), 340–351. https://doi.org/10.1111/j.1439-0485.2002.tb00032.x

Sanders, T., Schmittmann, L., Nascimento-Schulze, J. C., & Melzner, F. (2018). High calcification costs limit mussel growth at low salinity. *Frontiers in Marine Science*, *5*(OCT), 352. https://doi.org/10.3389/FMARS.2018.00352/BIBTEX

Sarà, G., Reid, G. K., Rinaldi, A., Palmeri, V., Troell, M., & Kooijman, S. (2012). Growth and reproductive simulation of candidate shellfish species at fish cages in the Southern Mediterranean: Dynamic Energy Budget (DEB) modelling for integrated multi-trophic aquaculture. *Aquaculture*, *324*, 259–266.

Scarponi, D., & Angeletti, L. (2008). Integration of palaeontological patterns in the sequence stratigraphy paradigm: a case study from Holocene deposits of the Po Plain (Italy). *GeoActa*, *7*, 1–13.

Scarponi, D., Azzarone, M., Kusnerik, K., Amorosi, A., Bohacs, K. M., Drexler, T. M., & Kowalewski, M. (2017). Systematic vertical and lateral changes in quality and time resolution of the macrofossil record: Insights from Holocene transgressive deposits, Po coastal plain, Italy. *Marine and Petroleum Geology*, *87*, 128–136. https://doi.org/10.1016/j.marpetgeo.2017.03.031

Scarponi, D., & Kowalewski, M. (2004a). Stratigraphic paleoecology: Bathymetric signatures and sequence overprint of mollusk associations from upper Quaternary sequences of the Po Plain, Italy. *Geology*, *32*(11), 989–992. https://doi.org/10.1130/G20808.1

Scarponi, D., & Kowalewski, M. (2004b). Stratigraphic paleoecology: Bathymetric signatures and sequence overprint of mollusk associations from upper Quaternary sequences of the Po Plain, Italy. *Geology*, *32*(11), 989–992. https://doi.org/10.1130/G20808.1

Scarponi, D., & Kowalewski, M. (2007). Sequence stratigraphic anatomy of diversity patterns: Late Quaternary benthic mollusks of the Po Plain, Italy. *PALAIOS*, *22*(3), 296–305. https://doi.org/10.2110/palo.2005.p05-020r

Schneider, C. A., Rasband, W. S., & Eliceiri, K. W. (2012). NIH Image to ImageJ: 25 years of image analysis. *Nature Methods*, *9*(7), 671–675. https://doi.org/10.1038/nmeth.2089

Schneidermann, N., & Harris, P. M. (1985). Carbonate Cements. *Carbonate Cements.* https://doi.org/10.2110/pec.85.36

Schofield, O., Ducklow, H. W., Martinson, D. G., Meredith, M. P., Moline, M. A., & Fraser, W. R. (2010). How do polar marine ecosystems respond to rapid climate change? *Science*, *328*(5985), 1520–1523. https://doi.org/10.1126/SCIENCE.1185779/ASSET/CB239015-9367-4926-84DC-ED33F944F564/ASSETS/GRAPHIC/328_1520_F2.JPEG

Schöne, B. R., & Giere, O. (2005). Growth increments and stable isotope variation in shells of the deep-sea hydrothermal vent bivalve mollusk Bathymodiolus brevior from the North Fiji Basin, Pacific Ocean. *Deep-Sea Research Part I: Oceanographic Research Papers*, *52*(10), 1896–1910. https://doi.org/10.1016/J.DSR.2005.06.003

Schöne, B. R., & Gillikin, D. P. (2013). Unraveling environmental histories from skeletal diaries — Advances in sclerochronology. *Palaeogeography, Palaeoclimatology, Palaeoecology*, *373*, 1–5. https://doi.org/10.1016/J.PALAEO.2012.11.026

Schöne, B. R., Oschmann, W., Rössler, J., Freyre Castro, A. D., Houk, S. D., Kröncke, I., Dreyer, W., Janssen, R., Rumohr, H., & Dunca, E. (2003). North Atlantic Oscillation dynamics recorded in shells of a long-lived bivalve mollusk. *Geology*, *31*(12), 1037–1040. https://doi.org/10.1130/G20013.1

Seed, R., & Richardson, C. A. (1999). Evolutionary traits in Perna viridis (Linnaeus) and Septifer virgatus (Wiegmann)(Bivalvia: Mytilidae). *Journal of Experimental Marine Biology and Ecology*, *239*(2), 273–287.

Siedlecki, S. A., Pilcher, D. J., Hermann, A. J., Coyle, K., & Mathis, J. (2017a). The Importance of Freshwater to Spatial Variability of Aragonite Saturation State in the Gulf of Alaska. *Journal of Geophysical Research: Oceans*, *122*(11), 8482–8502. https://doi.org/10.1002/2017JC012791

Siedlecki, S. A., Pilcher, D. J., Hermann, A. J., Coyle, K., & Mathis, J. (2017b). The Importance of Freshwater to Spatial Variability of Aragonite Saturation State in the Gulf of Alaska. *Journal of Geophysical Research: Oceans*, *122*(11), 8482–8502. https://doi.org/10.1002/2017JC012791

Sokolova, I., & Pörtner, H. (2001). Physiological adaptations to high intertidal life involve improved water conservation abilities and metabolic rate depression in Littorina saxatilis. *Marine Ecology Progress Series*, *224*, 171–186. https://doi.org/10.3354/meps224171

Stefani, M., & Vincenzi, S. (2005). The interplay of eustasy, climate and human activity in the late Quaternary depositional evolution and sedimentary architecture of the Po Delta system. *Marine Geology*, *222–223*(1–4), 19–48. https://doi.org/10.1016/j.margeo.2005.06.029

Steffani, C. N., & Branch, G. M. (2003). Growth rate, condition, and shell shape of Mytilus galloprovincialis: responses to wave exposure. *Marine Ecology Progress Series*, *246*, 197–209.

Stenzel, H. B. (1964). Oysters: Composition of the larval shell. *Science*, *145*(3628), 155–156. https://doi.org/10.1126/science.145.3628.155

Steyermark, A. C. (2002a). A high standard metabolic rate constrains juvenile growth. *Zoology*. https://doi.org/10.1078/0944-2006-00055

Steyermark, A. C. (2002b). A high standard metabolic rate constrains juvenile growth. *Zoology*, *105*(2), 147–151. https://doi.org/10.1078/0944-2006-00055

Sun, J., & Bhushan, B. (2012). Hierarchical structure and mechanical properties of nacre: A review. *RSC Advances*, *2*(20), 7617–7632. https://doi.org/10.1039/c2ra20218b

Suzuki, M., Saruwatari, K., Kogure, T., Yamamoto, Y., Nishimura, T., Kato, T., & Nagasawa, H. (2009). An acidic matrix protein, Pif, is a key macromolecule for nacre formation. *Science*, *325*(5946), 1388–1390. https://doi.org/10.1126/SCIENCE.1173793

Telesca, L., Michalek, K., Sanders, T., Peck, L. S., Thyrring, J., & Harper, E. M. (2018a). Blue mussel shell shape plasticity and natural environments: A quantitative approach. *Scientific Reports*, *8*(1). https://doi.org/10.1038/S41598-018-20122-9

Telesca, L., Michalek, K., Sanders, T., Peck, L. S., Thyrring, J., & Harper, E. M. (2018b). Blue mussel shell shape plasticity and natural environments: a quantitative approach. *Scientific Reports 2018 8:1*, *8*(1), 1–15. https://doi.org/10.1038/s41598-018-20122-9

Telesca, L., Peck, L. S., Sanders, T., Thyrring, J., Sejr, M. K., & Harper, E. M. (2019). Biomineralization plasticity and environmental heterogeneity predict geographical resilience patterns of foundation species to future change. *Global Change Biology*, *25*(12), 4179–4193.

Thomsen, J., & Melzner, F. (2010). Moderate seawater acidification does not elicit long-term metabolic depression in the blue mussel Mytilus edulis. *Marine Biology*, *157*(12), 2667–2676. https://doi.org/10.1007/S00227-010-1527-0

Tomašových, A., Albano, P. G., Fuksi, T., Gallmetzer, I., Haselmair, A., Kowalewski, M., Nawrot, R., Nerlović, V., Scarponi, D., & Zuschin, M. (2020a). Ecological regime shift preserved in the Anthropocene stratigraphic record. *Proceedings of the Royal Society B*, *287*(1929). https://doi.org/10.1098/RSPB.2020.0695

Tomašových, A., Albano, P. G., Fuksi, T., Gallmetzer, I., Haselmair, A., Kowalewski, M., Nawrot, R., Nerlović, V., Scarponi, D., & Zuschin, M. (2020b). Ecological regime shift preserved in the Anthropocene stratigraphic record. *Proceedings of the Royal Society B: Biological Sciences*, *287*(1929), 20200695. https://doi.org/10.1098/rspb.2020.0695

Tomašovỳch, A., Gallmetzer, I., Haselmair, A., Kaufman, D. S., Vidović, J., & Zuschin, M. (2017). Stratigraphic unmixing reveals repeated hypoxia events over the past 500 yr in the northern Adriatic Sea. *Geology*, *45*(4), 363–366. https://doi.org/10.1130/G38676.1

Trincardi, F., Amorosi, A., Bosman, A., Correggiari, A., Madricardo, F., & Pellegrini, C. (2020). Ephemeral rollover points and clinothem evolution in the modern Po Delta based on repeated bathymetric surveys. *Basin Research*, *32*(2), 402–418. https://doi.org/10.1111/bre.12426

Tushtev, K., Murck, M., & Grathwohl, G. (2008). On the nature of the stiffness of nacre. *Materials Science and Engineering C*, *28*, 1164–1172. https://doi.org/10.1016/j.msec.2007.10.039

v Moschino, M. M. (2006). Seasonal changes in physiological responses and evaluation of “well-being” in the Venus clam Chamelea gallina from the Northern Adriatic Sea. *Comp. Bioch. Physiol*, *145A*, 433–440.

Vacchi, M., Marriner, N., Morhange, C., Spada, G., Fontana, A., & Rovere, A. (2016). Multiproxy assessment of Holocene relative sea-level changes in the western Mediterranean: Sea-level variability and improvements in the definition of the isostatic signal. In *Earth-Science Reviews* (Vol. 155, pp. 172–197). Elsevier B.V. https://doi.org/10.1016/j.earscirev.2016.02.002

Vermeij, G. J. (1976). Interoceanic differences in vulnerability of shelled prey to crab predation. *Nature*, *260*(5547), 135–136. https://doi.org/10.1038/260135A0

Vihtakari, M., Ambrose, W. G., Renaud, P. E., Locke, W. L., Carroll, M. L., Berge, J., Clarke, L. J., Cottier, F., & Hop, H. (2017). A key to the past? Element ratios as environmental proxies in two Arctic bivalves. *Palaeogeography, Palaeoclimatology, Palaeoecology*, *465*, 316–332. https://doi.org/10.1016/J.PALAEO.2016.10.020

Wahl, M., Buchholz, B., Winde, V., Golomb, D., Guy-Haim, T., Müller, J., Rilov, G., Scotti, M., & Böttcher, M. E. (2015). A mesocosm concept for the simulation of near-natural shallow underwater climates: The Kiel Outdoor Benthocosms (KOB). *Limnology and Oceanography: Methods*, *13*(11), 651–663. https://doi.org/10.1002/LOM3.10055

Waldbusser, G. G., Brunner, E. L., Haley, B. A., Hales, B., Langdon, C. J., & Prahl, F. G. (2013). A developmental and energetic basis linking larval oyster shell formation to acidification sensitivity. *Geophysical Research Letters*, *40*(10), 2171–2176. https://doi.org/10.1002/GRL.50449

Warren Huntley, J., & Scarponi, D. (2015). Geographic variation of parasitic and predatory traces on mollusks in the northern Adriatic Sea, Italy: Implications for the stratigraphic paleobiology of biotic interactions. *Paleobiology*, *41*(1), 134–153. https://doi.org/10.1017/pab.2014.9

Watson, S. (2012). Marine invertebrate skeleton size varies with latitude, temperature and carbonate saturation: implications for global change and ocean acidification. *Global Change Biol*, *18*, 3026–3038.

Watson, S.-A., Peck, L. S., Tyler, P. A., Southgate, P. C., Tan, K. S., Day, R. W., & Morley, S. A. (2012). Marine invertebrate skeleton size varies with latitude, temperature and carbonate saturation: implications for global change and ocean acidification. *Global Change Biology*, *18*(10), 3026–3038. https://doi.org/10.1111/j.1365-2486.2012.02755.x

Weiner, S., & Dove, P. M. (2003a). An Overview of Biomineralization Processes and the Problem of the Vital Effect. *Reviews in Mineralogy and Geochemistry*, *54*(1), 1–29. https://doi.org/10.2113/0540001

Weiner, S., & Dove, P. M. (2003b). An Overview of Biomineralization Processes and the Problem of the Vital Effect. *Reviews in Mineralogy and Geochemistry*, *54*(1), 1–29. https://doi.org/10.2113/0540001

Weiner, S., & Dove, P. M. (2003c). An overview of biomineralization processes and the problem of the vital effect. *Reviews in Mineralogy and Geochemistry*, *54*(1), 1–29.

Weiner, S., Mahamid, J., Politi, Y., Ma, Y., & Addadi, L. (2009). Overview of the amorphous precursor phase strategy in biomineralization. *Frontiers of Materials Science in China*, *3*(2), 104–108. https://doi.org/10.1007/S11706-009-0036-X/METRICS

Weiss, I. M., Tuross, N., Addadi, L., & Weiner, S. (2002). Mollusc larval shell formation: amorphous calcium carbonate is a precursor phase for aragonite. *Journal of Experimental Zoology*, *293*(5), 478–491. https://doi.org/10.1002/JEZ.90004

Wittmer, J. M., Dexter, T. A., Scarponi, D., Amorosi, A., & Kowalewski, M. (2014). Quantitative bathymetric models for late quaternary transgressive-regressive cycles of the po plain, italy. *Journal of Geology*, *122*(6), 649–670. https://doi.org/10.1086/677901

Wootton, J. T., & Pfister, C. A. (2012). Carbon System Measurements and Potential Climatic Drivers at a Site of Rapidly Declining Ocean pH. *PLoS ONE*, *7*(12). https://doi.org/10.1371/JOURNAL.PONE.0053396

Wootton, J. T., Pfister, C. A., & Forester, J. D. (2008). Dynamic patterns and ecological impacts of declining ocean pH in a high-resolution multi-year dataset. *Proceedings of the National Academy of Sciences of the United States of America*, *105*(48), 18848–18853. https://doi.org/10.1073/PNAS.0810079105

Ye, F., Jurikova, H., Angiolini, L., Brand, U., Crippa, G., Henkel, D., Laudien, J., Hiebenthal, C., & Šmajgl, D. (2019). Variation in brachiopod microstructure and isotope geochemistry under low-pH–ocean acidification conditions. *Biogeosciences*, *16*(2), 617–642. https://doi.org/10.5194/bg-16-617-2019

Zeebe, R. E. (2012). History of Seawater Carbonate Chemistry, Atmospheric CO2, and Ocean Acidification. *Https://Doi.Org/10.1146/Annurev-Earth-042711-105521*, *40*, 141–165. https://doi.org/10.1146/ANNUREV-EARTH-042711-105521

Zhang, C., Li, S., Ma, Z., Xie, L., & Zhang, R. (2006). A novel matrix protein p10 from the nacre of pearl oyster (Pinctada fucata) and its effects on both CaCO 3 crystal formation and mineralogenic cells. *Marine Biotechnology*, *8*(6), 624–633. https://doi.org/10.1007/S10126-006-6037-1

Zuschin, M., & Stanton, R. J. (2001). Experimental Measurement of Shell Strength and its Taphonomic Interpretation. *PALAIOS*, *16*(2), 161–170. https://doi.org/10.1669/0883-1351(2001)016<0161:EMOSSA>2.0.CO;2

Chapter 2. Climate variation during the Holocene influenced the skeletal properties of *Chamelea gallina* shells in the North Adriatic Sea (Italy) (*Published in PLoSONE)*

Climate variation during the Holocene influenced the skeletal properties of *Chamelea gallina* shells in the North Adriatic Sea

Alessandro Cheli[1,2], Arianna Mancuso[1,2], Michele Azzarone[3], Simona Fermani[4], Jaap Kaandorp[5], Frederic Marin[6], Devis Montroni[4], Iryna Polishchuk[7], Fiorella Prada[1,2], Marco Stagioni[8], Giovanni Valdré[3,2], Boaz Pokroy[7], Giuseppe Falini[4,2]*, Stefano Goffredo[1,2]*, Daniele Scarponi[3,2]*

[1] Marine Science Group, Department of Biological, Geological and Environmental Sciences, University of Bologna, Bologna, Italy

[2] Fano Marine Center, The Inter-Institute Center for Research on Marine Biodiversity, Resources and Biotechnologies, Fano (PU), Italy

[3] Department of Biological, Geological and Environmental Sciences, University of Bologna, Bologna, Italy

[4] Department of Chemistry 'Giacomo Ciamician', University of Bologna, Via F. Selmi 2, 40126 Bologna, Italy

[5] Computational Science Laboratory, Faculty of Science, University of Amsterdam, Amsterdam, The Netherlands

[6] UMR CNRS 6282 Biogéosciences, Université de Bourgogne - Franche-Comté, Dijon, France

[7] Department of Materials Sciences and Engineering and the Russell Berrie Nanotechnology Institute, Technion – Israel Institute of Technology, Technion City, Haifa, Israel

[8] Marine Biology and Fisheries Laboratory of Fano, Department of Biological, Geological and Environmental Sciences, University of Bologna, (PU) Italy

*corresponding authors:

E-mail: giuseppe.falini@unibo.it (GF); s.goffredo@unibo.it (SG); daniele.scarponi@unibo.it (DS)

Abstract

Understanding how marine taxa will respond to near-future climate changes is one of the main challenges for management of coastal ecosystem services. Ecological studies that investigate relationships between the environment and shell properties of commercially important marine species are commonly restricted to latitudinal gradients or small-scale laboratory experiments. This paper aimed to explore the variations in shell features and growth of the edible bivalve *Chamelea gallina* from the Holocene sedimentary succession to present-day thanatocoenosis of the Po-Adriatic system (Italy). Comparing the Holocene sub-fossil record to modern thanatocoenoses allowed obtaining an insight of shell variations dynamics on a millennial temporal scale. Five shoreface-related, *C. gallina* rich, assemblages were considered: two from the Middle Holocene, when regional sea surface temperatures were higher than today, representing a possible analogue for the near-future global warming, one from the Late Holocene and two from the present-day thanatocoenoses. We investigated shell biometry and skeletal properties in relation to the valve length of *C. gallina*. Juveniles were found to be more porous than adults in all horizons. This suggested that *C. gallina* promoted an accelerated shell accretion with a higher porosity and lower density at the expense of a mechanically fragile shells. A positive correlation between sea surface temperatures and both micro-density and bulk density were found, with modern populations being less dense, likely due to lower aragonite saturation state at lower temperature, which could ultimately increase the energetic costs of shell formation. Since no variation was observed in shell $CaCO_3$ polymorphism (100% aragonite) or in compositional parameters among the analyzed horizons, the observed dynamics in skeletal parameters are likely not driven by a diagenetic recrystallization of the shell mineral phase. This study contributes to understand the response of *C. gallina* to climate-driven environmental shifts and offers insights for assessing anthropogenic impacts on this economic relevant species.

Introduction

Evaluating how marine ecosystems could respond to near-future global warming is critical to design proper conservation and management strategies, especially in coastal areas with increasing urbanization and resource overexploitation.

In the marine realm, calcifying macroinvertebrates such as corals, brachiopods and mollusks produce hard structures for support and protection that constitute high-resolution archives recording the environmental conditions that have prevailed during their life (Pérez-Huerta et al., 2018; Ye et al., 2019). Through the control exerted by intraskeletal macromolecules, mollusks can exert imprints on calcium carbonate biomineralization (Falini et al., 2015), influencing the polymorphism, morphology and chemistry of the shell in response to environmental changes (Gilbert, 2001; Lowenstam Heinz Adolf & Weiner Stephen, 1989; Rahman & Shinjo, 2011). Those biogenic structures can be useful tools to reconstruct the historical effects of climate change on marine organisms, thus allowing a better understanding of near-future dynamics.

Quantifying the effect of near future climate change on marine calcifying organisms requires long-term multi-generational studies for assessing their adaptability to changing environmental conditions (S.-A. Watson et al., 2012). Nevertheless, such studies are difficult to address in laboratory conditions. Natural latitudinal gradients could represent an alternative to laboratory experimental studies. In fact, this methodology allows to evaluate the effects of different environmental conditions, like temperature variations, along large-scale spatial gradients (Jansen et al., 2007; S.-A. Watson et al., 2012). A complementary approach is to investigate the recent fossil record. This line of research gives access to an archive of ecological responses to past climate transitions that could elucidate near-future scenarios of marine ecosystems under global warming (Scarponi et al., 2017; Tomašových et al., 2020b).

During the Holocene some time intervals were warmer than the present. Of these warmer periods, the longest was from about 9,000 to about 5,000 years before present (BP) (i.e., Holocene climate optimum HCO), with significantly higher temperatures than today at high latitudes (up to 4 ° C (Davis et al., 2003)). Holocene sedimentary successions are characterized by well-preserved remains of mollusk taxa with well-known ecological needs. Thus, it preserves a centennial record of environmental and biological dynamics that lead to present-day ecosystems. In this context, the recent sedimentary succession of the Po-Adriatic system (Italy) has been extensively investigated in the last decades and offers a high-resolution stratigraphic framework (for details see S1 Appendix “Geological setting”; (Amorosi, Barbieri, Bruno, Campo, Drexler, Hong, Rossi, et al., 2019; Amorosi et al., 1999b, 2017; Bruno et al., 2017; Frank Kenneth McKinney, 2007; Kowalewski et al., 2015; Nawrot et al., 2018; Scarponi et al., 2017; Scarponi & Kowalewski, 2007; Stefani & Vincenzi, 2005)). Hence, biomineralization dynamics in relation to millennial scale climate change can here be investigated in a well-resolved climate and stratigraphic framework.

Among economically relevant mollusks of the Adriatic Sea, the infaunal venerid bivalve *Chamelea gallina* seems to be particularly sensitive to environmental changes, showing shell morphology variations in response to environmental change (Gizzi, Caccia, Simoncini, Mancuso, Reggi, Fermani, Brizi, Fantazzini, Stagioni, Falini, et al., 2016b; Mancuso et al., 2019b; Ramon & Richardson, 1992; Romanelli et al., 2009). Previous studies have mainly focused on population dynamics, shell growth and composition of this species in the present-day Mediterranean and along latitudinal gradients ((Mancuso et al., 2019b) and reference therein). In contrast, there are no information about shell variations in relation to climate-driven environmental change along temporal gradients.

This study aimed to investigate the variations in skeletal features of *C. gallina* assemblages during the last 8,000 years from shoreface deposits and active shoreface settings of the Po-Adriatic system (Italy). This allowed to assess phenotypic variation occurred in time with different environmental conditions and determine how the impact of anthropogenic warming could affect this economically important bivalve species in the future. Biometry, composition and crystal structure of *C. gallina* shell were investigated in five shoreface-related horizons: two from the Middle Holocene, one from the Late Holocene and two from modern thanatocoenoses. Since diagenetic processes can occur over time, analyses of the taphonomic degradation status of the sub-fossil shells were carried out before comparing the results with modern thanatocoenosis.

Materials and methods

Specimens collection

Sub-fossil specimens (Holocene in age) of *C. gallina* were sampled from cores of the sedimentary successions of Po Coastal Plain drilled as part of a multidisciplinary project (Fig 1) (Amorosi et al., 2004; Scarponi & Kowalewski, 2004a). Two fossil horizons were collected from core 205-S6 (Comacchio, 44°68’N, 12°15’E), at depths of 17.2 m (code “CO1”) and 13.2 m (code “CO2”). The third sub-fossil horizon (code “CE”) was collected from core 240-S8 (Cervia 44°16'N, 12°20'E) at a depth of 13.1 m. All investigated horizons came from shoreface depositional environments characterized by sandy substrates and estimated water depth between ~5 and 10 m. Paleoenvironmental, paleobathymetric and paleogeographic reconstructions of the depositional environments of the Po-Adriatic system during the Holocene are detailed in previous studies (Bruno et al., 2017; Scarponi & Kowalewski, 2004a; Warren Huntley & Scarponi, 2015; Wittmer et al., 2014).

Modern samples of *C. gallina* were collected in the Northern Adriatic Sea off the coast of Goro (MGO; 44°75’N, 12°43’E) and Cervia (MCE; 44°30’N, 12°40’E). Samplings were performed by means of Van Veen Grab and scuba diving on the sandy bottom at 5.2 m and 5.3 m water depth. The sampling areas are about fifty kilometers away from each other and correspond roughly to the extraction areas of cores used in this study. Sampling operations were restricted to the top-most

10 cm of the taphonomically active zone (TAZ) of the sea bottom. This sampling allowed to collect a time-averaged record of shells estimated in tens of years, following the deposition rates reported in Trincardi et al. (Trincardi et al., 2020). This allowed a better comparison with cored sub-fossil horizons, in which the sampled shells came from a time span of few tens of years. No living organism was collected for this study.

Only valves of 5-30 mm length (maximum distance on the anterior-posterior axis) were considered for the analyses. The lower limit was defined by the technical difficulties in obtaining reliable measurements in very small specimens. The upper limit was due to the difficulty to collect whole shells over 30 mm in the sub-fossil horizons with 90 mm cores diameter and in finding valves over 30 mm in thanatocoenoses located in *C. gallina* harvesting areas.

Prior to any measurements, each valve was cleaned with a toothbrush and soaked in distilled water for two hours to remove any external residue on the shells surfaces. In addition, valves from modern Adriatic settings were immersed in a solution of distilled water and hydrogen peroxide (5 vol.%) for 24 h to eliminate any traces of organic material on the surface (e.g., epibionts). Then, the valves were dried in an oven at 37 °C for one night to remove any moisture that may influence following measurements. Samples were conserved at room temperature.

Radiocarbon dating measurements

A dating was performed exploiting the high-resolution stratigraphic framework developed for the Holocene succession of the Po Coastal Plain, which allowed to subdivide this ca. 30 m thick sedimentary package in millennial-scale sedimentary units (parasequences in (Amorosi et al., 2017)). Successively, radiocarbon dating was performed on five randomly selected valves to constrain the time span of the examined sample. Radiocarbon data were calibrated with Oxcal 4.2 (Ramsey & Lee, 2013), using the Intcal13 calibration curve (Reimer et al., 2013), Delta R (ΔR) = 139.0 ± 28.0 and obtained from CHRONO Marine Reservoir Database, Map No 235 (North Adriatic, Rimini, Italy).

Environmental parameters

Sea surface temperature (SST) for the Adriatic Sea in proximity of targeted shoreface settings were obtained from the global ocean OSTIA sea surface temperature and sea ice analysis databank (Copernicus Marine Environment Monitoring Service, n.d.). Mean annual SST was calculated from daily values measured from January 2010 to December 2019 (number of daily values = 3651 for each site).

As for sub-fossil *C. gallina* horizons, SST estimates were based on Alkenones unsaturation index, a widely applied proxy for past SST. Alkenones are long-chain methyl ketones synthesized by some single-celled algae found in marine sediments and whose carbon bond saturation index varies according to annual mean values at the SST (Conte et al., 2006). Jalali et al. (Jalali et al., 2016) produced a high-resolution SST record of the past 10,000 years based on alkenone paleothermometry for the central-northern Mediterranean Sea (Gulf of Lion). This site is at the same latitude of the North Adriatic Sea and shows a comparable physiographic setting. Estimated paleo-SST for the Gulf of Lion can be considered a reliable proxy for the study area too.

Shell parameters

Shell length (maximum distance on the anterior-posterior axis) and height (maximum distance on the dorsal-ventral axis) were measured using ImageJ software after data capture of each shell shape with a scanner (Acer Acerscan Prisa 620 ST 600 dpi). The shell width (maximum distance on the lateral axis of the valve) was measured with a caliper (± 0.05 mm).

Skeletal parameters were measured by buoyant weight (BW) analysis, using a density determination kit Ohaus Explorer Pro balance (± 0.1 mg; Ohaus Corp., Pine Brook, NJ, USA, see Gizzi et al. (Gizzi, Caccia, Simoncini, Mancuso, Reggi, Fermani, Brizi, Fantazzini, Stagioni, Falini, et al., 2016b)for details).

The BW measurement was repeated three times and the average was considered for statistical analysis. The BW technique allowed to estimate the variable of interest:

(i) micro-density or matrix density (mass per unit volume of the material which composes the shell, excluding the volume of pores; $g\cdot cm^{-3}$);

(ii) porosity: the volume of pores connected to the external surface (%);

(iii) bulk density: the density of the valve (including the volume of pores).

Correlations analyses between SST and skeletal parameters were performed to investigate any significant pattern developed over geological time as a function of temperature.

Differences in skeletal properties of *C. gallina* shells were also investigated in relation to animal sexual maturity (reached in modern specimens after 1 year of life (Romanelli et al., 2009) and length >18mm) in order to consider eventual differences in the biomineralization process during different stages of the bivalve’s life cycle.

Shell phase composition and microstructure

Nano-scale and micro-scale analyses of skeletal features were used to determine the mineral phase and an eventual recrystallization or alteration of the samples.

Prior to the analyses, samples were soaked in an ethanol solution (10 vol.%) and immersed in a bath sonicator (Falc Instruments S.r.l., UTA 18) for one minute. Subsequently, the valves were treated with a sodium hypochlorite solution (5 wt.%) for one hour, rinsed with distilled water and dried in a desiccator. About one-half of each shell was finely grounded in a mortar to obtain a homogenous powder.

X-ray powder diffraction (XRD) analyses were performed on six specimens for each horizon, by preparing a thin compact layer of the sample in a silica background signal free holder. Diffractograms for each sample were collected using an X'celerator detector fitted on a PANalytical X'Pert Pro diffractometer, using a Cu-Kα radiation generated at 40 kV and 40 mA. The data were collected within the 2θ range from 20° to 60° with a step size (Δ2θ) of 0.016° and a counting time of 60 s. Fixed anti-scatter and divergence slits of 1/2° were used with 10 mm beam mask. All measurements were carried out in a continuous mode. The XRD patterns were analyzed using the X'Pert HighScore Plus software (PANalytical).

High-resolution synchrotron X-ray powder diffraction (HR-XRPD) measurements were performed on three valves of the oldest horizon (CO1) and three of today's thanatocoenosis (MCE). The analysis was carried out on ID22 beamline at the European Synchrotron Radiation Facility (ESRF) in Grenoble, France, using a monochromatic radiation of 0.49599 Å. Each sample was transferred to a 0.9 mm glass capillary and measured three times at a fast rate (10 $\text{deg}\cdot\text{min}^{-1}$) at three different locations, while being rotated. This setup makes it possible to avoid beam damage and texture influences. Measurements were performed at room temperature and after *ex-situ* heating at 300 °C for 2 h in order to examine possible influence of the intracrystalline organics on the shell's unit cell. The unit cell parameters were extracted using Rietveld refinement method applied to a full diffraction pattern profile. Coherence length (nm) along specific crystallographic directions was derived by applying the line profile analysis to a specific diffraction peak. This was performed by fitting the diffraction peak profile to a Voigt function and deconvolution of the diffraction peak broadening into the Lorenzian and Gaussian widths.

Fourier-transform infrared spectroscopy (FTIR) analyses were performed on twelve valves for each site using a Nicolet IS10 Spectrometer (Thermo Electron Corporation) working in the 4,000–400 cm^{-1} range of wave numbers at a resolution of 2 cm^{-1}. The samples were analyzed as KBr pellets using a sample concentration of about 1 wt.%.

Thermogravimetric analysis (TGA) was used to estimate the organic matrix (OM) and the structurally associated intra-skeletal water content of each shell. The measurements were performed using a SDT Q900 instrument (TA Instruments). Five different valves were analyzed for each horizons measuring 10-15 mg of sample in a ceramic crucible. The analysis was carried out under nitrogen flow with a pre-equilibration at 30 °C, followed by a heating ramp from 30 °C to 850 °C using a 10 $°C\cdot min^{-1}$ heating rate.

Inductively coupled plasma optical emission spectroscopy (ICP-OES) measurements to evaluate the metal content of shells were performed on valves treated with sodium hypochlorite (5 wt.%) for 24 h, then rinsed with distilled water and dried in a desiccator. About 1 g of shell was dissolved in 3 mL of HCl and HNO_3 in a 1: 3 volume ratio, adjusting the volume with milliQ water until 5 mL. Solvents and reagents with trace analysis grade of purity were used. Three samples were measured for each level. Each sample was measured three times, 12 s each with 50 s of prerunning, using a Spectro Arcos-Ametek, ICP-OES with axial torch and high salinity kit.

Statistical analyses

Levene's test was used for testing homogeneity of variance while Kolmogorov-Smirnov's test was used for testing normality for environmental and shell parameters. Since assumptions for parametric statistics were not fulfilled, the non-parametric Kruskal-Wallis equality-of-populations rank test was used. Spearman's rank correlation coefficient was used to evaluate trend between shell parameters and sea surface temperature. In each horizon, rank-correlations were computed on all valves and also on two subgroups consisting of immature specimens (valve length <18 mm) and mature ones (>18 mm (Romanelli et al., 2009)). All statistical analyses were computed using RStudio software (RStudio Team, 2020).

Results

Dating and environmental parameters

Radiocarbon measurements ascribed two of the sub-fossil horizons to the Middle Holocene (CO2 and CE) and one to the Late Holocene (CO1) as reported in Table 1.

According to the data reported for the Gulf of Lion, estimated and measured SST appeared to cool down gradually moving from the oldest fossil horizon (CO1, 18.6 °C) to nowadays setting (MCE, 17.3 and MGO, 17.2 °C) (Kruskal-Wallis test, df = 4, $p < 0.001$; Table 1). The reconstructed SST trend for the Holocene showed a difference of ∼1.5 °C between middle Holocene and present day, a difference that is comparable with the current SST variation along the latitudinal gradient in the Adriatic Sea (Gizzi, Caccia, Simoncini, Mancuso, Reggi, Fermani, Brizi, Fantazzini, Stagioni, Falini, et al., 2016a)).

Table 1. Calibrated radiocarbon age, sea surface temperature (SST) and shell biometric parameters.

Horizon	n	^{14}C Age (ky BP)	SST (°C)	Length (mm)	Height (mm)	Width (mm)	Mass (g)
CO1	49	7.6 ± 0.1	18.6 ± 0.4	17.6 ± 0.9	14.2 ± 0.7	4.7 ± 0.2	0.66 ± 0.07
CO2	59	5.9 ± 0.1	18.2 ± 0.3	17.2 ± 0.8	14.8 ± 0.7	4.3 ± 0.2	0.74 ± 0.09
CE	52	2.6 ± 0.2	17.5 ± 0.5	15.7 ± 0.7	13.6 ± 0.6	3.9 ± 0.2	0.47 ± 0.06
MCE	73	modern	17.3 ± 0.1	16.7 ± 0.8	13.6 ± 0.6	4.0 ± 0.2	0.56 ± 0.06
MGO	68	modern	17.2 ± 0.1	17.3 ± 0.8	14.7 ± 0.7	4.3 ± 0.2	0.67 ± 0.08

Values for each horizon in chronological order. Radiocarbon measurements are reported in years `before present' (BP). For each parameter mean value and standard error are reported. n = number of collected specimens.

Shell parameters

All the measured shell parameters (i.e., length, height, width and mass; Tables 1 and 2) were homogeneous among horizons (Kruskal-Wallis test, $p > 0.05$, Table 1). In all investigated *C. gallina* assemblages, length correlated positively with height, width, and mass (S1 Fig). Shell length correlated with skeletal parameters (i.e., bulk-, micro-density and apparent porosity) except for apparent porosity and length of levels CO2 and MCE (S1 Fig). Skeletal parameters resulted significantly different among stratigraphic horizons both in the whole dataset and in the subgroups (i.e., mature and immature shells) (Tables 2 and 3).

In both cases, micro- and bulk density were positively correlated with SST, while apparent porosity correlated negatively with SST (Fig 2). The only exception was represented by the subgroup of mature shells, which showed no significant correlation between apparent porosity and SST (Fig. 2C).

Table 2. Mean value and standard error of shell skeletal parameters.

Horizon	**^{14}C Age (ky BP)**	**SST (°C)**	**Micro-density (g/cm^3)**	**Apparent Porosity (%)**	**Bulk Density (g/cm^3)**
CO1	7.6 ± 0.1	18.6 ± 0.4	2.81 ± 0.01	10.17 ± 0.55	2.52 ± 0.02
CO2	5.9 ± 0.1	18.2 ± 0.3	2.79 ± 0.01	8.58 ±0.42	2.55 ± 0.01
CE	2.6 ± 0.2	17.5 ± 0.5	2.80 ± 0.01	10.28 ± 0.72	2.52 ± 0.02
MCE	modern	17.3 ± 0.1	2.78 ± 0.01	9.87 ± 0.34	2.51 ± 0.01
MGO	modern	17.2 ± 0.1	2.78 ± 0.01	11.01 ± 0.59	2.47 ± 0.02
KW		***	***	*	***

Values for each horizon in chronological order. K-W = Kruskal-Wallis equality-of-populations rank test; * $p<0.05$, *** $p < 0.001$.

Table 3. Mean value and standard error of shell skeletal parameters for immature and mature shells.

	Horizon	**^{14}C Age (ky BP)**	**SST (°C)**	**Micro-density (g/cm^3)**	**Apparent Porosity (%)**	**Bulk Density (g/cm^3)**
Immature shell (≤18 mm)	CO1	7.6 ± 0.1	18.6 ± 0.4	2.78 ± 0.01	11.81 ± 0.8	2.45 ± 0.03
	CO2	5.9 ± 0.1	18.2 ± 0.3	2.77 ± 0.01	8.89 ± 0.7	2.52 ± 0.02
	CE	2.6 ± 0.2	17.5 ± 0.5	2.79 ± 0.01	12.04 ± 1.0	2.46 ± 0.03
	MCE	modern	17.3 ± 0.1	2.77 ± 0.004	10.67 ± 0.5	2.47 ± 0.01
	MGO	modern	17.2 ± 0.1	2.76 ± 0.004	13.54 ± 0.9	2.39 ± 0.03
	KW		***	***	***	***
Mature shell (>18 mm)	CO1	7.6 ± 0.1	18.6 ± 0.4	2.84 ± 0.004	8.60 ± 0.6	2.59 ± 0.02
	CO2	5.9 ± 0.1	18.2 ± 0.3	2.82 ± 0.002	8.24 ± 0.4	2.59 ± 0.01
	CE	2.6 ± 0.2	17.5 ± 0.5	2.82 ± 0.002	6.94 ± 0.4	2.63 ± 0.01
	MCE	modern	17.3 ± 0.1	2.80 ± 0.003	8.86 ± 0.3	2.55 ± 0.01
	MGO	modern	17.2 ± 0.1	2.79 ± 0.002	8.27 ± 0.3	2.56 ± 0.01
	KW		***	***	***	***

Values for each horizon in chronological order. K-W = Kruskal-Wallis equality-of-populations rank test; *** $p < 0.001$.

Shell phase composition and microstructure

The conventional XRD and FTIR analyses (Fig 3) of the shells from all levels showed only aragonite signals, no other mineral phase was detected. However, the HR-XRPD data (S2 Fig) allowed to precisely deduce the unit cell parameters, microstrain fluctuations and crystallite size. The heat treatment removed possible effects of the OM on the unit cell of the shells. The obtained data revealed that the intracrystalline OM induced an elongation of both the *a*- and *c*-axes and a contraction of the *b*-axis (Fig 4A). Values of the calculated lattice distortions vary from 0.15% to 0.20%, with the highest strain observed in the case of the modern sample (MCE). The line profile analysis allowed to derive the crystallite sizes along the <111> and <021> aragonite directions for the MCE sample, 0.221 and 0.183 µm, and CO1 samples, 0.275 and 0.231 µm, respectively. After the thermal treatment, the crystallite sizes were 0.158 and 0.139 µm for the MCE, and 0.179 and 0.171 µm for the CO1, respectively. (Fig 4 B-C).

The shell's skeletal weight loss measured by TGA before aragonite decomposition, in the temperature range between~150 and 450 °C, differed among horizons ($p< 0.05$), but no correlation with SST was found (S1 Table). The weight percentage of the OM and the associated intra-skeletal water was slightly lower in the case of the fossil horizons, where the values varied from 1.37 to 1.72 %, as compared to that of the both modern horizons with 1.79 and 1.83 %. (S1 Table).

The metal content analysis (ICP-OES) showed no differences between the fossil and modern horizons in the content of magnesium and strontium, two elements that may vary in response to a diagenetic alteration occurred over time (Bruckschen et al., 1995) (S1 Table).

Discussion

This study investigated the phenotypic variation of *C. gallina* in relation to SST trend in the Po-Adriatic system during the last ~8,000 years. By comparing the Holocene sub-fossil record to modern day thanatocoenoses, has been possible to get insight on skeletal dynamics on a millennial temporal scale. This allowed overcoming the time limits imposed by laboratory studies and assessing how rising SST and environmental-driven changes could affect this economically relevant bivalve in the future. The high temporal and stratigraphic resolution of the investigated succession offered an ideal venue to explore this scenario.

On a geologic time scale, the taphonomic status of a skeletal remain could be an indicator of its relative age (Flessa et al., 1993). This concept goes under the name of taphonomic clock (Kidwell & Behrensmeyer, 1993). Although intriguing, the taphonomic clock shows a variable reliability, as it is not only function of time since-death, but mainly depends on the time spent by the skeletal remain in the taphonomic active zone (TAZ) of the sediment layer, where it is exposed to physical and biological degradation processes (Tomašovỳch et al., 2017). In Holocene sub-fossils, most distinctive external features related to taphonomic alterations as a function of time would be expressed as lack of color, chalky surface or loss of glossiness. Other than aesthetic damages, deterioration of fossil remains also affects the preservation of the mineral phase that constitutes the shell. Indeed, in fossil records of biogenic calcium carbonate biominerals a partial or complete recrystallization might occur over time. This process might lead to recrystallization of aragonite into a more stable polymorph, such as calcite, or different minerals, such as calcium phosphate (Lynton S. Land, 1967).

Overall, a sustained variation in the mineral composition could deeply alter the original organization of the biomineral phase and in the end be responsible for spurious trends. In this study, if external and internal taphonomic degradations had occurred, older shells would have a chalky surface and would show a reduction in micro-density of shells, since calcite has a lower density than aragonite (2.71 $mg \cdot mm^{-3}$ vs 2.94 $mg \cdot mm^{-3}$ (Marszalek, 1982a)). On the contrary, our data report higher micro-density values in shells from the most ancient fossil horizons than in modern ones. Moreover, the application of both HR-XRPD and FTIR detected no other mineral phase than aragonite (Fig 3), the original mineralogy of *C. gallina* shell. Thus, we can assume no recrystallization process occurred in the geological time period examined.

The analyses of the HR-XRPD data allowed also to quantify the strain with the crystals due to the presence of the intra-crystalline OM. The obtained data on the lattice distortions and micro-structural parameters (microstrain fluctuations and crystallite size) were in line with those reported in the literature for the biogenic aragonite from other organisms (Pokroy et al., 2006a, 2007). The lattice strain was lower in the fossil samples (CO1) compared to the modern ones (MCE) (Fig 4), indicating a partial degradation of the organic matrix in the fossil samples. The values of the crystallite size after the thermal treatment, which is known to lead to the removal of the OM (Pokroy et al., 2006a, 2007), were lower than those of the non-treated samples and were quite similar for the both MCE and CO1 samples. The latter further confirms the presence of OM and supports its role in determining the lattice strain (Fig 4). Thus, we can safely state that in the sample CO1 the OM were still present, excluding a relevant re-crystallization of aragonite crystallite that should imply a loss of the strain, even if partially degraded. Moreover, we could speculate that degradation processes occurred mainly in the inter-crystallite fraction of the organic matrix rather than in the intra-crystallite one.

The fact that no recrystallization process occurred in the fossil shells was also confirmed by the values of the measured metal content that were constant among all samples, excluding important environmental fluid diffusion into the biomineral. This result was in agreement with previous studies reporting that in marine shallow settings certain parameters, such as high sedimentation rates, could rapidly sequester skeletal remains from the TAZ, increasing their preservation (Scarponi et al., 2017). In conclusion, for the sake of our study, these evidences allowed to rule out the possible influence of the taphonomic alteration of the mineral phase on the observed trends of the skeletal parameters.

C. gallina skeletal parameters differed between mature and immature clams (S1 Fig) in their biomineralization patterns. Higher apparent porosity was observed both in fossil and modern horizons for shells of small size, decreasing from more than 20 to less than 15% approaching the length at sexual maturity (about 18 mm (Romanelli et al., 2009)). High porosity influenced bulk density, which was conversely lower in small size shells. Micro-density followed the same pattern as bulk-density. This trend agreed with previous study carried out in living populations of *C. gallina* from the Adriatic Sea (Mancuso et al., 2019b). Hence, suggesting that Middle Holocene specimens of *C. gallina* in different climate-environmental contexts (Figs 4 and S1) exerted a similar physiologic control on biomineralization of calcium carbonate during their lifespan. In agreement with Mancuso et al. [24], adult specimens of *C. gallina* seemed to change their biomineralization behavior, showing small variations in apparent porosity and bulk density. This suggested that *C. gallina* promoted an accelerated shell accretion, in order to quickly reach the size required for sexual maturity, at the expense of possessing a less dense, more porous and mechanically weaker shell. Bulk and micro-density increased with increasing SST, for both mature and immature shells. Apparent porosity showed no correlation with SST in mature shells and a significant negative correlation in immature shells (Fig 2). The significant correlation in shell density with SST can be attributed to different mineralization rates driven by temperature and related aragonite saturation state. Warmer water masses reduce the thermodynamic work required to organisms to deposit calcium carbonate (Hall-Spencer & Harvey, 2019a; Siedlecki et al., 2017a), making the calcification less expensive in terms of metabolic cost (Clarke, 1993a). This enables an increase in calcification rates (Ries et al., 2009a). Comparable patterns have been detected also in brachiopods, where some species living in cold water showed a reduced calcium carbonate deposition and an increased organic matrix content compared to higher temperate settings, characterized by larger crystals and reduced organic matrix (hence denser shells (Cusack et al., 2012)).

Previous studies on *C. gallina* shells were conducted along a latitudinal gradient in the Adriatic Sea, including the area considered in this study (Gizzi, Caccia, Simoncini, Mancuso, Reggi, Fermani, Brizi, Fantazzini, Stagioni, Falini, et al., 2016b; Mancuso et al., 2019b). Mature shells of *C. gallina* of commercial size over 25 mm long were thinner, more porous and less resistant to fractures in warmer and more irradiated populations (Gizzi, Caccia, Simoncini, Mancuso, Reggi, Fermani, Brizi, Fantazzini, Stagioni, Falini, et al., 2016b; Mancuso et al., 2019b). On the other hand immature shells, less than 18 mm long, showed the opposite trend to mature ones, resulting in more porous and less dense shells with lower SST (Mancuso et al., 2019b). According to these results, local environmental parameters seemed to have a different influence on the biomineralization rate of mature shells compared to immature ones, likely due to different growth and metabolic rates (Mancuso et al., 2019b; Steyermark, 2002a). This might suggest that while immature clams have an energy surplus to better withstand environmental stress, mature clams are more dependent on their reserves (Myrand et al., 2002b).

Studies on mollusks and other macroinvertebrates highlight that calcification increases with aragonite saturation state (Clarke, 1993a; Ries et al., 2009a). Trends here depicted conforms to those patterns of biomineralization in warmer settings. However, no aragonite saturation data were available along the considered temporal gradient to investigate relationships between shell calcification and seawater chemistry in the studied area.

Although all samples were collected in the same area, a strong geomorphological evolution took place during the Holocene in response to the glacio-eustatic sea-level variations (Amorosi, Barbieri, Bruno, Campo, Drexler, Hong, Rossi, et al., 2019). The highest values for micro-density and bulk density of *C. gallina* shells were recorded during the Holocene climate optimum (HCO, 9-5 ky BP), when SSTs in the study area were higher than today. The North Western Adriatic coastal area was characterized by estuary systems, bounded seaward by a series of sandbars that isolated coastal lagoons and limited riverine plumes into the Adriatic (Fig 5) (Amorosi, Barbieri, Bruno, Campo, Drexler, Hong, Rossi, et al., 2019). Mancuso et al. (Mancuso et al., 2019b) reported that *C. gallina* populations could be negatively impacted by riverine influence (*i.e*., reduction of net calcification and linear extension rates). The positive correlation between temperature and shell density of *C. gallina* specimens found in the current study could be facilitated, other than higher aragonite saturation state due to past warmer conditions, by a more stable shoreface depositional setting due to reduced influence of riverine plumes. Indeed, in estuarine system mixing between freshwater and marine water occurs in the back barrier settings and not in the shallow marine zone where *C. gallina* thrives. By contrast, during the last part of the HCO, the weight of eustasy on the coastal dynamics of the study area largely vanished (Vacchi et al., 2016), and the study area transitioned (between 7.0 to 2.0 ky BP) to a wave-dominated and, after 2.0 ky BP, to a river-dominated deltaic system (Amorosi, Barbieri, Bruno, Campo, Drexler, Hong, Rossi, et al., 2019). The last geomorphologic configurations led to progressively increasing influence of riverine processes on the control of coastal dynamics and the storage-release of sediments (Li et al., 2018). The enhanced freshwater discharge in the nearshore area, especially during the last 2.0 ky BP, resulted in a strong progradation and the upbuilding of the modern Po Delta (Amorosi, Barbieri, Bruno, Campo, Drexler, Hong, Rossi, et al., 2019; Correggiari et al., 2005a) in a climatic context characterized by an overall decreasing trend in SST. The upbuilding of the modern Po Delta likely helped the installation of a low temperature and salinity wedge in the coastal area around it

(Gibson, 2002) and southward, due to action of anti-clock wise long-shore currents. Indeed, during flood events the modern Po river plume can influence the sea facing area in a radius of ~60 km (Brando et al., 2015). Freshwater plumes can reduce the SST between 2 °C to 6 °C, with a sensible effect down to 10 m of depth (Frascari et al., 2006). The drop in SST could have reduced the aragonite saturation state in the seawater, increasing the metabolic cost for calcification of *C. gallina*. Moreover, although *C. gallina* is euryhaline, the installation of suboptimal salinity level due to the riverine inflows, could lead to a reduced feeding activity and slower net calcification rates (Gizzi, Caccia, Simoncini, Mancuso, Reggi, Fermani, Brizi, Fantazzini, Stagioni, Falini, et al., 2016b; Heilmayer et al., 2004; Mancuso et al., 2019b; Sokolova & Pörtner, 2001). Additionally, the recorded decline of shell density could also be associated to the increasing water turbidity and oligotrophic conditions as the Po Delta advanced into the Adriatic Sea. Before ~5.0 ky BP (end of the HCO), the estuary-lagoon acted as a material sink, accommodating most of the sediments and nutrients debouched by the Po River (Amorosi, Barbieri, Bruno, Campo, Drexler, Hong, Rossi, et al., 2019; Kjerfve & Magill, 1989). This settings likely reduced the water turbidity, with positive repercussions on feeding activity (Ellis et al., 2002), providing *C. gallina* with spare metabolic energy to sustain higher net calcification and linear extension rates (Marsden, 2004). By contrast, during the onset of a wave dominated and then a fluvial dominated deltaic system the sediment and nutrients runoff directly into the shallow Adriatic Sea progressively increased (Amorosi, Barbieri, Bruno, Campo, Drexler, Hong, Rossi, et al., 2019). The resuspension of fine bottom sediments, could have increased the turbidity with serious consequences on the feeding activities of bivalves by reducing the rate of water pumped, increasing the period of valve closure (Loosanoff, 1962; Mancuso et al., 2019b) and damaging bivalves gills (Ellis et al., 2002), overall cutting the energy available for the skeletal construction.

The discrepancy between this and previous works in the shell density for mature clams (positive correlation with SST found in this study, VS negative correlation with SST found in Gizzi et al. (Gizzi, Caccia, Simoncini, Mancuso, Reggi, Fermani, Brizi, Fantazzini, Stagioni, Falini, et al., 2016b) and Mancuso et al. (Mancuso et al., 2019b), S4 Fig) suggested that this parameter is not only dependent on physical environmental factors (SST, salinity, aragonite saturation, sediments and nutrient supply), but is affected by a complex interplay between physical, biological and physiological factors, making clams response less predictable to changing environmental parameters. Moreover, since 2.0 ky BP, the anthropogenic influence on the Po Delta evolution constantly grew till to become dominant around the 17th century when river diversion and channels stabilization led to the growth of the modern Delta. These human interventions dictated an increase in sediments runoff, eutrophication events and anoxic events, overall participating in increasing the instability and stress of the nearshore environments, whose effects on *C. gallina* skeletal construction cannot be excluded. On a millennial time scale, temperature can be considered as a complex gradient that not only affects skeletal biomineralization directly by exerting a physiological response but also indirectly, by influencing the geomorphologic configuration and environmental parameters of *C. gallina* biotope.

Conclusion

Chamelea gallina shells appeared to be sensitive to changes in seawater temperature. At the macroscale level, specimens from past fossil horizons, living in warmer water, presented a denser, less porous shells than modern specimens. The significant correlation between temperature and skeletal density remained consistent even when dividing the total dataset into two minor subgroups and analysing sexually mature and immature individuals, separately.

At the microscale level, the shells were all composed of pure aragonite, presenting a perfectly preserved mineral phase with no relevant diagenetic alteration and only a slight degradation of the inter-crystalline organic phase. Hence, the observed difference in micro-density is not ascribable to any of the parameters here measured. Other factors not investigated in this study, such as occluded porosity and intra-crystalline water content, may be at the origin of the observed differences.

This study along temporal gradient represented a complementary approach to previous studies conducted along a latitudinal gradient in the Adriatic Sea and together improved our understanding of the response of this economically relevant species to a changing environment in face to seawater warming.

Acknowledgments

The research leading to these results has been conceived under the International PhD Program “Innovative Technologies and Sustainable Use of Mediterranean Sea Fishery and Biological Resources” (www.FishMed-PhD.org). This study represents partial fulfilment of the requirements for the Ph.D. thesis of Alessandro Cheli at the FishMed PhD Program (University of Bologna, Italy).

The authors acknowledge discussions with M. Kowalewski (University of Florida) and R. Nawrot (University of Vienna).

References

Addadi, L., Raz, S., & Weiner, S. (2003). Taking advantage of disorder: Amorphous calcium carbonate and its roles in biomineralization. *Advanced Materials*, *15*(12), 959–970. https://doi.org/10.1002/ADMA.200300381

Addadi, L., & Weiner, S. (2014). Biomineralization: mineral formation by organisms. *Physica Scripta*, *89*(9), 098003. https://doi.org/10.1088/0031-8949/89/9/098003

Aizenberg, J., Tkachenko, A., Weiner, S., Addadi, L., & Hendler, G. (2001). Calcitic microlenses as part of the photoreceptor system in brittlestars. *Nature 2001 412:6849*, *412*(6849), 819–822. https://doi.org/10.1038/35090573

Amorosi, A., Barbieri, G., Bruno, L., Campo, B., Drexler, T., Hong, W., & Fielding, C. (2019). Three-fold nature of coastal progradation during the Holocene eustatic highstand, Po Plain, Italy–close correspondence of stratal character with distribution patterns. *Sedimentology*, *66*.

Amorosi, A., Barbieri, G., Bruno, L., Campo, B., Drexler, T. M., Hong, W., Rossi, V., Sammartino, I., Scarponi, D., Vaiani, S. C., & Bohacs, K. M. (2019). Three-fold nature of coastal progradation during the Holocene eustatic highstand, Po Plain, Italy – close correspondence of stratal character with distribution patterns. *Sedimentology*, *66*(7), 3029–3052. https://doi.org/10.1111/sed.12621

Amorosi, A., Bruno, L., Campo, B., Morelli, A., Rossi, V., Scarponi, D., Hong, W., Bohacs, K. M., & Drexler, T. M. (2017). Global sea-level control on local parasequence architecture from the Holocene record of the Po Plain, Italy. *Marine and Petroleum Geology*, *87*, 99–111. https://doi.org/10.1016/j.marpetgeo.2017.01.020

Amorosi, A., Colalongo, M., Fusco, F., Pasini, G., & Fiorini, F. (1999a). Glacio-eustatic control of continental-shallow marine cyclicity from late quaternary deposits of the southeastern Po Plain, northern Italy. *Quat Res*, *52*.

Amorosi, A., Colalongo, M. L., Fiorini, F., Fusco, F., Pasini, G., Vaiani, S. C., & Sarti, G. (2004). Palaeogeographic and palaeoclimatic evolution of the Po Plain from 150-ky core records. *Global and Planetary Change*, *40*(1–2), 55–78. https://doi.org/10.1016/S0921-8181(03)00098-5

Amorosi, A., Colalongo, M. L., Fusco, F., Pasini, G., & Fiorini, F. (1999b). Glacio-eustatic control of continental-shallow marine cyclicity from late quaternary deposits of the southeastern Po Plain, northern Italy. *Quaternary Research*, *52*(1), 1–13. https://doi.org/10.1006/qres.1999.2049

Anagnostou, E., Sherrell, R. M., Gagnon, A., LaVigne, M., Field, M. P., & McDonough, W. F. (2011). Seawater nutrient and carbonate ion concentrations recorded as P/Ca, Ba/Ca, and U/Ca in the deep-sea coral Desmophyllum dianthus. *Geochimica et Cosmochimica Acta*, *75*(9), 2529–2543.

Andrisoa, A., Lartaud, F., Rodellas, V., Neveu, I., & Stieglitz, T. C. (2019). Enhanced Growth Rates of the Mediterranean Mussel in a Coastal Lagoon Driven by Groundwater Inflow . In *Frontiers in Marine Science* (Vol. 6).

Azzarone, M., Pellegrini, C., Barbieri, G., Rossi, V., Gamberi, F., Trincardi, F., Scarponi, D., Barbieri, G., & Rossi, V. (2020). Linking benthic fauna and seismic facies to improve stratigraphic reconstructions: the case of the Mid-Adriatic Deep since the late glacial period (Central Adriatic Sea). *Bollettino Della Società Paleontologica Italiana*, *59*(1), 9–23. https://doi.org/10.4435/BSPI.2020.03

Bajt, O., Ramšak, A., Milun, V., Andral, B., Romanelli, G., Scarpato, A., Mitrić, M., Kupusović, T., Kljajić, Z., Angelidis, M., Çullaj, A., & Galgani, F. (2019a). Assessing chemical contamination in the coastal waters of the Adriatic Sea using active mussel biomonitoring with Mytilus galloprovincialis. *Marine Pollution Bulletin*, *141*, 283–298. https://doi.org/10.1016/J.MARPOLBUL.2019.02.007

Bajt, O., Ramšak, A., Milun, V., Andral, B., Romanelli, G., Scarpato, A., Mitrić, M., Kupusović, T., Kljajić, Z., Angelidis, M., Çullaj, A., & Galgani, F. (2019b). Assessing chemical contamination in the coastal waters of the Adriatic Sea using active mussel biomonitoring with Mytilus galloprovincialis. *Marine Pollution Bulletin*, *141*, 283–298. https://doi.org/10.1016/J.MARPOLBUL.2019.02.007

Barnes, D. K. A., & Peck, L. S. (2008). Vulnerability of Antarctic shelf biodiversity to predicted regional warming. *Climate Research*, *37*(2–3), 149–163. https://doi.org/10.3354/CR00760

Beer, N. A., Wing, S. R., & Hu, Y. (2011). Physical versus biological control of element incorporation into biogenic carbonate: an in situ experiment in a New Zealand fjord. *Marine Ecology Progress Series*, *433*, 289–301.

Bemis, B. E., Spero, H. J., Bijma, J., & Lea, D. W. (1998). Reevaluation of the oxygen isotopic composition of planktonic foraminifera: Experimental results and revised paleotemperature equations. *Paleoceanography*, *13*(2), 150–160. https://doi.org/10.1029/98PA00070

Beniash, E., Addadi, L., & Weiner, S. (1999). Cellular control over spicule formation in sea urchin embryos: A structural approach. *Journal of Structural Biology*, *125*(1), 50–62. https://doi.org/10.1006/JSBI.1998.4081

Bergström, P., & Lindegarth, M. (2016a). Environmental influence on mussel (Mytilus edulis) growth – A quantile regression approach. *Estuar. Coast. Shelf Sci.*, *171*, 123–132. https://doi.org/10.1016/j.ecss.2016.01.040

Bergström, P., & Lindegarth, M. (2016b). Environmental influence on mussel (Mytilus edulis) growth - A quantile regression approach. *Estuarine, Coastal and Shelf Science*, *171*, 123–132. https://doi.org/10.1016/J.ECSS.2016.01.040

Bertness, M. D., & Grosholz, E. (1985). Population dynamics of the ribbed mussel, Geukensia demissa: the costs and benefits of an aggregated distribution. *Oecologia*, *67*(2), 192–204.

Beyer, J., Green, N. W., Brooks, S., Allan, I. J., Ruus, A., Gomes, T., Bråte, I. L. N., & Schøyen, M. (2017). Blue mussels (Mytilus edulis spp.) as sentinel organisms in coastal pollution monitoring: A review. *Marine Environmental Research*, *130*, 338–365. https://doi.org/https://doi.org/10.1016/j.marenvres.2017.07.024

Brando, V. E., Braga, F., Zaggia, L., Giardino, C., Brando, V. E., Braga, F., Zaggia, L., Giardino, C., Bresciani, M., Matta, E., Bellafiore, D., Ferrarin, C., Maicu, F., Benetazzo, A., Bonaldo, D., Falcieri, F. M., Coluccelli, A., Russo, A., & Carniel, S. (2015). High-resolution satellite turbidity and sea surface temperature observations of river plume interactions during a significant flood event BLASCO-Blending Laboratory And Satellite techniques for detecting CyanObacteria View project HAZADR View project High-resolution satellite turbidity and sea surface temperature observations of river plume interactions during a significant flood event. *Ocean Sci*, *11*, 1–11. https://doi.org/10.5194/os-11-909-2015

Bråte, I. L. N., Hurley, R., Iversen, K., Beyer, J., Thomas, K. V., Steindal, C. C., Green, N. W., Olsen, M., & Lusher, A. (2018). Mytilus spp. as sentinels for monitoring microplastic pollution in Norwegian coastal waters: A qualitative and quantitative study. *Environmental Pollution*, *243*, 383–393. https://doi.org/10.1016/J.ENVPOL.2018.08.077

Bruckschen, P., Bruhn, F., Meijer, J., Stephan, A., & Veizer, J. (1995). Diagenetic alteration of calcitic fossil shells: Proton microprobe (PIXE) as a trace element tool. *Nuclear Inst. and Methods in Physics Research, B*, *104*(1–4), 427–431. https://doi.org/10.1016/0168-583X(95)00424-6

Bruno, L., Amorosi, A., Severi, P., & Costagli, B. (2017). Late Quaternary aggradation rates and stratigraphic architecture of the southern Po Plain, Italy. *Basin Research*, *29*(2), 234–248. https://doi.org/10.1111/bre.12174

Bruno, L., Campo, B., Di Martino, A., Hong, W., & Amorosi, A. (2019). Peat layer accumulation and post-burial deformation during the mid-late Holocene in the Po coastal plain (Northern Italy). *Basin Research*, *31*(3), 621–639. https://doi.org/10.1111/bre.12339

Busse, C., Homs, J. L., Gustafsson, D., Palmert, F., Sjödin, B., Moverare, J. J., Simonsson, K., & Leidermark, D. (2016). A finite element study of the effect of crystal orientation and misalignment on the crack driving force in a single-crystal superalloy. *Proceedings of the ASME Turbo Expo: Turbomachinery Technical Conference and Exposition*, 1–8. https://doi.org/10.1115/GT2016-56305

Carter, J. G., & Clark, G. R. (1985). Classification and Phylogenetic Significance of Molluscan Shell Microstructure. *Series in Geology*, *Notes for Short Course*, *13*, 50–71. https://doi.org/10.1017/S0271164800001093

Chateigner, D., Hedegaard, C., & Wenk, H. R. (2000). Mollusc shell microstructures and crystallographic textures. *Journal of Structural Geology*, *22*(11–12), 1723–1735. https://doi.org/10.1016/S0191-8141(00)00088-2

Chauvaud, L., Lorrain, A., Dunbar, R. B., Paulet, Y.-M., rard Thouzeau, G., ric Jean, F., Guarini, J.-M., Mucciarone, D., Lorrain, A., Dunbar, R. B., Paulet, Y., Thouzeau, G., Jean, F., Guarini, J., & Mucciarone, D. (2005). Shell of the Great Scallop Pecten maximus as a high-frequency archive of paleoenvironmental changes. *Geochemistry, Geophysics, Geosystems*, *6*(8). https://doi.org/10.1029/2004GC000890

Cheli, A., Mancuso, A., Azzarone, M., Fermani, S., Kaandorp, J., Marin, F., Montroni, D., Polishchuk, I., Prada, F., Stagioni, M., Valdré, G., Pokroy, B., Falini, G., Goffredo, S., & Scarponi, D. (2021a). Climate variation during the Holocene influenced the skeletal properties of Chamelea gallina shells in the North Adriatic Sea (Italy). *PLOS ONE*, *16*(3), e0247590. https://doi.org/10.1371/JOURNAL.PONE.0247590

Cheli, A., Mancuso, A., Azzarone, M., Fermani, S., Kaandorp, J., Marin, F., Montroni, D., Polishchuk, I., Prada, F., Stagioni, M., Valdré, G., Pokroy, B., Falini, G., Goffredo, S., &

Scarponi, D. (2021b). Climate variation during the Holocene influenced the skeletal properties of Chamelea gallina shells in the North Adriatic Sea (Italy). *PLOS ONE*, *16*(3), e0247590. https://doi.org/10.1371/JOURNAL.PONE.0247590

Clark, M. S. (2020). Molecular mechanisms of biomineralization in marine invertebrates. *Journal of Experimental Biology*, *223*(11). https://doi.org/10.1242/JEB.206961

Clarke, A. (1993a). Temperature and Extinction in the Sea: A Physiologist's View. *Paleobiology*, *19*(4), 499–518.

Clarke, A. (1993b). Temperature and extinction in the sea: a physiologist's view. *Paleobiology*, *19*, 499–518.

Coll, M., Piroddi, C., Steenbeek, J., Kaschner, K., Lasram, F. B. R., Aguzzi, J., Ballesteros, E., Bianchi, C. N., Corbera, J., Dailianis, T., Danovaro, R., Estrada, M., Froglia, C., Galil, B. S., Gasol, J. M., Gertwage, R., Gil, J., Guilhaumon, F., Kesner-Reyes, K., … Voultsiadou, E. (2010). The Biodiversity of the Mediterranean Sea: Estimates, Patterns, and Threats. *PLOS ONE*, *5*(8), e11842. https://doi.org/10.1371/JOURNAL.PONE.0011842

Conte, M. H., Sicre, M. A., Rühlemann, C., Weber, J. C., Schulte, S., Schulz-Bull, D., & Blanz, T. (2006). Global temperature calibration of the alkenone unsaturation index (U 37k) in surface waters and comparison with surface sediments. *Geochemistry, Geophysics, Geosystems*, *7*(2). https://doi.org/10.1029/2005GC001054

Cooley, S. R., & Doney, S. C. (2009). Anticipating ocean acidification's economic consequences for commercial fisheries. *Environmental Research Letters*, *4*(2). https://doi.org/10.1088/1748-9326/4/2/024007

Copernicus Marine Environment Monitoring Service. (n.d.). *Global Ocean OSTIA Sea Surface Temperature and Sea Ice Analysis — European Environment Agency*. https://www.eea.europa.eu/data-and-maps/data/external/global-ocean-ostia-sea-surface

Correggiari, A., Cattaneo, A., & Trincardi, F. (2005a). The modern Po Delta system: Lobe switching and asymmetric prodelta growth. *Marine Geology*, *222–223*(1–4), 49–74. https://doi.org/10.1016/j.margeo.2005.06.039

Correggiari, A., Cattaneo, A., & Trincardi, F. (2005b). The modern Po Delta system: Lobe switching and asymmetric prodelta growth. *Marine Geology*, *222–223*(1–4), 49–74. https://doi.org/10.1016/J.MARGEO.2005.06.039

Crane, R. L., & Denny, M. W. (2022). Bivalves maintain repair when faced with chronically repeated mechanical stress. *Journal of Experimental Biology*, *225*(10), jeb243813. https://doi.org/10.1242/jeb.243813

Currey, J. D., & Taylor, J. D. (1974). The mechanical behaviour of some molluscan hard tissues. *Journal of Zoology*, *173*(3), 395–406. https://doi.org/10.1111/j.1469-7998.1974.tb04122.x

Cusack, M., Huerta, A. P., & EIMF. (2012). Brachiopods recording seawater temperature-A matter of class or maturation? *Chemical Geology*, *334*, 139–143. https://doi.org/10.1016/j.chemgeo.2012.10.021

Dalgi, G., Okumuş, I., & Karaycel, S. (2010). The effect of fishing on growth of the clam Chamelea gallina (Bivalvia: Veneridae) from the Turkish Black Sea coast. *Journal of the*

Marine Biological Association of the United Kingdom, *90*(2), 261–265. https://doi.org/10.1017/S0025315409000939

Dauphin, Y. (2016). Biomineralization. *Encyclopedia of Inorganic and Bioinorganic Chemistry*, 1–15. https://doi.org/10.1002/9781119951438.EIBC0017.PUB2

Davis, B. A. S., Brewer, S., Stevenson, A. C., Guiot, J., Allen, J., Almqvist-Jacobson, H., Ammann, B., Andreev, A. A., Argant, J., Atanassova, J., Balwierz, Z., Barnosky, C. D., Bartley, D. D., De Beaulieu, J. L., Beckett, S. C., Behre, K. E., Bennett, K. D., Berglund, B. E. B., Beug, H. J., … Zernitskaya, V. P. (2003). The temperature of Europe during the Holocene reconstructed from pollen data. *Quaternary Science Reviews*, *22*(15–17), 1701–1716. https://doi.org/10.1016/S0277-3791(03)00173-2

Degobbis, D., Gilmartin, M., & Revelante, N. (1986). An annotated nitrogen budget calculation for the northern Adriatic Sea. *Marine Chemistry*, *20*(2), 159–177. https://doi.org/10.1016/0304-4203(86)90037-X

Deng, Z., & Li, L. (2021). Intrinsic Mechanical Properties of Individual Biogenic Mineral Units in Biomineralized Skeletons. *ACS Biomaterials Science and Engineering*. https://doi.org/10.1021/acsbiomaterials.0c01587

Denny, M. W., & Gaylord, B. (2010). Marine ecomechanics. *Annu Rev Mar Sci*, *2*, 89–114.

Dhami, N. K., Reddy, M. S., & Mukherjee, M. S. (2013). Biomineralization of calcium carbonates and their engineered applications: A review. *Frontiers in Microbiology*, *4*(OCT), 314. https://doi.org/10.3389/FMICB.2013.00314/BIBTEX

Dillon, E. M., Lafferty, K. D., McCauley, D. J., Bradley, D., Norris, R. D., Caselle, J. E., DiRenzo, G. v., Gardner, J. P. A., & O'Dea, A. (2020). Dermal denticle assemblages in coral reef sediments correlate with conventional shark surveys. *Methods in Ecology and Evolution*, *11*(3), 362–375. https://doi.org/10.1111/2041-210X.13346

DP Häder, H. K. R. S. R. W. (2007). Effects of solar UV radiation on aquatic ecosystems and interactions with climate change. *Photochem. Photobiol. Sci.*, *6*, 267–285.

Dunca, E., Schöne, B. R., & Mutvei, H. (2005). Mutvei's solution: An ideal agent for resolving microgrowth structures of biogenic carbonates. *Palaeogeogr. Palaeoclimatol. Palaeoecol.*, *228*(1–2), 149–166. https://doi.org/10.1016/j.palaeo.2005.03.050

E Arneri, G. G. R. P. B. A. (1995). Age and growth of Chamelea gallina (Bivalvia: Veneridae) in the Central Adriatic Sea obtained by thin sections. *Rapp. Comm. Int. Mer Médit*, *34*, 17.

Ellis, J., Cummings, V., Hewitt, J., Thrush, S., & Norkko, A. (2002). Determining effects of suspended sediment on condition of a suspension feeding bivalve (*Atrina zelandica*): Results of a survey, a laboratory experiment and a field transplant experiment. *Journal of Experimental Marine Biology and Ecology*, *267*(2), 147–174. https://doi.org/10.1016/S0022-0981(01)00355-0

Epstein, S., & Lowenstam, H. A. (1953). Temperature-Shell-Growth Relations of Recent and Interglacial Pleistocene Shoal-Water Biota from Bermuda. *The Journal of Geology*, *61*(5), 424–438. https://doi.org/10.1086/626110

Eyster, L. S., & Morse, M. P. (1984). Early shell formation during molluscan embryogenesis, with new studies on the surf clam, Spisula solidissima. *Integrative and Comparative Biology*, *24*(4), 871–882. https://doi.org/10.1093/icb/24.4.871

Falini, G., Albeck, S., Weiner, S., & Addadi, L. (1996). Control of aragonite or calcite polymorphism by mollusk shell macromolecules. *Science*, *271*(5245), 67–69. https://doi.org/10.1126/SCIENCE.271.5245.67

Falini, G., Fermani, S., & Goffredo, S. (2015). Coral biomineralization: A focus on intra-skeletal organic matrix and calcification. In *Seminars in Cell and Developmental Biology* (Vol. 46, pp. 17–26). Academic Press. https://doi.org/10.1016/j.semcdb.2015.09.005

FAO. (2020). The State of World Fisheries and Aquaculture. *Sustainability in Action*. https://doi.org/10.4060/ca9229en

Fermani, S., Džakula, B. N., Reggi, M., Falini, G., & Kralj, D. (2017). Effects of magnesium and temperature control on aragonite crystal aggregation and morphology. *CrystEngComm*, *19*(18), 2451–2455.

Fitzer, S. C., Cusack, M., Phoenix, V. R., & Kamenos, N. A. (2014). Ocean acidification reduces the crystallographic control in juvenile mussel shells. *Journal of Structural Biology*, *188*(1), 39–45. https://doi.org/10.1016/J.JSB.2014.08.007

Fitzer, S. C., Vittert, L., Bowman, A., Kamenos, N. A., Phoenix, V. R., & Cusack, M. (2015). Ocean acidification and temperature increase impact mussel shell shape and thickness: Problematic for protection? *Ecology and Evolution*, *5*(21), 4875–4884. https://doi.org/10.1002/ECE3.1756

Flessa, K. W., Cutler, A. H., & Meldahl, K. H. (1993). Time and Taphonomy: Quantitative Estimates of Time-Averaging and Stratigraphic Disorder in a Shallow Marine Habitat. In *Paleobiology* (Vol. 19, Issue 2).

Fox, D. L., & Coe, W. R. (1943). Biology of the California sea-mussel (Mytilus californianus). II. Nutrition, metabolism, growth and calcium deposition. *Journal of Experimental Zoology*, *93*(2), 205–249. https://doi.org/10.1002/JEZ.1400930204

Frank Kenneth McKinney. (2007). *The Northern Adriatic Ecosystem: Deep Time in a Shallow Sea* . Columbia University Press.

Frascari, F., Spagnoli, F., Marcaccio, M., & Giordano, P. (2006). Anomalous Po River flood event effects on sediments and the water column of the northwestern Adriatic Sea. *Climate Research*, *31*(2–3), 151–165. https://doi.org/10.3354/cr031151

Furuhashi, T., Schwarzinger, C., Miksik, I., Smrz, M., & Beran, A. (2009). Molluscan shell evolution with review of shell calcification hypothesis. *Comparative Biochemistry and Physiology Part B: Biochemistry and Molecular Biology*, *154*(3), 351–371. https://doi.org/10.1016/J.CBPB.2009.07.011

Gaspar, M. B., Pereira, A. M., Vasconcelos, P., & Monteiro, C. C. (2004). Age and growth of Chamelea gallina from the Algarve coast (southern Portugal): Influence of seawater temperature and gametogenic cycle on growth rate. *Journal of Molluscan Studies*, *70*(4), 371–377. https://doi.org/10.1093/MOLLUS/70.4.371

Gazeau, F., Parker, L. M., Comeau, S., Gattuso, J. P., O'Connor, W. A., Martin, S., Pörtner, H. O., & Ross, P. M. (2013). Impacts of ocean acidification on marine shelled molluscs. *Marine Biology*, *160*(8), 2207–2245. https://doi.org/10.1007/S00227-013-2219-3

Gibson, R. N. , M. B. and R. J. A. Atkinson. (2002). Impact of changes in flow of freshwater on estuarine and open coastal habitats and the associated organisms. *Oceanography and Marine Biology: An Annual Review 40*, 233–309. https://doi.org/10.1201/9780203180594.ch5

Gilbert, S. F. (2001). Ecological developmental biology: Developmental biology meets the real world. *Developmental Biology*, *233*(1), 1–12. https://doi.org/10.1006/dbio.2001.0210

Gizzi, F., Caccia, M. G., Simoncini, G. A., Mancuso, A., Reggi, M., Fermani, S., Brizi, L., Fantazzini, P., Stagioni, M., & Falini, G. (2016). Shell properties of commercial clam Chamelea gallina are influenced by temperature and solar radiation along a wide latitudinal gradient. *Scientific Reports*, *6*(1), 1–12.

Gizzi, F., Caccia, M. G., Simoncini, G. A., Mancuso, A., Reggi, M., Fermani, S., Brizi, L., Fantazzini, P., Stagioni, M., Falini, G., Piccinetti, C., & Goffredo, S. (2016a). Shell properties of commercial clam Chamelea gallina are influenced by temperature and solar radiation along a wide latitudinal gradient. *Scientific Reports 2016 6:1*, *6*(1), 1–12. https://doi.org/10.1038/srep36420

Gizzi, F., Caccia, M. G., Simoncini, G. A., Mancuso, A., Reggi, M., Fermani, S., Brizi, L., Fantazzini, P., Stagioni, M., Falini, G., Piccinetti, C., & Goffredo, S. (2016b). Shell properties of commercial clam *Chamelea gallina* are influenced by temperature and solar radiation along a wide latitudinal gradient. *Scientific Reports*, *6*(1), 36420. https://doi.org/10.1038/srep36420

Gizzi, F., Caccia, M. G., Simoncini, G. A., Mancuso, A., Reggi, M., Fermani, S., Brizi, L., Fantazzini, P., Stagioni, M., Falini, G., Piccinetti, C., & Goffredo, S. (2016c). Shell properties of commercial clam Chamelea gallina are influenced by temperature and solar radiation along a wide latitudinal gradient. *Scientific Reports*, *6*. https://doi.org/10.1038/SREP36420

Goldberg, E. (1975). The mussel watch-a first step in global marine monitoring. *Mar. Pollut. Bull.*, *6*(7), 111.

Gosling, E. (2015). *Marine bivalve molluscs*. John Wiley & Sons.

Grazioli, E., Guerranti, C., Pastorino, P., Esposito, G., Bianco, E., Simonetti, E., Rainis, S., Renzi, M., & Terlizzi, A. (2022). Review of the Scientific Literature on Biology, Ecology, and Aspects Related to the Fishing Sector of the Striped Venus (Chamelea gallina) in Northern Adriatic Sea. *Journal of Marine Science and Engineering*, *10*(9), 1328. https://doi.org/10.3390/JMSE10091328/S1

Grienke, U., Silke, J., & Tasdemir, D. (2014). Bioactive compounds from marine mussels and their effects on human health. *Food Chemistry*, *142*, 48–60. https://doi.org/10.1016/J.FOODCHEM.2013.07.027

Hahn, S., Rodolfo-Metalpa, R., Griesshaber, E., Schmahl, W. W., Buhl, D., Hall-Spencer, J. M., Baggini, C., Fehr, K. T., & Immenhauser, A. (2012). Marine bivalve shell geochemistry and ultrastructure from modern low pH environments: Environmental effect versus experimental bias. *Biogeosciences, 9*(5), 1897–1914. https://doi.org/10.5194/BG-9-1897-2012

Hall-Spencer, J. M., & Harvey, B. P. (2019a). Ocean acidification impacts on coastal ecosystem services due to habitat degradation. *Emerging Topics in Life Sciences, 3*(2), 197–206. https://doi.org/10.1042/etls20180117

Hall-Spencer, J. M., & Harvey, B. P. (2019b). Ocean acidification impacts on coastal ecosystem services due to habitat degradation. *Emerging Topics in Life Sciences, 3*(2), 197–206. https://doi.org/10.1042/ETLS20180117

Harley, C. D. G. (2011). Climate change, keystone predation, and biodiversity loss. *Science, 334*(6059), 1124–1127. https://doi.org/10.1126/SCIENCE.1210199

Heilmayer, O., Brey, T., & Portner, H. O. (2004). Growth efficiency and temperature in scallops: a comparative analysis of species adapted to different temperatures. *Functional Ecology, 18*(5), 641–647. https://doi.org/10.1111/j.0269-8463.2004.00905.x

Hofmann, G. E., Barry, J. P., Edmunds, P. J., Gates, R. D., Hutchins, D. A., Klinger, T., & Sewell, M. A. (2010). The effect of Ocean acidification on calcifying organisms in marine ecosystems: An organism-to-ecosystem perspective. *Annual Review of Ecology, Evolution, and Systematics, 41*, 127–147. https://doi.org/10.1146/ANNUREV.ECOLSYS.110308.120227

Hofmann, G. E., Smith, J. E., Johnson, K. S., Send, U., Levin, L. A., Micheli, F., Paytan, A., Price, N. N., Peterson, B., Takeshita, Y., Matson, P. G., de Crook, E., Kroeker, K. J., Gambi, M. C., Rivest, E. B., Frieder, C. A., Yu, P. C., & Martz, T. R. (2011). High-frequency dynamics of ocean pH: A multi-ecosystem comparison. *PLoS ONE, 6*(12). https://doi.org/10.1371/JOURNAL.PONE.0028983

Huang, W., Restrepo, D., Jung, J. Y., Su, F. Y., Liu, Z., Ritchie, R. O., McKittrick, J., Zavattieri, P., & Kisailus, D. (2019). Multiscale Toughening Mechanisms in Biological Materials and Bioinspired Designs. *Advanced Materials, 31*, 1901561. https://doi.org/10.1002/adma.201901561

Jalali, B., Sicre, M.-A., Bassetti, M.-A., & Kallel, N. (2016). Holocene climate variability in the North-Western Mediterranean Sea (Gulf of Lions). *Climate of the Past, 12*(1), 91–101. https://doi.org/10.5194/cp-12-91-2016

Jamieson, J. C. (2004). Phase Equilibrium in the System Calcite-Aragonite. *The Journal of Chemical Physics, 21*(8), 1385. https://doi.org/10.1063/1.1699228

Jansen, J. M., Pronker, A. E., Kube, S., Sokolowski, A., Sola, J. C., Marquiegui, M. A., Schiedek, D., Wendelaar Bonga, S., Wolowicz, M., & Hummel, H. (2007). Geographic and seasonal patterns and limits on the adaptive response to temperature of *European Mytilus* spp. and *Macoma balthica* populations. *Oecologia, 154*(1), 23–34. https://doi.org/10.1007/s00442-007-0808-x

Kidwell, S. M. (2015). Biology in the Anthropocene: Challenges and insights from young fossil records. *Proceedings of the National Academy of Sciences, 112*(16), 4922–4929. https://doi.org/10.1073/PNAS.1403660112

Kidwell, S. M., & Behrensmeyer, A. K. (1993). Taphonomic approaches to time resolution in fossil assemblages: Introduction. *Short Courses in Paleontology, 6,* 1–8. https://doi.org/10.1017/s2475263000001021

Kjerfve, B., & Magill, K. E. (1989). Geographic and hydrodynamic characteristics of shallow coastal lagoons. *Marine Geology, 88*(3–4), 187–199. https://doi.org/10.1016/0025-3227(89)90097-2

Klein, R. T., Lohmann, K. C., & Thayer, C. W. (1996). SrCa and 13C12C ratios in skeletal calcite of Mytilus trossulus: Covariation with metabolic rate, salinity, and carbon isotopic composition of seawater. *Geochimica et Cosmochimica Acta, 60*(21), 4207–4221. https://doi.org/10.1016/S0016-7037(96)00232-3

Knoll, A. H. (2003). Biomineralization and Evolutionary History. *Reviews in Mineralogy and Geochemistry, 54*(1), 329–356. https://doi.org/10.2113/0540329

Kong, Y., Jing, G., Yan, Z., Li, C., Gong, N., Zhu, F., Li, D., Zhang, Y., Zheng, G., Wang, H., Xie, L., & Zhang, R. (2009). Cloning and characterization of Prisilkin-39, a novel matrix protein serving a dual role in the prismatic layer formation from the oyster Pinctada fucata. *Journal of Biological Chemistry, 284*(16), 10841–10854. https://doi.org/10.1074/JBC.M808357200

Kowalewski, M., Wittmer, J. M., Dexter, T. A., Amorosi, A., & Scarponi, D. (2015). Differential responses of marine communities to natural and anthropogenic changes. *Proceedings of the Royal Society B: Biological Sciences*, *282*(1803), 20142990. https://doi.org/10.1098/rspb.2014.2990

Kroeker, K. J., Kordas, R. L., Crim, R. N., & Singh, G. G. (2010). Meta-analysis reveals negative yet variable effects of ocean acidification on marine organisms. *Ecology Letters*, *13*(11), 1419–1434. https://doi.org/10.1111/J.1461-0248.2010.01518.X

Kroeker, K. J., Kordas, R. L., & Harley, C. D. G. (2017). Embracing interactions in ocean acidification research: Confronting multiple stressor scenarios and context dependence. *Biology Letters*, *13*(3). https://doi.org/10.1098/RSBL.2016.0802

Kroeker, K. J., Sanford, E., Rose, J. M., Blanchette, C. A., Chan, F., Chavez, F. P., Gaylord, B., Helmuth, B., Hill, T. M., Hofmann, G. E., McManus, M. A., Menge, B. A., Nielsen, K. J., Raimondi, P. T., Russell, A. D., & Washburn, L. (2016a). Interacting environmental mosaics drive geographic variation in mussel performance and predation vulnerability. *Ecology Letters*, *19*(7), 771–779. https://doi.org/10.1111/ELE.12613

Kroeker, K. J., Sanford, E., Rose, J. M., Blanchette, C. A., Chan, F., Chavez, F. P., Gaylord, B., Helmuth, B., Hill, T. M., Hofmann, G. E., McManus, M. A., Menge, B. A., Nielsen, K. J., Raimondi, P. T., Russell, A. D., & Washburn, L. (2016b). Interacting environmental mosaics drive geographic variation in mussel performance and predation vulnerability. *Ecology Letters*, *19*(7), 771–779. https://doi.org/10.1111/ELE.12613

Lemasson, A., & Knights, M. (2021). Differential responses in anti-predation traits of the native oyster Ostrea edulis and invasive Magallana gigas to ocean acidification and warming. *Marine Ecology Progress Series, 665,* 87–102.

Leonard, G. H., Bertness, M. D., & Yund, P. O. (1999). Crab predation, waterborne cues, and inducible defenses in the blue mussel, Mytilus edulis. *Ecology, 80*(1), 1–14.

Li, H. X., Ma, L. S., Lin, L., Ni, Z. X., Xu, X. R., Shi, H. H., Yan, Y., Zheng, G. M., & Rittschof, D. (2018). Microplastics in oysters Saccostrea cucullata along the Pearl River Estuary, China. *Environmental Pollution*, *236*, 619–625. https://doi.org/10.1016/j.envpol.2018.01.083

Lippmann, F. (1973). *Sedimentary carbonate minerals*. Springer Verlag.

Loo, L. O., & Rosenberg, R. (1989). Bivalve suspension-feeding dynamics and benthic-pelagic coupling in an eutrophicated marine bay. *Journal of Experimental Marine Biology and Ecology*, *130*(3), 253–276. https://doi.org/10.1016/0022-0981(89)90167-6

Loosanoff, V. L. (1962). *Effects of turbidity on some larval and adult bivalves*.

Lorens, R. B., & Bender, M. L. (1980). The impact of solution chemistry on Mytilus edulis calcite and aragonite. *Geochimica et Cosmochimica Acta*, *44*(9), 1265–1278.

Lorrain, A., Paulet, Y.-M., Chauvaud, L., Dunbar, R., Mucciarone, D., & Fontugne, M. (2004). δ13C variation in scallop shells: increasing metabolic carbon contribution with body size? *Geochimica et Cosmochimica Acta*, *68*(17), 3509–3519.

Lowenstam, H. A. (1954). Factors affecting the aragonite: calcite ratios in carbonate-secreting marine organisms. *The Journal of Geology*, *62*(3), 284–322.

Lowenstam, H. A. (1981). Minerals Formed by Organisms. *Science*, *211*(4487), 1126–1131. https://doi.org/10.1126/SCIENCE.7008198

Lowenstam, H. A., & Weiner, S. (1989a). *On biomineralization*. Oxford University Press on Demand.

Lowenstam, H. A., & Weiner, S. (1989b). *On Biomineralization* (Oxford University Press on Demand, Ed.). https://books.google.it/books?hl=it&lr=&id=16znCwAAQBAJ&oi=fnd&pg=PR7&dq=Lowenstam,+H.+A.%3B+Weiner,+S.,+On+Biomineralization.+New+York,+1989.+&ots=7xDD6oWe1E&sig=L8GoWmGPA1zzMypvdlcDo8sJI4I&redir_esc=y#v=onepage&q=Lowenstam%2C%20H.%20A.%3B%20Weiner%2C%20S.%2C%20On%20Biomineralization.%20New%20York%2C%201989.&f=false

Lowenstam Heinz Adolf, & Weiner Stephen. (1989). On Biomineralization. In *On Biomineralization*. Oxford University Press.

Lutz, R. A., & Rhoads, D. C. (1980). *Growth patterns within the molluscan shell: an overview*. 750.

Lynton S. Land. (1967). Diagenesis of Skeletal Carbonates. *SEPM Journal of Sedimentary Research*, *Vol. 37*(3), 914–930. https://doi.org/10.1306/74d717d5-2b21-11d7-8648000102c1865d

M Ramón, C. R. (1992). Age determination and shell growth of Chamelea gallina (Bivalvia: Veneridae) in the western Mediterranean. *Mar. Ecol. Prog. Ser.*, *89*, 15–23.

Mackenzie, C. L., Ormondroyd, G. A., Curling, S. F., Ball, R. J., Whiteley, N. M., & Malham, S. K. (2014a). Ocean Warming, More than Acidification, Reduces Shell Strength in a Commercial Shellfish Species during Food Limitation. *PLOS ONE*, *9*(1), e86764. https://doi.org/10.1371/JOURNAL.PONE.0086764

Mackenzie, C. L., Ormondroyd, G. A., Curling, S. F., Ball, R. J., Whiteley, N. M., & Malham, S. K. (2014b). Ocean Warming, More than Acidification, Reduces Shell Strength in a Commercial Shellfish Species during Food Limitation. *PLOS ONE*, *9*(1), e86764.

Magnabosco, G., Giuri, D., Di Bisceglie, A. P., Scarpino, F., Fermani, S., Tomasini, C., & Falini, G. (2021). New material perspective for waste seashells by covalent functionalization. *ACS Sustainable Chemistry and Engineering*, *9*(18), 6203–6208. https://doi.org/10.1021/acssuschemeng.1c01306

Mancuso, A., Stagioni, M., Prada, F., Scarponi, D., Piccinetti, C., & Goffredo, S. (2019a). Environmental influence on calcification of the bivalve Chamelea gallina along a latitudinal gradient in the Adriatic Sea. *Scientific Reports*, *9*(1), 11198. https://doi.org/10.1038/S41598-019-47538-1

Mancuso, A., Stagioni, M., Prada, F., Scarponi, D., Piccinetti, C., & Goffredo, S. (2019b). Environmental influence on calcification of the bivalve *Chamelea gallina* along a latitudinal gradient in the Adriatic Sea. *Scientific Reports*, *9*(1), 11198. https://doi.org/10.1038/s41598-019-47538-1

Mancuso, A., Stagioni, M., Prada, F., Scarponi, D., Piccinetti, C., & Goffredo, S. (2019c). Environmental influence on calcification of the bivalve Chamelea gallina along a latitudinal gradient in the Adriatic Sea. *Scientific Reports*, *9*(1), 11198. https://doi.org/10.1038/s41598-019-47538-1

Mancuso, A., Stagioni, M., Prada, F., Scarponi, D., Piccinetti, C., & Goffredo, S. (2019d). Environmental influence on calcification of the bivalve Chamelea gallina along a latitudinal gradient in the Adriatic Sea. *Scientific Reports*, *9*(1), 11198. https://doi.org/10.1038/s41598-019-47538-1

Mann, S. (1993). Molecular tectonics in biomineralization and biomimetic materials chemistry. *Nature 1993 365:6446*, *365*(6446), 499–505. https://doi.org/10.1038/365499a0

Marchetti, R., Provini, A., & Crosa, G. (1989). Nutrient load carried by the River Po into the Adriatic Sea, 1968–1987. *Marine Pollution Bulletin*, *20*(4), 168–172. https://doi.org/10.1016/0025-326X(89)90487-6

Marin, F., le Roy, N., & Marie, B. (2012a). The formation and mineralization of mollusk shell. *Frontiers in Bioscience*, *4*, 1099.

Marin, F., le Roy, N., & Marie, B. (2012b). The formation and mineralization of mollusk shell. *Frontiers in Bioscience*, *4*, 1099.

Marsden, I. (2004). Effects of reduced salinity and seston availability on growth of the New Zealand little-neck clam *Austrovenus stutchburyi*. *Marine Ecology Progress Series*, *266*, 157–171. https://doi.org/10.3354/meps266157

Marszalek, D. S. (1982a). The role of heavy skeletons in vertical movements of non-motile zooplankton. *Marine Behaviour and Physiology*, *8*(4), 295–303. https://doi.org/10.1080/10236248209387026

Marszalek, D. S. (1982b). The role of heavy skeletons in vertical movements of non-motile zooplankton. *Marine & Freshwater Behaviour & Phy*, *8*(4), 295–303.

Martinez, M., Mangano, M. C., Maricchiolo, G., Genovese, L., Mazzola, A., & Sarà, G. (2018). Measuring the effects of temperature rise on Mediterranean shellfish aquaculture. *Ecological Indicators*, *88*, 71–78. https://doi.org/10.1016/j.ecolind.2018.01.002

Maselli, V., & Trincardi, F. (2013). Man made deltas. *Scientific Reports*, *3*(1), 1–7. https://doi.org/10.1038/srep01926

Monari, M., Serrazanetti, G. P., Foschi, J., Matozzo, V., Marin, M. G., & Cattani, O. (2007). Effects of salinity on the clam Chamelea gallina haemocytes. Part II: Superoxide dismutase response. *Marine Biology*, *151*(3), 1059–1068. https://doi.org/10.1007/S00227-006-0544-5/METRICS

Montroni, D. (2020). *Hierarchically organized chitin-based matrices*. University of Bologna.

Morello, E. B., Froglia, C., Atkinson, R. J. A., & Moore, P. G. (2005). Hydraulic dredge discards of the clam (Chamelea gallina) fishery in the western Adriatic Sea, Italy. *Fisheries Research*, *76*(3), 430–444. https://doi.org/10.1016/J.FISHRES.2005.07.002

Morse, J. W., Andersson, A. J., & Mackenzie, F. T. (2006). Initial responses of carbonate-rich shelf sediments to rising atmospheric pCO2 and “ocean acidification”: Role of high Mg-calcites. *Geochimica et Cosmochimica Acta*, *70*(23), 5814–5830. https://doi.org/10.1016/J.GCA.2006.08.017

Muñoz-Moya, E., García-Herrera, C. M., Lagos, N. A., Abarca-Ortega, A. F., Checa, A. G., & Harper, E. M. (2022). Evaluation of remodeling and geometry on the biomechanical properties of nacreous bivalve shells. *Scientific Reports*, *12*(1), 1–11.

Myrand, B., Tremblay, R., & Sévigny, J. M. (2002a). Selection against blue mussels (Mytilus edulis L.) homozygotes under various stressful conditions. *Journal of Heredity*, *93*(4), 238–248. https://doi.org/10.1093/jhered/93.4.238

Myrand, B., Tremblay, R., & Sévigny, J.-M. (2002b). Selection against blue mussels (*Mytilus edulis* L.) homozygotes under various stressful conditions. *The Journal of Heredity*. https://doi.org/DOI 10.1093/jhered/93.4.238

Nagarajan, R., Lea, S. E. G., & Goss-Custard, J. D. (2006). Seasonal variations in mussel, Mytilus edulis L. shell thickness and strength and their ecological implications. *Journal of Experimental Marine Biology and Ecology*, *339*(2), 241–250.

Nash, M. C., Opdyke, B. N., Troitzsch, U., Russell, B. D., Adey, W. H., Kato, A., Diaz-Pulido, G., Brent, C., Gardner, M., Prichard, J., & Kline, D. I. (2012). Dolomite-rich coralline algae in reefs resist dissolution in acidified conditions. *Nature Climate Change 2012 3:3*, *3*(3), 268–272. https://doi.org/10.1038/nclimate1760

Nawrot, R., Scarponi, D., Azzarone, M., Dexter, T. A., Kusnerik, K. M., Wittmer, J. M., Amorosi, A., & Kowalewski, M. (2018). Stratigraphic signatures of mass extinctions: ecological and sedimentary determinants. *Proceedings of the Royal Society B: Biological Sciences*, *285*(1886), 20181191. https://doi.org/10.1098/rspb.2018.1191

Niu, Y.-Q., Liu, J.-H., Aymonier, C., Fermani, S., Kralj, D., Falini, G., & Zhou, C.-H. (2022). Calcium carbonate: controlled synthesis, surface functionalization, and nanostructured materials. *Chemical Society Reviews*, *51*, 7883–7943.

Nudelman, F., Shimoni, E., Klein, E., Rousseau, M., Bourrat, X., Lopez, E., Addadi, L., & Weiner, S. (2008). Forming nacreous layer of the shells of the bivalves Atrina rigida and Pinctada margaritifera: An environmental- and cryo-scanning electron microscopy study. *Journal of Structural Biology*, *162*, 290–300. https://doi.org/10.1016/j.jsb.2008.01.008

Olson, I. C., Kozdon, R., Valley, J. W., & Gilbert, P. U. P. A. (2012). Mollusk shell nacre ultrastructure correlates with environmental temperature and pressure. *Journal of the American Chemical Society*, *134*(17), 7351–7358. https://doi.org/10.1021/ja210808s

Orban, E., di Lena, G., Nevigato, T., Casini, I., Caproni, R., Santaroni, G., & Giulini, G. (2007). Nutritional and commercial quality of the striped venus clam, Chamelea gallina, from the Adriatic sea. *Food Chemistry*, *101*(3), 1063–1070. https://doi.org/10.1016/J.FOODCHEM.2006.03.005

P Moura, M. G. C. M. (2009). Age determination and growth rate of a Callista chione population from the southwestern coast of Portugal. Aquat. *Biol.*, *5*, 97–106.

Palmer, A. R. (1981). Do carbonate skeletons limit the rate of body growth? *Nature*, *292*(5819), 150–152.

Palmer, A. R. (1983). Relative cost of producing skeletal organic matrix versus calcification: evidence from marine gastropods. *Marine Biology*, *75*(2), 287–292.

Parsons, K. E. (1997). Contrasting patterns of heritable geographic variation in shell morphology and growth potential in the marine gastropod Bembicium vittatum: evidence from field experiments. *Evolution*, *51*(3), 784–796.

Pauly, M., Kamenos, N. A., Donohue, P., & LeDrew, E. (2015). Coralline algal Mg-O bond strength as a marine pCO2 proxy. *Geology*, *43*(3), 267–270. https://doi.org/10.1130/G36386.1

Pavicic, J., Raspor, B., & Martincic, D. (1993). Quantitative determination of metallothionein-like proteins in mussels. Methodological approach and field evaluation. *Marine Biology*, *115*, 435–444. https://doi.org/10.1038/164914a0

Penney, R. W., Hart, M. J., & Templeman, N. D. (2007). Shell Strength and Appearance in Cultured Blue Mussels Mytilus edulis, M. trossulus, and M. edulis × M. trossulus Hybrids. *North American Journal of Aquaculture*, *69*(3), 281–295. https://doi.org/10.1577/A06-044.1

Pérez-Huerta, A., Coronado, I., & Hegna, T. A. (2018). Understanding biomineralization in the fossil record. In *Earth-Science Reviews* (Vol. 179, pp. 95–122). Elsevier B.V. https://doi.org/10.1016/j.earscirev.2018.02.015

Perry, R. S., Mcloughlin, N., Lynne, B. Y., Sephton, M. A., Oliver, J. D., Perry, C. C., Campbell, K., Engel, M. H., Farmer, J. D., Brasier, M. D., & Staley, J. T. (2007). Defining biominerals and organominerals: Direct and indirect indicators of life. *Sedimentary Geology*, *201*(1–2), 157–179. https://doi.org/10.1016/J.SEDGEO.2007.05.014

Pfister, C. A., Roy, K., Wootton, J. T., McCoy, S. J., Paine, R. T., Suchanek, T. H., & Sanford, E. (2016). Historical baselines and the future of shell calcification for a foundation species in a changing ocean. *Proceedings of the Royal Society B: Biological Sciences*, *283*(1832). https://doi.org/10.1098/RSPB.2016.0392

Pokroy, B., Fitch, A. N., Marin, F., Kapon, M., Adir, N., & Zolotoyabko, E. (2006a). Anisotropic lattice distortions in biogenic calcite induced by intra-crystalline organic molecules. *Journal of Structural Biology*, *155*(1), 96–103. https://doi.org/10.1016/j.jsb.2006.03.008

Pokroy, B., Fitch, A. N., Marin, F., Kapon, M., Adir, N., & Zolotoyabko, E. (2006b). Anisotropic lattice distortions in biogenic calcite induced by intra-crystalline organic molecules. *Journal of Structural Biology*, *155*(1), 96–103. https://doi.org/10.1016/J.JSB.2006.03.008

Pokroy, B., Fitch, A. N., & Zolotoyabko, E. (2007). Structure of biogenic aragonite (CaCO3). *Crystal Growth and Design*, *7*(9), 1580–1583. https://doi.org/10.1021/cg060842v

Poulain, P. M. (2001). Adriatic Sea surface circulation as derived from drifter data between 1990 and 1999. *Journal of Marine Systems*, *29*(1–4), 3–32. https://doi.org/10.1016/S0924-7963(01)00007-0

Proćków, M., Proćków, J., Błażej, P., & Mackiewicz, P. (2018). The influence of habitat preferences on shell morphology in ecophenotypes of Trochulus hispidus complex. *Science of The Total Environment*, *630*, 1036–1043. https://doi.org/https://doi.org/10.1016/j.scitotenv.2018.02.311

Purroy, A., Milano, S., Schöne, B. R., Thébault, J., & Peharda, M. (2018). Drivers of shell growth of the bivalve, Callista chione (L. 1758) – Combined environmental and biological factors. *Mar. Environ. Res.*, *134*, 138–149. https://doi.org/10.1016/j.marenvres.2018.01.011

Rahman, M. A., & Shinjo, R. (2011). *Biocalcification of Corals and their Response to Global Climate Change*.

Ramon, M., & Richardson, C. A. (1992). Age determination and shell growth of Chamelea gallina (Bivalvia: Veneridae) in the western Mediterranean. *Marine Ecology Progress Series*, *89*(1), 15–23. https://doi.org/10.3354/meps089015

Ramsey, C. B., & Lee, S. (2013). Recent and Planned Developments of the Program OxCal. *Radiocarbon*, *55*(2), 720–730. https://doi.org/10.1017/s0033822200057878

Rasband, W. S. (n.d.). *ImageJ, U. S. National Institutes of Health, Bethesda, Maryland, USA, https://imagej.nih.gov/ij/, 1997-2018.*

Reimer, P. J., Bard, E., Bayliss, A., Beck, J. W., Blackwell, P. G., Ramsey, C. B., Buck, C. E., Cheng, H., Edwards, R. L., Friedrich, M., Grootes, P. M., Guilderson, T. P., Haflidason, H., Hajdas, I., Hatté, C., Heaton, T. J., Hoffmann, D. L., Hogg, A. G., Hughen, K. A., … van der Plicht, J. (2013). IntCal13 and Marine13 Radiocarbon Age Calibration Curves 0–50,000 Years cal BP. *Radiocarbon*, *55*(4), 1869–1887. https://doi.org/10.2458/azu_js_rc.55.16947

Ren, D., Feng, Q., & Bourrat, X. (2011). Effects of additives and templates on calcium carbonate mineralization in vitro. *Micron*, *42*(3), 228–245. https://doi.org/10.1016/J.MICRON.2010.09.005

Ries, J. B., Cohen, A. L., & McCorkle, D. C. (2009a). Marine calcifiers exhibit mixed responses to CO2-induced ocean acidification. *Geology*, *37*(12), 1131–1134. https://doi.org/10.1130/G30210A.1

Ries, J. B., Cohen, A. L., & McCorkle, D. C. (2009b). Marine calcifiers exhibit mixed responses to CO2-induced ocean acidification. *Geology*, *37*(12), 1131–1134. https://doi.org/10.1130/G30210A.1

Romanelli, M., Cordisco, A. C., & Giovanardi, O. (2009). The long-term decline of the *Chamelea gallina* L. (Bivalvia: Veneridae) clam fishery in the Adriatic Sea: is a synthesis possible? *Acta Adriatica*, *50*(2), 171–205.

RStudio Team. (2020). *RStudio: Integrated Development for R. RStudio*. RStudio, PBC.

Russo, A., Rabitti, S., & Bastianini, M. (2002). Decadal Climatic Anomalies in the Northern Adriatic Sea Inferred from a New Oceanographic Data Set. *Mar. Ecol.*, *23*(SUPPL. 1), 340–351. https://doi.org/10.1111/j.1439-0485.2002.tb00032.x

Sanders, T., Schmittmann, L., Nascimento-Schulze, J. C., & Melzner, F. (2018). High calcification costs limit mussel growth at low salinity. *Frontiers in Marine Science*, *5*(OCT), 352. https://doi.org/10.3389/FMARS.2018.00352/BIBTEX

Sarà, G., Reid, G. K., Rinaldi, A., Palmeri, V., Troell, M., & Kooijman, S. (2012). Growth and reproductive simulation of candidate shellfish species at fish cages in the Southern Mediterranean: Dynamic Energy Budget (DEB) modelling for integrated multi-trophic aquaculture. *Aquaculture*, *324*, 259–266.

Scarponi, D., & Angeletti, L. (2008). Integration of palaeontological patterns in the sequence stratigraphy paradigm: a case study from Holocene deposits of the Po Plain (Italy). *GeoActa*, *7*, 1–13.

Scarponi, D., Azzarone, M., Kusnerik, K., Amorosi, A., Bohacs, K. M., Drexler, T. M., & Kowalewski, M. (2017). Systematic vertical and lateral changes in quality and time resolution of the macrofossil record: Insights from Holocene transgressive deposits, Po coastal plain, Italy. *Marine and Petroleum Geology*, *87*, 128–136. https://doi.org/10.1016/j.marpetgeo.2017.03.031

Scarponi, D., & Kowalewski, M. (2004a). Stratigraphic paleoecology: Bathymetric signatures and sequence overprint of mollusk associations from upper Quaternary sequences of the Po Plain, Italy. *Geology*, *32*(11), 989–992. https://doi.org/10.1130/G20808.1

Scarponi, D., & Kowalewski, M. (2004b). Stratigraphic paleoecology: Bathymetric signatures and sequence overprint of mollusk associations from upper Quaternary sequences of the Po Plain, Italy. *Geology*, *32*(11), 989–992. https://doi.org/10.1130/G20808.1

Scarponi, D., & Kowalewski, M. (2007). Sequence stratigraphic anatomy of diversity patterns: Late Quaternary benthic mollusks of the Po Plain, Italy. *PALAIOS*, *22*(3), 296–305. https://doi.org/10.2110/palo.2005.p05-020r

Schneider, C. A., Rasband, W. S., & Eliceiri, K. W. (2012). NIH Image to ImageJ: 25 years of image analysis. *Nature Methods*, *9*(7), 671–675. https://doi.org/10.1038/nmeth.2089

Schneidermann, N., & Harris, P. M. (1985). Carbonate Cements. *Carbonate Cements.* https://doi.org/10.2110/pec.85.36

Schofield, O., Ducklow, H. W., Martinson, D. G., Meredith, M. P., Moline, M. A., & Fraser, W. R. (2010). How do polar marine ecosystems respond to rapid climate change? *Science*, *328*(5985), 1520–1523. https://doi.org/10.1126/SCIENCE.1185779/ASSET/CB239015-9367-4926-84DC-ED33F944F564/ASSETS/GRAPHIC/328_1520_F2.JPEG

Schöne, B. R., & Giere, O. (2005). Growth increments and stable isotope variation in shells of the deep-sea hydrothermal vent bivalve mollusk Bathymodiolus brevior from the North Fiji Basin, Pacific Ocean. *Deep-Sea Research Part I: Oceanographic Research Papers*, *52*(10), 1896–1910. https://doi.org/10.1016/J.DSR.2005.06.003

Schöne, B. R., & Gillikin, D. P. (2013). Unraveling environmental histories from skeletal diaries — Advances in sclerochronology. *Palaeogeography, Palaeoclimatology, Palaeoecology*, *373*, 1–5. https://doi.org/10.1016/J.PALAEO.2012.11.026

Schöne, B. R., Oschmann, W., Rössler, J., Freyre Castro, A. D., Houk, S. D., Kröncke, I., Dreyer, W., Janssen, R., Rumohr, H., & Dunca, E. (2003). North Atlantic Oscillation dynamics recorded in shells of a long-lived bivalve mollusk. *Geology*, *31*(12), 1037–1040. https://doi.org/10.1130/G20013.1

Seed, R., & Richardson, C. A. (1999). Evolutionary traits in Perna viridis (Linnaeus) and Septifer virgatus (Wiegmann)(Bivalvia: Mytilidae). *Journal of Experimental Marine Biology and Ecology*, *239*(2), 273–287.

Siedlecki, S. A., Pilcher, D. J., Hermann, A. J., Coyle, K., & Mathis, J. (2017a). The Importance of Freshwater to Spatial Variability of Aragonite Saturation State in the Gulf of Alaska. *Journal of Geophysical Research: Oceans*, *122*(11), 8482–8502. https://doi.org/10.1002/2017JC012791

Siedlecki, S. A., Pilcher, D. J., Hermann, A. J., Coyle, K., & Mathis, J. (2017b). The Importance of Freshwater to Spatial Variability of Aragonite Saturation State in the Gulf of Alaska. *Journal of Geophysical Research: Oceans*, *122*(11), 8482–8502. https://doi.org/10.1002/2017JC012791

Sokolova, I., & Pörtner, H. (2001). Physiological adaptations to high intertidal life involve improved water conservation abilities and metabolic rate depression in Littorina saxatilis. *Marine Ecology Progress Series*, *224*, 171–186. https://doi.org/10.3354/meps224171

Stefani, M., & Vincenzi, S. (2005). The interplay of eustasy, climate and human activity in the late Quaternary depositional evolution and sedimentary architecture of the Po Delta system. *Marine Geology*, *222–223*(1–4), 19–48. https://doi.org/10.1016/j.margeo.2005.06.029

Steffani, C. N., & Branch, G. M. (2003). Growth rate, condition, and shell shape of Mytilus galloprovincialis: responses to wave exposure. *Marine Ecology Progress Series*, *246*, 197–209.

Stenzel, H. B. (1964). Oysters: Composition of the larval shell. *Science*, *145*(3628), 155–156. https://doi.org/10.1126/science.145.3628.155

Steyermark, A. C. (2002a). A high standard metabolic rate constrains juvenile growth. *Zoology*. https://doi.org/10.1078/0944-2006-00055

Steyermark, A. C. (2002b). A high standard metabolic rate constrains juvenile growth. *Zoology*, *105*(2), 147–151. https://doi.org/10.1078/0944-2006-00055

Sun, J., & Bhushan, B. (2012). Hierarchical structure and mechanical properties of nacre: A review. *RSC Advances*, *2*(20), 7617–7632. https://doi.org/10.1039/c2ra20218b

Suzuki, M., Saruwatari, K., Kogure, T., Yamamoto, Y., Nishimura, T., Kato, T., & Nagasawa, H. (2009). An acidic matrix protein, Pif, is a key macromolecule for nacre formation. *Science*, *325*(5946), 1388–1390. https://doi.org/10.1126/SCIENCE.1173793

Telesca, L., Michalek, K., Sanders, T., Peck, L. S., Thyrring, J., & Harper, E. M. (2018a). Blue mussel shell shape plasticity and natural environments: A quantitative approach. *Scientific Reports*, *8*(1). https://doi.org/10.1038/S41598-018-20122-9

Telesca, L., Michalek, K., Sanders, T., Peck, L. S., Thyrring, J., & Harper, E. M. (2018b). Blue mussel shell shape plasticity and natural environments: a quantitative approach. *Scientific Reports 2018 8:1*, *8*(1), 1–15. https://doi.org/10.1038/s41598-018-20122-9

Telesca, L., Peck, L. S., Sanders, T., Thyrring, J., Sejr, M. K., & Harper, E. M. (2019). Biomineralization plasticity and environmental heterogeneity predict geographical resilience patterns of foundation species to future change. *Global Change Biology*, *25*(12), 4179–4193.

Thomsen, J., & Melzner, F. (2010). Moderate seawater acidification does not elicit long-term metabolic depression in the blue mussel Mytilus edulis. *Marine Biology*, *157*(12), 2667–2676. https://doi.org/10.1007/S00227-010-1527-0

Tomašových, A., Albano, P. G., Fuksi, T., Gallmetzer, I., Haselmair, A., Kowalewski, M., Nawrot, R., Nerlović, V., Scarponi, D., & Zuschin, M. (2020a). Ecological regime shift preserved in the Anthropocene stratigraphic record. *Proceedings of the Royal Society B*, *287*(1929). https://doi.org/10.1098/RSPB.2020.0695

Tomašových, A., Albano, P. G., Fuksi, T., Gallmetzer, I., Haselmair, A., Kowalewski, M., Nawrot, R., Nerlović, V., Scarponi, D., & Zuschin, M. (2020b). Ecological regime shift preserved in the Anthropocene stratigraphic record. *Proceedings of the Royal Society B: Biological Sciences*, *287*(1929), 20200695. https://doi.org/10.1098/rspb.2020.0695

Tomašovỳch, A., Gallmetzer, I., Haselmair, A., Kaufman, D. S., Vidović, J., & Zuschin, M. (2017). Stratigraphic unmixing reveals repeated hypoxia events over the past 500 yr in the northern Adriatic Sea. *Geology*, *45*(4), 363–366. https://doi.org/10.1130/G38676.1

Trincardi, F., Amorosi, A., Bosman, A., Correggiari, A., Madricardo, F., & Pellegrini, C. (2020). Ephemeral rollover points and clinothem evolution in the modern Po Delta based on repeated bathymetric surveys. *Basin Research*, *32*(2), 402–418. https://doi.org/10.1111/bre.12426

Tushtev, K., Murck, M., & Grathwohl, G. (2008). On the nature of the stiffness of nacre. *Materials Science and Engineering C*, *28*, 1164–1172. https://doi.org/10.1016/j.msec.2007.10.039

v Moschino, M. M. (2006). Seasonal changes in physiological responses and evaluation of “well-being” in the Venus clam Chamelea gallina from the Northern Adriatic Sea. *Comp. Bioch. Physiol*, *145A*, 433–440.

Vacchi, M., Marriner, N., Morhange, C., Spada, G., Fontana, A., & Rovere, A. (2016). Multiproxy assessment of Holocene relative sea-level changes in the western Mediterranean: Sea-level variability and improvements in the definition of the isostatic signal. In *Earth-Science Reviews* (Vol. 155, pp. 172–197). Elsevier B.V. https://doi.org/10.1016/j.earscirev.2016.02.002

Vermeij, G. J. (1976). Interoceanic differences in vulnerability of shelled prey to crab predation. *Nature*, *260*(5547), 135–136. https://doi.org/10.1038/260135A0

Vihtakari, M., Ambrose, W. G., Renaud, P. E., Locke, W. L., Carroll, M. L., Berge, J., Clarke, L. J., Cottier, F., & Hop, H. (2017). A key to the past? Element ratios as environmental proxies in two Arctic bivalves. *Palaeogeography, Palaeoclimatology, Palaeoecology*, *465*, 316–332. https://doi.org/10.1016/J.PALAEO.2016.10.020

Wahl, M., Buchholz, B., Winde, V., Golomb, D., Guy-Haim, T., Müller, J., Rilov, G., Scotti, M., & Böttcher, M. E. (2015). A mesocosm concept for the simulation of near-natural shallow underwater climates: The Kiel Outdoor Benthocosms (KOB). *Limnology and Oceanography: Methods*, *13*(11), 651–663. https://doi.org/10.1002/LOM3.10055

Waldbusser, G. G., Brunner, E. L., Haley, B. A., Hales, B., Langdon, C. J., & Prahl, F. G. (2013). A developmental and energetic basis linking larval oyster shell formation to acidification sensitivity. *Geophysical Research Letters*, *40*(10), 2171–2176. https://doi.org/10.1002/GRL.50449

Warren Huntley, J., & Scarponi, D. (2015). Geographic variation of parasitic and predatory traces on mollusks in the northern Adriatic Sea, Italy: Implications for the stratigraphic paleobiology of biotic interactions. *Paleobiology*, *41*(1), 134–153. https://doi.org/10.1017/pab.2014.9

Watson, S. (2012). Marine invertebrate skeleton size varies with latitude, temperature and carbonate saturation: implications for global change and ocean acidification. *Global Change Biol*, *18*, 3026–3038.

Watson, S.-A., Peck, L. S., Tyler, P. A., Southgate, P. C., Tan, K. S., Day, R. W., & Morley, S. A. (2012). Marine invertebrate skeleton size varies with latitude, temperature and carbonate saturation: implications for global change and ocean acidification. *Global Change Biology*, *18*(10), 3026–3038. https://doi.org/10.1111/j.1365-2486.2012.02755.x

Weiner, S., & Dove, P. M. (2003a). An Overview of Biomineralization Processes and the Problem of the Vital Effect. *Reviews in Mineralogy and Geochemistry*, *54*(1), 1–29. https://doi.org/10.2113/0540001

Weiner, S., & Dove, P. M. (2003b). An Overview of Biomineralization Processes and the Problem of the Vital Effect. *Reviews in Mineralogy and Geochemistry*, *54*(1), 1–29. https://doi.org/10.2113/0540001

Weiner, S., & Dove, P. M. (2003c). An overview of biomineralization processes and the problem of the vital effect. *Reviews in Mineralogy and Geochemistry*, *54*(1), 1–29.

Weiner, S., Mahamid, J., Politi, Y., Ma, Y., & Addadi, L. (2009). Overview of the amorphous precursor phase strategy in biomineralization. *Frontiers of Materials Science in China*, *3*(2), 104–108. https://doi.org/10.1007/S11706-009-0036-X/METRICS

Weiss, I. M., Tuross, N., Addadi, L., & Weiner, S. (2002). Mollusc larval shell formation: amorphous calcium carbonate is a precursor phase for aragonite. *Journal of Experimental Zoology*, *293*(5), 478–491. https://doi.org/10.1002/JEZ.90004

Wittmer, J. M., Dexter, T. A., Scarponi, D., Amorosi, A., & Kowalewski, M. (2014). Quantitative bathymetric models for late quaternary transgressive-regressive cycles of the po plain, italy. *Journal of Geology*, *122*(6), 649–670. https://doi.org/10.1086/677901

Wootton, J. T., & Pfister, C. A. (2012). Carbon System Measurements and Potential Climatic Drivers at a Site of Rapidly Declining Ocean pH. *PLoS ONE*, *7*(12). https://doi.org/10.1371/JOURNAL.PONE.0053396

Wootton, J. T., Pfister, C. A., & Forester, J. D. (2008). Dynamic patterns and ecological impacts of declining ocean pH in a high-resolution multi-year dataset. *Proceedings of the National Academy of Sciences of the United States of America*, *105*(48), 18848–18853. https://doi.org/10.1073/PNAS.0810079105

Ye, F., Jurikova, H., Angiolini, L., Brand, U., Crippa, G., Henkel, D., Laudien, J., Hiebenthal, C., & Šmajgl, D. (2019). Variation in brachiopod microstructure and isotope geochemistry under low-pH–ocean acidification conditions. *Biogeosciences*, *16*(2), 617–642. https://doi.org/10.5194/bg-16-617-2019

Zeebe, R. E. (2012). History of Seawater Carbonate Chemistry, Atmospheric CO2, and Ocean Acidification. *Https://Doi.Org/10.1146/Annurev-Earth-042711-105521*, *40*, 141–165. https://doi.org/10.1146/ANNUREV-EARTH-042711-105521

Zhang, C., Li, S., Ma, Z., Xie, L., & Zhang, R. (2006). A novel matrix protein p10 from the nacre of pearl oyster (Pinctada fucata) and its effects on both CaCO 3 crystal formation and mineralogenic cells. *Marine Biotechnology*, *8*(6), 624–633. https://doi.org/10.1007/S10126-006-6037-1

Zuschin, M., & Stanton, R. J. (2001). Experimental Measurement of Shell Strength and its Taphonomic Interpretation. *PALAIOS*, *16*(2), 161–170. https://doi.org/10.1669/0883-1351(2001)016<0161:EMOSSA>2.0.CO;2

Figures

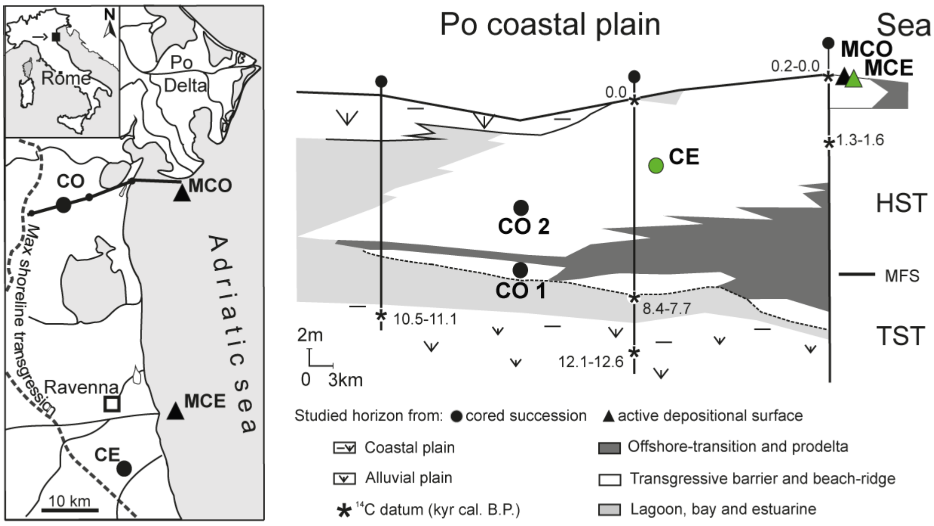

Fig 1. Study area map and stratigraphic framework of the latest Quaternary Po-Adriatic sedimentary succession. In the left panel, black dots mark the locations of sampled cores (CO1, CO2, CE), black triangles mark sampled thanatocoenosis from present-day shoreface environments (MCE, MCO), and the black solid line represents the along-dip cross section of the Po coastal plain (right panel). Right panel shows sketched climate driven environmental changes within the study area during the Holocene, see also Fig. 2. Acronyms: MFS= Maximum flooding surface; TST= transgressive systems tract; HST= highstand systems tract.

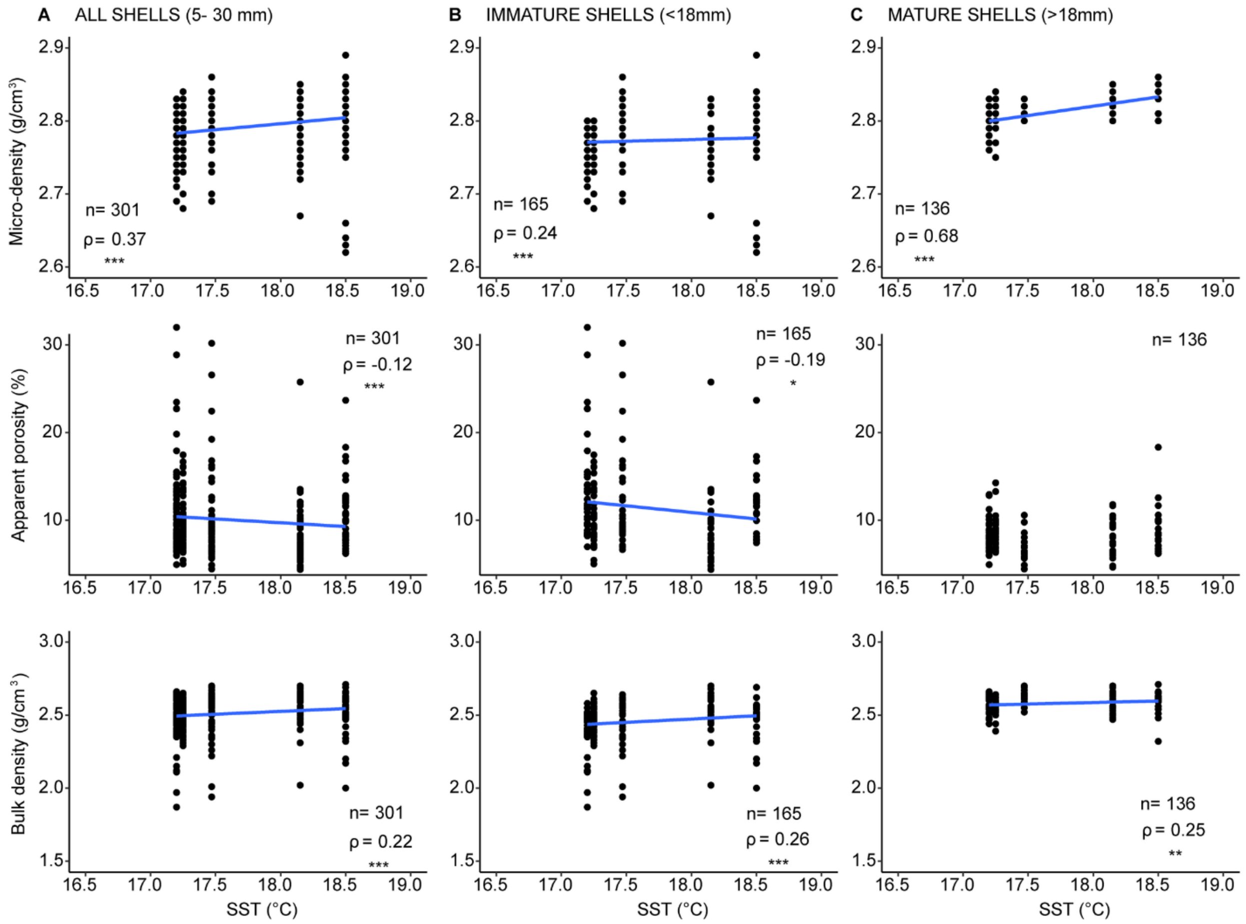

Fig 2. Relationship between shell skeletal parameters and SST. (A): whole dataset, (B): immature shells and (C): mature shells. n = total specimens analyzed; ρ = Spearman's determination coefficient; * p < 0.05; ** p < 0.01; *** p < 0.001.

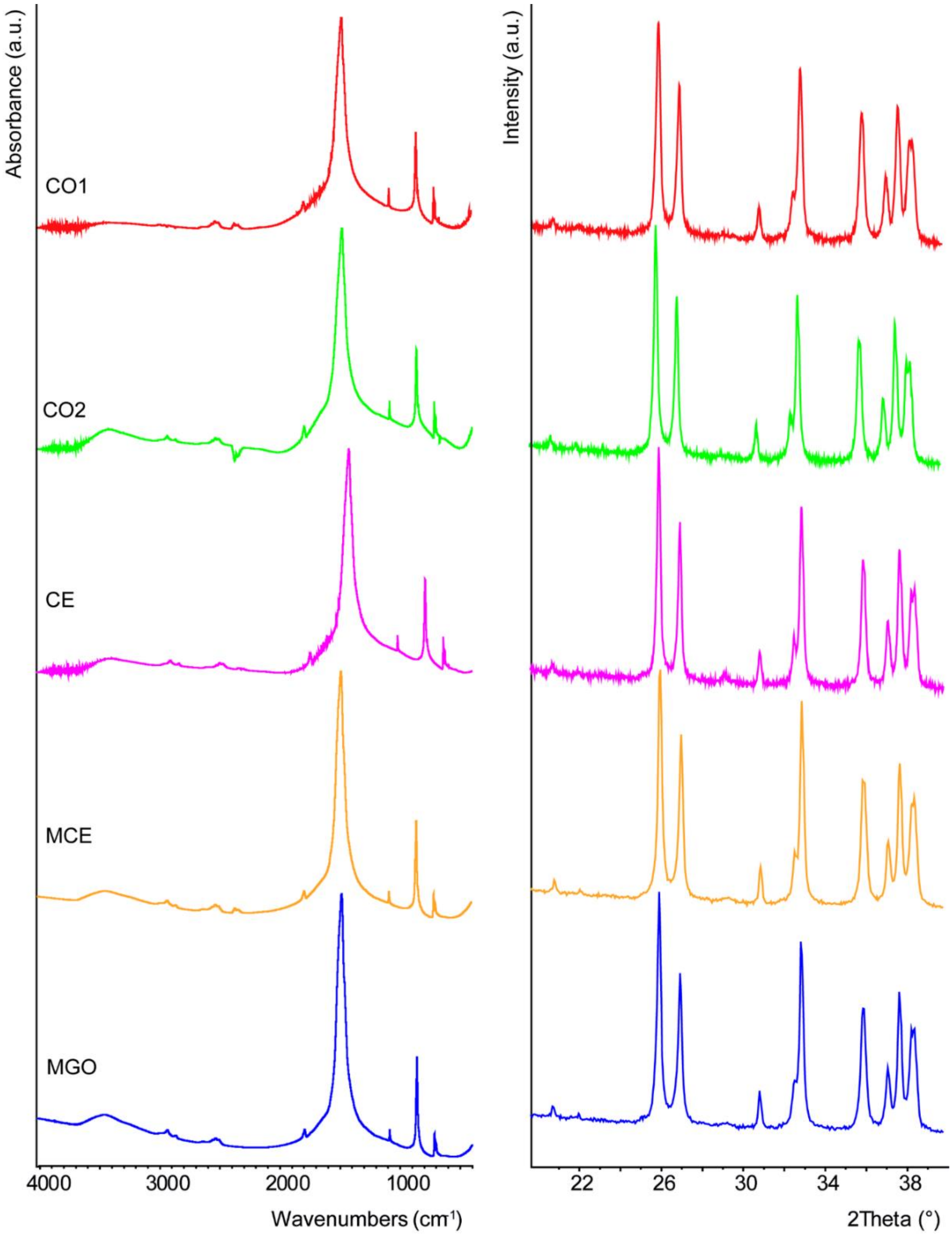

Fig 3. Fourier-transform infrared (FTIR) spectra (on the left chart) and X-ray powder diffraction (XRD) patterns (on the right chart) from grinded shells of *C. gallina*. A representative diffraction pattern and FTIR spectrum is shown for each level from the older samples (top) to more recent ones (bottom).

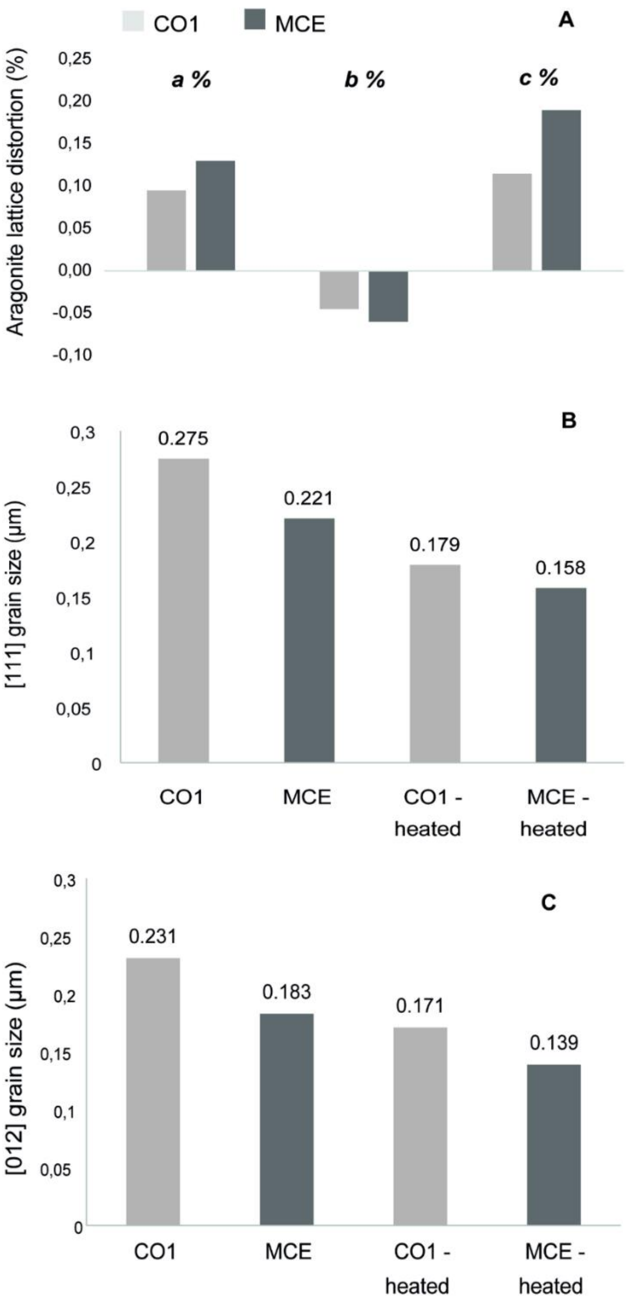

Fig 4. HR-XRPD data. (A) Distortions along a, b, and c axis of aragonite due to the presence of the intraskeletal organic matrix. Crystallite sizes of aragonite along the (B) (111) and (C) (021) directions, respectively, of pristine and thermal-treated samples.

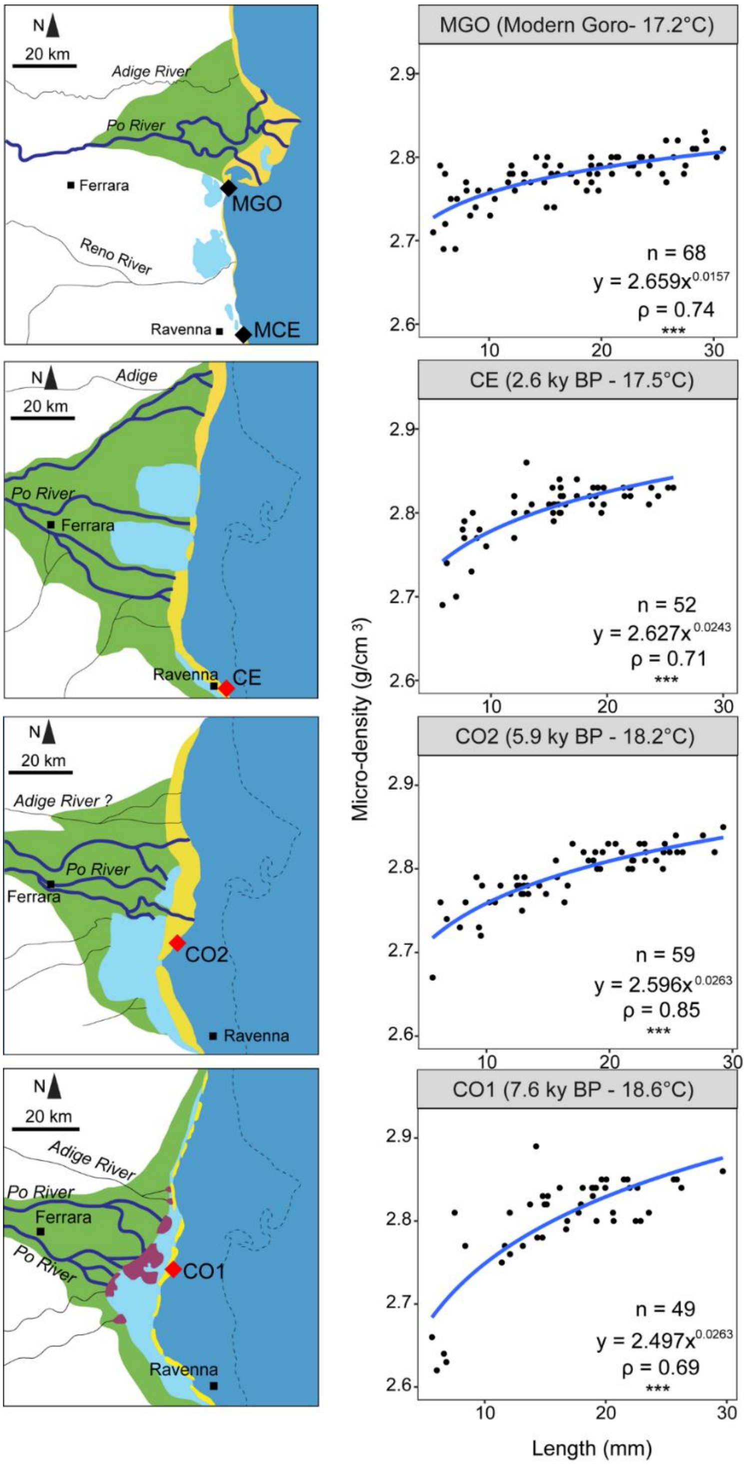

Fig 5. Po Delta evolution through time and variation in micro-density recorded within the five horizons investigated. Of the two modern settings, only Goro (MGO) data are reported since they show comparable patterns and SSTs (all analyses are shown in S1 Fig). The dotted line represents the modern Po Delta shoreline. n = number of valves; ρ = Spearman's determination coefficient; * $p < 0.05$; ** $p < 0.01$; *** $p < 0.001$. Geomorphologic map after Amorosi et al., 2017 modified).

Supporting information

Geological setting

The Po coastal plain, treasures records of past environmental shifts that reflect the complex interplay between climate driven sea-level changes and coastal dynamics (Amorosi et al., 1999b; Scarponi & Kowalewski, 2004a). Stratigraphic paleobiology investigations over the past years led to a high-resolution framework of the study area in term of environmental and biological dynamics, here briefly sketched. The latest Quaternary (<30 ky BP) succession of the Po coastal plain is a few tens of meters thick (Fig 1). This succession displays a wedge-shaped package of coastal and marine units recording the recent interplay between local sediment supply and accommodation space.

The fluvial-channel and associated floodplain deposits of the lower part of the succession are interpreted to record progradation and aggradation during the last glacial maximum and the onset of sea-level rise (<14.5 ky BP). At that time the Po Delta was located near the Mid-Adriatic Deep and the Northern Adriatic was entirely subaerially exposed (Azzarone et al., 2020). In the study area, these glacial and early transgressive alluvial and marsh deposits are overlaid by a few meters of shallow marine fossil rich sandstones forming elongated shoreline-parallel barriers and delimiting inland a back-barrier brackish zone and bay-head deltas in correspondence of the estuaries fluvial mouths (Bruno et al., 2019); Fig 1). These elongated shoreface-related bodies recorded short-lived intervals of rapid sedimentation (Scarponi et al., 2017) linked to sea-level stillstand phases in the overall post-glacial transgression of the Adriatic shelf. After the transgression reached its peak and in response to a deceleration of the sea-level rise (~7.0 until 2.0 ka BP) an early phase of slow progradation of bay-head deltas (ca. 5 m/year), initially filled great part of the back barrier area and then, by delta-lobe switching processes and sediment redistribution, built mainland attached and continuous beaches (Fig 1). Hence, during the middle Holocene the physiography of the study area transitioned from a barrier-lagoon-estuary system to wave dominated coastal and deltaic systems (Amorosi, Barbieri, Bruno, Campo, Drexler, Hong, Rossi, et al., 2019). These environmental dynamics are recorded in the sedimentary succession by aggradational to slightly progradational stacking of beach and barrier sandy units characterized by shallowing upward trends (Amorosi et al., 2017; Scarponi & Angeletti, 2008; Scarponi & Kowalewski, 2004a; Wittmer et al., 2014), passing inland to floodplain and wetland deposits. During this phase, the distal part of Po-Adriatic deltaic system continued to experience a phase of sediment starvation due to the trapping of coarse-grained sediments in the nearshore area and around the river outlets (Amorosi, Barbieri, Bruno, Campo, Drexler, Hong, Rossi, et al., 2019;

Scarponi et al., 2017). From 2.0 ka BP onward, the deltaic and coastal systems of Emilia-Romagna experienced a period of increased rivers discharge that promoted a strong progradation phase and the transition from wave-dominated to river-dominated deltaic systems shifting spatially due to multiple episodes of river avulsion. The last 800 years record the up building of the present-day morphological configuration. In 1152 AD the last natural Po river major avulsion occurred. The Po delta shifted northward respect to its previous location and during the last 400 years built its present-day morphological configuration (Maselli & Trincardi, 2013).

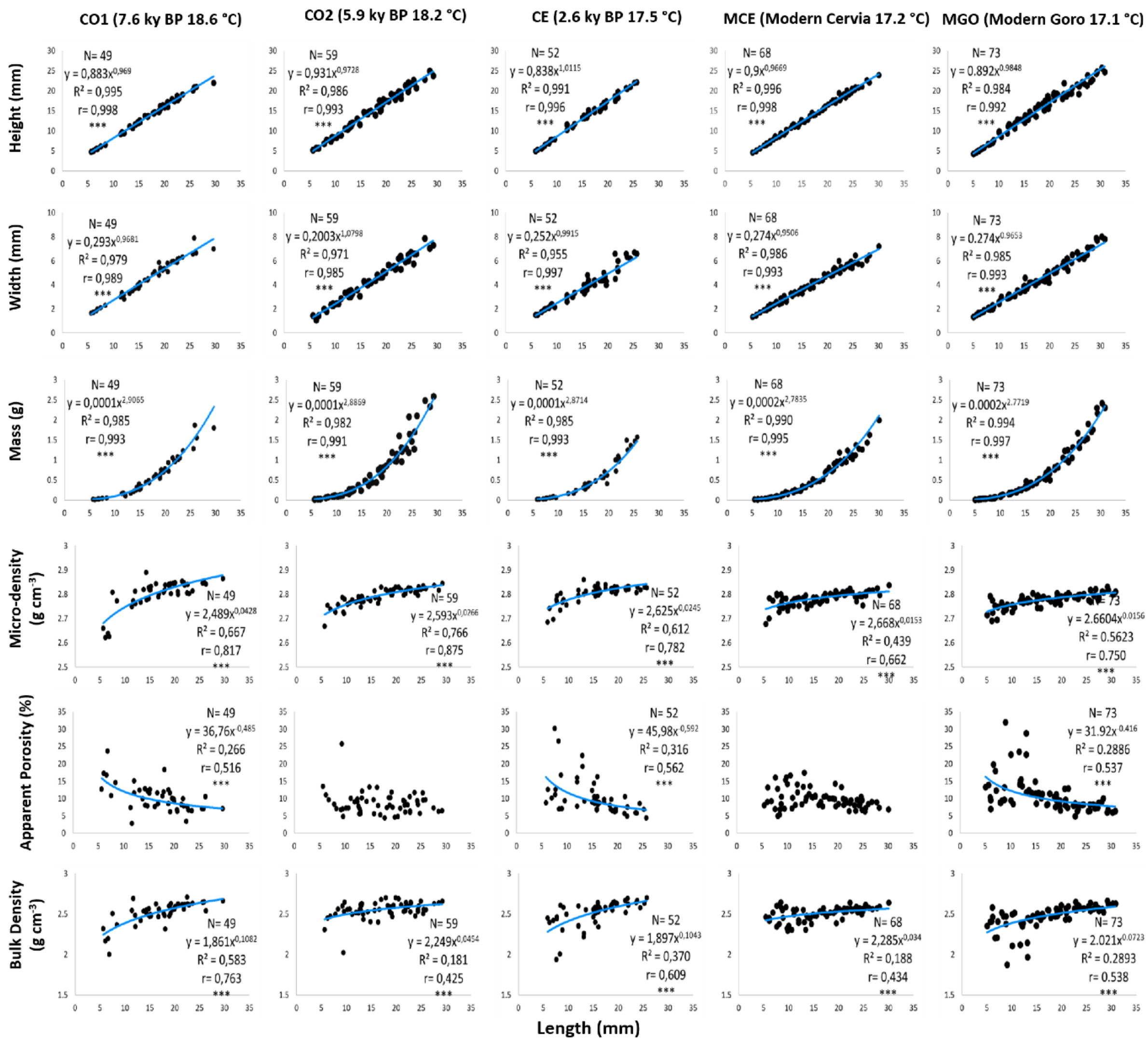

S1

Fig S1. Correlation of the skeletal and biometric parameters with shell length in the different horizons; n = number of valves; r = Spearman coefficient of determination; * $p<0.05$; ** $p<0.01$; *** $p<0.001$.

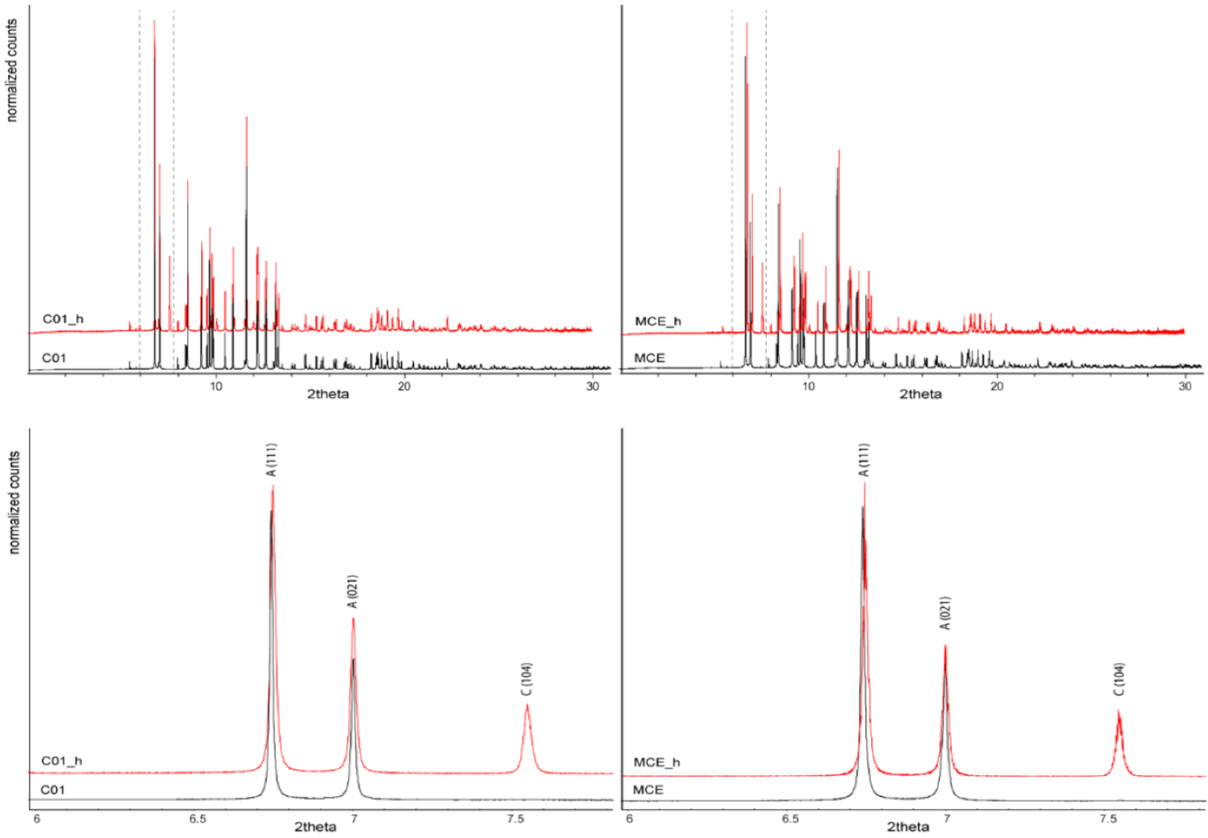

S2

Fig S2. HR-XRPD patterns of the samples MCE and CO1. The suffix _h indicates the thermally treated samples. At the bottom enlargements of the diffraction patterns in the 2theta region of main interest are reported. The Miller index is reported among brackets. C = calcite; A = aragonite.

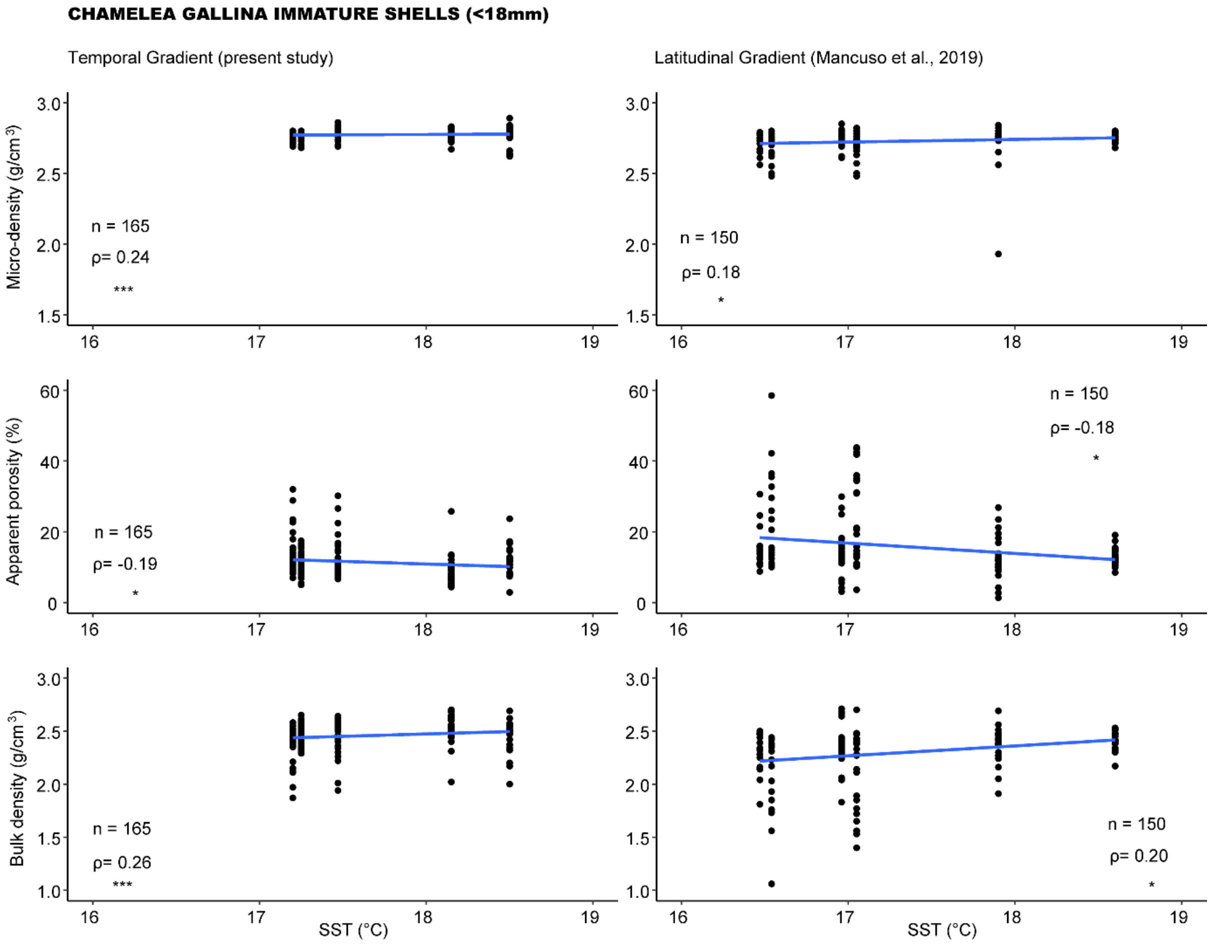

S3

Fig S3. Comparison of the relationship between shell skeletal parameters and SST in immature shells between this work and Mancuso et al. 2019; n = number of valves; ρ = Spearman coefficient of determination; * p<0.05; ** p<0.01; *** p<0.001.

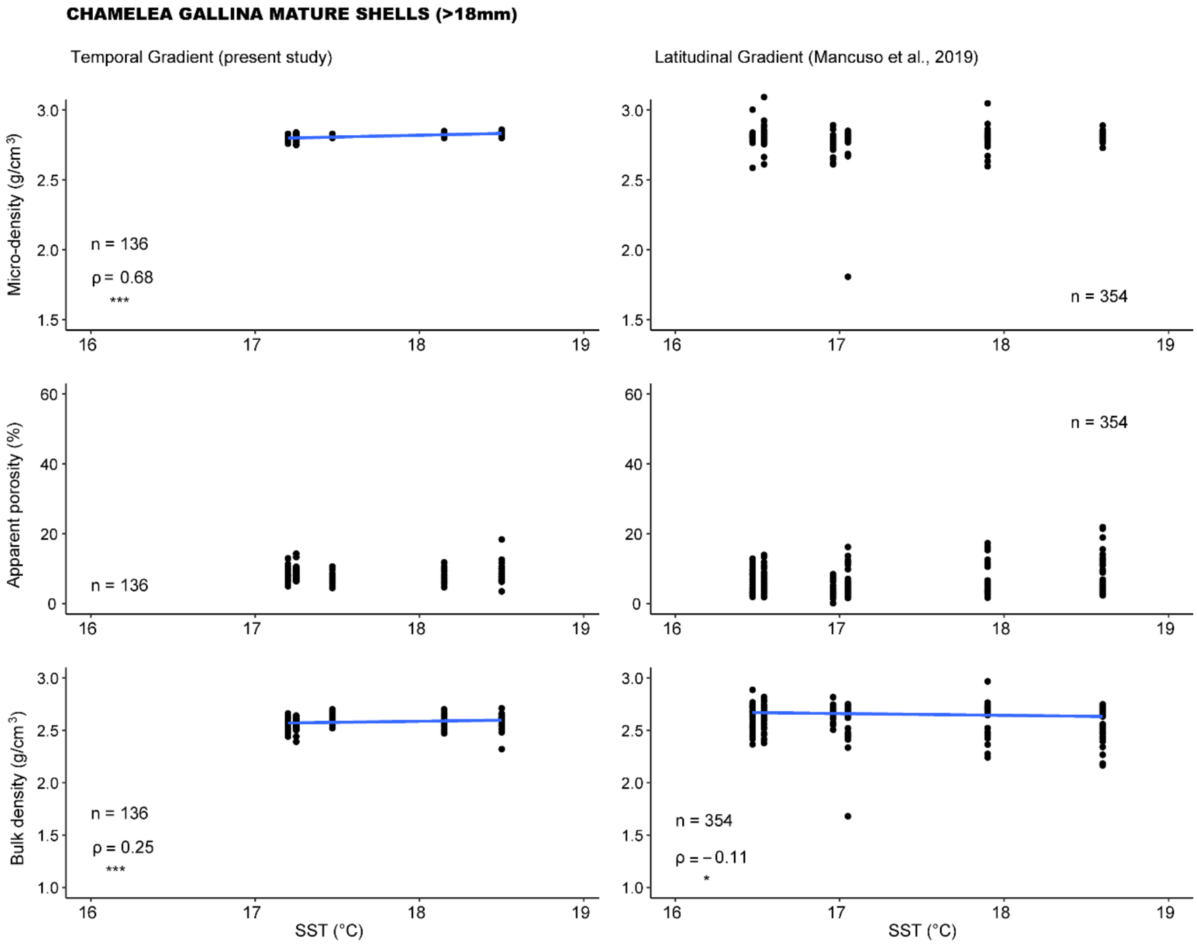

S4

Fig S4. Comparison of the relationship between shell skeletal parameters and SST in mature shells between this work and Mancuso et al., 2019; n = number of valves; ρ = Spearman coefficient of determination; * $p<0.05$; ** $p<0.01$; *** $p<0.001$.

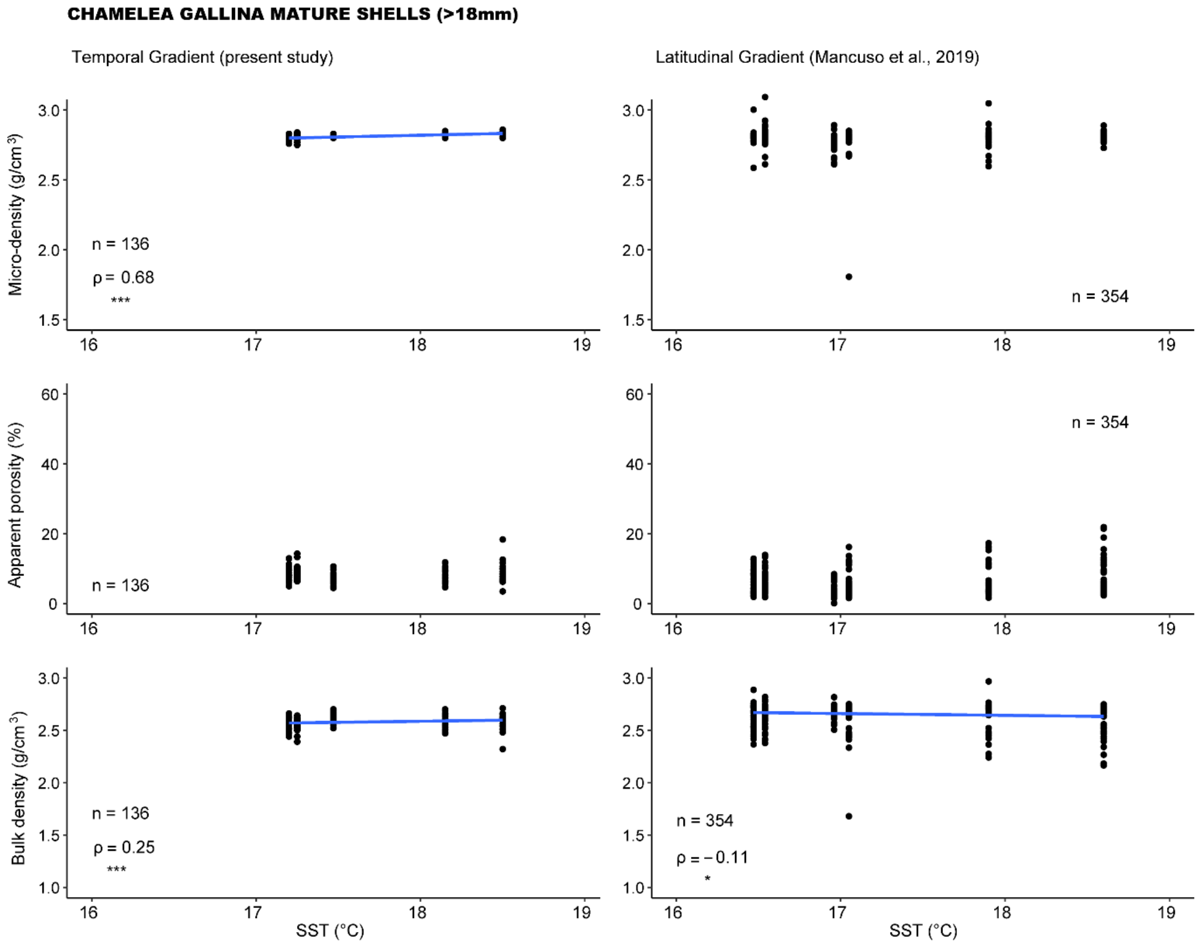

S5

Fig S5. Comparison of the relationship between shell skeletal parameters and SST for the entire C. gallina dataset (i.e., including both immature and mature specimens) between this work and Mancuso et al., 2019; n = number of valves; ρ = Spearman coefficient of determination; * p<0.05; ** p<0.01; *** p<0.001.

Level	^{14}C Age (ky BP)	SST (°C)	OM (%)	Mg ppm	Sr ppm
CO1	7.6 ± 0.1	18.6 ± 0.4	1.72 ± 0.03	58 ± 5	36 ± 2
CO2	5.9 ± 0.1	18.2 ± 0.3	1.37 ± 0.04	60 ± 10	40 ± 20
CE	2.6 ± 0.2	17.5 ± 0.5	1.60 ± 0.06	50 ± 20	60 ± 20
MCE	modern	17.3 ± 0.1	1.83 ± 0.02	40 ± 10	30 ± 9
MGO	modern	17.2 ± 0.1	1.79 ± 0.05	50 ± 20	40 ± 20
K-W			*		

S1 Table. Mean value and standard error of weight percentage loss as determined by TGA, and trace element analysis results. Values for each horizon in chronological order. K-W = Kruskal-Wallis equality-of-populations rank test; * $p<0.05$

References

1. Amorosi A, Colalongo ML, Fusco F, Pasini G, Fiorini F. Glacio-eustatic control of continental-shallow marine cyclicity from late quaternary deposits of the southeastern Po Plain, northern Italy. Quat Res. 1999;52: 1–13. doi:10.1006/qres.1999.2049

2. Scarponi D, Kowalewski M. Stratigraphic paleoecology: Bathymetric signatures and sequence overprint of mollusk associations from upper Quaternary sequences of the Po Plain, Italy. Geology. 2004;32: 989–992. doi:10.1130/G20808.1

3. Azzarone M, Pellegrini C, Barbieri G, Rossi V, Gamberi F, Trincardi F, et al. Linking benthic fauna and seismic facies to improve stratigraphic reconstructions: the case of the Mid-Adriatic Deep since the late glacial period (Central Adriatic Sea). Boll della Soc Paleontol Ital. 2020;59: 9–23. doi:10.4435/BSPI.2020.03

4. Bruno L, Campo B, Di Martino A, Hong W, Amorosi A. Peat layer accumulation and post-burial deformation during the mid-late Holocene in the Po coastal plain (Northern Italy). Basin Res. 2019;31: 621–639. doi:10.1111/bre.12339

5. Scarponi D, Azzarone M, Kusnerik K, Amorosi A, Bohacs KM, Drexler TM, et al. Systematic vertical and lateral changes in quality and time resolution of the macrofossil record: Insights from Holocene transgressive deposits, Po coastal plain, Italy. Mar Pet Geol.

2017;87: 128–136. doi:10.1016/j.marpetgeo.2017.03.031

6. Amorosi A, Barbieri G, Bruno L, Campo B, Drexler TM, Hong W, et al. Three-fold nature of coastal progradation during the Holocene eustatic highstand, Po Plain, Italy – close correspondence of stratal character with distribution patterns. Fielding C, editor. Sedimentology. 2019;66: 3029–3052. doi:10.1111/sed.12621

7. Amorosi A, Bruno L, Campo B, Morelli A, Rossi V, Scarponi D, et al. Global sea-level control on local parasequence architecture from the Holocene record of the Po Plain, Italy. Mar Pet Geol. 2017;87: 99–111. doi:10.1016/j.marpetgeo.2017.01.020

8. Wittmer JM, Dexter TA, Scarponi D, Amorosi A, Kowalewski M. Quantitative bathymetric models for late quaternary transgressive-regressive cycles of the po plain, italy. J Geol. 2014;122: 649–670. doi:10.1086/677901

9. Scarponi D, Angeletti L. Integration of palaeontological patterns in the sequence stratigraphy paradigm: a case study from Holocene deposits of the Po Plain (Italy). GeoActa. 2008;7: 1–13.

10. Maselli V, Trincardi F. Man made deltas. Sci Rep. 2013;3: 1–7. doi:10.1038/srep01926

Chapter 3. Assessing long term *Chamelea gallina* age and growth dynamics on a millennial temporal scale in the Northern Adriatic Sea (Italy) *(manuscript in preparation)*

Assessing long term *Chamelea gallina* age and growth dynamics on a millennial temporal scale in the Northern Adriatic Sea (Italy)

Alessandro Cheli[1,2], Arianna Mancuso[1,2], Fiorella Prada[2,3], Daniele Scarponi[1,2] Giuseppe Falini[2,4], Stefano Goffredo[1,2]

[1] Department of Biological, Geological and Environmental sciences - BIGEA, University of Bologna, Bologna, Italy
[2] Fano Marine Center, The Inter-Institute Center for Research on Marine Biodiversity, Resources and Biotechnologies, Fano (PU), Italy
[3] Environmental Biophysics and Molecular Ecology Program, Department of Marine and Coastal Sciences, Rutgers, The State University of New Jersey, New Brunswick, New Jersey, USA
[4] Department of Chemistry "Giacomo Ciamician", University of Bologna, Bologna, Italy

Abstract

This study investigates the influence of environmental changes on long term age and growth dynamics of the bivalve *Chamelea gallina* in the Po-Adriatic System (Italy). *C. gallina* is a valuable economic species in the Mediterranean Sea, expected to be impacted by numerous anthropogenic stressors that threaten its biological and economic sustainability. Here we investigated age and growth parameters (bulk density, linear extension, and net calcification rates) of *C. gallina* shells by comparing sub-fossil remains from the middle Holocene (between ~8 and ~5 kyr cal. BP) with present-day Adriatic shoreface deposits. This allowed to analyse *C. gallina* long-term response to changing environmental conditions, in particular the decreasing trend in sea surface temperature from the Holocene to nowadays. Three independent aging techniques were used (counting of shell surface growth rings, counting of internal bands in the shell section and analysis of 18O/16O ratio) to determine the Von Bertalanffy growth functions for each analysed horizon. This, in turn, allowed us to estimate the linear extension rate and net calcification rate, evaluated also in relation to animal sexual maturity to detect any possible variation of biomineralization behaviour during organism development. A previous study on the same *C. gallina* populations observed that temperatures variation induced macro-scale variations in shell skeletal parameters, with shells from the warmer middle Holocene setting characterized by a denser and less porous exoskeleton than modern ones.

Despite the reported differences in skeletal properties of *C. gallina* shells in the analysed temporal gradient, we found no significant variation between the growth of middle-Holocene and present-day horizons. Linear extension and net calcification rates remained constant in the last 8000 years in *C. gallina* populations of the Po-Adriatic System. When analysing immature and mature shells separately, we observed a similar decrease in extension rate and net calcification rate with increasing animal age in all horizons, highlighting a very fast growth in the first stages of life in order to likely quickly attain the size of sexual maturity.

The comparison between sub-fossil and modern specimens from comparable setting of the Northern Adriatic Sea allowed to evaluate long term *C. gallina* biomineralization dynamics on a millennial temporal scale, offering insights into its adaptive capacities to changing environment.

Introduction

Anthropogenic stressors, particularly warming and ocean acidification (among many others), are predicted to be the major driving forces in shaping coastal ecosystem and their services in the next century. Some coastal areas have already experienced substantial changes in mean seawater temperature and acidity levels, in some cases equal to or greater than conditions originally predicted in future ocean scenarios (Hofmann et al., 2011; Kroeker et al., 2016a; Wahl et al., 2015; Wootton et al., 2008; Wootton & Pfister, 2012). There is increasing concern about the effects of those hazards on marine calcifying organisms like mollusks, corals and echinoderms, which rely on calcium carbonate exoskeletons for structural support and mechanical strength (Addadi & Weiner, 2014).

Among calcifiers, bivalves are considered highly sensitive to environmental changes (Cooley & Doney, 2009) since many factors can influence their energy allocation patterns and the process of shell formation (Bergström & Lindegarth, 2016a; Kroeker et al., 2016a; Telesca et al., 2018a), affecting the structural integrity and the protection of these organisms against abiotic and biotic factors. Multiple environmental parameters can influence the calcification responses of bivalves like pCO_2 (Fitzer et al., 2014; Gazeau et al., 2013; Kroeker et al., 2010; Pfister et al., 2016), temperature (Fitzer et al., 2015), wave exposure (Fox & Coe, 1943), food availability (Hahn et al., 2012; Thomsen & Melzner, 2010; Waldbusser et al., 2013) and predation pressure (Vermeij, 1976). Their effect can be reflected in the variation of growth rate and overall size (Mancuso et al., 2019a; Thomsen & Melzner, 2010), shell morphology (Fitzer et al., 2015; Mackenzie et al., 2014a; Pfister et al., 2016), and mineralogical plasticity (Nash et al., 2012; Pauly et al., 2015).

A good understanding of long-term dynamics in the context of major environmental shifts is required to narrow the uncertainty regarding organismal responses to ongoing climate changes. While laboratory studies enable the isolation of a specific stressor, field studies are necessary to widely understand the effects of stressors in a natural and more complex system. Nevertheless, the time required to detect long-term population dynamics can be prohibitive (Hofmann et al., 2010; Pfister et al., 2016). In this light, well-resolved, fossil-rich sedimentary successions record ecological responses to past climatic shifts, far beyond the limited timescales of direct ecological monitoring, typically restricted to the most recent decades (e.g., Dillon et al., 2020; Kidwell, 2015; Tomašových et al., 2020). As major calcareous organisms with an extensive fossil record, marine calcifying organisms can be considered valuable recorders of past environmental change in marine habitats (Bemis et al., 1998; Chauvaud et al., 2005; Lutz & Rhoads, 1980; Schöne & Gillikin, 2013; Vihtakari et al., 2017). In particular, mollusk shells archive historical data due to their seasonal deposition of carbonate material, retaining high-resolution temporal records of the ambient physical and chemical conditions during growth (Klein et al., 1996; Purroy et al., 2018; Schöne et al., 2003).

The infaunal venerid bivalve *Chamelea gallina* (Linnaeus, 1758) is one of the most important fishery resources of the Adriatic Sea, with annual catches for about 15,000 tonnes (for the year 2018). *C. gallina* is abundant in shoreface settings at depths ranging from 0 to 12 m up to 1–2 nautical miles (nm) off the coast (Morello et al., 2005; Moschino, 2006). It is particularly abundant in the central and northern Adriatic Sea, where the massive Po River outflow and the currents along the Italian coast provide abundant nutrients, particles, and organic matter (Orban et al., 2007). Previous studies have mainly focused on population dynamics, shell growth and composition of this species in the present-day Mediterranean (Gizzi et al., 2016; Mancuso et al., 2019 and reference therein). It has been observed that the biomineralization of *C. gallina* populations in the Adriatic Sea is influenced by environmental changes, with variations in shell density, thickness and growth in response to varying water temperature, solar radiation, salinity and food availability along a latitudinal gradient (Gizzi, Caccia, Simoncini, Mancuso, Reggi, Fermani, Brizi, Fantazzini, Stagioni, Falini, et al., 2016c; Mancuso et al., 2019a).

C. gallina long term dynamic in shell properties in response to past climate-driven environmental change was firstly investigated by Cheli et al. (2021), that investigated variations in shell biometric, skeletal and microstructural features on a millennial temporal scale, by comparing fossil remains and modern population of the Northern Adriatic Sea. Macro-scale variations in skeletal parameters were observed, with modern specimens displaying less dense and more porous shells than fossils one, likely due to a lower aragonite saturation state at a lower temperature.

The same fossil and modern assemblages investigated in Cheli et al. (2021) have been examined in this study, with the aim of verifying any possible influence of past climate transitions on age and growth dynamics of *C. gallina.* Those parameters were not addressed in the previous work but are fundamental in assessing populations dynamics and necessary for efficient fishery management. Age and growth parameters (bulk density, linear extension, and net calcification rates) of *C. gallina* were investigated along a temporal gradient of 8000 years, in two different geomorphologic configurations of North Adriatic coastal systems along the Holocene (estuarine vs. deltaic system). Four shoreface-related *C. gallina* horizons have been evaluated: two from the present-day Adriatic setting and two from the Middle Holocene, when regional sea temperatures were higher than today, thus representing a possible analogy for the increase of sea temperatures predicted for the end of this century.

Shells were measured and aged using three independent methods (shell surface growth rings, shell internal bands and stable isotope composition) to determine the Von Bertalanffy growth functions for each horizon and calculate the derived growth parameters linear extension rate and net calcification rate. In addition, differences in skeletal and growth properties of *C. gallina* shells were also investigated concerning animal sexual maturity (reached in modern specimens at length around 18mm) to consider eventual differences in the biomineralization process during different stages of the bivalve’s life cycle.

This study could allow the reconstruction of *C. gallina* natural range of variability on time-scale well beyond the ecological monitoring or small-scale experiments and offer insights on the possible adaptive capacities of *C. gallina* facing near-future anthropogenic warming.

Materials and methods

Study area and geological setting

The Northern Adriatic Sea is a semi-enclosed, shallow basin characterized by a wide shelf with a low topographic gradient of 0.02° and an average depth of 35 m (Poulain, 2001). It extends ~350 km southward from the Gulf of Trieste and is delimited westward by Italy and eastward by the Balkan Peninsula. The Italian coasts are primarily sandy and are strongly influenced by the Po River flow, that affect the water circulation in the north Adriatic and plays a fundamental role in the bio-geochemical processes of the basin. The Po is the largest Italian river, supplying over 50 % of freshwater input to the Northern Adriatic basin (Degobbis et al., 1986) and about 20 % of the total river discharge in the Mediterranean Sea (Russo & Artegiani, 1996).

The Po coastal plain preserves records of past environmental shifts that reflect the interplay between coastal dynamics and climate-driven sea-level changes (Amorosi et al., 1999a; Scarponi & Kowalewski, 2004b). In particular during the Holocene, a strong geo-morphological change occurred in response to the glacioeustatic sea-level variations (Amorosi, Barbieri, Bruno, Campo, Drexler, Hong, & Fielding, 2019). Stratigraphic paleobiology investigations over the past years led to a high-resolution framework of the study area in terms of environmental and biological dynamics. During the Holocene early climate optimum (HCO, 9–7 ky BP), the north-western Adriatic coast was characterized by estuary systems bounded seaward by a series of coastal lagoons that limited riverine plumes into the Adriatic Sea (Amorosi, Barbieri, Bruno, Campo, Drexler, Hong, & Fielding, 2019). By contrast, during the last part of the HCO (i.e., between 7.0 to 5 ky BP), the area transitioned firstly to a wave-dominated and, after 2.0 ky BP, to a river-dominated deltaic system (Amorosi, Barbieri, Bruno, Campo, Drexler, Hong, & Fielding, 2019). The last geomorphologic configurations led to the progressively increasing influence of riverine processes on the control of coastal dynamics and the storage-release of sediments. The enhanced freshwater discharge in the nearshore area, especially during the last 2.0 ky BP, resulted in a strong progradation and the upbuilding of the modern Po Delta (Correggiari et al., 2005b) in a climatic context characterized by an overall decreasing trend in SST.

Specimen collection

The analyses compared two specific time intervals: the mid-Holocene (between ~8 and ~5 kyr cal. BP) documented in subsurface cores and the present day represented by the surficial dead assemblages of the northern Adriatic Sea. The age of the samples was based on direct radiocarbon dating of the fossil material and timing of the parasequence development in the study area. The samples of fossiliferous deposits were acquired from previously investigated cores, whereas the data on the surficial assemblages derive from new sampling efforts.

Details on age determination methods, sampling design, specimens' collection and preparation and estimate of environmental parameters can be found in Cheli et al. (2021) and a brief description is here reported in supplementary material.

Determination of age and growth parameters

Age was measured in a subsample of 30 shells of different sizes in each horizon, using three methods: shell surface growth rings, shell internal bands (shell cross-sections), and stable $\delta^{18}O$ composition (Fig. 1). By counting the total number of visible external and internal rings in each shell, the age-length keys were obtained for the two methods and fitted with the von Bertalanffy growth (VBG) functions,

$$L_t = L_{inf}[1 - e^{-k(t)}]$$

Where L_t is the individual length at age t, L_{inf} is asymptotic length (maximum expected length in the population), K is a growth constant, and t is the age of the individual. Two growth curves for each horizon were produced, and a chi-square test of maximum likelihood ratios was used to examine the significance of differences in growth functions between the two ageing methods. Kimura's method allows testing several hypotheses to compare the two curves by simultaneously analyzing one or more growth parameters. The FSA (Simple Fisheries Stock Assessment Methods) and the Fishmethods packages in R studio were used for these purposes. If no differences were revealed between VBG curves from shell surface growth rings and internal bands, generalized growth curves for each site were constructed by merging age-length keys from both methods. The resulting generalised VBG function for each site was considered for extrapolating age in all the remaining shells. Finally, age was calculated from the inverse of the generalized VBG function of each site:

$$t = \frac{1}{k * ln\left(\frac{L_{inf}}{L_{inf} - L)}\right)}$$

To validate the data from the two counting rings methods and the generalized VBG curves, oxygen isotopic measurements ($\delta^{18}O$) were carried out at the Isotope biogeochemistry laboratory, Department of earth & planetary sciences, Washington University in St Louis. $\delta^{18}O$ measurements were carried out on “spot” samples collected from the prismatic layer and the cross-lamellar layer and drilled in sequence along the shell growth direction by a single diamond drill. Dried homogenized powdered samples were treated with helium, then an acidified solution consisting of 104% orthophosphoric acid was addedand left to react for 1 hour at 70 °C. Each piece was analyzed using a Thermo Gasbench preparation system attached to a Thermo Delta V Advantage mass spectrometer in continuous flow mode. Age resulted from counting lighter δ^{18}O (summer) and heavier δ^{18}O (winter) peaks were plotted with the age-length key from the two ageing methods.

Shell linear extension rates were obtained with the length/age ratio (cm y^{-1}), while the net calcification rate (mass of $CaCO_3$ deposited per year per unit area, (g cm^2 y^{-1}) was calculated for each shell by the formula:

net calcification (g cm^{-2} y^{-1}) = bulk density (g cm^{-3}) x shell extension (cm y^{-1}).

Correlations analyses between skeletal and growth parameters and SST were performed to investigate any significant pattern developed over geological time as a function of temperature. Differences in growth of *C. gallina* shells were also investigated concerning animal sexual maturity (reached in modern specimens at a length of around 18mm) to consider eventual differences in the biomineralization process during different stages of the bivalve’s life cycle.

Shell ageing methods details

For counting surface external rings, which appeared as smooth clefts on the shell surface and as strong pigmented lines across the anterior-posterior axis, shells were scanned in a transmitted light to enhance contrast of surface’s ridge and highlight bands at different densities.

In order to estimate age by means of shell sectioning, the valves were embedded in epoxy resin under vacuum at room temperature, followed by 24 h hardening. For counting internal bands, the shells were sectioned along the anterior-posterior axis, from the umbo to the ventral margin, using an electrodeposited diamond cutting blade. Sections were subsequently ground using successive finger grits (600, 1200, 2400 μm) and polished with abrasive allumina compound (3M Perfect-it III Extrafine Paste). Finally, the sections were ultrasonically cleaned, rinsed in purified water and dried. Shell sections were then examined and photographed under oblique light at low magnification in order to identify internal growth bands. In each section the number of annual growth rings was determined by counting the alternating opaque (carbonate matrix) and translucent (carbonate-organic matrix) increments visible on the shell cross-section (E Arneri, 1995) using a dissecting microscope under reflected light at low magnification (6.4 X). Assuming that the growth rings are laid down yearly, the age of each clam was estimated by counting all the translucent zones.

To validate the data from the two counting rings methods, oxygen isotopic measurements ($\delta^{18}O$) were carried out on “spot” samples collected in sequence from the umbo to the ventral edge of 3 shells of different dimensions for each site. Dried homogenized powdered samples were treated with helium then added an acidified solution consisting of 104% orthophosphoric acid and left to react for 1 hour at 70 °C. Each sample was then analyzed using a Thermo Gasbench preparation system attached to a Thermo Delta V Advantage mass spectrometer in continuous flow mode. Each run of samples was accompanied by 10 reference carbonates (Carrara Z) and 2 control samples (Fletton Clay). Carrara Z has been calibrated to VPDB using the international standard NBS19. Age resulted from counting lighter $\delta^{18}O$ (summer) and heavier $\delta^{18}O$ (winter) peaks were then plotted with the age-length key from the two ageing methods.

Statistical analyses

Levene’s test was used to test homogeneity of variance, while Kolmogorov-Smirnov’s test was used to test normality for environmental and shell parameters. Since assumptions for parametric statistics were not fulfilled, the non-parametric Kruskal-Wallis equality-of-populations rank test was used. Spearman’s rank correlation coefficient was used to evaluate the trend between shell parameters and sea surface temperature. In each horizon, rank correlations were computed on all valves and also on two subgroups consisting of immature specimens (valve length <18 mm) and mature ones (>18 mm). All statistical analyses were computed using RStudio software (RStudio Team, 2020).

Results

Dating and environmental parameters

Radiocarbon measurements ascribed the two sub-fossil horizons to the Middle Holocene; in particular, horizon CO1 was dated 7.6 ± 0.1 ky BP, while horizon CO2 was dated 5.9 ± 0.1 ky BP. Estimated and measured SST varied among horizons along the temporal gradient (Kruskal-Wallis test, $df = 5$, $p < 0.001$; Table 1). The reconstructed SST trend showed a difference of ∼1.5°C between the middle Holocene and present-day cooling down gradually from the oldest horizon (CO1, 18.6°C) to nowadays setting (MCE, 17.3 and MGO, 17.1°C; Table 1).

Shell growth and skeletal parameters

Shell age did not differ among horizons for both external rings and internal bands (Kruskal-Wallis test, $df = 5$ and $p > 0.05$). There were no significant differences among the growth curves obtained from the external and internal rings within each site. Therefore, a generalized VBG curve was obtained for each site (Fig. 2). The $\delta^{18}O$ values along the shell growth direction exhibited a roughly sinusoidal sequence of lower (summer) and higher (winter) values, and the number of observed seasons allowed age estimation. Age from $\delta^{18}O$ values validated the data from the other two ageing methods fitting the VBG curves (Fig. 2). At each site, shell growth parameters were significantly correlated with shell age (Fig. 3). Linear extension rates and net calcification rates decreased with shell age at all sites (Fig. 3).

Variation of growth parameters was then analyzed in relation to environmental variables along the temporal gradient. Linear extension rate and net calcification rate showed no significant correlation with SST variation (Fig. 4). Correlations with the environment were also performed separately in the immature and mature shells; in all groups, bulk density were positively correlated with SST, while no correlation was found for the other parameters (Fig. 5).

Discussion

This study investigated the variation in shell age and growth parameters of the bivalve *C. gallina* in relation to SST trend in the Po-Adriatic system during the last ~8,000 years. By comparing the Holocene sub-fossil record to modern-day assemblages, it has been possible to gain insight into growth dynamics on a millennial temporal scale, overcoming the time limits imposed by laboratory studies.

A previous study investigated biometric, skeletal, and microstructural features of *C. gallina* shells along the same temporal gradient (Cheli et al., 2021a). At the microscale level, the shells were composed of pure aragonite with a perfectly preserved mineral phase and no relevant diagenetic alteration, except for a slight degradation of the inter-crystalline organic phase (Cheli et al., 2021a). At the macroscale level *C. gallina* shells appeared sensitive to changes in seawater temperature: specimens from past sub-fossil horizons living in warmer water presented denser and less porous shells than modern specimens (Cheli et al., 2021a). Here we examined shell age and growth in four of the previously analyzed assemblages, in relation to shell age and growth dynamics, crucial parameters for responsible fisheries management. Specifically, we compared two horizons dated 7.6 ± 0.1 and 5.9 ± 0.1 ky BP, coming from a warmer environmental context and characterized by a lower fluvial influence due to the estuarine configuration of the river Po mouth, with modern populations sampled in two localities of the Emilia Romagna coast, south of the Po Delta. To better understand the overall biomineralization dynamic, in this discussion we will refer to the findings of both the present study and the previous one of Cheli et al. 2021.

Through the count of shell external and internal growth rings, we estimated the age of a subsample of *C. gallina* shells for each investigated horizon, used to build growth curves with the Von Bertalanffy function. Both methods were validated by $\delta^{18}O$ profiles along the shell growth direction, resulting in appropriate and reasonably accurate age estimation of *C. gallina* specimens. The observed values for the estimated maximum shell length (L_{inf}) and von Bertalanffy growth constants (k) were in conformity with data from previous studies on *C. gallina* in the Adriatic Sea (Dunca et al., 2005; Mancuso et al., 2019a), in the Western Mediterranean Sea (Schöne & Giere, 2005) and the Algarve coast (P Moura, 2009).

As previously observed for mollusks and other organisms (Mancuso et al., 2019a; Myrand et al., 2002a; Steyermark, 2002b), *C. gallina* extension rate decreased with increasing length (Fig. 3), highlighting a fast growth in the first year of life, while in the second year, the growth rate had more than halved. Decreasing linear extension rates with age determine a reduction in net calcification rates, partly countered by increasing bulk density (Fig. 3).

A significant positive correlation was previously observed for bulk density and micro-density in both mature and immature shells in relation to past SST variations, while apparent porosity showed no correlation in mature shells and a significant negative correlation in immature shells (Cheli et al., 2021a). The significant correlation in shell density with SST can be attributed to different mineralization rates driven by temperature and related aragonite saturation state. Warmer water masses reduce the thermodynamic work required to organisms to deposit calcium carbonate (Pokroy et al., 2006b), making the biomineralization less expensive in terms of metabolic cost (Siedlecki et al., 2017b) and enabling an increase in calcification rates (Hall-Spencer & Harvey, 2019b). Comparable patterns have also been detected in brachiopods, where some species living in cold water showed a reduced calcium carbonate deposition and an increased organic matrix content compared to higher temperate settings, characterized by larger crystals and reduced organic matrix (hence denser shells (Clarke, 1993b)). Total $CaCO_3$ deposited by the organism results from the interplay between linear extension rate and shell bulk density. Despite the differences observed in the skeletal parameters related to the SST trend and different environmental context (see study area), the growth parameters (linear extension and net calcification) do not show significant variations in the analyzed fossil and modern horizons (tab 2; Fig. 4), neither when considering immature and mature shells separately (tab 3; Fig. 5). The fossil horizons from Holocene and modern settings show homogeneous linear extension rates and a decreasing trend in bulk density from the Holocene to nowadays. Nevertheless, the net calcification rate remains constant among the horizons, likely not significantly influenced by temperature variations and by the geomorphological evolution that occurred in the study area in the last 8,000 years. This could be interpreted as phenotypic plasticity exerted by *C. gallina* populations in this area, which has shown the ability to maintain similar growth rates in different environmental contexts.

This result contrasts with the outcome of other studies conducted on *C. gallina* growth and mineralization in relation to environmental factors, that showed how the abiotic or biotic factors can influence the shell growth rate, like spawning, food availability, type of substratum, depth, light, temperature, salinity, and population density (Dalgi et al., 2010; Gaspar et al., 2004). Nevertheless, a recent review of all the studies conducted on the biology of *C. gallina* in the Adriatic Sea (Grazioli et al., 2022) founds numerous discrepancies in results, highlighting how the interaction of several environmental factors at the local level can strongly influence *C. gallina* responses.

In particular, previous studies on *C. gallina* shells were conducted along a latitudinal gradient in the Adriatic Sea, including the area considered in this study (Gizzi, Caccia, Simoncini, Mancuso, Reggi, Fermani, Brizi, Fantazzini, Stagioni, Falini, et al., 2016c; Mancuso et al., 2019a). Gizzi et al. found that shells of *C. gallina* of commercial size over 25 mm long were thinner, more porous and less resistant to fractures in warmer and more irradiated populations (Gizzi, Caccia, Simoncini, Mancuso, Reggi, Fermani, Brizi, Fantazzini, Stagioni, Falini, et al., 2016c) . On the other hand, immature shells, less than 18 mm long, showed the opposite trend to mature ones, resulting in more porous and less dense shells with lower SST(Gizzi, Caccia, Simoncini, Mancuso, Reggi, Fermani, Brizi, Fantazzini, Stagioni, Falini, et al., 2016c). Mancuso et al. (2019) observed a positive correlation between net calcification rates and increasing solar radiation, sea surface temperature and salinity and decreasing Chlorophyll concentration in immature and mature shells. Moving far from the Po delta towards South, warmer seawater, low fluctuations in salinity and oligotrophic conditions suggested that these environmental conditions may be most favourable for the clam *C. gallina*, leading to higher net calcification rates (Mancuso et al., 2019a). Net calcification rates were significantly reduced in sites around the Po delta, possibly due to a lower temperature and reduced salinity that increase the energetic costs of shell formation with decreasing aragonite saturation state (Mancuso et al., 2019a).

The discrepancy between this work and the previous ones regarding growth parameters (no variation of linear extension and net calcification rate with SST found in this study, VS Positive correlation with SST found in Mancuso et al.) suggested that these parameters are not only dependent on physical environmental factors (SST, salinity, aragonite saturation, sediments and nutrient supply) but are affected by a complex interplay between physical, biological and physiological factors, making *C. gallina* response less predictable to changing environmental parameters. Besides, local environmental parameters seemed to have a different influence on the biomineralization rate of mature shells compared to immature ones, likely due to different growth and metabolic rates (Gizzi, Caccia, Simoncini, Mancuso, Reggi, Fermani, Brizi, Fantazzini, Stagioni, Falini, et al., 2016c; Ries et al., 2009b).

In the context of climate change and ocean warming, the phenotypic plasticity observed in this work for the populations living in the Po-Adriatic system may lead us to think that *C. gallina* can adapt to changing environmental scenarios. Nonetheless, it should be noted that the results obtained from this study refer to a time scale of thousands of years, from the middle Holocene to nowadays, with no relevant anthropogenic pressure in the area until a few centuries ago. Starting from 2.0 ky BP, the anthropogenic influence on the Po Delta system began to grow till it became dominant around the 17th century when river diversion and channel stabilization led to the growth of the modern Delta (Amorosi, Barbieri, Bruno, Campo, Drexler, Hong, & Fielding, 2019). These human interventions dictated an increase in sediments runoff, eutrophication events, and anoxic events, increasing the instability and stress of the nearshore environments, whose effects on *C. gallina* skeletal construction cannot be excluded.

Overall, we can state that temperature can be considered as a complex gradient that influences calcium carbonate ($CaCO_3$) availability, affecting the energy cost of shell formation (S. Watson, 2012), and influencing biotic and abiotic components in the marine environment, such as the presence of phytoplankton both in terms of density and distribution and dissolved oxygen concentration (M Ramón, 1992). The concentration of food supply is one of the factors that most influence the growth of filter-feeding bivalves (DP Häder, 2007). Furthermore, temperature has indirectly affected the geomorphologic configuration of the study area, shaping the structure of the Po River Delta, whose flow strongly influenced the distribution of phytoplankton and reduced salinity values, exposing *C. gallina* to seasonal solid variations (Russo et al., 2002). The growing eutrophication also influences this complex environmental scenario. The records of the Po River nutrient load (Monari et al., 2007), seawater transparency (Siedlecki et al., 2017b), and anoxic events of the past decades (Sanders et al., 2018) all suggest that the anthropogenic nutrient input is increasingly affecting the marine environment. Slow growth rates associated with eutrophicated habitats have been recorded previously for the bivalve *Cerastoderma edule* (Marchetti et al., 1989) and the bivalve *Austrovenus stutchburyi* (Loo & Rosenberg, 1989). Anthropogenic pressure is also exerted in terms of solid fishing effort. This, added to the many other cited factors, contributes to creating a complex environmental scenario that increases the difficulty in trying to predict the response of *C. gallina* to changing environmental parameters.

Conclusion

This study integrates the results of the previous work Cheli et al 2021 by adding a description of long-term growth dynamics of *Chamelea gallina* populations of the Northern Adriatic Sea, from the middle Holocene to nowadays. This made possible to depict a more complete description of the overall biomineralization process (including biometry, skeletal parameters, microstructure characterization and calcification) of *C. gallina* and how it was influenced by variations in temperature and environmental context over a millennial time scale.

At a macro-scale level *C. gallina* shells were affected by changes in seawater temperature, showing a denser, less porous shells in specimens from past warmer settings, respect to modern samples. Surprisingly those differences were not reflected on *C. gallina* growth in the examined time period, suggesting a possible long-term phenotypic adaptive capacity. The observed trends in both skeletal and growth parameters with SST variation remained consistent even when analysing sexually mature and immature individuals separately, indicating only a minor influence of sexual maturation in the biomineralization behaviour during organism life.

These findings are in disagreement with results produced by previous studies on *C. gallina* biomineralization, highlighting how the combination of specific biotic and abiotic conditions at the local level can strongly influence the final organism response. Using different and complementary approaches like laboratory experiments, field studies and analysis of the fossil record can ultimately help to understand the weight of different environmental factors and their combined effect, together improving our understanding of the response of this economically relevant species to a changing environment in face to seawater warming.

Acknowledgments

This study is a partial fulfillment of the requirements for a PhD thesis of A. Cheli the PhD Course of Innovative Technologies and Sustainable Use of Mediterranean Sea Fishery and Biological Resources (FishMed-PhD) (University of Bologna, Italy).

Figures and tables

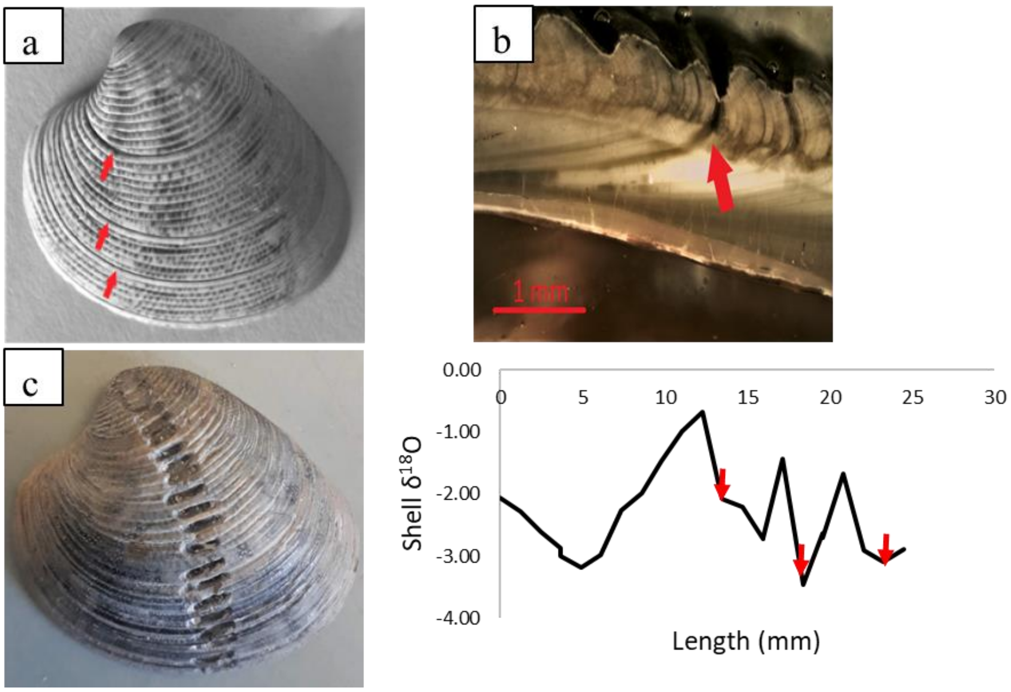

Figure 1. **Shell ageing methods**. (a) external growth rings; (b) Internal annual growth band in the shell section; (c) Samples for shell oxygen isotope analysis, collected along the growth axis; age is indicated by the sequence of lower (summer) and higher (winter) δ18O values recorded by the shells, as visible in the graph.

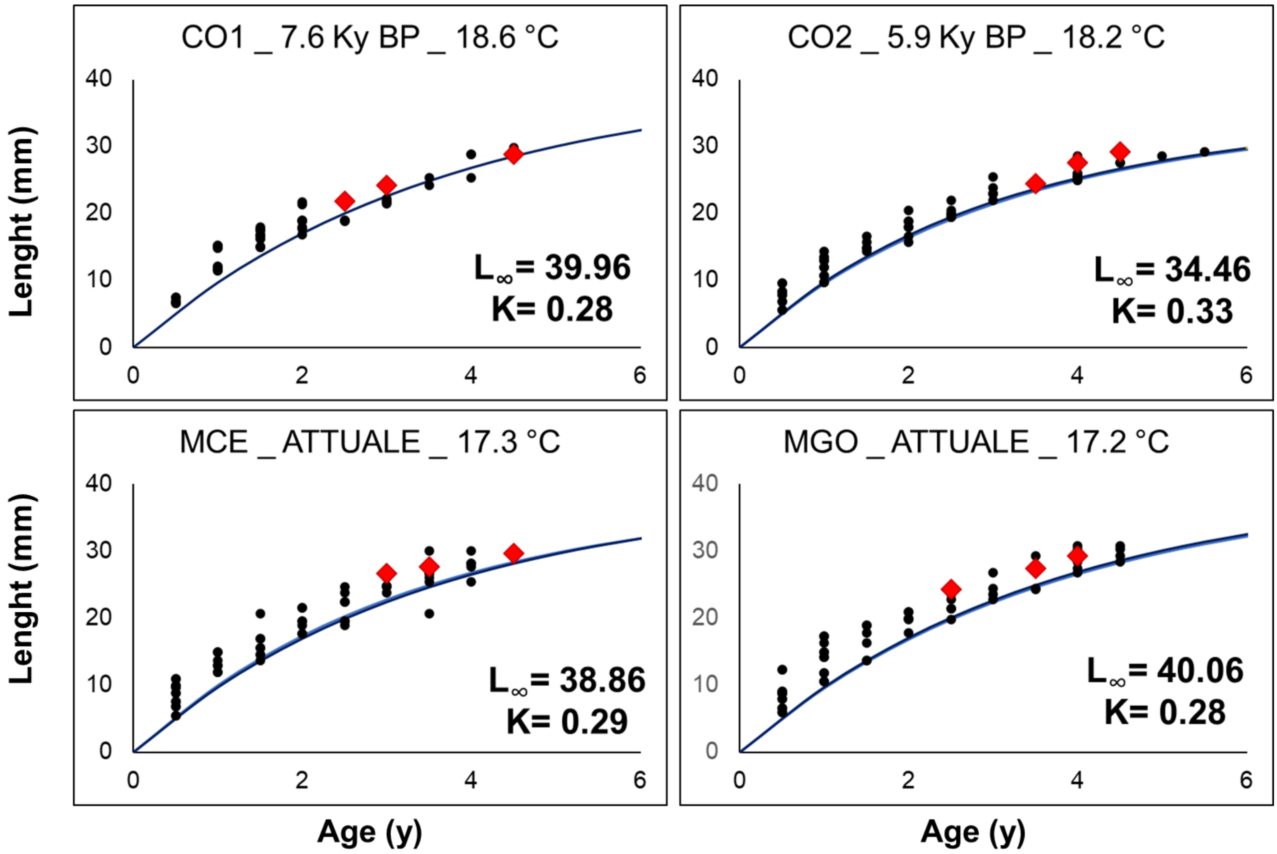

Figure 2. Von Bertalanfy growth curves. The generalised generalized age-length von Bertalanfy

growth curve in each horizon was obtained by all data from the two ageing methods (counting external rings and internal rings). Red diamonds are the ages obtained from the $\delta^{18}O$ profiles along the shell growth axis and are figured as validation to the counting ageing methods fitting the curves. L_{inf}: asymptotic length (maximum expected length in the population); K: growth constant

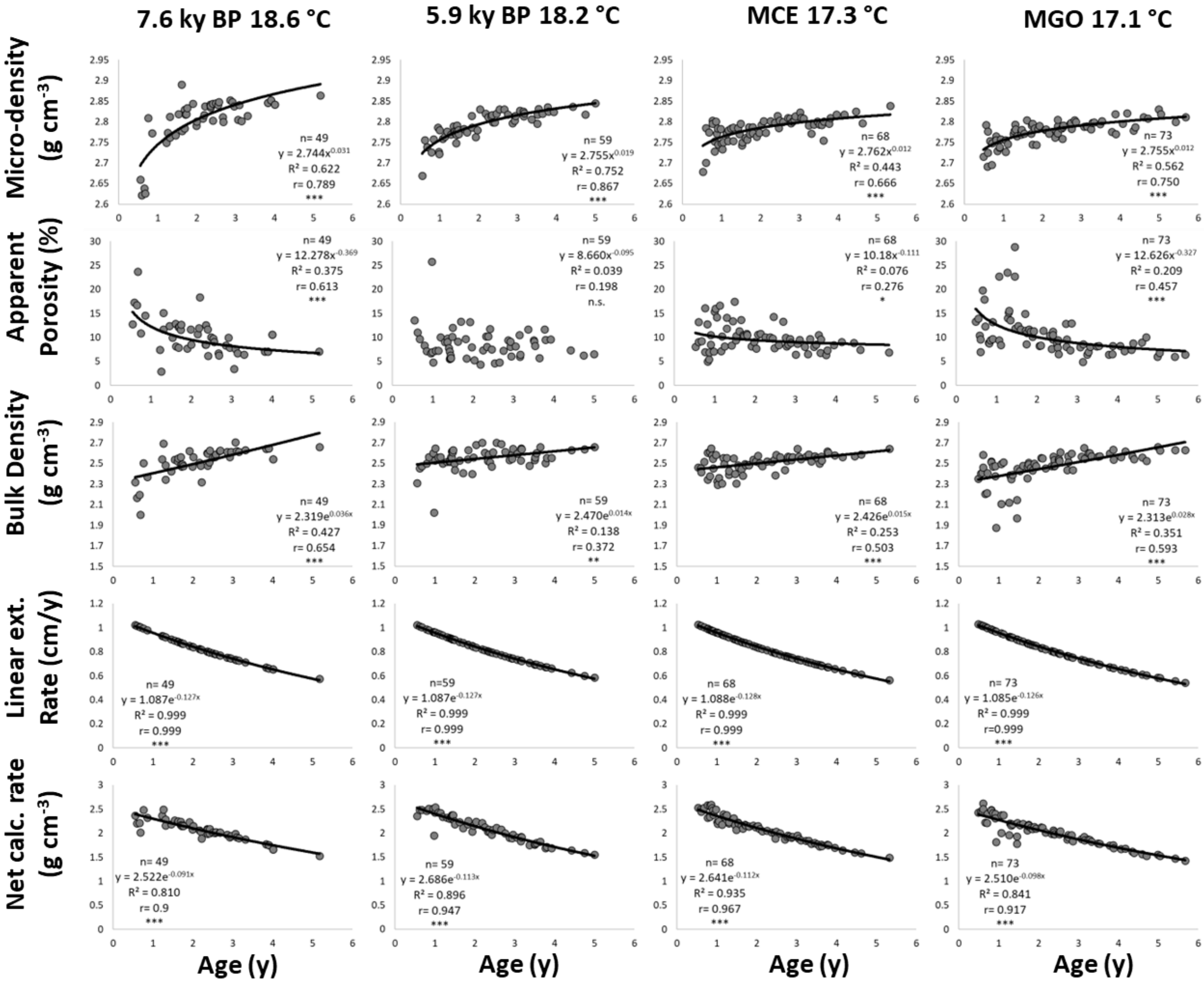

Figure 3. Correlation of the skeletal and growth parameters with shell age in the different horizons; n = number of valves; r = Spearman coefficient of determination; n.s. not significant, * $p<0.05$; ** $p<0.01$; *** $p<0.001$.

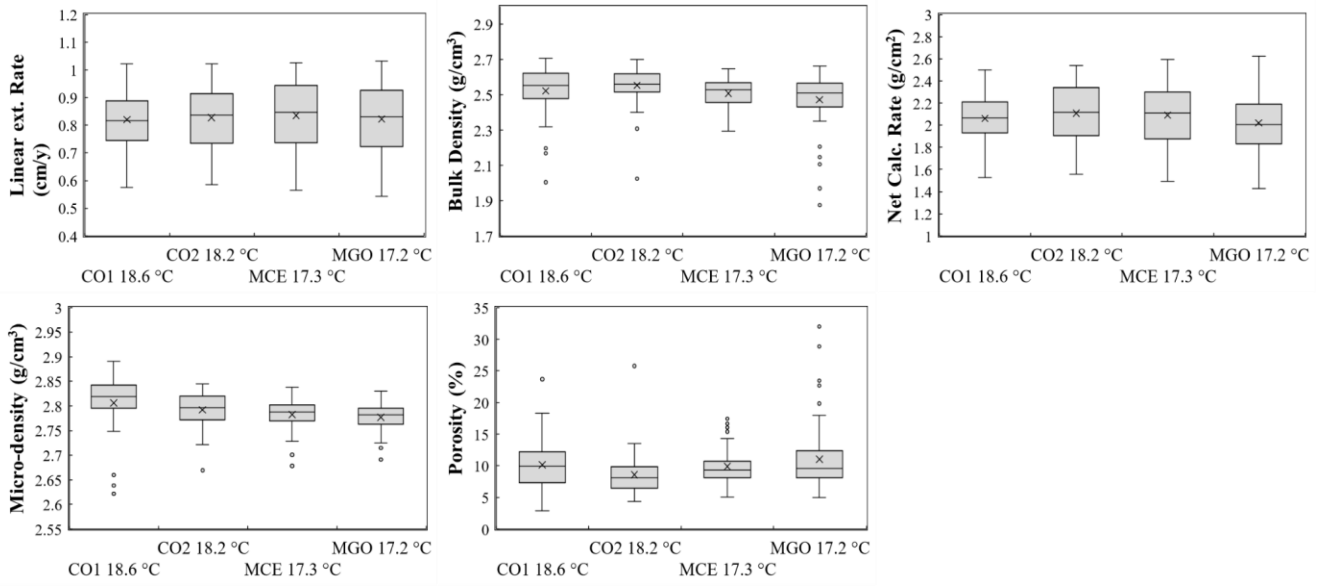

Figure 4. Variation of shell growth and skeletal parameter among horizons

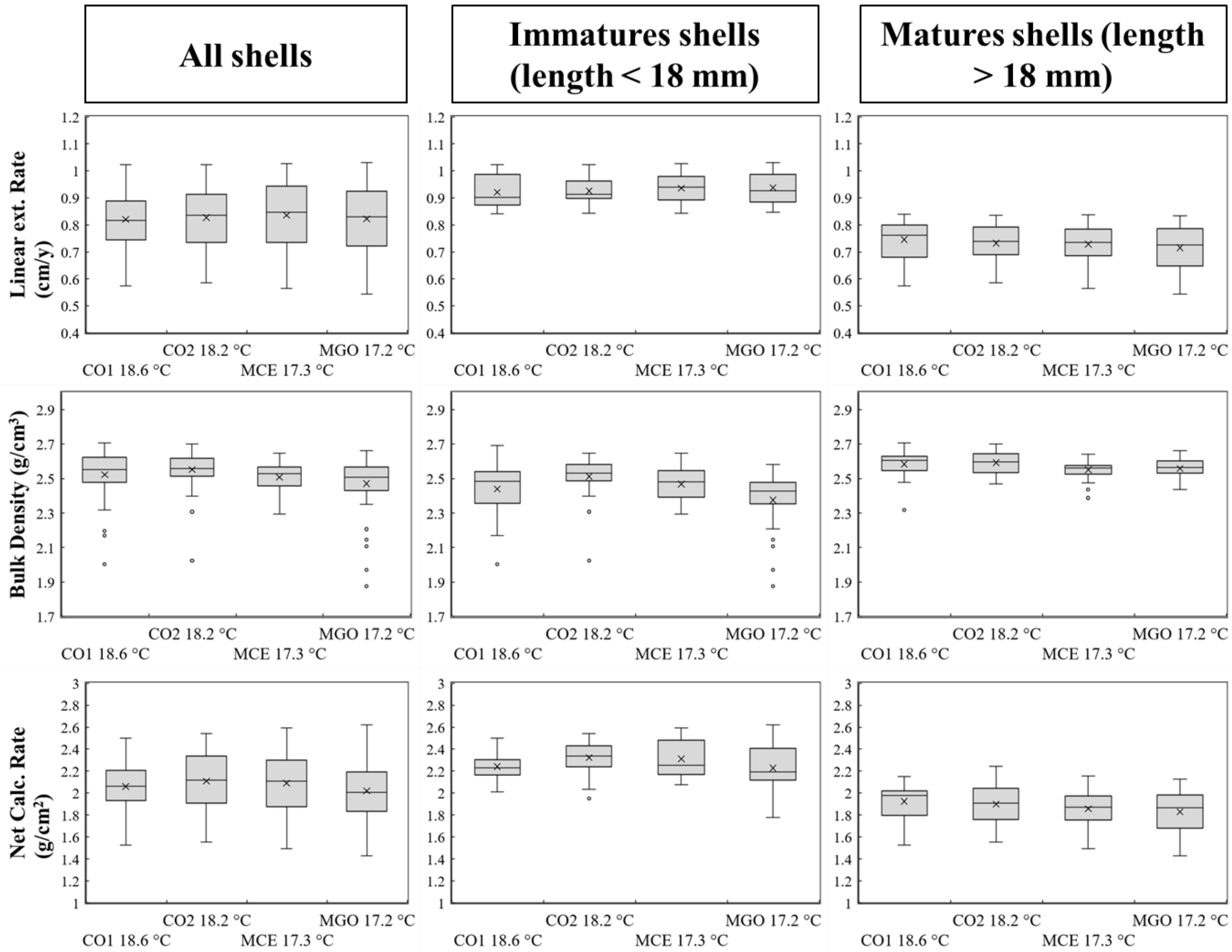

Figure 5. Variation of shell skeletal parameter among horizons considering different age classes

Horizon	n	14C Age (ky BP)	SST (°C)	Generalised VBGF	
				Linf	k
CO1	49	7.6 ± 0.1	18.6 ± 0.4	38.27	0.29
CO2	59	5.9 ± 0.1	18.2 ± 0.3	34.46	0.33
MCE	68	modern	17.3 ± 0.1	38.86	0.29
MGO	73	modern	17.1 ± 0.1	40.06	0.28
KW			***	n.s.	n.s.

Table 1. Calibrated radiocarbon age, sea surface temperature (SST) and Von Bertalanffy growth parameter. Values for each horizon in chronological order. Radiocarbon measurements are reported in years `before present' (BP). L_{inf} and K estimated from the generalised Von Bertalanffy growth function by pooling the data for external and internal bands. n = number of collected specimens. K-W = Kruskal-Wallis equality-of-populations rank test; n.s. not significant, *** p < 0.001.

Horizon	Length (mm)	Micro-density (g/cm3)	Apparent Porosity (%)	Bulk Density (g/cm3)	Linear extension rate (cm/y)	Net calcifcation (g/cm2 y)
CO1	17.6 ± 0.9	2.81 ± 0.01	10.17 ± 0.55	2.52 ± 0.02	0.84 ± 0.01	2.1 ± 0.03
CO2	17.2 ± 0.8	2.79 ± 0.01	8.58 ±0.42	2.55 ± 0.01	0.82 ± 0.02	2.08 ± 0.04
MCE	16.7 ± 0.8	2.78 ± 0.01	9.87 ± 0.34	2.51 ± 0.01	0.85 ± 0.01	2.12 ± 0.03
MGO	17.3 ± 0.8	2.78 ± 0.01	11.01 ± 0.59	2.47 ± 0.02	0.84 ± 0.01	2.08 ± 0.03
KW	n.s.	***	**	***	n.s.	n.s.

Table 2. Mean value and standard error of shell skeletal and growth parameters. Values for each horizon in chronological order. K-W = Kruskal-Wallis equality-of-populations rank test; n.s. not significant, ** p<0.01, *** p < 0.001.

	Horizon	n	Length (mm)	Micro-density (g/cm3)	Apparent Porosity (%)	Bulk Density (g/cm3)	Linear extension rate (cm/y)	Net calcifcation (g/cm2 y)
Immature shell	CO1	24	12.6 ± 0.7	2.78 ± 0.014	11.81 ± 0.8	2.45 ± 0.03	0.9 ± 0.01	2.22 ± 0.03
	CO2	31	12.1 ± 0.5	2.77 ± 0.006	8.89 ± 0.7	2.52 ± 0.02	0.91 ± 0.01	2.32 ± 0.03
	MCE	38	11.4 ± 0.6	2.77 ± 0.004	10.67 ± 0.5	2.47 ± 0.01	0.93 ± 0.01	2.3 ± 0.03
	MGO	38	11.5 ± 0.6	2.76 ± 0.004	13.54 ± 0.9	2.39 ± 0.03	0.93 ± 0.01	2.22 ± 0.03
	KW		n.s.	***	***	***	n.s.	n.s.
Mature shell	CO1	25	22.2 ± 0.6	2.84 ± 0.004	8.60 ± 0.6	2.59 ± 0.02	0.74 ± 0.01	1.90 ± 0.03
	CO2	28	22.8 ± 0.5	2.82 ± 0.002	8.24 ± 0.4	2.59 ± 0.01	0.73 ± 0.01	1.87 ± 0.03
	MCE	30	23.6 ± 0.6	2.80 ± 0.003	8.86 ± 0.3	2.55 ± 0.01	0.72 ± 0.01	1.83 ± 0.03
	MGO	35	23.1 ± 0.5	2.79 ± 0.002	8.27 ± 0.3	2.56 ± 0.01	0.71 ± 0.01	1.8 ± 0.03
	KW		n.s.	***	n.s.	***	n.s.	n.s.

Table 3. **Mean value and standard error of shell skeletal and growth parameters for immature and mature shells.** Values for each horizon in chronological order. K-W = Kruskal-Wallis equality-of-populations rank test; n.s. not significant, *** p < 0.001.

Supplementary material

Specimens' collection (from Cheli et. al 2021)

In particular, the two horizons from the Holocene were collected from core 205-S6 (Comacchio, 44°68'N, 12°15'E), respectively, at depths of 17.2 m (code "CO1") and 13.2 m (code "CO2"). Both horizons came from shoreface depositional environments characterized by sandy substrates and estimated water depth between 5 and 10 m.

Modern samples of *C. gallina* were collected in the Northern Adriatic Sea off the coast of Goro (code "MGO"; 44°75'N, 12°43'E) and Cervia (code "MCE"; 44°30'N, 12°40'E), two sites near to the extraction areas of cores used in this study and distant about fifty kilometers away from each other. Samplings were performed during scuba diving and using Van Veen Grab on the sandy bottom, ranging from 1 to 5 m water depth. Sampling operations were confined to the top-most 10 cm of the taphonomically active zone (TAZ) of the sea bottom. This sampling allowed us to collect a time-averaged record of shells estimated in tens of years, following the deposition rates reported in Trincardi *et al*. This allowed a better comparison between modern and sub-fossil horizons, the latter consisting of shells from tens of years. No living organism was collected for this study.

Only shells of 5–30 mm in length (the maximum distance on the anterior-posterior axis) were considered for the analyses. The lower size limit was defined by the technical difficulties in obtaining reliable measurements in very small specimens. The upper size limit was due to the difficulty of collecting whole shells over 30 mm in the sub-fossil horizons with 90 mm cores diameter.

Before any measurements, each valve was cleaned with a toothbrush and soaked in distilled water for two hours to remove any external residue on the shell's surfaces. In addition, valves from modern settings were immersed in a solution of distilled water and hydrogen peroxide (5 vol.%) for 24 h to eliminate any traces of organic material (e.g., epibionts). Then, the valves were dried in an oven at 37°C for one night to remove any moisture that may influence subsequent measurements.

Environmental parameters

Sea surface temperature (SST) for the Adriatic Sea of modern settings was obtained from the global ocean OSTIA sea surface temperature and sea ice analysis databank (https://ghrsst-pp.metoffice.gov.uk). Mean annual SST was calculated from daily values from January 2010 to

December 2019 (number of daily values = 3651 for each site). SST estimates for sub-fossil horizons were based on the Alkenones unsaturation index, a widely applied proxy for past SST and obtained from the high-resolution SST record of the past 10,000 years for the central-northern Mediterranean Sea (Gulf of Lion; (Jalali et al., 2016), considered a comparable physiographic setting for the North Adriatic Sea.

Shell biometrics and skeletal parameters

Shell length (the maximum distance on the anterior-posterior axis) was measured using ImageJ software after data capture of each shell shape with a scanner (Acer Acerscan Prisa 620 ST 600 dpi), and dry shell weight was measured using an analytical balance (±0.1 mg).

Between 50 and 70 shells of different sizes from each site were used for the analyses after being divided into two groups according to their size: immature shells (up to 18 mm) and mature ones (over 18 mm).

Skeletal parameters were measured by buoyant weight (BW) analysis using a density determination kit Ohaus Explorer Pro balance (± 0.1 mg; Ohaus Corp., Pine Brook, NJ, USA) as reported in Gizzi *et al*.

The BW measurement was repeated three times, and the average was considered for statistical analysis. The BW technique allowed us to estimate the variable of interest:

i. micro-density (mass per unit volume of the material which composes the shell, excluding the volume of pores; $g \cdot cm^{-3}$);
ii. apparent porosity: the volume of pores connected to the external surface (%);
iii. bulk density: shell mass/volume ratio, including the volume of pores, the volume of pores; $g \cdot cm^{-3}$).

References

Addadi, L., & Weiner, S. (2014). Biomineralization: mineral formation by organisms. *Physica Scripta*, *89*(9), 098003. https://doi.org/10.1088/0031-8949/89/9/098003

Amorosi, A., Barbieri, G., Bruno, L., Campo, B., Drexler, T., Hong, W., & Fielding, C. (2019). Three-fold nature of coastal progradation during the Holocene eustatic highstand, Po Plain, Italy–close correspondence of stratal character with distribution patterns. *Sedimentology*, *66*.

Amorosi, A., Colalongo, M., Fusco, F., Pasini, G., & Fiorini, F. (1999). Glacio-eustatic control of continental-shallow marine cyclicity from late quaternary deposits of the southeastern Po Plain, northern Italy. *Quat Res*, *52*.

Bemis, B. E., Spero, H. J., Bijma, J., & Lea, D. W. (1998). Reevaluation of the oxygen isotopic composition of planktonic foraminifera: Experimental results and revised paleotemperature equations. *Paleoceanography*, *13*(2), 150–160. https://doi.org/10.1029/98PA00070

Bergström, P., & Lindegarth, M. (2016). Environmental influence on mussel (Mytilus edulis) growth – A quantile regression approach. *Estuar. Coast. Shelf Sci.*, *171*, 123–132. https://doi.org/10.1016/j.ecss.2016.01.040

Chauvaud, L., Lorrain, A., Dunbar, R. B., Paulet, Y.-M., rard Thouzeau, G., ric Jean, F., Guarini, J.-M., Mucciarone, D., Lorrain, A., Dunbar, R. B., Paulet, Y., Thouzeau, G., Jean, F., Guarini, J., & Mucciarone, D. (2005). Shell of the Great Scallop Pecten maximus as a high-frequency archive of paleoenvironmental changes. *Geochemistry, Geophysics, Geosystems*, *6*(8). https://doi.org/10.1029/2004GC000890

Cheli, A., Mancuso, A., Azzarone, M., Fermani, S., Kaandorp, J., Marin, F., Montroni, D., Polishchuk, I., Prada, F., Stagioni, M., Valdré, G., Pokroy, B., Falini, G., Goffredo, S., & Scarponi, D. (2021). Climate variation during the Holocene influenced the skeletal properties of Chamelea gallina shells in the North Adriatic Sea (Italy). *PLOS ONE*, *16*(3), e0247590. https://doi.org/10.1371/JOURNAL.PONE.0247590

Clarke, A. (1993). Temperature and extinction in the sea: a physiologist's view. *Paleobiology*, *19*, 499–518.

Cooley, S. R., & Doney, S. C. (2009). Anticipating ocean acidification's economic consequences for commercial fisheries. *Environmental Research Letters*, *4*(2). https://doi.org/10.1088/1748-9326/4/2/024007

Correggiari, A., Cattaneo, A., & Trincardi, F. (2005). The modern Po Delta system: Lobe switching and asymmetric prodelta growth. *Marine Geology*, *222–223*(1–4), 49–74. https://doi.org/10.1016/J.MARGEO.2005.06.039

Dalgi, G., Okumuş, I., & Karaycel, S. (2010). The effect of fishing on growth of the clam Chamelea gallina (Bivalvia: Veneridae) from the Turkish Black Sea coast. *Journal of the Marine Biological Association of the United Kingdom*, *90*(2), 261–265. https://doi.org/10.1017/S0025315409000939

Degobbis, D., Gilmartin, M., & Revelante, N. (1986). An annotated nitrogen budget calculation for the northern Adriatic Sea. *Marine Chemistry*, *20*(2), 159–177. https://doi.org/10.1016/0304-4203(86)90037-X

Dillon, E. M., Lafferty, K. D., McCauley, D. J., Bradley, D., Norris, R. D., Caselle, J. E., DiRenzo, G. v., Gardner, J. P. A., & O'Dea, A. (2020). Dermal denticle assemblages in coral reef sediments correlate with conventional shark surveys. *Methods in Ecology and Evolution*, *11*(3), 362–375. https://doi.org/10.1111/2041-210X.13346

DP Häder, H. K. R. S. R. W. (2007). Effects of solar UV radiation on aquatic ecosystems and interactions with climate change. *Photochem. Photobiol. Sci.*, *6*, 267–285.

Dunca, E., Schöne, B. R., & Mutvei, H. (2005). Mutvei's solution: An ideal agent for resolving microgrowth structures of biogenic carbonates. *Palaeogeogr. Palaeoclimatol. Palaeoecol.*, *228*(1–2), 149–166. https://doi.org/10.1016/j.palaeo.2005.03.050

E Arneri, G. G. R. P. B. A. (1995). Age and growth of Chamelea gallina (Bivalvia: Veneridae) in the Central Adriatic Sea obtained by thin sections. *Rapp. Comm. Int. Mer Médit*, *34*, 17.

Fitzer, S. C., Cusack, M., Phoenix, V. R., & Kamenos, N. A. (2014). Ocean acidification reduces the crystallographic control in juvenile mussel shells. *Journal of Structural Biology*, *188*(1), 39–45. https://doi.org/10.1016/J.JSB.2014.08.007

Fitzer, S. C., Vittert, L., Bowman, A., Kamenos, N. A., Phoenix, V. R., & Cusack, M. (2015). Ocean acidification and temperature increase impact mussel shell shape and thickness: Problematic for protection? *Ecology and Evolution*, *5*(21), 4875–4884. https://doi.org/10.1002/ECE3.1756

Fox, D. L., & Coe, W. R. (1943). Biology of the California sea-mussel (Mytilus californianus). II. Nutrition, metabolism, growth and calcium deposition. *Journal of Experimental Zoology*, *93*(2), 205–249. https://doi.org/10.1002/JEZ.1400930204

Gaspar, M. B., Pereira, A. M., Vasconcelos, P., & Monteiro, C. C. (2004). Age and growth of Chamelea gallina from the Algarve coast (southern Portugal): Influence of seawater temperature and gametogenic cycle on growth rate. *Journal of Molluscan Studies*, *70*(4), 371–377. https://doi.org/10.1093/MOLLUS/70.4.371

Gazeau, F., Parker, L. M., Comeau, S., Gattuso, J. P., O'Connor, W. A., Martin, S., Pörtner, H. O., & Ross, P. M. (2013). Impacts of ocean acidification on marine shelled molluscs. *Marine Biology*, *160*(8), 2207–2245. https://doi.org/10.1007/S00227-013-2219-3

Gizzi, F., Caccia, M. G., Simoncini, G. A., Mancuso, A., Reggi, M., Fermani, S., Brizi, L., Fantazzini, P., Stagioni, M., Falini, G., Piccinetti, C., & Goffredo, S. (2016). Shell properties of commercial clam Chamelea gallina are influenced by temperature and solar radiation along a wide latitudinal gradient. *Scientific Reports*, *6*. https://doi.org/10.1038/SREP36420

Grazioli, E., Guerranti, C., Pastorino, P., Esposito, G., Bianco, E., Simonetti, E., Rainis, S., Renzi, M., & Terlizzi, A. (2022). Review of the Scientific Literature on Biology, Ecology, and Aspects Related to the Fishing Sector of the Striped Venus (Chamelea gallina) in Northern Adriatic Sea. *Journal of Marine Science and Engineering*, *10*(9), 1328. https://doi.org/10.3390/JMSE10091328/S1

Hahn, S., Rodolfo-Metalpa, R., Griesshaber, E., Schmahl, W. W., Buhl, D., Hall-Spencer, J. M., Baggini, C., Fehr, K. T., & Immenhauser, A. (2012). Marine bivalve shell geochemistry and ultrastructure from modern low pH environments: Environmental effect versus experimental bias. *Biogeosciences*, *9*(5), 1897–1914. https://doi.org/10.5194/BG-9-1897-2012

Hall-Spencer, J. M., & Harvey, B. P. (2019). Ocean acidification impacts on coastal ecosystem services due to habitat degradation. *Emerging Topics in Life Sciences*, *3*(2), 197–206. https://doi.org/10.1042/ETLS20180117

Hofmann, G. E., Barry, J. P., Edmunds, P. J., Gates, R. D., Hutchins, D. A., Klinger, T., & Sewell, M. A. (2010). The effect of Ocean acidification on calcifying organisms in marine ecosystems: An organism-to-ecosystem perspective. *Annual Review of Ecology, Evolution, and Systematics, 41*, 127–147. https://doi.org/10.1146/ANNUREV.ECOLSYS.110308.120227

Hofmann, G. E., Smith, J. E., Johnson, K. S., Send, U., Levin, L. A., Micheli, F., Paytan, A., Price, N. N., Peterson, B., Takeshita, Y., Matson, P. G., de Crook, E., Kroeker, K. J., Gambi, M. C., Rivest, E. B., Frieder, C. A., Yu, P. C., & Martz, T. R. (2011). High-frequency dynamics of ocean pH: A multi-ecosystem comparison. *PLoS ONE*, *6*(12). https://doi.org/10.1371/JOURNAL.PONE.0028983

Kidwell, S. M. (2015). Biology in the Anthropocene: Challenges and insights from young fossil records. *Proceedings of the National Academy of Sciences*, *112*(16), 4922–4929. https://doi.org/10.1073/PNAS.1403660112

Klein, R. T., Lohmann, K. C., & Thayer, C. W. (1996). SrCa and 13C12C ratios in skeletal calcite of Mytilus trossulus: Covariation with metabolic rate, salinity, and carbon isotopic composition of seawater. *Geochimica et Cosmochimica Acta*, *60*(21), 4207–4221. https://doi.org/10.1016/S0016-7037(96)00232-3

Kroeker, K. J., Kordas, R. L., Crim, R. N., & Singh, G. G. (2010). Meta-analysis reveals negative yet variable effects of ocean acidification on marine organisms. *Ecology Letters*, *13*(11), 1419–1434. https://doi.org/10.1111/J.1461-0248.2010.01518.X

Kroeker, K. J., Sanford, E., Rose, J. M., Blanchette, C. A., Chan, F., Chavez, F. P., Gaylord, B., Helmuth, B., Hill, T. M., Hofmann, G. E., McManus, M. A., Menge, B. A., Nielsen, K. J., Raimondi, P. T., Russell, A. D., & Washburn, L. (2016). Interacting environmental mosaics drive geographic variation in mussel performance and predation vulnerability. *Ecology Letters*, *19*(7), 771–779. https://doi.org/10.1111/ELE.12613

Loo, L. O., & Rosenberg, R. (1989). Bivalve suspension-feeding dynamics and benthic-pelagic coupling in an eutrophicated marine bay. *Journal of Experimental Marine Biology and Ecology*, *130*(3), 253–276. https://doi.org/10.1016/0022-0981(89)90167-6

Lutz, R. A., & Rhoads, D. C. (1980). *Growth patterns within the molluscan shell: an overview*. 750.

M Ramón, C. R. (1992). Age determination and shell growth of Chamelea gallina (Bivalvia: Veneridae) in the western Mediterranean. *Mar. Ecol. Prog. Ser.*, *89*, 15–23.

Mackenzie, C. L., Ormondroyd, G. A., Curling, S. F., Ball, R. J., Whiteley, N. M., & Malham, S. K. (2014). Ocean Warming, More than Acidification, Reduces Shell Strength in a Commercial Shellfish Species during Food Limitation. *PLOS ONE*, *9*(1), e86764. https://doi.org/10.1371/JOURNAL.PONE.0086764

Mancuso, A., Stagioni, M., Prada, F., Scarponi, D., Piccinetti, C., & Goffredo, S. (2019). Environmental influence on calcification of the bivalve Chamelea gallina along a latitudinal gradient in the Adriatic Sea. *Scientific Reports, 9*(1), 11198. https://doi.org/10.1038/S41598-019-47538-1

Marchetti, R., Provini, A., & Crosa, G. (1989). Nutrient load carried by the River Po into the Adriatic Sea, 1968–1987. *Marine Pollution Bulletin*, *20*(4), 168–172. https://doi.org/10.1016/0025-326X(89)90487-6

Monari, M., Serrazanetti, G. P., Foschi, J., Matozzo, V., Marin, M. G., & Cattani, O. (2007). Effects of salinity on the clam Chamelea gallina haemocytes. Part II: Superoxide dismutase response. *Marine Biology*, *151*(3), 1059–1068. https://doi.org/10.1007/S00227-006-0544-5/METRICS

Morello, E. B., Froglia, C., Atkinson, R. J. A., & Moore, P. G. (2005). Hydraulic dredge discards of the clam (Chamelea gallina) fishery in the western Adriatic Sea, Italy. *Fisheries Research*, *76*(3), 430–444. https://doi.org/10.1016/J.FISHRES.2005.07.002

Myrand, B., Tremblay, R., & Sévigny, J. M. (2002). Selection against blue mussels (Mytilus edulis L.) homozygotes under various stressful conditions. *Journal of Heredity*, *93*(4), 238–248. https://doi.org/10.1093/jhered/93.4.238

Nash, M. C., Opdyke, B. N., Troitzsch, U., Russell, B. D., Adey, W. H., Kato, A., Diaz-Pulido, G., Brent, C., Gardner, M., Prichard, J., & Kline, D. I. (2012). Dolomite-rich coralline algae in reefs resist dissolution in acidified conditions. *Nature Climate Change 2012 3:3*, *3*(3), 268–272. https://doi.org/10.1038/nclimate1760

Orban, E., di Lena, G., Nevigato, T., Casini, I., Caproni, R., Santaroni, G., & Giulini, G. (2007). Nutritional and commercial quality of the striped venus clam, Chamelea gallina, from the Adriatic sea. *Food Chemistry*, *101*(3), 1063–1070. https://doi.org/10.1016/J.FOODCHEM.2006.03.005

P Moura, M. G. C. M. (2009). Age determination and growth rate of a Callista chione population from the southwestern coast of Portugal. Aquat. *Biol.*, *5*, 97–106.

Pauly, M., Kamenos, N. A., Donohue, P., & LeDrew, E. (2015). Coralline algal Mg-O bond strength as a marine pCO2 proxy. *Geology*, *43*(3), 267–270. https://doi.org/10.1130/G36386.1

Pfister, C. A., Roy, K., Wootton, J. T., McCoy, S. J., Paine, R. T., Suchanek, T. H., & Sanford, E. (2016). Historical baselines and the future of shell calcification for a foundation species in a changing ocean. *Proceedings of the Royal Society B: Biological Sciences*, *283*(1832). https://doi.org/10.1098/RSPB.2016.0392

Pokroy, B., Fitch, A. N., Marin, F., Kapon, M., Adir, N., & Zolotoyabko, E. (2006). Anisotropic lattice distortions in biogenic calcite induced by intra-crystalline organic molecules. *Journal of Structural Biology*, *155*(1), 96–103. https://doi.org/10.1016/J.JSB.2006.03.008

Poulain, P. M. (2001). Adriatic Sea surface circulation as derived from drifter data between 1990 and 1999. *Journal of Marine Systems*, *29*(1–4), 3–32. https://doi.org/10.1016/S0924-7963(01)00007-0

Purroy, A., Milano, S., Schöne, B. R., Thébault, J., & Peharda, M. (2018). Drivers of shell growth of the bivalve, Callista chione (L. 1758) – Combined environmental and biological factors. *Mar. Environ. Res.*, *134*, 138–149. https://doi.org/10.1016/j.marenvres.2018.01.011

Ries, J. B., Cohen, A. L., & McCorkle, D. C. (2009). Marine calcifiers exhibit mixed responses to CO2-induced ocean acidification. *Geology*, *37*(12), 1131–1134. https://doi.org/10.1130/G30210A.1

Russo, A., Rabitti, S., & Bastianini, M. (2002). Decadal Climatic Anomalies in the Northern Adriatic Sea Inferred from a New Oceanographic Data Set. *Mar. Ecol.*, *23*(SUPPL. 1), 340–351. https://doi.org/10.1111/j.1439-0485.2002.tb00032.x

Sanders, T., Schmittmann, L., Nascimento-Schulze, J. C., & Melzner, F. (2018). High calcification costs limit mussel growth at low salinity. *Frontiers in Marine Science*, *5*(OCT), 352. https://doi.org/10.3389/FMARS.2018.00352/BIBTEX

Scarponi, D., & Kowalewski, M. (2004). Stratigraphic paleoecology: Bathymetric signatures and sequence overprint of mollusk associations from upper Quaternary sequences of the Po Plain, Italy. *Geology*, *32*(11), 989–992. https://doi.org/10.1130/G20808.1

Schöne, B. R., & Giere, O. (2005). Growth increments and stable isotope variation in shells of the deep-sea hydrothermal vent bivalve mollusk Bathymodiolus brevior from the North Fiji Basin, Pacific Ocean. *Deep-Sea Research Part I: Oceanographic Research Papers*, *52*(10), 1896–1910. https://doi.org/10.1016/J.DSR.2005.06.003

Schöne, B. R., & Gillikin, D. P. (2013). Unraveling environmental histories from skeletal diaries — Advances in sclerochronology. *Palaeogeography, Palaeoclimatology, Palaeoecology*, *373*, 1–5. https://doi.org/10.1016/J.PALAEO.2012.11.026

Schöne, B. R., Oschmann, W., Rössler, J., Freyre Castro, A. D., Houk, S. D., Kröncke, I., Dreyer, W., Janssen, R., Rumohr, H., & Dunca, E. (2003). North Atlantic Oscillation dynamics recorded in shells of a long-lived bivalve mollusk. *Geology*, *31*(12), 1037–1040. https://doi.org/10.1130/G20013.1

Siedlecki, S. A., Pilcher, D. J., Hermann, A. J., Coyle, K., & Mathis, J. (2017). The Importance of Freshwater to Spatial Variability of Aragonite Saturation State in the Gulf of Alaska. *Journal of Geophysical Research: Oceans*, *122*(11), 8482–8502. https://doi.org/10.1002/2017JC012791

Steyermark, A. C. (2002). A high standard metabolic rate constrains juvenile growth. *Zoology*, *105*(2), 147–151. https://doi.org/10.1078/0944-2006-00055

Telesca, L., Michalek, K., Sanders, T., Peck, L. S., Thyrring, J., & Harper, E. M. (2018). Blue mussel shell shape plasticity and natural environments: A quantitative approach. *Scientific Reports*, *8*(1). https://doi.org/10.1038/S41598-018-20122-9

Thomsen, J., & Melzner, F. (2010). Moderate seawater acidification does not elicit long-term metabolic depression in the blue mussel Mytilus edulis. *Marine Biology*, *157*(12), 2667–2676. https://doi.org/10.1007/S00227-010-1527-0

Tomašových, A., Albano, P. G., Fuksi, T., Gallmetzer, I., Haselmair, A., Kowalewski, M., Nawrot, R., Nerlović, V., Scarponi, D., & Zuschin, M. (2020). Ecological regime shift preserved in the Anthropocene stratigraphic record. *Proceedings of the Royal Society B*, *287*(1929). https://doi.org/10.1098/RSPB.2020.0695

v Moschino, M. M. (2006). Seasonal changes in physiological responses and evaluation of “well-being” in the Venus clam Chamelea gallina from the Northern Adriatic Sea. *Comp. Bioch. Physiol*, *145A*, 433–440.

Vermeij, G. J. (1976). Interoceanic differences in vulnerability of shelled prey to crab predation. *Nature*, *260*(5547), 135–136. https://doi.org/10.1038/260135A0

Vihtakari, M., Ambrose, W. G., Renaud, P. E., Locke, W. L., Carroll, M. L., Berge, J., Clarke, L. J., Cottier, F., & Hop, H. (2017). A key to the past? Element ratios as environmental proxies in two Arctic bivalves. *Palaeogeography, Palaeoclimatology, Palaeoecology*, *465*, 316–332. https://doi.org/10.1016/J.PALAEO.2016.10.020

Wahl, M., Buchholz, B., Winde, V., Golomb, D., Guy-Haim, T., Müller, J., Rilov, G., Scotti, M., & Böttcher, M. E. (2015). A mesocosm concept for the simulation of near-natural shallow underwater climates: The Kiel Outdoor Benthocosms (KOB). *Limnology and Oceanography: Methods*, *13*(11), 651–663. https://doi.org/10.1002/LOM3.10055

Waldbusser, G. G., Brunner, E. L., Haley, B. A., Hales, B., Langdon, C. J., & Prahl, F. G. (2013). A developmental and energetic basis linking larval oyster shell formation to acidification sensitivity. *Geophysical Research Letters*, *40*(10), 2171–2176. https://doi.org/10.1002/GRL.50449

Watson, S. (2012). Marine invertebrate skeleton size varies with latitude, temperature and carbonate saturation: implications for global change and ocean acidification. *Global Change Biol*, *18*, 3026–3038.

Wootton, J. T., & Pfister, C. A. (2012). Carbon System Measurements and Potential Climatic Drivers at a Site of Rapidly Declining Ocean pH. *PLoS ONE*, *7*(12). https://doi.org/10.1371/JOURNAL.PONE.0053396

Wootton, J. T., Pfister, C. A., & Forester, J. D. (2008). Dynamic patterns and ecological impacts of declining ocean pH in a high-resolution multi-year dataset. *Proceedings of the National Academy of Sciences of the United States of America*, *105*(48), 18848–18853. https://doi.org/10.1073/PNAS.0810079105

Chapter 4. Assessing biotic response to anthropogenic forcing using mollusc assemblages from the Po-Adriatic System (Italy) *(Published in GSL Special Publication "Conservation Palaeobiology of Marine Ecosystems")*

Assessing biotic response to anthropogenic forcing using mollusc assemblages from the Po-Adriatic System (Italy)

Daniele Scarponi*[1,4], Alexis Rojas[2], Rafał Nawrot[3], Alessandro Cheli[1,4], Michał Kowalewski[5]

[1]*Dipartimento di Scienze Biologiche, Geologiche e Ambientali, University of Bologna, 40126, Italy*

[2]*Department of Computer Science, University of Helsinki, 00560, Finland*

[3]*Department of Palaeontology, University of Vienna, 1090, Austria*

[4]*Fano Marine Center, The Inter-Institute Center for Research on Marine Biodiversity, Resources and Biotechnologies, 61032, Italy*

[5]*Florida Museum of Natural History, University of Florida, FL 32611, USA*

ORCID ID: D. Scarponi 0000-0001-5914-4947; A. Rojas 0000-0002-1063-9102; R. Nawrot 0000-0002-5774-7311; A. Cheli 0000-0002-4656-4632; M. Kowalewski 0000-0002-8575-4711.

***** Corresponding author, e-mail: daniele.scarponi@unibo.it

Abstract

Preserving adaptive capacities of coastal ecosystems in the Anthropocene requires an understanding of their natural variability prior to modern times. We quantified responses of nearshore mollusks assemblages to past environmental changes using 101 samples (~57300 specimens) retrieved from the subsurface Holocene succession and present-day seabed of the Po-Adriatic System (Italy). Present-day assemblages shifted in their faunal composition with respect to their mid-late Holocene counterparts. Major differences are observed in lower nearshore settings, where present-day samples show higher heterogeneity, reduced standardised richness, reduced relative abundance of *Lentidium mediterraneum*, and increased relative abundance of *Varicorbula gibba*, scavengers (genus *Tritia*), and deposit feeders (nuculid bivalves). A dominance of infaunal opportunistic species and shifts towards detritus-feeding and scavenging are often associated with disturbed benthic habitats. Our results suggest that the ongoing anthropogenic stressors (mainly bottom trawling and non-native species) are currently shifting benthic communities into novel states outside the range of natural variability archived in the fossil record.

Keywords: Conservation Palaeobiology, Mediterranean, Holocene, Anthropocene, Ecosystem services.

Introduction

In the last centuries, humans have been impacting the natural dynamics of the Earth system (Steffen et al., 2020), changing the rates and magnitudes of environmental processes and, by means of direct and indirect cascading effects (e.g., Heithaus et al., 2008), altering the distribution of organisms and structure of ecosystems across the globe. It has been estimated that more than half of the terrestrial biotas have been directly and strongly impacted by human activities (e.g., Mittermeier et al., 2003) such as urbanization, overexploitation of natural resources, and introduction of non-native species either for sustenance purposes or accidentally (IUCN, 2000). These processes, in turn, have led to habitat degradation, affecting the structure and functioning of ecosystems, and thus the overall biodiversity of the Earth. For continental biotas early warnings on the undesired effects of globalization and industrialization were documented since the last century (e.g., d'Arge and Kneese, 1972; Wilson, 1987) and were more readily observable than in the ocean (Dirzo et al., 2014). In the marine realm, researchers have started to document human-induced changes in marine and coastal ecosystems only more recently (Lenhan and Peterson, 1998; Newell and Ott, 1999; Kowalewski et al., 2000; Jackson et al., 2001; Kidwell, 2007; Lotze et al., 2006; Edelist et al., 2013; McCauley et al., 2015; Tomašových et al., 2019; Jouffray et al., 2020; Steiger et al., 2022). These studies documented that the long history of intensive human utilisation of ecosystem services in some areas (e.g., Adriatic Sea) exceeded the adaptive capacity of local biotas, with a potential risk of pushing modern ecosystems toward different ecological states and driving the decline of economically important species (Burgess et al., 2013; McCauley et al., 2015; Bargione et al., 2021). But, to what extent are present-day ecosystems or key species already being affected by human impacts? Will continuing anthropogenic pressures result in sustained ecosystem regime shifts or extinctions of key species in the near future?

To narrow the uncertainty in answering these questions, it is necessary to understand the variability of ecosystems or individual species under natural conditions, with no, or at most limited, human interference. Documenting the magnitude of past changes is essential for defining marine ecosystem baselines, which can be used to evaluate present-day ecosystem status, set realistic conservation goals, assess efficacy of restoration efforts, and mitigate future human impacts (e.g., Kowalewski et al., 2000; Jackson et al., 2001; Dietl et al., 2015). However, ecological studies provide a relatively short record by which to measure ecosystem changes, and disentangling present-day natural factors from anthropogenic forcing is often a challenging, if not impossible, task (e.g., Pitacco et al., 2019). Geohistorical data, including the youngest fossil record, are thus needed to understand the status and variability of marine ecosystems prior to major phases of human impact (Kowalewski et al., 2000; Jackson et al., 2001; Lotze et al., 2006, 2011; Dietl and Flessa, 2011; Kidwell and Tomašových, 2013; Kidwell, 2015).

Here, we focused on the Adriatic Sea, which is part of the Mediterranean basin—a global hotspot of marine biodiversity due to its exceptional rates of endemism combined with a relatively large spatial extent (Myers et al., 2000; Coll et al., 2010; CEPF, 2022). At the same time the Adriatic Sea is being affected by multiple anthropogenic stressors and has already been highly impacted by human activities (e.g., Furlan et al., 2019 and references therein). Habitat loss and degradation, pollution, eutrophication, overfishing, and invasive species are major causes of changes in the Adriatic coastal ecosystems, with many of these pressures operating for decades or centuries (e.g., Coll et al., 2010; Lotze et al., 2011).

In this study, aimed at providing a deeper historical perspective, we compared mid-late Holocene assemblages preserved in the subsurface stratigraphic record of the Po coastal plain (Northern Italy; Fig. 1) with surficial assemblages that accumulated along the Po Delta and Emilia Romagna coastline during the Anthropocene (*sensu* Crutzen, 2002 and references therein). To ensure environmental comparability through time, the study focused on aggrading-to-prograding shallow marine and coarse-grained successions of the Po-Adriatic System. Specifically, we evaluated changes in the composition of mollusc assemblages between the present-day fluvial influenced coastal shoreface and delta front settings with sustained sedimentary inputs (hereafter referred to as “nearshore”) and their mid-late Holocene counterparts representing a time interval when anthropogenic pressure were notably less significant (between ~6 and 0.5 kyr cal BP i.e., prior to the early modern period). This study contributes to the area of near-time Conservation Palaeobiology that provides the framework against which to evaluate extant biotic dynamics (Dietl et al., 2015).

Background

Near-time Conservation Palaeobiology in its role of synthetic discipline helping the conservation of ecosystem functions uses fossil archives to define the reference condition (baseline) of an ecosystem (or its components) against which to compare modern ecological structure of the same ecosystem (Flessa, 2002). Detected changes should aid in predicting future states of ecosystems and populations in a scenario of increasing global warming and anthropogenic impacts (Kowalewski, 2001; Currano et al., 2008, 2016; Dietl and Flessa, 2017; Tyler and Schneider, 2018; Slater et al., 2022). This role is especially needed in highly anthropized areas, like the Adriatic, one of the most impacted basins of the Mediterranean Sea (e.g., Furlan et al., 2019). In this region, Conservation Palaeobiology approach has been used extensively to document both biotic changes through time, and to disentangle natural vs. anthropogenic drivers of these changes (Barmawidjaja et al., 1995; Scarponi et al., 2017a; Schnedl et al., 2018; Gallmetzer et al., 2019; Tomašových et al., 2021; Barbieri et al., 2021; Cheli et al., 2021).

Our work builds directly on previous studies by Kowalewski et al. (2015) and Scarponi et al. (2022). The first study, using macrobenthic fossil assemblages from the subsurface marine succession of the Po coastal plain evaluated quantitatively ecosystem changes at the coarse spatial scale (multiple depositional systems) across the Late Pleistocene and Holocene interglacials and contrasted such changes against the data available for present-day assemblages of the Northern Adriatic Sea. Specifically, the study focused on two stratigraphic units, dominated by a large suite of coastal, shallow-marine, and deltaic deposits, documenting the present (pre-Anthropocene) and last interglacial conditions of the Po-Adriatic System. Quantitative comparisons were conducted at very coarse spatial and environmental scales by merging data from all marine depositional systems recorded within each time-period. Kowalewski et al. (2015) observed high congruence of mollusc fossil assemblages from the penultimate and the current interglacial time intervals, and attributed this concordant pattern to either a resilient or persistent response of the Adriatic benthic communities. The recurrence of the same community composition in two distinct stratigraphic units separated by ~100.000 years (i.e., from the Late Pleistocene and Holocene) can indicate either ecological persistence, if associations continue through the perturbation, or strong resilience, if the community shifts to a novel state upon perturbation, but then rebounds to its previous state with the return of pre-disturbance environmental conditions.

To distinguish between these two scenarios, Scarponi et al. (2022) conducted a new study based on a more constrained paleoenvironmental framework (only nearshore settings considered) and incorporating data from the lowstand nearshore deposits of the Po-Adriatic System, accumulated during the last late glacial phase and preserved in the sedimentary record of the Central Adriatic Sea (see Pellegrini et al., 2018; Azzarone et al., 2020). The fossil record recovered from sediment cores in the Po-Adriatic System indicated that nearshore assemblages of the penultimate and the current (pre-Anthropocene) interglacial were indistinguishable statistically from one another despite notably different assemblage composition during the intervening glacial conditions. These results suggested that the nearshore mollusc associations of the northwestern Adriatic Sea should be resilient to the limited rise of sea surface temperatures predicted for the near future but stand in stark contrast to benthic community responses to recent anthropogenic impacts in this region (Kowalewski et al., 2015). The latter study, however, did not evaluate if those anthropogenic changes affected the entire onshore-offshore gradient or were only limited to specific bathymetric zones. Nevertheless, recent conservation palaeobiology studies conducted in the northeastern Adriatic Sea documented a strong shift in the faunal composition of mollusc assemblages that occurred during the last centuries in more offshore settings (20-40 m e.g., Mautner et al., 2018; Gallmetzer et al., 2019). In contrast, the Holocene-to-present-day changes along the nearshore settings in the western part of the basin directly influenced by Po river discharge have remained underexplored.

Study area

The Northern Adriatic is an epicontinental, semi-enclosed, shallow sea (average depth 35 m), which is characterised by a wide shelf with a low topographic gradient of 0.02° (Poulain et al., 2001). The Northern Adriatic Sea extends ~350 km southward from the Gulf of Trieste and is delimited westward by Italy and eastward by the Balkan Peninsula. The Italian coasts of the northwestern Adriatic Sea are mostly sandy and—in the few cases where the landscape has not been modified—separated from the coastal plain by a few-meters-high dune system (Sistilli et al., 2015). The submerged portion of the beach (either shoreface or delta front) is delimited landward by a reduced swash zone (foreshore) and offshore by the depth at which the sediment could be remobilised by waves and currents (i.e., closure depth principle, see Nicholls et al., 1996). Within this bathymetric interval, two sub-environments can be identified. The upper zone (= upper nearshore), where the flux of sediment is nearly constant, is a dynamic environment represented by highly mobile bars and troughs changing their morphology and location at temporal scales of days to years. The lower zone (= lower nearshore) is a depositional setting characterized by a more stable profile, where only storm waves can strongly re-shape bottom morphology (at the scale of decades to centuries). Beyond that, a transition zone occurs where morphological changes develop on longer time scales and finer sediments are increasingly common. In other words, beach subdivision is defined here as a function of the local wave energy expected in a predetermined time-window. The longer the time interval considered, the greater probability that a wave able to interact with deeper seabed can occur. Using a time-interval of 100 years as predetermined time window, the submerged beach in this part of the western Adriatic Sea extends down to a 10 m isobath. As for the boundary between the lower and upper nearshore, this limit is commonly placed approximately at 4 m water depth (Sistilli et al., 2015).

Another important element of the northwestern Adriatic Sea is the Po Delta that represents the most readily observable sub-aerial morphologic feature recording coastal progradation of the last few millennia after the relative sea level stabilization (Amorosi et al., 2016). However, the past sea-level dynamics are recorded below the Po coastal plain, where a sequence of wedge-shaped marine sedimentary bodies records the waxing and waning of the Northern Adriatic Sea during the most recent glacial-interglacial cycles (e.g., Amorosi et al., 1999; Scarponi and Kowalewski, 2004; Amorosi et al., 2016, Campo et al., 2020). The uppermost wedge-shape unit, mainly Holocene in age, has been studied in detail during the last decades (e.g., Amorosi et al., 1999; Scarponi et al., 2013; Bruno et al., 2017; Cheli et al., 2021; Rossi et al., 2021). The lowermost boundary of this unit is the transgressive surface (TS), a boundary of regional extent, that can be readily recognized in cores using lithologic and palaeontological data (Bruno et al., 2017). Above the TS, estuarine to shallow marine deposits of variable thickness (e.g., Scarponi et al., 2017b) document the late phase of post-glacial sea-level rise and the maximum marine ingression (dated around 7.0 kyr; Rossi et al., 2021 and references therein). This overall retrogradational set of units is overlain by an aggradational-to-increasingly-progradational succession of silty-mud to coarser grained coastal and deltaic facies (e.g., Amorosi et al., 2019). When considered jointly, these geological lines of evidence indicate that during the middle Holocene the physiography of the study area transitioned from barrier-lagoon-estuary systems to wave-dominated coastal and deltaic systems (Amorosi et al., 2019). Subsequently, during the late Holocene, (2.0 kyr cal. BP till mid-20th century), the deltaic and coastal systems of Emilia-Romagna experienced a period of increased river discharge that promoted a strong progradation phase and the transition from wave-dominated to river-dominated deltaic systems shifting laterally due to multiple episodes of river avulsion (e.g., Amorosi et al., 2019). During the last decades coastal progradation in the Northern Adriatic Sea seems to have stopped or slowed down due to anthropogenic subsidence and sea-level rise (see Cencini 1998; Gambolati et al., 1999; Da Lio and Tosi, 2018; Ninfo et al., 2018; Meli et al., 2021).

Methods

The analyses compared two specific time intervals: (1) the mid-late Holocene (between ~6 and ~0.5 kyr cal. BP) documented in subsurface cores, and (2) the present day represented by the surficial assemblages accumulating along the Po Delta and Emilia Romagna coastlines, mainly during the last 100 years (Scarponi et al., 2013). The age of the samples was based on direct radiocarbon dating of the fossil material and timing of the parasequence development in the study area, see Appendix S1; Amorosi et al., 2017). The samples of fossiliferous deposits preserved in the subsurface of the Po coastal plain (Fig. 1) were acquired from previously investigated cores, whereas the data on the surficial assemblages derive from new sampling efforts combined with previously collected samples recorded in the Italian Mollusc Database of the Santa Teresa research center—National Agency for New Technologies, Energy and Sustainable Economic Development (ENEA) (Bedulli et al., 1984).

Data selection criteria

To limit possible biases due to different taphonomic conditions and to ensure environmental comparability, the analyses were restricted to samples from nearshore settings, sampled along the Emilia Romagna and the Po Delta coastline (Fig. 1). Samples from backshore deposits were not considered. Samples from ENEA database that recorded only the live assemblage counts were also excluded.

Mid-late Holocene samples were derived from cores and ranged in volume between ~110 and ~375 cm^3 each, whereas surficial assemblages from present-day settings were collected by different methods, mainly Van Veen Grab (8000 cm^3) and short cores (400 cm^3) (Appendix S1). Core samples were treated following a standard procedure reported in Wittmer et al. (2014). For the ENEA samples only the taxonomic list, specimen counts, and sampling method (i.e., SCUBA diving, dredge, grab, and fishing net) were reported (Appendixes S1-S2). We restricted our analyses to molluscs (bivalves, gastropods and scaphopods), which dominated the studied macrobenthic assemblages. Analyses were conducted at species level. Because the great majority of bivalve specimens were represented by individual valves, their final counts were divided by two to account for disarticulation (Scarponi and Kowalewski, 2004).

The assignment of mid-late Holocene samples to nearshore setting was based on stratigraphic, sedimentological and micropalaeontological lines of evidence reported in literature (see Appendix S1 columns “facies associations”). Samples were then included in either upper or lower nearshore based on their estimated water depth following procedure reported in Wittmer et al. (2014), summarized here briefly. For each species retrieved in a sample and present in the ENEA database (Santa Teresa research center; Bedulli et al., 1984), its preferred bathymetry was estimated, as the present-day abundance-weighted average preferred depth (PD). Then a water depth estimate for each sample was obtained by computing the mean PD of all the species retrieved in a sample weighted by their abundances.

Quantitative analyses

The molluscan assemblages in the two time intervals were examined by comparing sample-standardised diversity (richness and evenness), changes in relative abundance of dominant species, trophic structure, and substrate relationship. Taxonomic composition and diversity were analysed at environmental (nearshore) and sub-environmental levels (upper and lower nearshore).

Bivariate and multivariate methods along with network analyses were used to compare assemblage composition representing the investigated environmental units. Finally, trophic structure and substrate relationships in both time intervals were investigated by assessing the relative abundances of various feeding and substrate preference groups among the 10 most abundant species.

Multivariate analyses. The compositional variation in mollusc assemblages was first assessed by means of ordination analyses. The dataset for ordination analyses was restricted to samples with at least 20 specimens, and singletons (species occurring in only one sample) were removed (Wittmer et al., 2014). To check for volatility and sensitivity of the results, a more restrictive dataset was employed, consisting of samples with at least 60 specimens (singletons removed as well) (Scarponi et al., 2022). The sample-by-species matrices have been standardised (Wisconsin double relativisation) or transformed (4-root-transformed relative abundances) to reduce the effect of hyper-abundant taxa. The indirect ordination was performed by non-metric multidimensional scaling (NMDS) using Bray-Curtis (BC) distance measure (k = 3 dimensions) on both the standardised and transformed matrices. In addition, permutation-based multivariate analysis of variance (PERMANOVA) was employed to evaluate differences in centroids of the multivariate groups of samples between the two time intervals. Here sub-environments represent groups, so that permutations occur across the two time intervals within sub-environments only. Average BC dissimilarity of nearshore samples from their group centroid, as well as pairwise BC dissimilarity between the samples were used as measure of compositional heterogeneity (beta diversity) within each environment and time interval (Anderson et al., 2006).

Network analyses. We created multilayer network representations of the mid-late Holocene and present-day records by using the same dataset employed for the NMDS. Here we conceptualised those records as complex systems with a two-layered structure in which one layer described taxonomic composition and the other quantified sedimentologically defined relationships (Fig. S1). Nodes in those networks represent samples, taxa, and environmental zones—based on sedimentological attributions (Appendixes S3-S4). This multilayer framework has been used in palaeobiological research to create temporal networks in which layers represent ordered time intervals, such as consecutive geological stages (Rojas et al., 2021) or equal time bins (Pilotto et al., 2022). However, in this study, the layers in the assembled networks did not represent time intervals but biological and sedimentological constraints in the underlying geohistorical data. We used the Infomap framework, a higher-order approach that operates on multilayer networks (Edler et al., 2017), to reveal the network's modular structure. Because the underlying data were sparse, the assembled networks were small, and the optimized solutions did not exhibit a hierarchical organization. Indeed, standard network clustering provides limited information on the large-scale organization of the studied systems. To overcome this limitation, we used varying Markov time models (Rojas et al., 2022) that allowed us to explore the larger-scale modular patterns of the mid-late Holocene succession and present-day nearshore seabed of the Adriatic Sea at different resolutions. In the Map Equation framework, the parameter Markov time sets the scale of the modules (Kheirkhahzadeh et al., 2016). We obtained the optimised partitions of the assembled networks for a range of Markov time values using the following Infomap arguments: N = 500, i = multilayer, flow-model = undirected, markov-time, multilayer-relax-rate = 0.8. The multilayer-relax rate (*r*) is the probability to relax the constraint of a random walker visiting a sample in one layer for moving towards the same sample in the other layer as described in Rojas et al. (2021). We used an alluvial diagram to visualize changes in the modular structure across the different Markov time models. Each column in the alluvial diagram represents the network partition obtained at the given Markov time. For each partition, nodes (i.e., samples, taxa, and depositional features) grouped into modules are represented as vertically aligned rectangles, with height proportional to their flow volume (i.e., long-term visit rates of nodes describing the behaviour of the random walk). Horizontal streamlines connect sets of nodes in adjacent networks, with height proportional to the node's flow (Rojas at al. 2022). The alluvial diagrams provided here represent 98% of the network flow and were created using the Alluvial diagram app available on https://www.mapequation.org.

Bivariate analyses. Spearman's coefficient was used to measure the strength of the rank correlation between selected bio-environmental descriptors that are thought to be relevant for the sampled nearshore assemblages: sample depth, standardised richness, relative abundance of economically valuable species, and relative abundance of non-native species. NMDS sample scores were correlated with these bio-environmental descriptors to shed light on the potential drivers of variation in assemblage composition captured by the ordination patterns. In addition, comparison of the rank abundance distribution of species (i.e., proportion of individuals representing each species) was employed to evaluate changes in structure of the regional species pool across the two time intervals.

Quantitative analyses were performed in R (R Development Team, 2018, v 3.6). Codes and data are provided in the supporting information. The Infomap software package (Edler et al., 2017) was used for clustering the assembled networks. Results can be reproduced using the Infomap Online freely available at https://www.mapequation.org.

Results

The dataset examined (i.e., samples with at least 20 specimens and singletons excluded) consisted of 30 assemblages (28,949 specimens representing 67 species in total) from present-day nearshore settings and 71 samples (28,332 specimens and 58 species) from the comparable settings of the mid-late Holocene (Appendix S1). Present-day samples cover the entire bathymetric gradient of the nearshore setting (i.e., 0-10 m water depth, see Methods), whereas the mid-late Holocene samples do not extend beyond 8 m water depth. The NMDS ordinations, regardless of the matrix transformation or sample size threshold applied (Figs. 2; S2-S4), showed only partial overlap between present-day and mid-late Holocene nearshore assemblages, with samples from the lower nearshore grouping separately according to their age. In addition, the upper and lower nearshore are well separated from each other in both time intervals (Figs. 2; S2-S4). Similar patterns are revealed by the network analysis. The higher-order Markov dynamics on the assembled networks captured the large-scale structure of the dataset by explicitly delineating two modules (representing 98% of the network flow) comprised of strongly connected sets of species, samples, and sedimentological features, that can be directly interpreted as lower and upper nearshore sub-environments (Fig. 3). Furthermore, the Holocene nearshore sub-environments show a higher mixing at the boundary. That is, the modules representing upper and lower settings overlap or share a few samples due to the uncertainty inherent to the sedimentological descriptions in the fossil data or reflecting Holocene to present-day changes in the Po-Adriatic System.

Rarefied diversity, water depth and per-sample relative abundance of edible taxa (Figs. 2, S2-S3) are significantly correlated with NMDS1 (ρ = 0.63–0.69 and p-values << 0.001 in all cases), whereas correlation between NMDS2 and sample-standardised diversity or abundance of economically relevant taxa depends on the matrix treatment (Wisconsin standardisation vs. 4th-root transformation, respectively; Figs. 2, S2-S3). PERMANOVA based on species abundance data reported consistently different assemblage composition between nearshore samples of the two time-intervals (Table 1).

Comparison of BC pairwise dissimilarities between the samples provides evidence of higher heterogeneity within present-day nearshore settings (mean BC dissimilarity = 0.72), than within the mid-late Holocene nearshore settings (mean BC dissimilarity = 0.33; Table 2). The lower heterogeneity in mid-late Holocene nearshore was likely driven by lower turnover (i.e., higher congruence of sample taxonomic composition) among the upper nearshore samples (mean BC dissimilarity = 0.15), while in present-day assemblages heterogeneity was comparable in both sub-environments (mean BC dissimilarities = 0.60 and 0.65; Table 2). Differences in heterogeneity within nearshore deposits of the two-time intervals were also supported by multivariate dispersion of the two sample groups around their centroids (Fig. S5), and by the higher-order Markov dynamics that revealed non-trivial modules at higher Markov times on the network representing present-day nearshore seabeds (Fig. 3). The nearshore settings of the two time intervals are also distinct from one another due to the occurrence of non-native species, here defined as those taxa that were initially distributed outside the central-eastern Mediterranean Sea. While the presence of non-native species is widespread in the investigated area (i.e., 87% of present-day samples record at least one non-native species; Appendix S1), they are more common in the deeper nearshore settings (Fig. S6c), but their relative abundance is generally limited (always <10% of per-sample abundance).

Mid-late Holocene assemblages display an expected monotonic increase of the standardised diversity and relative abundance of economically relevant species moving from upper to lower nearshore settings (Fig. 4), with shallower samples characterized by their lower abundance (median relative abundance <10%) compared to deeper settings (median relative abundance of 35%, but rarely exceeding 50% of the specimens per sample; Figs. 2, 4; S6). This pattern is more complex in present-day nearshore settings, which are characterized by a lack of monotonic relationship between rarefied species richness and economically valuable taxa, which commonly attain relative abundances >50% in both upper and lower nearshore samples (Fig. 4). In present-day settings, when the economically relevant species are dominant (i.e., abundance >50%), rarefied species richness usually decreases considerably (Fig. 4).

A very similar set of species dominates nearshore environments in both time intervals, with eight out of the top ten most abundant species shared between them, and more than 90% of the specimens retrieved in both time intervals is represented by infaunal, filter feeders (Table S1). However, in present-day assemblages the accidentally introduced non-native bivalve *Anadara* gr. *kagoshimensis* is recorded among the top species (Table 3) and the dominance of *Lentidium mediterraneum* is less pronounced than in mid-late Holocene samples. Although *L. mediterraneum* in the network analysis is the highest ranked species in both modules representing upper nearshore settings of the investigated time-intervals, the contribution of the individual taxa to the modules delineated in both networks (Tables S2; S3), as measured in terms of the flow (see Pilotto et al., 2022), highlights the mid-late Holocene to present-day shift in their relative importance (Fig. 5; Table 3). Apart from the non-native species *A.* gr. *kagoshimensis* present along the entire gradient, the lower nearshore assemblages appear to have undergone more notable changes since the late Holocene compared with the upper nearshore assemblages. These changes involved the exclusion of *L. mediterraneum* from the 10 most abundant species and the increase in opportunistic, scavenger, and deposit feeder taxa such as *Varicorbula gibba*, *Tritia varicosa*, and *Nucula nitidosa.*

Discussion

Our study provides an evaluation of assemblage dynamics in the nearshore settings of the Northern Adriatic Sea over the last several thousand years, based on the analysis of fossil mollusc remains. Thus, it provides a palaeoecological baseline against which it is possible to assess recent shifts in mollusc assemblages from the present-day nearshore settings.

Biotic response in the Anthropocene: Nearshore

NMDS and network analyses both provide evidence supporting a modularity within nearshore environments corresponding to two groups of samples with distinct species composition (Figs. 2-3, 5). This modularity parallels the morphodynamic zonation of the Adriatic nearshore zone (Sistilli et al., 2015). The observed patterns in relative species abundance and dominance of infaunal filter feeders in both time intervals (Tables 3, S1; Appendix S1), suggest that the identity of the most abundant species populating nearshore settings has not changed notably over the last several thousand years, except for the addition of non-native taxa (e.g., the accidentally introduced *A.* gr. *kagoshimensis)* or aquaculture-related molluscs such as *Mytilus edulis*, *Ruditapes philippinarum* (Appendix S1). Thus, the present-day nearshore mollusc assemblages retain the basic structure of the assemblages that thrived in comparable environments during the mid-late Holocene. This finding is encouraging. However, strong impacts are observed in deeper (~10-40 m water depth) soft-bottom settings of the Northern Adriatic Sea, where the composition of molluscs assemblages shifted markedly during the 20th century compared to the late Holocene baseline (Vidovic et al., 2016; Galltmezter et al., 2017; 2019; Mautner et al., 2018; Tomasovych et al., 2020; Haselmair et al., 2021). This profound ecological change reduced species richness and led to a decline in abundance of grazers and deposit feeders, and increase of stress-related species (e.g., *V. gibba;* Fuksi et al., 2018; Tomašových et al., 2020). Thus, the offshore benthic communities in the Northern Adriatic Sea are substantially different from those of a few thousand years ago and do not show the high geographic heterogeneity in faunal composition that characterized the late Holocene (Galltmezter et al., 2019; Haselmair et al., 2021). Similar compositional shifts in benthic communities were also observed over the last century in ecological surveys of living assemblages (e.g., Crema et al., 1991; Chiantore et al., 2001).

In contrast to these more offshore habitats, our data suggest that while the present-day northwestern Adriatic nearshore seabed is directly impacted by a number of human stressors (see below), those stressors have not significantly reshaped (so far) the taxonomic and functional compositions of the shallow-water benthic assemblages. The presence of non-native species in targeted nearshore settings is widespread but they are still largely limited in terms of their relative abundance (Fig. S4; Table 3). When the upper and lower nearshore samples are examined separately, the mid-late Holocene and present-day assemblages diverge in terms of species abundances and diversity structure (Figs. 2, 5; S6; Table 3). Multivariate analyses indicate that water depth, rarefied species richness and relative abundance of economically relevant edible species are the main factors responsible for the variation in assemblage composition captured by the NMDS1 axis. Bathymetry drives the shift of nearshore samples toward lower axis 1 values. As noted above the present-day samples cover the entire bathymetric gradient of the nearshore setting (i.e., 0-10 m water depth, see Methods), whereas the mid-late Holocene samples do not extend beyond ~8 m water depth. However, the shift of the present-day upper nearshore samples toward lower NMDS1 values (Fig. 2; S2-S4) is determined by the other two correlates (diversity and relative abundance of economically relevant edible species; Figs. 2; S6). Overall, species thriving in shallower settings seem to be more resilient than those thriving in the deeper part of the investigated gradient (i.e., lower nearshore). Finally, samples found in lower nearshore settings, despite containing the same set of taxa show completely different diversity and dominance structure in the two time intervals (Figs. 2, 5; S2-S6, Table 3). Although we posit here that anthropogenic factors are the primary drivers of the shifts in the structure of mollusc assemblages, natural climatic changes during the Holocene (e.g., Marriner et al. 2022) might have also played a role. The lack of regional sea surface palaeotemperature records from the Northern Adriatic Sea precludes direct assessment of the extent to which the climatic fluctuations might have contributed to late Holocene shifts in community composition. However, the fact that there is a higher congruence in the taxonomic composition of nearshore assemblages from samples (Fig. S5) that encompass an overall multimillennial cooling trend (even if limited) in the Mediterranean during the mid-late Holocene (pre-Anthropocene, Jalali et al., 2016), indicates that changes in seawater temperatures are unlikely to have been a primary causative explanation for detected patterns.

Upper nearshore. NMDS and correlation analyses (Figs. 2; S5; Table 1) document a moderate shift toward reduced dominance of *L. mediterraneum* and a modest increase in hard-substrate (e.g., *Mytilus*) and non-native species (e.g., *A.* gr. *kagoshimensis*), which led to an increase in standardised diversity (Figs. 2; S4, S6) and shift toward lower NMDS1 scores. This change is supported by the multilayer network analysis showing that a limited number of taxa are clustered into the module depicting upper nearshore settings in the mid-late Holocene network. In contrast to the present-day counterpart, this module does not include hard-substrate or non-native species. These patterns could be explained by the intense development of coastal infrastructure (e.g., groins and breakwaters, piers) over the last century. The infrastructure development impacted more than half of the sampled shoreline (Cencini, 1998; Dafforn et al., 2015) and provided artificial hard-substrates further facilitating spread of non-native species (Airoldi et al., 2015). Shallow marine infrastructure increases heterogeneity of coastal habitats, which in turn can increase species diversity (habitat heterogeneity hypothesis, MacArthur and MacArthur 1961; Almond et al., 2021) by favoring hard-substrate species. These effects are especially relevant in the study areas, which during the Holocene was characterized by a very limited extent of natural hard-substrate habitats.

Another factor driving diversity in present-day upper nearshore settings is the decreasing dominance of *L. mediterraneum* (75% in present-day assemblages vs. 95% during the mid-late Holocene; Table 3). Although the shift is noticeable, *L. mediterraneum* abundance tends to be variable both spatially and temporally (e.g., Occhipinti-Ambrogi et al., 2002). Due to our limited sampling effort (i.e., small number of samples) of present-day upper nearshore settings, make it difficult to evaluate if the drop in abundance mostly reflects a sampling artifact or an anthropogenic signal linked to higher habitat heterogeneity recently developed along the Adriatic coastline. The ongoing land-use changes like wetland draining, expansion of agriculture, urbanization, road construction, and waterway regulation affected the area since late Roman times, but with the highest intensity during the last two centuries. Indeed, the Greek geographer Strabo reported, around 2000 years ago, that the Po Delta and surrounding coastal areas were a continuous almost uninterrupted series of wetlands and rivers (Horace, 1923). It is noteworthy that *L. mediterraneum* thrives in euryhaline shallow marine settings, especially at the mouth of rivers (Massé, 1972), and can withstand eutrophic waters and high sedimentation rates (Ambrogi and Bedulli, 1981). Since the 17th century (but on a large scale during the late 19th-20th centuries) hydraulic works of river diversions and merging, as well as wetland drainage took place. Along the Po Delta and Emilia Romagna coastlines less than 5% of freshwater marshes and <30% of salt marshes that existed in the area during the Roman times are still present, and the coastline is now dominated by recreational facilities, harbors, and other infrastructures (Cencini, 1998). In the second half of the 20th century the Emilia-Romagna coastal plain became one of the popular tourist destinations of the Mediterranean Sea. However, in protected areas with limited anthropogenic stressors like the Po Delta Biosphere Reserve, *L. mediterraneum* is found with an overwhelming abundance (but see also Occhipinti-Ambrogi et al., 2002). In this area *L. mediterraneum* is widely dominant in water depth <2.5 m, with a mean population density of 130,000 ind/m^2 and reaching relative abundances of 95% in macrobenthic communities (Ambrogi and Bedulli, 1981; see Table 3 for comparison with mid-late Holocene upper nearshore settings).

Finally, the increase in non-native species due to aquaculture activities (mainly *R. philippinarum, Magallana gigas*) and accidental introductions (e.g.,, *Rapana venosa*, *Anadara* gr. *kagoshimensis*; Appendix S1) appears to have played a minor role in the region. As for *R. philippinarum,* while not very abundant in high-energy nearshore habitats, the taxon is one of the most successful non-native species in brackish settings along the entire northwestern Adriatic coastline. Introduced in the region during the early 1980s for farming purposes (Cesari and Pelizzato, 1985), it expanded along the coast colonising a variety of brackish settings and replacing the native *R. decussatus*. Expansion of the *R. philippinarum* aquaculture is also responsible for the introduction of other non-native species such as the seaweed *Gracilaria vermiculophylla* (Sfriso et al., 2012; Airoldi et al., 2016).

In summary, the separation of present-day and mid-late Holocene assemblages observed in our multivariate analyses (Figs. 2; S2-S5; Table 1) is driven by the reduced dominance of *L. mediterraneum* along the heavily urbanized settings of the northwestern Adriatic, as well as, to a lesser degree, by the increase in species richness (Fig. S6d) possibly due to coastal development and appearance of non-native species that were accidentally or intentionally introduced to the region (Fig. S6c).

Lower nearshore. In such settings, present-day assemblages show a higher magnitude of changes with respect to their mid-late Holocene counterparts (Fig. 2; S2-S3; Table 3; S2). First, *L. mediterraneum* is no longer present among the 10 most abundant species in this sub-environment, being replaced by the other Mediterranean corbulid—*V. gibba* (Table 3). *L. mediterraneum* is not even grouped into the network module representing the present-day lower nearshore settings (Table S3). *V. gibba* dominance is often related to environmental instability driven by oxygen depletion, turbidity or sustained sediment fluxes both in benthic communities (e.g., Pérès and Picard, 1964; Hrs-Brenko, 2006) and Pliocene-Quaternary Mediterranean fossil assemblages (e.g., Dominici, 2001; Amorosi et al., 2002). According to Ambrogi and Bedulli (1981), *L. mediterraneum* is still one of the most abundant species in lower nearshore settings of the Po Delta (especially between 5 m and 8 m water depth), whereas in deeper settings *V. gibba* is more abundant and sometimes dominant (see also Occhipinti-Ambrogi et al., 2002). The shift in dominance between *L. mediterraneum* and *V. gibba* from the mid-late Holocene toward present-day observed in our data, however, needs further investigation, as the two-time intervals are not uniformly sampled along the bathymetric gradient (Fig. 2d). This bias in sampling coverage could explain at least in part the switch in dominance of the two corbulids (Table 3). The pattern, however, may also reflect an ecological signal related to anthropogenic disturbances, already documented in other parts of the Adriatic Sea. In fact, previous studies focused on soft-bottom habitats of the Northern Adriatic Sea attributed the 20th century dominance of *V. gibba* (= *Corbula gibba*) and *Tritia varicosa* (= *Nassarius pygmaeus*) to trawling-enhanced remobilization of the Adriatic seabed and to increase in frequency of anoxia events driven by eutrophication (e.g., Crema et al., 1991; Giani et al., 2012; Gallmetzer et al., 2017; Tomašových et al., 2020). Such repeated stressors tend to reduce ecosystem complexity and keep macrobenthic communities permanently at an early stage of recovery with moderate diversity and high abundance of opportunistic, resistant species such as *V. gibba* and scavenger taxa (e.g., *T. varicosa*) (Table 3; Occhipinti-Ambrogi et al., 2005; Tomašových et al., 2018), while epifauna is more patchily distributed (Riedel et al., 2012). Our findings are concordant with these previous studies. However, improved sampling coverage of the entire nearshore bathymetric gradient in the mid-late Holocene record is necessary to limit the effects of potential sampling biases.

It is noteworthy that the present-day lower nearshore assemblages characterised by the reduced standardised diversity (Fig. S6a), tend to be dominated by the economically relevant *Chamelea gallina,* an edible infaunal bivalve. This species contributed the most to the network delineation of the lower nearshore settings in the present-day network (Table S3). While hypoxic events in the Northern Adriatic Sea are becoming less common comparing to the 1970s and 1980s (Rinaldi et al., 1991), the seabed is still intensively trawled along almost its entire bathymetric profile (Russo et al., 2020 and references therein). A fleet of hydraulic dredgers (ca. 450 vessels) operates on the sandy coastal bottoms (3-15 m water depth) in the Northern Adriatic Sea (Romanelli et al., 2009) exploiting *C. gallina*. The areas hosting commercially exploitable densities of this species are swept around 2.0 times each year on average, with peaks of 20 times a year (Morello et al., 2005). Our data reinforce the ongoing concerns regarding impact of trawling on the lower nearshore seabed, especially on benthic biodiversity. When standardised richness per sample is plotted as a function of the relative abundance of economically relevant edible species, the lower nearshore assemblages show a strong drop in median sample-level diversity (Fig. 4). The increase in abundance of such species, that is a peculiar feature of the studied present-day assemblages, is probably related to the 20th century expansion of marine invertebrate fisheries and aquaculture. Opportunistic species like *C. gallina* or *V. gibba* benefit most from novel environmental conditions provided by urban seas like the Adriatic. These taxa, given their ecological requirements, can thrive best in human-impacted areas. In addition, the “law of large numbers” may apply in this context. The “law” states that the most abundant species remain most abundant because they tend to produce more offspring than the less abundant species (Di Michele et al., 2004). Both features confer to this species a strong adaptive potential to face the environmental perturbations to which it is continuously subjected. However, even in the case of *C. gallina*, human impacts exert negative effects on its populations. According to Bargione et al. (2021 and references therein), forty years ago *C. gallina* annual yield in the Adriatic Seaa was 4-to-5 times higher than it is today (15,000–20,000 tons/year). Nevertheless, while human exploitation of molluscs as a food source has significantly altered community compositions, populations of exploited species like *C. gallina* are still able to persist given responsible management. However, species less tolerant to anthropogenic stressors that decreased in abundance from the mid-late Holocene (e.g., *Bittium*, *Spisula*; Table 1), would require the establishment of larger protected areas that should allow them to survive and to sustain populations in other parts of the basin via larval dispersal.

Perspectives

We used sample-level metrics of community composition and diversity to evaluate nearshore habitats over the last few millennia and assess long-term changes in Adriatic coastal mollusc assemblages. Adriatic geohistorical records highlight a marked shift between nearshore assemblages from the two investigated time intervals. Compared to the mid-late Holocene baseline, present-day molluscan assemblages show an increase in standardised diversity in upper nearshore settings due to increase in habitat heterogeneity and introduction of non-native species. The increase in standardised species diversity of surficial assemblages reflects local mixing of dead organisms by physical processes across upper nearshore communities that are more heterogenous today than they were in the past. The elevated spatial heterogeneity of mollusc assemblages is likely attributable to transformation and fragmentation of coastal habitats driven by human activities in the most recent centuries. In lower nearshore settings, on the other hand the decrease in standardised diversity and the rise of opportunistic taxa signal a strong anthropogenic transformation of these habitats related to eutrophication, increased frequency of hypoxic events and intense bottom trawling. Given the economic and socio-cultural importance of shellfish fisheries in the Mediterranean basin, it will be difficult to set the Holocene baseline for lower nearshore environments as an achievable (or desirable) restoration goal. Conservation strategies in such settings need to accept and incorporate human societies as part of the ecosystem (urban sea, Dafforn et al., 2015) and consider them as one of the major stakeholders that should be involved in the sustainable management of coastal ecosystems. The historical perspective provided in this study should allow us to establish better conservation strategies.

Acknowledgements

The authors thank A. Baseotto and G. Tugnoli for their help in fieldwork and sample processing. Marcelo Rivadeneira, an anonymous reviewer, and Stefano Dominici (handling editor) for their helpful comments. This study represents partial fulfillment of the requirements for the Ph.D. thesis of Alessandro Cheli at the FishMed PhD Program (University of Bologna, Italy).

Funding

The research was funded by the RFO grant: 2021, PI D. Scarponi and the NSF grants: EAR-1559196 and EAR-0920075, PI M.Kowalewski.

References

Airoldi L., Ponti M., Abbiati M. (2016). Conservation challenges in human dominated seascapes: The harbour and coast of Ravenna. Regional Studies in Marine Science, 8, 308-318, https://doi.org/10.1016/j.rsma.2015.11.003

Airoldi, L., Turon, X., Perkol-Finkel, S., Rius, M. (2015). Corridors for aliens but not for natives: effects of marine urban sprawl at a regional scale. Diversity and Distributions, 21(7), 755-768, https://doi.org/10.1111/ddi.12301

Almond P.M., Linse K., Dreutter S., Grant S.M., Griffiths H.J., Whittle R.J., Mackenzie M., Reid W.D.K. (2021). In-situ Image Analysis of Habitat Heterogeneity and Benthic Biodiersity in the Prince Gustav Channel, Eastern Antartctic Peninsula. Frontiers in Marine Science, 8, 614496, https://doi.org/10.3389/fmars.2021.614496

Ambrogi R., Bedulli D., (1981) Notes on macrobenthos in the area facing the Po River Delta. Rapp. Comm. Int. Mer. Médit., 27(4), 169-170.

Amorosi A., Barbieri G., Bruno L., Campo B., Drexler T.M., Hong W., Rossi V., Sammartino I., Scarponi D., Vaiani S.C. (2019). Three-fold nature of coastal progradation during the Holocene eustatic highstand, Po Plain, Italy—close correspondence of stratal character with distribution patterns. Sedimentology 66, 3029-3052, https://doi.org/10.1111/sed.12621

Amorosi A., Bruno L., Campo B., Morelli A., Rossi V., Scarponi D., Hong W., Bohacs K., Drexler T.M. (2017). Global sea-level control on local parasequence architecture from the Holocnee record of the Po Plain, Italy. Marine and Petroleum Geology, 87, 99-111, https://doi.org/0.1016/j.marpetgeo.2017.01.020.

Amorosi A., Colalongo M.L., Pasini G., Preti D. (1999). Sedimentary response to Late Quaternary sea-level changes in the Romagna coastal plain (northern Italy). Sedimentology, 46(1), 99-121.

Amorosi A., Maselli V., Trincardi F. (2016). Onshore to offshore anatomy of a late Quaternary source-to-sink system (Po Plain-Adriatic Sea, Italy). Earth-Science Reviews, 153, 212–237, https://doi.org/10.1016/j.earscirev.2015.10.010

Amorosi A., Scarponi D., Ricci Lucchi F. (2002). Palaeoenvironmental changes in the Pliocene Intra-Apenninic Basin, near Bologna (Northern Italy). Geobios, 35(1), 7-18, https://doi.org/10.1016/S0016-6995(02)00044-X

Anderson, M.J., Ellingsen, K.E., McArdle, B.H. (2006). Multivariate dispersion as a measure of beta diversity. Ecology letters, *9*(6), 683-693.

Azzarone M., Pellegrini C., Barbieri G., Rossi V., Gamberi F., Trincardi F., Scarponi D. (2020). Linking benthic fauna and seismic facies to improve stratigraphic reconstructions: the case of the Mid-Adriatic Deep since the late glacial period (Central Adriatic Sea). Boll. Soc. Pal. 59, 9-23.

Barbieri G., Rossi V., Ghosh A., Vaiani S.C. (2020). Conservation paleobiology as a tool to define reference conditions in naturally stressed transitional settings: Micropaleontological insights from the Holocene of the Po coastal plain (Italy). Water, 12(12), 3420, https://doi.org/10.3390/w12123420

Bargione G., Donato F., Barone G., Virgili M., Penna P., Lucchetti A. (2021). *Chamelea gallina* reproductive biology and Minimum Conservation Reference Size: implications for fishery management in the Adriatic Sea. BMC Zoology, 6(1), 1-16, https://doi.org/10.1186/s40850-021-00096-4

Barmawidjaja D.M., Van der Zwaan G.J., Jorissen F.J., Puskaric S. (1995). 150 years of eutrophication in the northern Adriatic Sea: evidence from a benthic foraminiferal record. Marine Geology, *122*(4), 367-384, https://doi.org/10.1016/0025-3227(94)00121-Z

Bedulli D., Dell'Angelo B., Piani P., Spada G., Zurlini G., Bruschi A. (1984). Census of the distribution of the Italian Marine Mollusca. Nova Thalassia, suppl. 6, 585–590.

Bruguière J.G. (1789). Encyclopédie méthodique ou par ordre de matières. Histoire naturelle des vers, volume 1. Paris: Pancoucke. 1-344

Bruno L., Bohacs K.M., Campo B., Drexler T.M., Rossi V., Sammartino I., Scarponi D., Hong W., Amorosi A., (2017). Early Holocene transgressive palaeogeography in the Po coastal plain (northern Italy). Sedimentology 64, 1792e1816, https://doi.org/10.1111/sed.12374

Burgess M.G., Polasky S., Tilman, D. (2013). Predicting overfishing and extinction threats in multispecies fisheries. Proceedings of the National Academy of Sciences 110(40), 15943-378 15948, https://doi.org/10.1073/pnas.1314472110

Campo B., Bruno L., Amorosi A. (2020). Basin-scale stratigraphic correlation of late Pleistocene-Holocene (MIS52-MIS1) strata across the rapidly subsiding Po Basin (northern Italy). Quaternary Science Reviews, 237, 106300, https://doi.org/10.1016/j.quascirev.2020.106300

Cencini C.P. (1998) Processes and Human Activities in the Evolution of the Po Delta, Italy. J. Coast. Res. 14-3, 774–793.

CEPF (2022) Explore the Biodiversity Hotspots. Critical Ecosystem Partnership Fund. https://www.cepf.net/our-work/biodiversity-hotspots

Cesari, P., Pellizzato, M. (1985) Molluschi pervenuti in Laguna di Venezia per apporti volontari o casuali. Acclimazione di *Saccostrea commercialis* (Iredale and Roughely, 1933) e di *Tapes philippinarum* (Adams and Reeve, 1850). Bollettino Malacologico, 21, 237-274.

Cheli A., Mancuso A., Azzarone M., Fermani S., Kaandorp J., Marin F., ... Scarponi D. (2021). Climate variation during the Holocene influenced the skeletal properties of Chamelea gallina shells in the North Adriatic Sea (Italy). Plos one, 16(3), e0247590, https://doi.org/10.1371/journal.pone.0247590

Chiantore M., Bedulli D., Cattaneo-Vietti R., Schiaparelli S., Albertelli G. (2001) Long-term changes in the Mollusc-Echinoderm assemblages in the north and coastal middle Adriatic Sea." Atti della Associazione Italiana di Oceanologia e Limnologia 14, 63-75.

Coll M., Piroddi C., Steenbeek J., Kaschner K., Ben Rais Lasram F., Aguzzi J., ... Voultsiadou E. (2010). The biodiversity of the Mediterranean Sea: estimates, patterns, and threats. PloS one, 5(8), e11842, https://doi.org/10.1371/journal.pone.0011842

Crema R., Castelli A., Prevedelli D. (1991). Long term eutrophication effects on macrofaunal communities in northern Adriatic Sea. Marine Pollution Bulletin 22, 503e508, https://doi.org/10.1016/0025-326X(91)90405-H

Crutzen, P. J. (2002). Geology of mankind—the Anthropocene. Nature 415, 23.

Currano E.D., Wilf P., Wing S.L., Labandeira C.C., Lovelock E.C., Royer D.L. (2008). Sharply increased insect herbivory during the Paleocene–Eocene Thermal Maximum. Proceedings of the National Academy of Science, 12, 1960-1964, https://doi.org/10.1073/pnas.0708646105

Currano E.D., Laker R., Flynn A.G., Fogt K.K., Stradtman H., Wing S.L. 2016 Consequences of elevated temperature and pCO2 on insect folivory at the ecosystem level: perspectives from the fossil record. Ecology and Evolution, 6(13), 4318-4331, https://doi.org/10.1002/ece3.2203

d'Arge, R.C., Kneese, A. V. (1972). Environmental quality and international trade. International organization, 26(2), 419-465.

Dafforn K.A., Glasby T.M., Airoldi L., Rivero N.K., Mayer-Pinto M., Johnston E.L. (2015). Marine urbanization: an ecological framework for designing multifunctional artificial structures. Frontiers in Ecology and the Environment, 13(2), 82-90, https://doi.org/10.1890/140050

DiMichele, W.A., Behrensmeyer, A.K., Olszewski, T.D., Labandeira, C.C., Pandolfi, J.M., Wing, S.L., Bobe, R. (2004). Long-term stasis in ecological assemblages: evidence from the fossil record. Annual Review of Ecology, Evolution, and Systematics, 1, 285-322.

Dietl G.P., Flessa K.W. (2011). Conservation Paleobiology: Putting the dead to work. Trends in Ecology and Evolution, 26(1), 30-37, https://doi.org/10.1016/j.tree.2010.09.010

Dietl G.P., Flessa K.W. (2017). Conservation Paleobiology. Science and Practice. The University of Chicago Press.

Dietl G.P., Kidwell S.M., Brenner M., Burney D.A.; Flessa, K.W., Jackson, S.T, Koch, P.L. (2015). Conservation Paleobiology: Leveraging Knowledge of the Past to Inform Conservation and Restoration. Annual Review of Earth and Planetary Sciences. 43, 79-103, https://doi.org/10.1146/annurev-earth-040610-133349

Dirzo R., Young H.S., Galetti M., Ceballos G., Isaac N.J.B., Collen B. (2014). Defaunation in the Anthropocene. Science 345, 401–406, https://doi.org/10.1126/science.1251817

Da Lio C., Tosi L. (2018). Land subsidence in the Friuli Venezia Giulia coastal plain, Italy: 1992-2010 results from SAR-based interferometry. Science of the Total Environment, 633, 752-764, https://doi.org/10.1016/j.scitotenv.2018.03.244

Dominici S. (2001). Taphonomy and paleoecology of shallow marine macrofossil assemblages in a collisional setting (late Pliocene-early Pleistocene, western Emilia, Italy). Palaios, 16: 336-353 https://doi.org/10.1669/0883-1351(2001)016<0336:TAPOSM>2.0.CO;2

Edelist D., Rilov G., Golani D., Carlton J.T., Spanier E. (2013). Restructuring the Sea: profound shifts in the world’s most invaded marine ecosystem. Diversity and Distributions 19: 69–77. https://doi.org/10.1111/ddi.12002

Edler D., Bohlin L., Rosvall M. (2017). Mapping Higher-Order Network Flows in Memory and Multilayer Networks with Infomap. Algorithms 10, 112, https://doi.org/10.3390/a10040112

Flessa, K. W. (2002). Conservation paleobiology. American Paleontologist, 10(1), 2-5.

Fuksi T., Tomašových A., Gallmetzer I., Haselmair A., Zuschin M. (2018). 20th century increase in body size of a hypoxia-tolerant bivalve documented by sediment cores from the northern Adriatic Sea (Gulf of Trieste). Marine Pollution bulletin, 135, 361-375, https://doi.org/10.1016/j.marpolbul.2018.07.004

Furlan E., Torresan S., Critto A., Lovato T., Solidoro C., Lazzari P., Marcomini A. (2019). Cumulative Impact Index for the Adriatic Sea: Accounting for interactions among climate and anthropogenic pressures. Science of the Total Environment, 670, 379-397, https://doi.org/10.1016/j.scitotenv.2019.03.021

Gallmetzer, I., Haselmair, A., Tomašových, A., Stachowitsch, M., Zuschin, M. (2017). Responses of molluscan communities to centuries of human impact in the northern Adriatic Sea. PLoS One, 12(7), e0180820, https://doi.org/10.1371/journal.pone.0180820

Gallmetzer I., Haselmair A., Tomašových A., Mautner A.K., Schnedl S.M., Cassin D., Zonta R., Zuschin M. (2019) Tracing origin and collapse of Holocene benthic baseline communities in the northern Adriatic Sea. Palaios, 34, 121-145, https://doi.org/10.2110/palo.2018.068

Gambolati G., Teatini P., Tomasi L., Gonella M. (1999) Coastline regression of the Romagna region, Italy, due to natural and anthropogenic land subsidence and sea level rise. Water resources research, 35 (1) 163-184, https://doi.org/10.1029/1998WR900031

Giani M., Djakovac T., Degobbis D., Cozzi S., Solidoro C., Umani S.F. (2012). Recent changes in the marine ecosystems of the northern Adriatic Sea. Estuarine, Coastal and Shelf Science, 115, 1-13, https://doi.org/10.1016/j.ecss.2012.08.023

Haselmair A, Gallmetzer I, Tomašových A, Wieser A.M., Übelhör A., Zuschin M. (2021) Basin-wide infaunalisation of benthic soft-bottom communities driven by anthropogenic habitat degradation in the northern Adriatic Sea. Marine Ecology Progress Series 671, 45-65, https://doi.org/10.3354/meps13759

Heithaus M.R., Frid A., Wirsing A.J., Worm B. (2008). Predicting ecological consequences of marine top predator declines. Trends in ecology & evolution 23(4), 202-210, https://doi.org/10.1016/j.tree.2008.01.003

Horace L.J. (1923). Strabo geography. Books 3-5, with an English translation. Harvard University Press. London.

Hrs-Brenko, M. (2006). The basket shell, *Corbula gibba* Olivi, 1792 (Bivalve Mollusks) as a species resistant to environmental disturbances: A review. Acta Adriatica: international journal of Marine Sciences, *47*(1), 49-64.

Jackson, J. B., Kirby, M. X., Berger, W. H., Bjorndal, K. A., Botsford, L. W., Bourque, B. J., ... Warner, R. R. (2001). Historical overfishing and the recent collapse of coastal ecosystems. Science, 293(5530), 629-637, https://doi.org/10.1126/science.1059199.

Jalali B, Sicre M.A, Bassetti M.A, Kallel N. Holocene climate variability in the North-Western Mediterranean Sea (Gulf of Lions). Clim Past. 2016; 12: 91–101. https://doi.org/10.5194/cp-12-91-201.

Jouffray J.B., Blasiak R., Norström A.V., Österblom H., Nyström, M. (2020). The blue acceleration: the trajectory of human expansion into the ocean. One Earth 2(1), 43-54, https://doi.org/10.1016/j.oneear.2019.12.016

Kheirkhahzadeh M., Lancichinetti A., Rosvall M. (2016). Efficient community detection of network flows for varying Markov times and bipartite networks. Physical Review E 93, 032309, https://doi.org/10.1103/PhysRevE.93.032309

Kidwell S.M. (2007). Discordance between living and death assemblages as evidence for anthropogenic ecological change. Proceedings of the National Academy of Sciences, 104(45), 17701-17706, https://doi.org/10.1073/pnas.0707194104

Kidwell S.M. (2015). Biology in the Anthropocene: Challenges and insights from young fossil records. Proceedings of the National Academy of Sciences, 112(16), 4922-4929, https://doi.org/10.1073/pnas.1403660112

Kidwell S.M., Tomašových A. (2013). Implications of time-averaged death assemblages for ecology and conservation biology. Annual Review of Ecology, Evoution, and Systematics, 44, 539-563, https://doi.org/10.1130/G37017.1

Kowalewski M., Serrano G.E.A., Flessa K.W., Goodfriend G.A. (2000). Dead delta's former productivity: two trillion shells at the mouth of the Colorado River. *Geology*, *28*(12), 1059-1062, https://doi.org/10.1130/0091-7613(2000)28<1059:DDFPTT>2.0.CO;2

Kowalewski M. (2001). Applied Marine Paleoecology: An Oxymoron or Reality? Palaios 16(4), 309-310, https://doi.org/10.1669/0883-1351(2001)016<0309:AMPAOO>2.0.CO;2

Kowalewski M., Wittmer J.M., Dexter T.A., Amorosi A., Scarponi D. (2015). Differential responses of marine communities to natural and anthropogenic changes. Proceedings of the Royal Society B: Biological Sciences, 282(1803), 20142990, https://doi.org/10.1098/rspb.2014.2990

International Union for Conservation of Nature (2000). IUCN guidelines for the prevention of biodiversity loss caused by alien invasive species. Gland: IUCN.

Lenhan H.S., Peterson C.H. (1998). How habitat degradation through fishery disturbance enhance impacts of hypoxia on oyster reefs. Ecological Applications, 8(1), 128-140, https://doi.org/10.1890/1051-0761(1998)008[0128:HHDTFD]2.0.CO;2

Lotze H. K., Lenihan H.S., Bourque B.J., Bradbury R.H., Cooke R.G., Kay M.C., ... & Jackson, J. B. (2006). Depletion, degradation, and recovery potential of estuaries and coastal seas. Science, 312(5781), 1806-1809, https://doi.org/10.1126/science.1128035

Lotze H.K., Coll M., Dunne J.A. (2011). Historical changes in marine resources, food-web structure and ecosystem functioning in the Adriatic Sea, Mediterranean. Ecosystems, 14, 198–222, https://doi.org/10.1007/s10021-010-9404-8.

MacArthur R. H., MacArthur J. (1961). On bird species diversity. Ecology 42, 594-598.

Marriner N., Kaniewski D., Pourkerman M., Devillers B. (2022). Anthropocene tipping point reverses long-term Holocene cooling of the Mediterranean Sea: A meta-analysis of the basin's Sea Surface Temperature records. Earth-Science Reviews, 227, p.103986. https://doi.org/10.1016/j.earscirev.2022.103986

Masse H. (1972). Contribution a l'etude de la macrofaune des peuplements des sables fins infralittoraux des cotes de Provence. VII-Discussion, comparaison et interpretation des donnees quantitatives. Tethys,~ (2): 397-422

Mautner A.K., Gallmetzer I., Haselmair A., Schnedl S.M., Tomasovych A., Zuschin M. (2018). Holocene ecosystem shifs and human-induced loss of Arca and Ostrea beds in the north-eastern Adriatic Sea. Marine Pollution Bulletin, 126, 19-30, https://doi.org/10.1016/j.marpolbul.2017.10.084

Meli, M., Olivieri, M., Romagnoli, C. (2021). Sea-level change along the emilia-romagna coast from tide gauge and satellite altimetry. Remote Sensing, 13(1), 1-26, https://doi.org/10.3390/rs13010097

McCauley D.J., Pinsky M.L., Palumbi S.R., Estes J.A., Joyce F.H., Warner R.R. (2015) Marine defaunation: Animal loss in the Global Ocean. Science, 347, 1255641, https://doi.org/10.1126/science.1255641

Mittermeier R.A., Mittermeier C.G., Gil P.R., Pilgrim J. (2003) Wilderness Earth’s Last Wild Places. University of Chicago Press.

MolluscaBase eds. (2022). MolluscaBase. Accessed at https://www.molluscabase.org on 2022-11-13. doi:10.14284/448

Morello, E.B., Froglia, C., Atkinson, R.J.A., Moore, P.G. (2005). Hydraulic dredge discards of the clam (*Chamelea gallina)* fishery in the western Adriatic Sea, Italy. Fisheries Research, 76(3), 430-444, https://doi.org/10.1016/j.fishres.2005.07.002

Myers, N., Mittermeier, R. A., Mittermeier, C. G., Da Fonseca, G. A., & Kent, J. (2000). Biodiversity hotspots for conservation priorities. Nature, 403(6772), 853-858, https://doi.org/10.1038/35002501

Newell, R.I., Ott, J.A. (1999). Macrobenthic communities and eutrophication. Ecosystems at the Land-Sea Margin: Drainage Basin to Coastal Sea, 55, 265-293, https://doi.org/10.1029/CE055p0265

Nicholls, R. J., Birkemeier, W. A., & Hallermeier, R. J. (1996). Application of the depth of closure concept. Coastal Engineering Proceedings, 1(25). https://doi.org/10.9753/icce.v25.%p

Ninfo, A., Ciavola, P., Billi, P. (2018). The Po Delta is restarting progradation: geomorphological evolution based on a 47-years Earth Observation dataset. Scientific Reports 8, 3457, https://doi.org/10.1038/s41598-018-21928-3

Occhipinti-Ambrogi A., Marchini A., Cantone G., Castelli A., Chimenz C., Cormaci M., ... & Piraino, S. (2011). Alien species along the Italian coasts: an overview. Biological invasions, 13(1), 215-237, https://doi.org/10.1007/s10530-010-9803-y

Occhipinti-Ambrogi A., Favruzzo M., Savini D. (2002). Multi-Annual variations of macrobenthos along the Emilia-Romagna coast (Northern Adriatic). Marine Ecology, 23(Supplement 1), 307-319, https://doi.org/10.1111/j.1439-0485.2002.tb00029.x

Occhipinti-Ambrogi A., Savini D., Forni G. (2005). Macrobenthos community structural changes off Cesenatico coast (Emilia Romagna, Northern Adriatic), a six-year monitoring programme. Science of the Total Environment, 353(1-3), 317-328, https://doi.org/10.1016/j.scitotenv.2005.09.021

Pellegrini C., Asioli A., Bohacs K.M., Drexler T.M., Feldman H.R., Sweet M.L., ... & Trincardi, F. (2018). The late Pleistocene Po River lowstand wedge in the Adriatic Sea: Controls on architecture variability and sediment partitioning. Marine and Petroleum Geology, 96, 16-50. https://doi.org/10.1016/j.marpetgeo.2018.03.002

Pérès J.M., Picard J. 1964 Nouveau manuel de bionomie benthique de la mer Méditerranée. Station Marine d'Endoume.

Pilotto F., Rojas A., Buckland PI. (2022) Late Holocene anthropogenic landscape change in northwestern Europe impacted insect biodiversity as much as climate change did after the last Ice Age. Proceedings of the Royal Society B., 289, 20212734, https://doi.org/10.1098/rspb.2021.2734

Pitacco V., Reizopoulou S., Sfriso A., Sfriso A., Mistri M., Munari C. (2019). The difficulty of disentangle natural from anthropogenic forcing factors makes the evaluation of ecological quality problematic: A case study from Adriatic lagoons. Marine Environmental Research, 150, 104756, https://doi.org/10.1016/j.marenvres.2019.104756

Poulain PM., Kourafalou V.H., Cushman-Roisin B. (2001) Northern Adriatic Sea. In: Cushman-Roisin B., Gačić M., Poulain PM., Artegiani A. (eds) Physical Oceanography of the Adriatic Sea. Springer, Dordrecht. https://doi.org/10.1007/978-94-015-9819-4_5

R Core Team (2018) R: A language and environment for statistical computing. R Foundation for Statistical Computing. R Foundation for Statistical Computing, Vienna, Austria. URL https://www.R-project.org/

Rinaldi A., Montanari G., Ghetti A., Ferrari C.R. (1992) Anossie nelle acque costiere dell'Adriatico nord-occidentale. Loro evoluzione e conseguenze sull'ecosistema bentonico. Biologia Marina 1 (Suppl. Notiziario S.I.B.M), 79e-89.

Riedel B., Zuschin M., Stachowitsch M. (2012) Tolerance of benthic macrofauna to hypoxia and anoxia in shallow coastal seas: a realistic scenario: Marine Ecology Progress Series, 458, 39-52, https://doi.org/10.3354/meps09724

Rojas A., Calatayud J., Kowalewski M., Neuman M., Rosvall M. (2021). A multiscale view of the Phanerozoic fossil record reveals the three major biotic transitions. Communication Biology 4, 309, https://doi.org/10.1038/s42003-021-01805-y

Rojas A., Eriksson A., Neuman M., Edler D., Bl öcker, Rosvall M.. (2022). A natural history of networks: Higher-order network modelling for research in paleobiology. bioRxiv (pre-print) doi: https://doi.org/10.1101/2022.09.26.509538

Romanelli M., Cordisco C.A., Giovanardi O. (2009). The long-term decline of the *Chamelea gallina* L. (Bivalvia: Veneridae) clam fishery in the Adriatic Sea: is a synthesis possible? Acta Adriatica, 50(2), 171-205, https://doi.org/10.32582/aa.50.2.233

Rossi V., Barbieri G., Vaiani S.C., Cacciari M., Bruno L., Campo B., Marchesini M., Marvelli S., Amorosi A. (2021). Millennial-scale shifts in microtidal ecosystems during the Holocene: dynamics and drivers of change from the Po Plain coastal record (NE Italy). Journal of Quaternary Science, 36(6), 961-979, https://doi.org/10.1002/jqs.3322

Russo E., Anelli Monti M., Mangano M.C., Raffaeta A., Sarà G., Silvestri G., Pranovi F. (2020). Temporal and spatial patterns of trawl fishing activities in the Adriatic Sea (Central Mediterranean Sea, GDA17). Ocean and Coastal Management 192, 105231, https://doi.org/10.1016/j.ocecoaman.2020.105231

Say T. (1822). An account of some of the marine shells of the United States. Journal of the Academy of Natural Sciences, Philadelphia. 2(1): 221-248.

Scarponi D., Kowalewski M., (2004). Stratigraphic paleoecology: bathymetric signatures and sequence overprint of mollusk associations from upper Quaternary sequences of the Po Plain. Italy. Geology 32, 989e992, https://doi.org/10.1130/G20808.1

Scarponi D., Kaufman D., Amorosi A., Kowalewski M. (2013). Sequence stratigraphy and the resolution of the fossil record. Geology 41, 239e242, https://doi.org/10.1130/G33849.1

Scarponi D., Azzarone M., Kowalewski M., Huntley J.W. (2017a). Surges in trematode prevalence linked to centennial-scale flooding events in the Adriatic. Scientific Reports, 7(1), 5732, https://doi.org/10.1038/s41598-017-05979-6

Scarponi D., Azzarone M., Kusnerik K., Amorosi A., Bohacs K.M., Drexler T.M., Kowalewski M. (2017). Systematic vertical and lateral changes in quality and time resolution of the macrofossil record: Insights from Holocene transgressive deposits, Po coastal plain, Italy. Marine and Petroleum Geology, 87, 128-136, https://doi.org/10.1016/j.marpetgeo.2017.03.031

Scarponi D., Nawrot R., Azzarone M., Pellegrini C., Gamberi F., Trincardi F., Kowalewski M. (2022). Resilient biotic response to long-term climate change in the Adriatic Sea. Global Change Biology 28(13), 4041-4053, https://doi.org/10.1111/gcb.16168

Schnedl S.M., Haselmair A., Gallmetzer I., Mautner A.K., Tomašových A., Zuschin M. (2018). Molluscan benthic communities at Brijuni Islands (northern Adriatic Sea) shaped by Holocene sea-level rise and recent human eutrophication and pollution. Holocene, 28(11), 1801-1817, https://doi.org/10.1177/0959683618788651

Sfriso A., Wolf M.A., Maistro S., Sciuto K., Moro I. (2012). Spreading and autoecology of the invasive species *Gracilaria vermiculophylla* (Gracilariales, Rhodophyta) in the lagoons of the north-western Adriatic Sea (Mediterranean Sea, Italy). Estuar. Coast. Shelf Sci. 114, 192-198, https://doi.org/10.1016/j.ecss.2012.07.024

Sistilli F., Scarelli F., Stecchi F., Fabbri S., Cantelli L., Gabbianelli G. (2015). Spatial and temporal evolution and morphodynamic zonation fo the Ravenna shoreface. Coastal and Marittime Mediterranean Conference, 89-92. http://dx.doi.org/10.5150/cmcm.2015.018.

Steffen W., Richardson K., Rockström J., Schellnhuber H.J., Dube O.P., Dutreuil S., Timothy M. Lenton T.M., Lubchenco J. (2020). The emergence and evolution of Earth System Science. Nature Reviews Earth & Environment, 1, 54-63. https://doi.org/10.1038/s43017-019-0005-6

Slater S.M., Bown P., Twitchett R.J., Danise S., Vajda V. (2022). Global record of “ghost” nannofossils reveals plankton resilience to high CO2 and warming. Science, 376(6595), 853-856, 10.1126/science.abm7330

Steger J., Bošnjak M., Belmaker J., Galil B.S., Zuschin M., Albano P.G. (2022). Non-indigenous molluscs in the Eastern Mediterranean have distinct traits and cannot replace historic ecosystem functioning. Global Ecology and Biogeography, 31(1), 89-102, https://doi.org/10.1111/geb.13415

Todd P.A., Heery E.C., Loke L.H.L., Thurstan R.H., Kotze D.J., Swan C. (2019). Towards an urban marine ecology: characterizing the drivers, patterns and processes of marine ecosystems in coastal cities. Oikos 128: 1215-1242, https://doi.org/10.1111/oik.05946

Tomašových A., Gallmetzer I., Haselmair A., Kaufman D.S., Borut M., Zuschin M. (2019). A decline in molluscan carbonate production driven by the loss of vefetated habitats encoded in the Holocene sedimentary record of the Gulf of Trieste. Sedimentology 66(3), 781-807, https://doi.org/10.1111/sed.12516

Tomašových A., Albano P.G., Fuksi T., Gallmetzer I., Haselmair A., Kowalewski M., Nawrot R., Nerlovic V., Scarponi D., Zuschin M. (2020) Ecological regime shift preserved in the Anthropocene stratigraphic record. Proceedings of the Royal Society B., 287, 20200695, https://doi.org/10.1098/rspb.2020.0695

Tyler C.L., Schneider C.L. (2018). An overview of conservation paleobiology. Marine conservation paleobiology, https://doi.org/1-10. 10.1007/978-3-319-73795-9_1

Vidović J., Nawrot R., Gallmetzer I., Haselmair A., Tomašových A., Stachowitsch M., Ćosović V., Zuschin M. (2016). Anthropogenically induced environmental changes in the northeastern Adriatic Sea in the last 500 years (Panzano Bay, Gulf of Trieste). Biogeosciences, 13(21), 5965-5981.

Wittmer J.M., Dexter T.A., Scarponi D., Amorosi A., Kowalewski M. (2014). Quantitative bathymetric models for late quaternary transgressive-regressive cycles of the po plain, Italy. Journal of Geology, 122(6), 649-670, https://doi.org/10.1086/677901

TABLES AND FIGURES CAPTIONS

Table 1. Permutational analysis of variance (PERMANOVA). Results (based on 999 permutations), indicate statistically significant differences between the nearshore units of the two-time intervals. Within our nested design, nearshore is a factor whereas upper and lower nearshore are considered as levels (i.e., strata) of our factor, so that permutations occur only within each level and not across all levels. Given the strong differences in the number of samples from the compared units (see Table 2), we apply PERMANOVA comparatively and not as a formal statistical test. PERMANOVA is based on the same dataset utilised for NMDS analyses (i.e., samples with ≥ 20 specimens and to species occurring in more than one sample excluded).

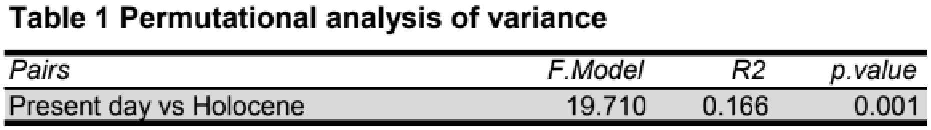

Table 1 Permutational analysis of variance

Pairs	*F.Model*	*R2*	*p.value*
Present day vs Holocene	19.710	0.166	0.001

Table 2. Pairwise comparisons of samples (n ≥ 20) using Bray-Curtis dissimilarity. Compositional heterogeneity within targeted environments and sub-environments during Holocene (H) and present-day (P) samples, estimated by pairwise Bray-Curtis dissimilarity between the samples**.** Abbreviations: IQR = interquartile range; 0.25Q = first quartile; 0.75Q = third quartile; n = number of pairwise comparisons computed following the formula: n = 0.5 * (n-1).

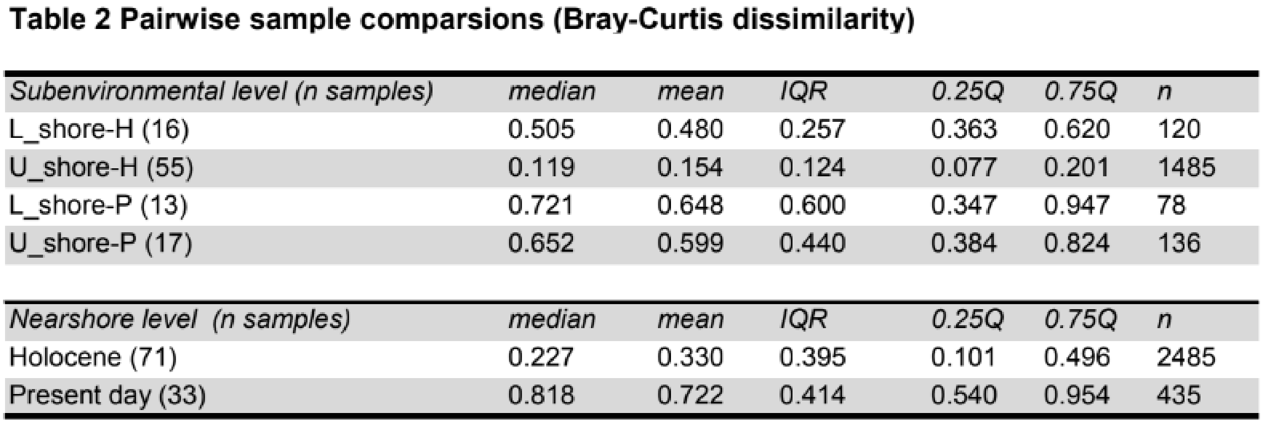

Table 2 Pairwise sample comparsions (Bray-Curtis dissimilarity)

Subenvironmental level (n samples)	*median*	*mean*	*IQR*	*0.25Q*	*0.75Q*	*n*
L_shore-H (16)	0.505	0.480	0.257	0.363	0.620	120
U_shore-H (55)	0.119	0.154	0.124	0.077	0.201	1485
L_shore-P (13)	0.721	0.648	0.600	0.347	0.947	78
U_shore-P (17)	0.652	0.599	0.440	0.384	0.824	136

Nearshore level (n samples)	*median*	*mean*	*IQR*	*0.25Q*	*0.75Q*	*n*
Holocene (71)	0.227	0.330	0.395	0.101	0.496	2485
Present day (33)	0.818	0.722	0.414	0.540	0.954	435

Table 3. Ten most abundant taxa in Holocene and present-day nearshore settings. The ten most abundant species (relative abundance) in Holocene and present-day settings and their ranking at nearshore and sub-environmental level. Bivalves counts were divided by two, due to disarticulation. Taxonomic notes: *Anadara* gr. *kagoshimensis* includes also *A. transversa* (Say, 1822), which both are non-native species from southern Asia. The reports of *A. inaequivalvis*

(Bruguière, 1789), in the ENEA dataset are treated as misidentifications of. *A.* gr. *kagoshimensis*. Based on Philip Bouchet communication *A. inaequivalvis* is a valid species that does not occur in the Mediterranean as an introduced species (Molluscabase eds., 2022).

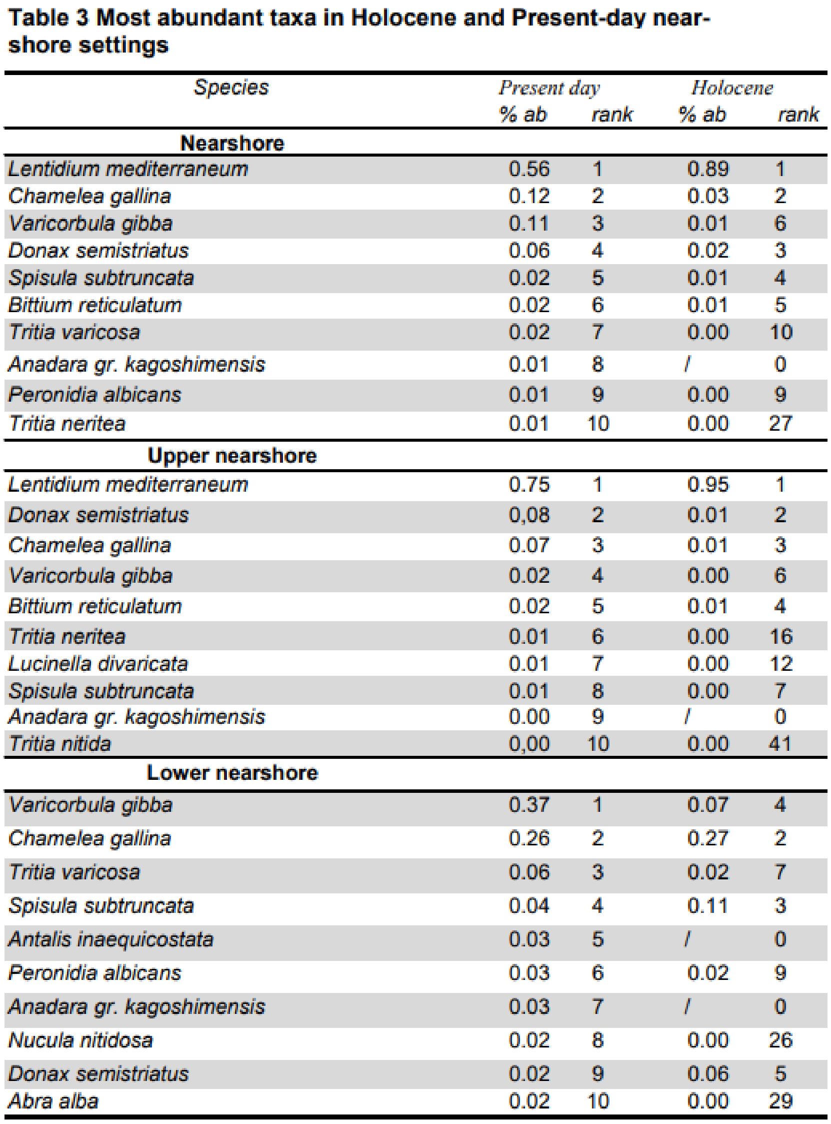

Table 3 Most abundant taxa in Holocene and Present-day near-shore settings

Species	Present day		Holocene	
	% ab	rank	% ab	rank
Nearshore				
Lentidium mediterraneum	0.56	1	0.89	1
Chamelea gallina	0.12	2	0.03	2
Varicorbula gibba	0.11	3	0.01	6
Donax semistriatus	0.06	4	0.02	3
Spisula subtruncata	0.02	5	0.01	4
Bittium reticulatum	0.02	6	0.01	5
Tritia varicosa	0.02	7	0.00	10
Anadara gr. kagoshimensis	0.01	8	/	0
Peronidia albicans	0.01	9	0.00	9
Tritia neritea	0.01	10	0.00	27
Upper nearshore				
Lentidium mediterraneum	0.75	1	0.95	1
Donax semistriatus	0,08	2	0.01	2
Chamelea gallina	0.07	3	0.01	3
Varicorbula gibba	0.02	4	0.00	6
Bittium reticulatum	0.02	5	0.01	4
Tritia neritea	0.01	6	0.00	16
Lucinella divaricata	0.01	7	0.00	12
Spisula subtruncata	0.01	8	0.00	7
Anadara gr. kagoshimensis	0.00	9	/	0
Tritia nitida	0,00	10	0.00	41
Lower nearshore				
Varicorbula gibba	0.37	1	0.07	4
Chamelea gallina	0.26	2	0.27	2
Tritia varicosa	0.06	3	0.02	7
Spisula subtruncata	0.04	4	0.11	3
Antalis inaequicostata	0.03	5	/	0
Peronidia albicans	0.03	6	0.02	9
Anadara gr. kagoshimensis	0.03	7	/	0
Nucula nitidosa	0.02	8	0.00	26
Donax semistriatus	0.02	9	0.06	5
Abra alba	0.02	10	0.00	29

Figure 1. **Map of the study area**. Blue squares represent the georeferenced sediment core locations along the Po coastal plain of Emilia Romagna. The red dots indicate locations of the present-day surficial samples. Numbers next to the symbols indicate the nearshore samples retrieved in each location.

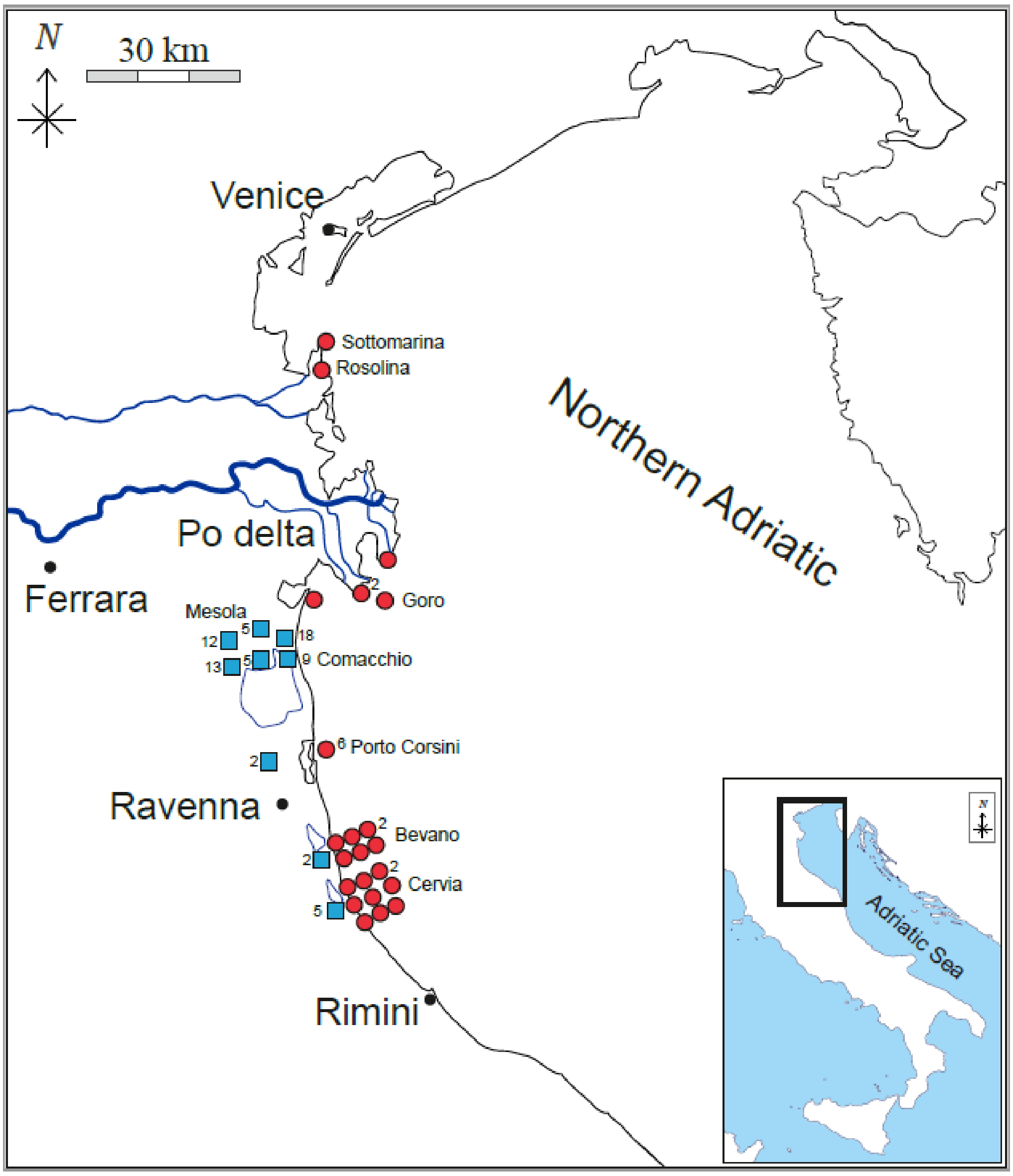

Figure 2. **Nonmetric multidimensional scaling (NMDS) and rank correlation analyses**. A) NMDS 3-D ordination (axes 1 and 2, see figure S4 for axes 1 and 3) of nearshore samples with at least 20 specimens (singletons excluded). Samples are symbol- and colour-coded according to the time interval and sub-environment. The size of each symbol corresponds to the log transformed sample size. Convex hulls delimit the ordination space occupied by each nearshore group of samples: brown = present day, blue = mid-late Holocene. B) Correlation between NMDS axis 1 sample scores (NMDS1) and species diversity rarefied to 20 specimens. C) Correlation between NMDS1 and relative abundance of economically relevant edible species recovered in each sample (see Appendix S2 for details). D) Correlation between NMDS1 and the water depth assigned to each sample (see Methods for details). In each panel samples are symbol- and colour-coded according to the time interval and sub-environments: U-shore_H = mid-late Holocene upper nearshore; L-shore_H = mid-late Holocene lower nearshore; U-shore_P = present-day upper

nearshore; L-shore_P = present-day lower nearshore. In b–d panels, Spearman's correlation coefficient (ρ) is reported also for NMDS axis 2 sample scores. Correlation between sample NMDS scores and key community parameters is statistically significant ($p << 0.001$) in all comparisons except for NMDS2 vs % edible species and sample water depth ($p > 0.7$).

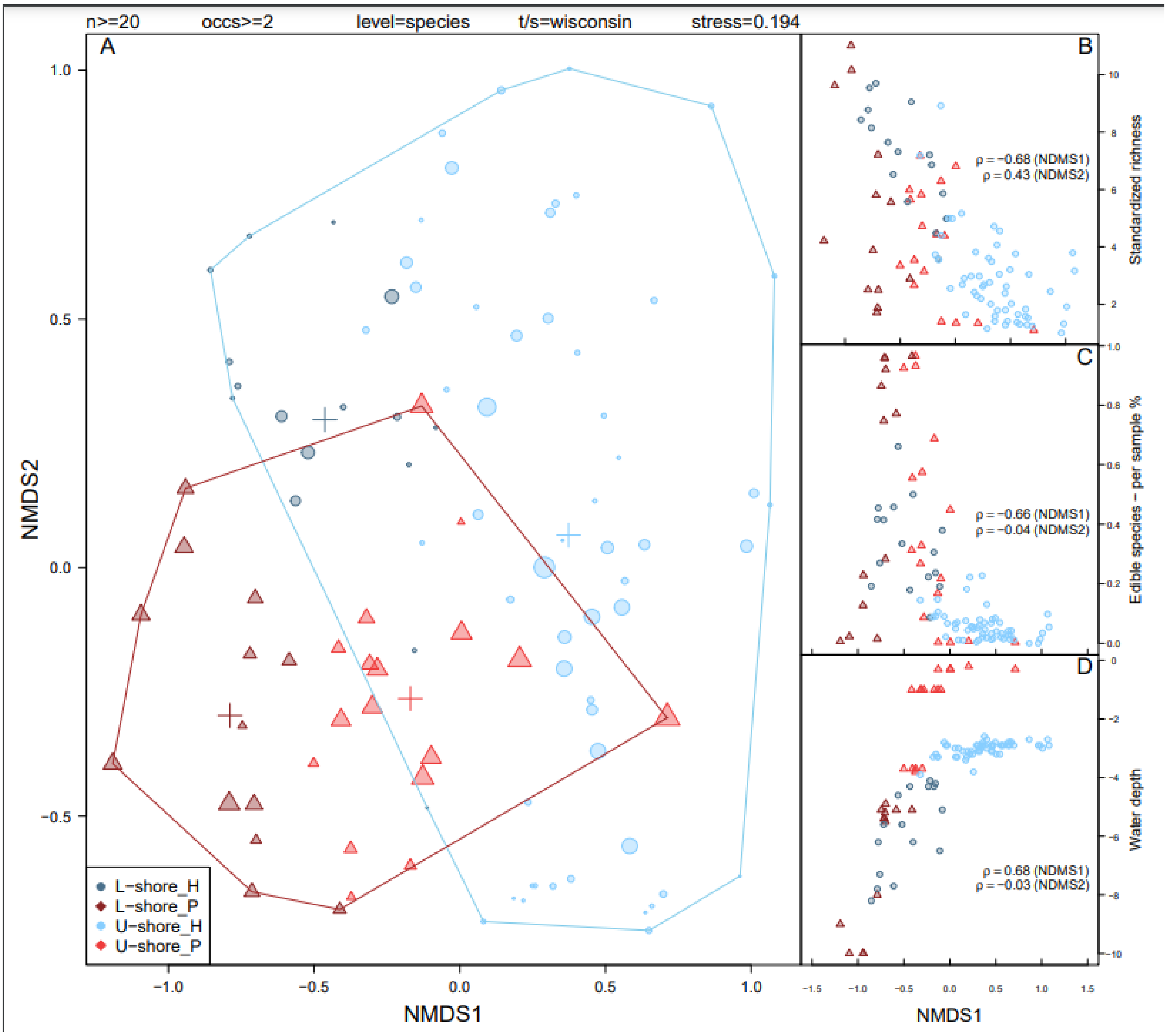

Figure 3. Varying Markov time models of the networks representing the mid-late Holocene succession (A) and present-day nearshore seabed (B) of the Po-Adriatic system. This alluvial diagram highlights changes in module assignments of nodes between network partitions obtained at different Markov times (Kheirkhahzadeh et al., 2016). The partition capturing the two-step dynamics on the links (Markov time = 2) is highlighted and its modular structure is used to colour nodes in other partitions.

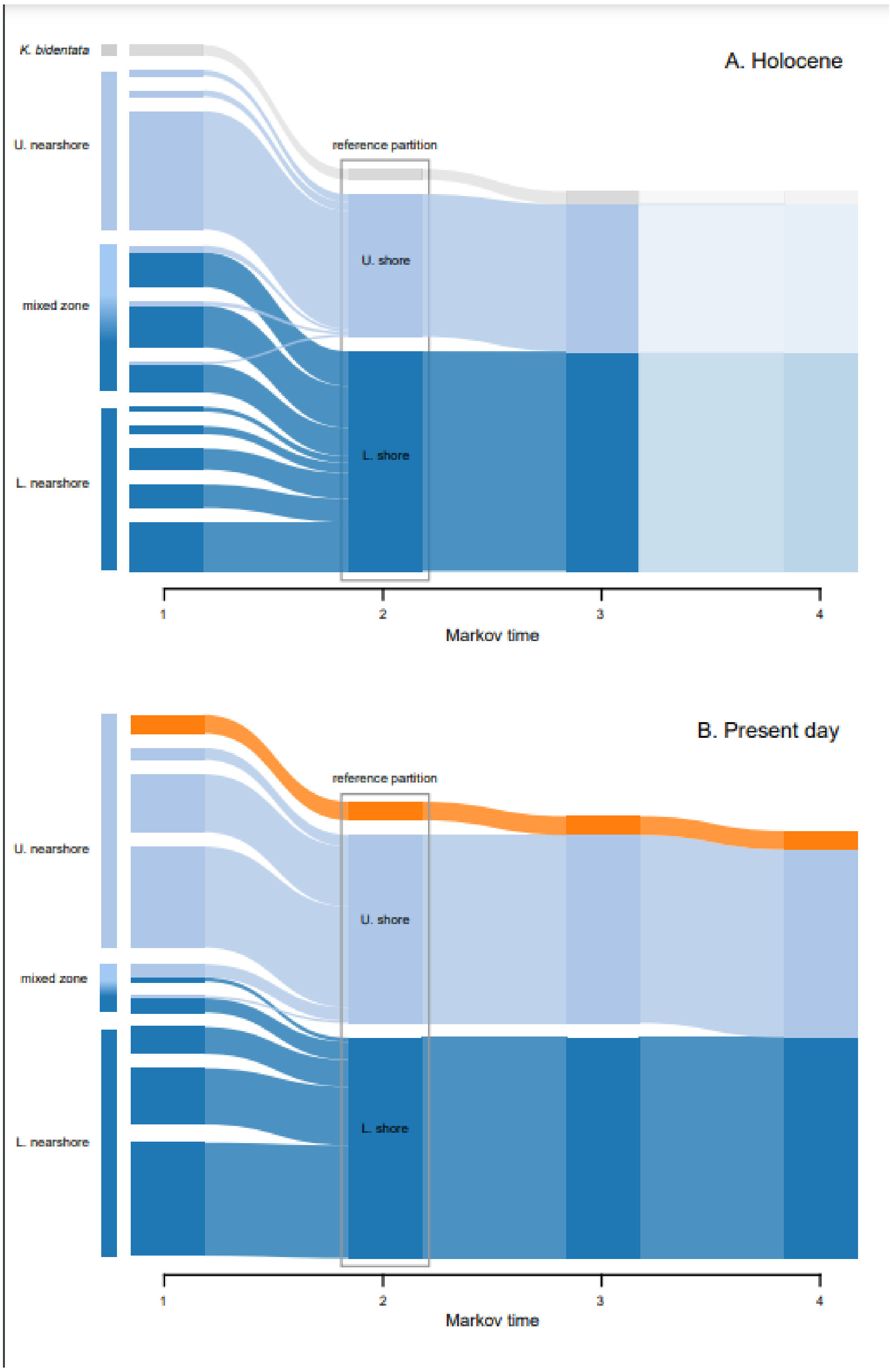

Figure 4. Relationship between economically relevant edible species (relative abundance per sample) and standardised diversity in targeted nearshore settings. Lines are Lowess functions based on samples pooled at nearshore level (blue circles = mid-late Holocene, brown triangles = present day). Standardised richness shows different behaviours in the analysed time intervals: Holocene assemblages show a moderate increase in both economically relevant taxa and standardised diversity between the upper and lower nearshore settings. The pattern is much less clear in present-day settings, with standardised diversity much more variable in lower nearshore samples. Economically relevant species tend to reach dominance more frequently only in the

present-day assemblages. U-shore_H = mid-late Holocene upper nearshore; L-shore_H = mid-late Holocene lower nearshore; U-shore_P = present-day upper nearshore; L-shore_P = present-day lower nearshore.

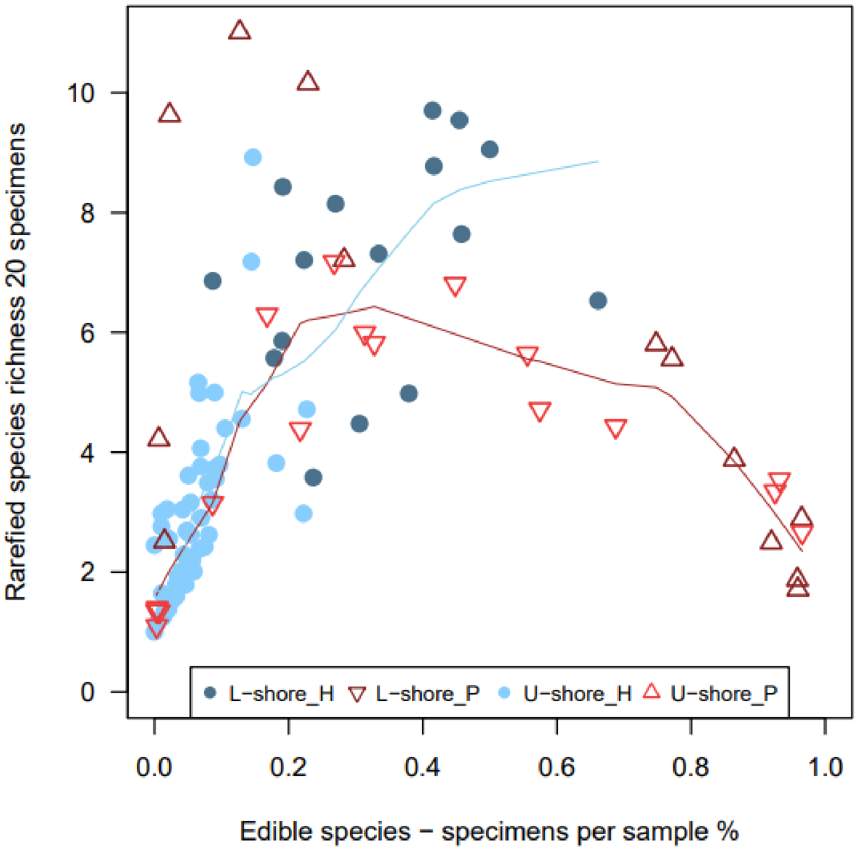

Figure 5. Modular patterns of the networks representing the mid-late Holocene succession and present-day nearshore seabed of the Northern Adriatic Sea (reference partitions). This alluvial diagram highlights changes in assignment of the taxa to nearshore sub-environments between the two time intervals. Although both networks show a similar modular structure, some taxa clustered into the module representing the Holocene lower nearshore belong to the module representing the present-day upper nearshore.

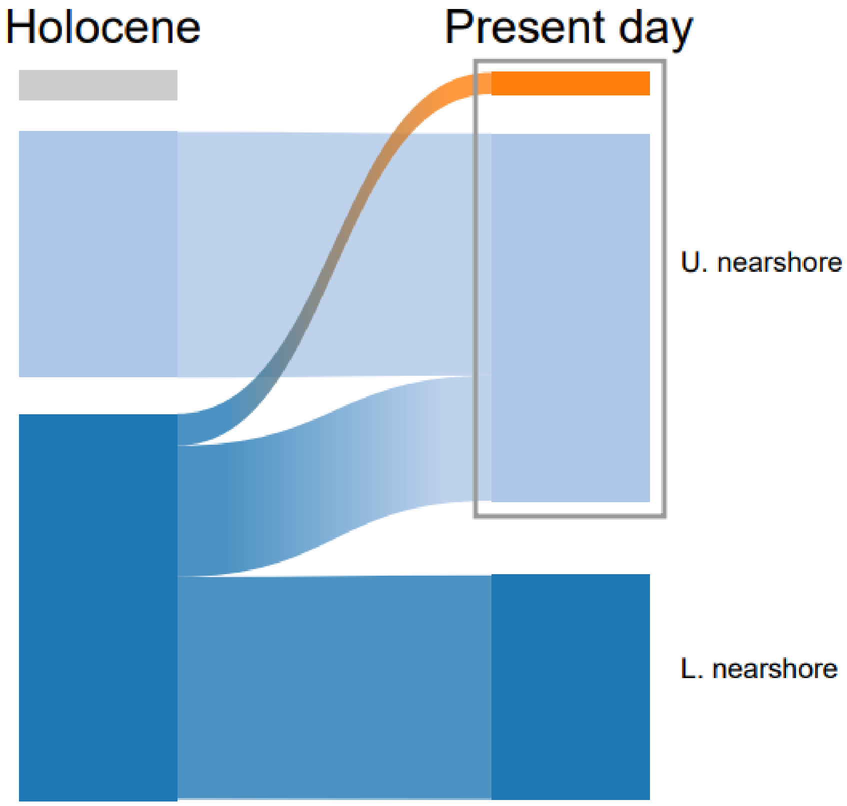
Holocene
Present day
U. nearshore
L. nearshore

Supplementary material for

Assessing biotic response to anthropogenic forcing using mollusc assemblages from the Po-Adriatic System (Italy)

Daniele Scarponi[1], Alexis Rojas[2], Rafał Nawrot[3], Alessandro Cheli[1,4], Michał Kowalewski[5]

Corresponding author email: daniele.scarponi@unibo.it

This PDF file includes:
Figures S1 to S6
Tables S1 to S3
Appendixes S1 to S4 captions and R-script information
References

Appendixes S1 to S4 and R-script files can be downloaded here: ---------

Supplementary figures

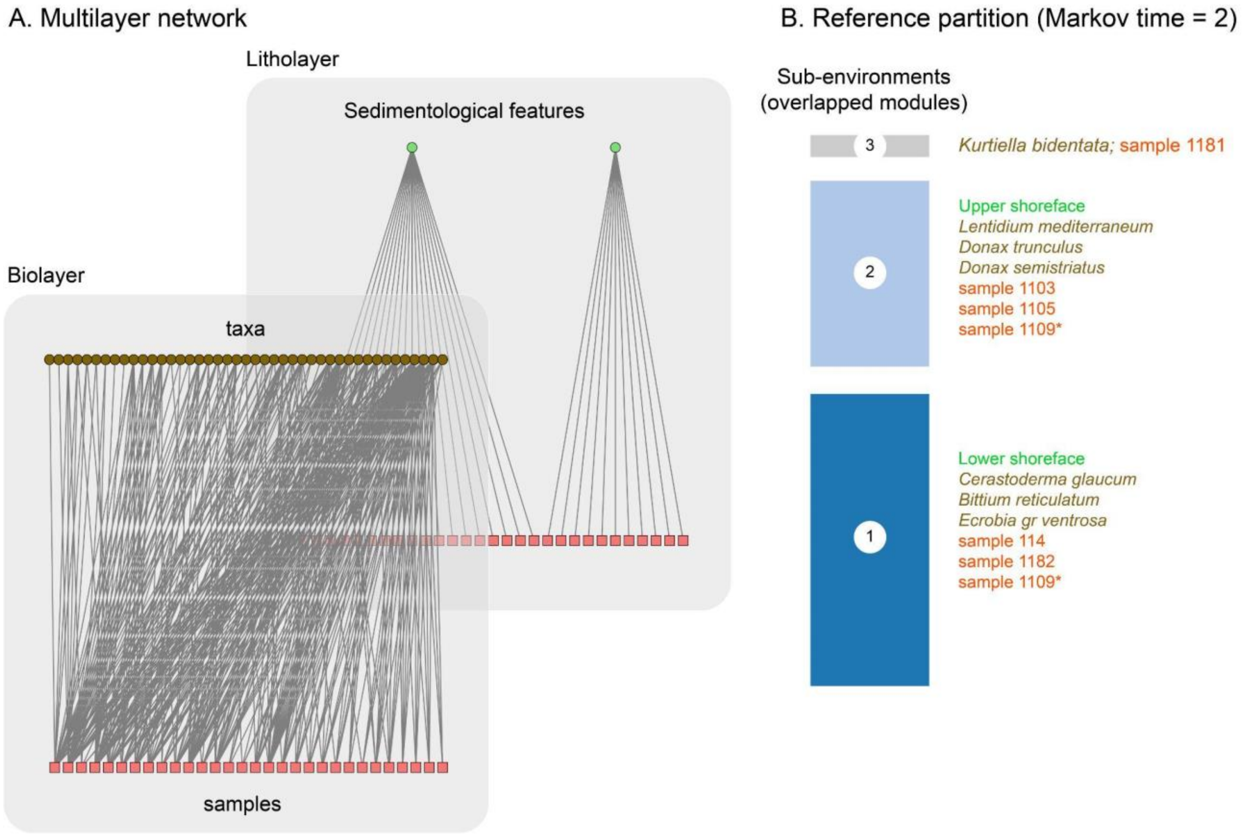

Figure S1. Multilayer network representation of the mid-late Holocene succession of the Po-Adriatic System. A) One layer describes the taxonomic composition of samples and the other describes their depositional environments. B) Holocene nearshore sub-environments. This alluvial diagram represents the network partition obtained when modeling the two-step dynamics on the links (Markov time = 2) (Kheirkhahzadeh et al. 2016). Infomap modules are shown as coloured bars with height proportional to the number of nodes. They comprise highly connected taxa, samples, and sedimentological features and can be directly interpreted as upper and lower shoreface sub-environments. Some higher ranked nodes per module are plotted, including one of the samples clustered into modules 1 and 2 to highlight the module overlapping in the reference partition.

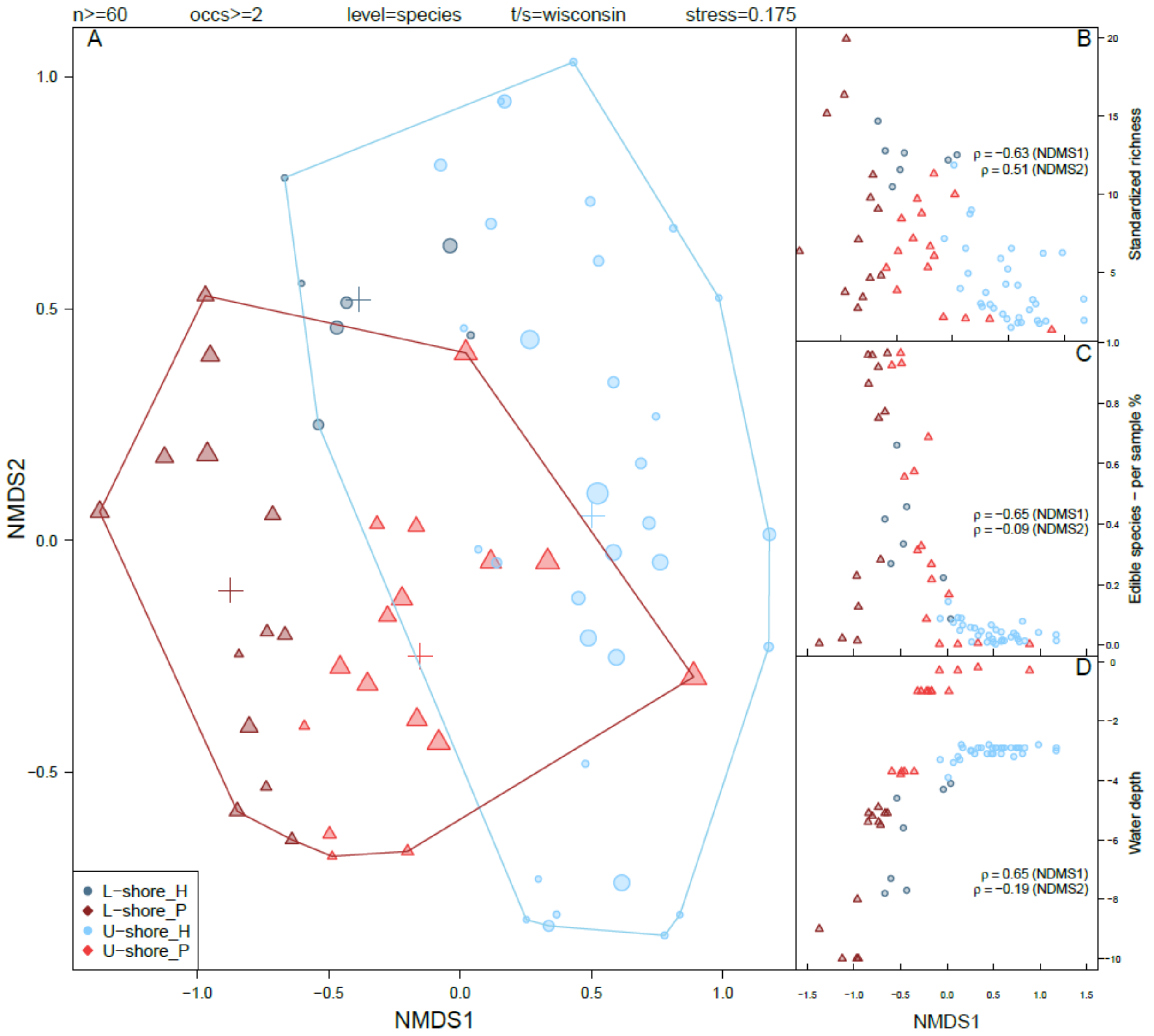

Figure S2. Nonmetric multidimensional scaling (NMDS) and rank correlation analyses at higher sample threshold (n ≥ 60 specimens) applying Wisconsin double standardisation. A) NMDS 3-D ordination (axes 1 and 2) of nearshore samples (Bray-Curtis dissimilarity index). The size of each point is the log transformed sample size. Convex hulls delimit the ordination space occupied by each nearshore group of samples: brown—present day, blue—Holocene. B) Correlation between NMDS axis 1 sample scores (NMDS1) and species diversity rarefied to 60 specimens. C) Correlation between NMDS1 and relative abundance of economically relevant edible species recovered in each sample (see Appendix S2 for details). D) Correlation between NMDS1 and the water depth assigned to each sample (see Methods for details). In each panel samples are symbol- and colour-coded according to the time interval and sub-environments: U-shore_H = mid-late Holocene upper nearshore; L-shore_H = mid-late Holocene lower nearshore; U-shore_P = present-day upper nearshore; L-shore_P = present-day lower nearshore. In b–d panels, Spearman’s correlation coefficient (ρ) is reported also for NMDS axis 2 sample scores.

Correlation between NMDS1 and key community parameters is statistically significant ($p << 0.001$) in all comparisons except for NMDS2 vs. % edible species and sample water depth ($p > 0.3$).

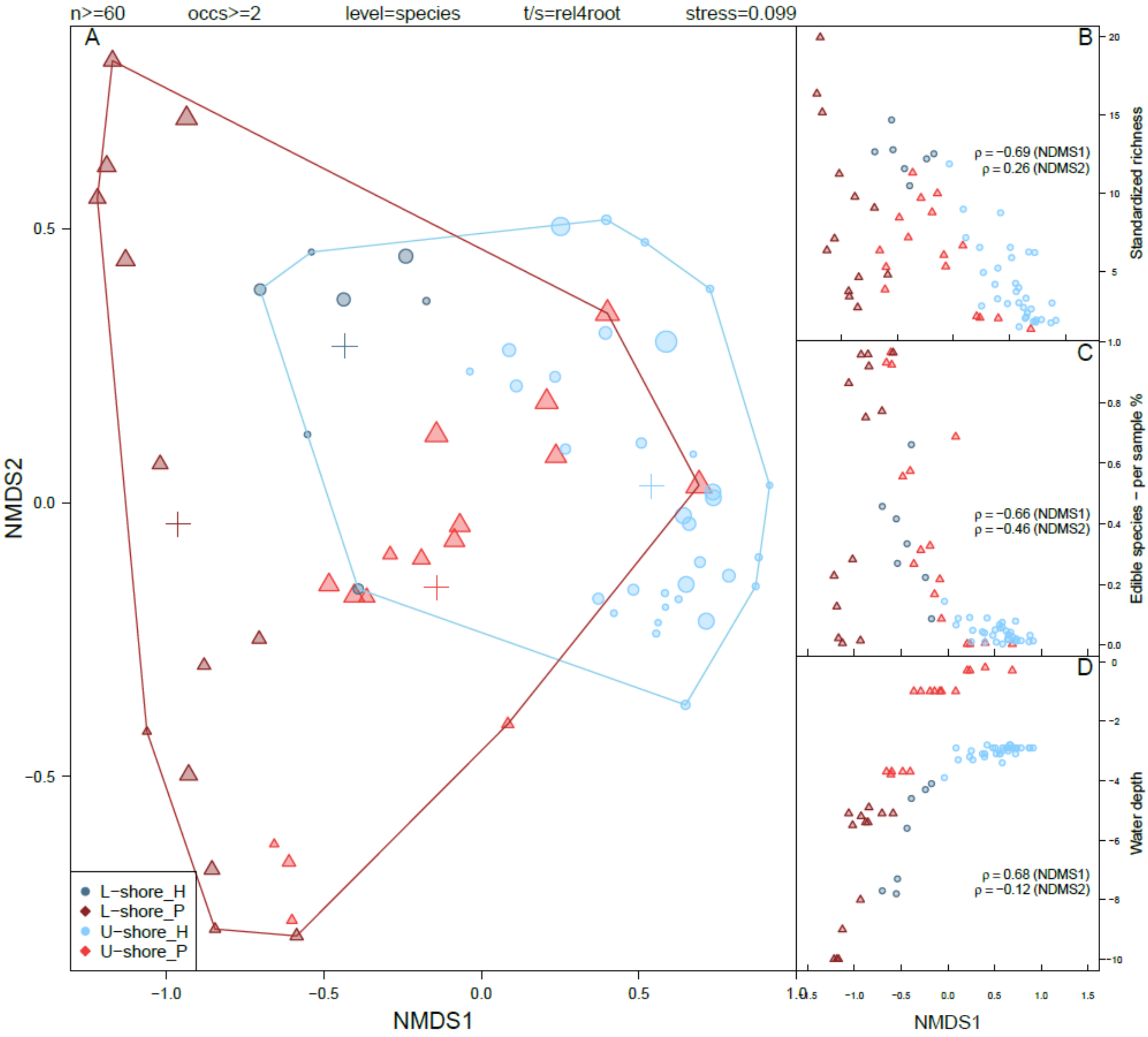

Figure S3. Nonmetric multidimensional scaling (NMDS) and rank correlation analyses at higher sample threshold (n ≥ 60 specimens) based on the fourth square root transformed relative abundances of species (rel4root). A) NMDS 3-D ordination (axes 1 and 2) of nearshore samples (Bray-Curtis dissimilarity index). The size of each point is the log transformed sample size. Convex hulls delimit the ordination space occupied by each nearshore group of samples: brown—present day, blue—Holocene. B) Correlation between NMDS axis 1 sample scores (NMDS1) and species diversity rarefied to 60 specimens. C) Correlation between NMDS1 and relative abundance of economically relevant edible species (see Appendix S2 for details). D) Correlation between NMDS1 and the water depth assigned to each sample (see Methods for details). In each panel samples are symbol- and colour-coded according to the time interval and sub-environments: U-shore_H = mid-late Holocene upper nearshore; L-shore_H = mid-late Holocene lower nearshore; U-shore_P = present-day upper nearshore; L-shore_P = present-day lower nearshore. In b–d panels, Spearman's correlation coefficient (ρ) is reported also for NMDS axis 2 sample scores. Correlation between sample NMDS scores and key community parameters is statistically significant (p << 0.001) in all comparisons except for NMDS2 vs. sample water depth (p-value > 0.3).

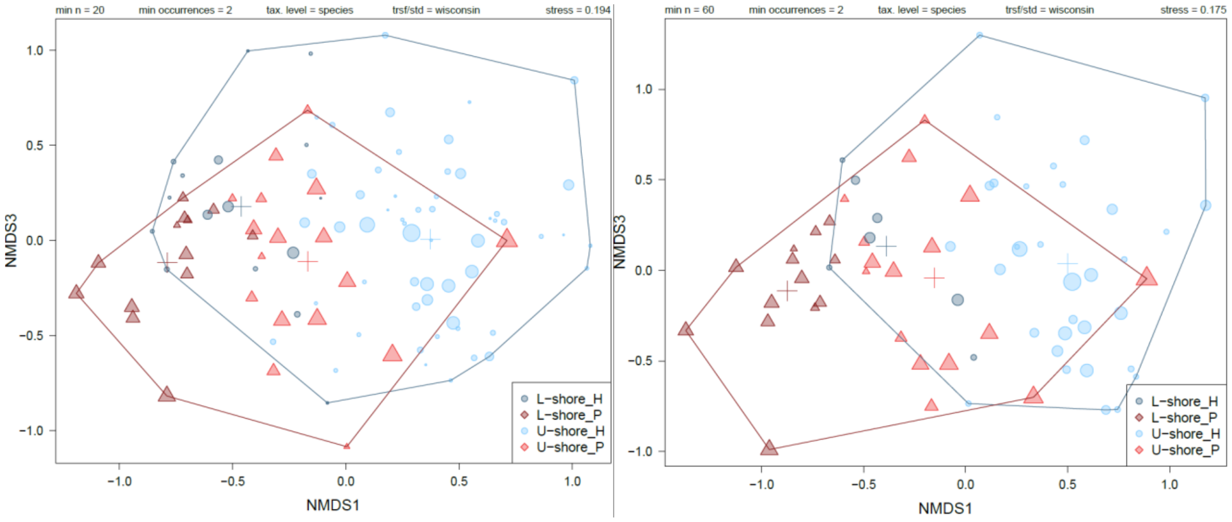

Figure S4. Nonmetric multidimensional scaling (NMDS) axes 1 and 3 of nearshore samples of the Po-Adriatic System. Bray-Curtis dissimilarity index and Wisconsin standardisation applied on a data matrix with singletons excluded. Panels show NMDS outputs based on samples with at least 20 (left) or 60 (right) specimens. Samples are symbol- and colour-coded according to the time intervals and sub-environments as in figures S2 and S3.

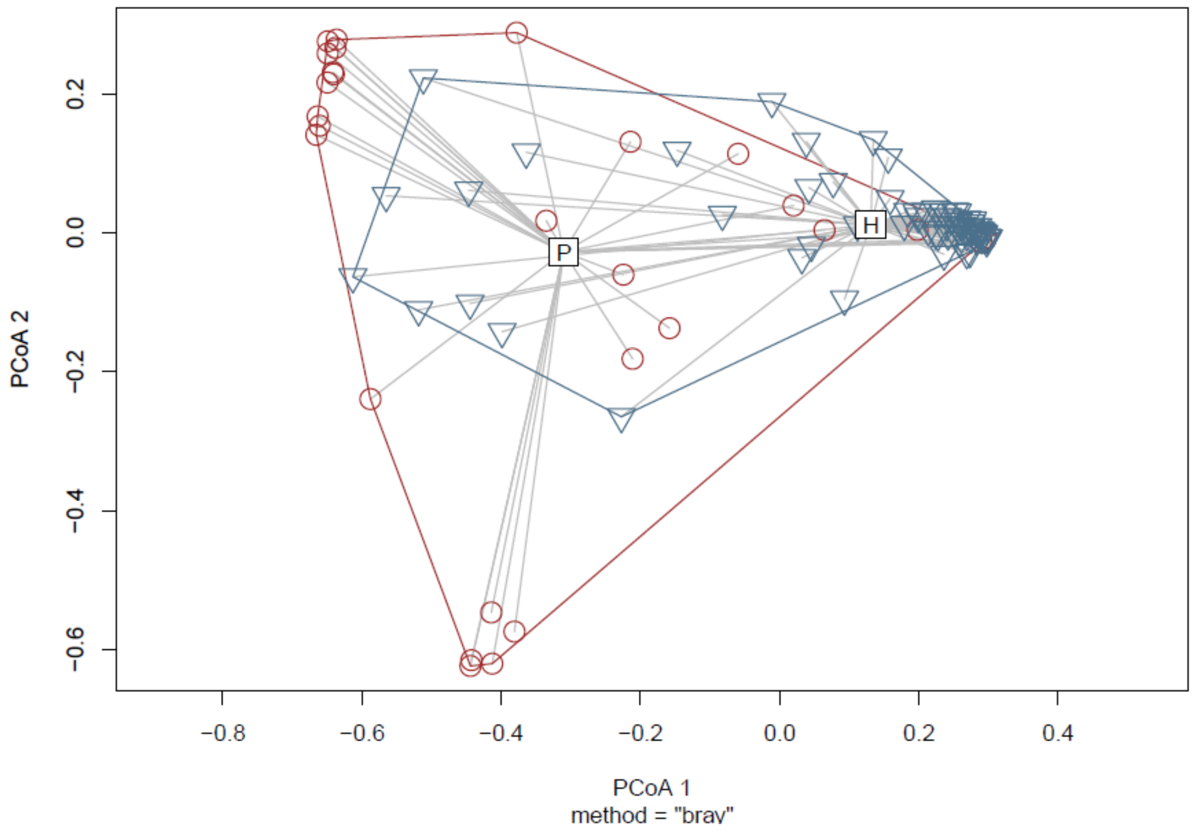

Figure S5. Principal coordinates analysis illustrating multivariate dispersion (a measure of beta diversity) in mid-late Holocene and present-day nearshore assemblages of the Po-Adriatic System. Average Bray-Curtis distance of samples to their group centroids is 0.526 for present day (P) and 0.245 for mid-late Holocene (H) nearshore sample groups. Tests for homogeneity of multivariate dispersions (999 permutations) and ANOVA both indicate statistically significant ($p < 0.05$) differences between the two time intervals. Samples are symbol- and colour-coded according to the time intervals (brown circles = present day; blue triangles = Holocene).

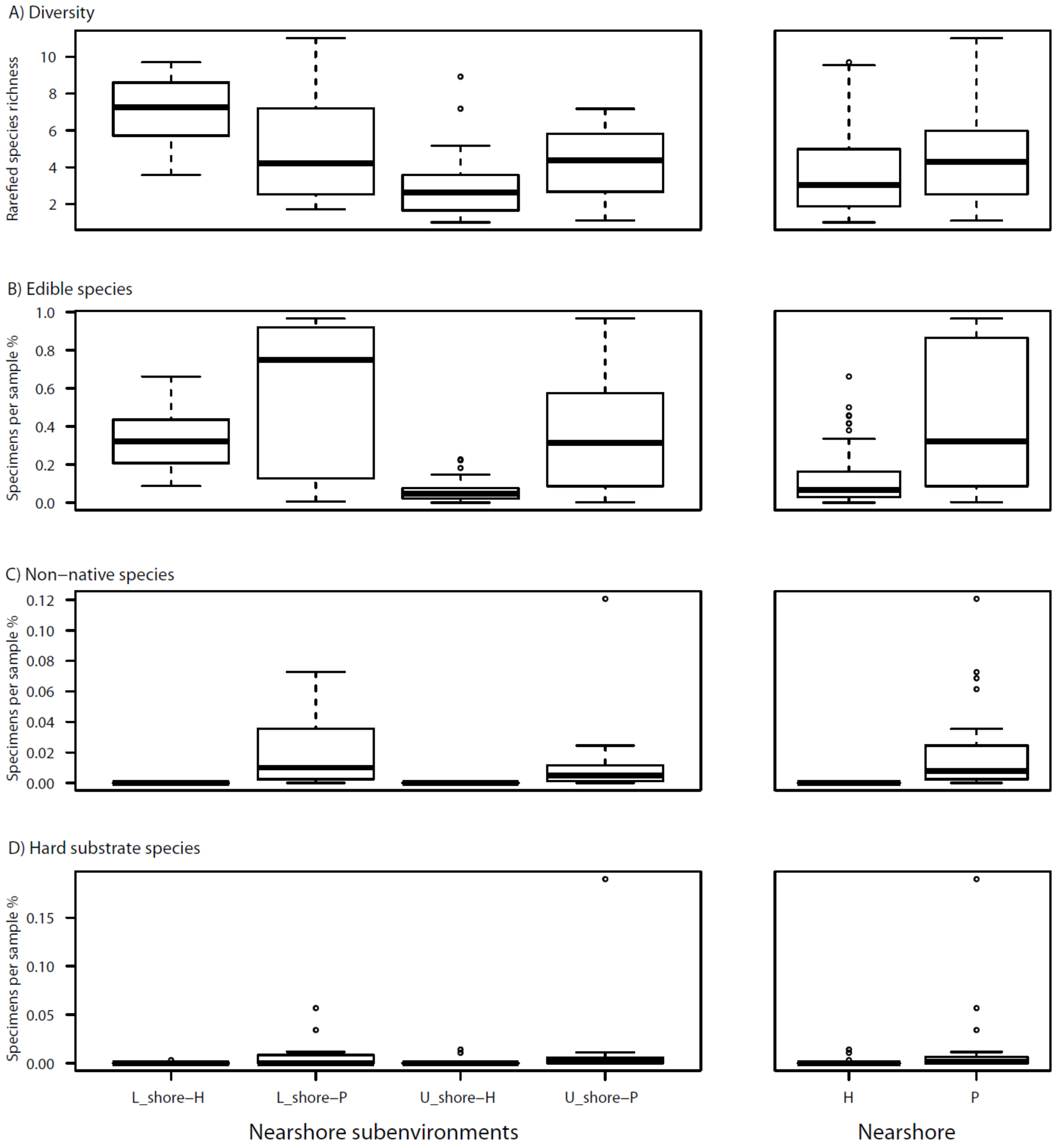

Figure S6. Bio-environmental descriptors of nearshore assemblages of the Po-Adriatic System (only samples with n ≥ 20 specimens considered). A) Rarefied species richness (at 20 specimens per sample). B) Per sample relative abundance of edible species that are economically relevant in the study area (Appendix S2). C) Per sample relative abundance of non-native species in the study area (Appendix S2). Non-native species are those that were initially distributed outside the central-eastern Mediterranean. D) Per sample relative abundance of species thriving on hard substrates (Appendix S2). The present-day increase of taxa related to hard substrates is minimal, but their presence is relatively widespread with respect to mid-late Holocene assemblages, in which such species were recovered in 3 upper nearshore and 1 lower nearshore samples (out of 71 samples investigated).

Supplementary tables

Taxon	Author	Substrate	Feeding	Nearshore-H %
Lentidium mediterraneum	(CostaO.G.,1839)	IN	SU	0.889
Chamelea gallina	(Linneo,1758)	IN	SU	0.033
Donax semistriatus	Poli,1795	IN	SU	0.015
Spisula subtruncata	(DaCosta,1778)	IN	SU	0.012
Bittium reticulatum	(DaCosta,1778)	EP	HE	0.010
Varicorbula gibba	(Olivi,1792)	IN	SU	0.009
Ecrobia gr. *ventrosa*	NA	EP	HE	0.005
Bela formica	Nordisieck,1977	EP	CAR	0.003
Peronidia albicans	Gmelin,1791	IN	DE	0.002
Tritia varicosa	(Lamarck,1822)	IN	CAR	0.002
Taxon	**Author**	**Substrate**	**Feeding**	**Nearshore-P %**
Lentidium mediterraneum	(CostaO.G.,1839)	IN	SU	0.562
Chamelea gallina	(Linneo,1758)	IN	SU	0.115
Varicorbula gibba	(Olivi,1792)	IN	SU	0.111
Donax semistriatus	Poli,1795	IN	SU	0.063
Spisula subtruncata	(DaCosta,1778)	IN	SU	0.017
Bittium reticulatum	(DaCosta,1778)	EP	HE	0.016
Tritia varicosa	(Lamarck,1822)	IN	CAR	0.015
Anadara gr. *kagoshimensis*	NA	SI	SU	0.010
Peronidia albicans	Gmelin,1791	IN	DE	0.009
Tritia neritea	(Linneo,1758)	IN	CAR	0.009

Table S1. The ten most abundant taxa in the investigated mid-late Holocene and present-day mollusc assemblages of the Po-Adriatic System. This table contains substrate and trophic information on the 10 most abundant taxa (relative abundance) retrieved in the Holocene (H) and present-day (P) time intervals. Abbreviations: IN—infaunal, SI—semi-infaunal, EP—epifaunal, SU—suspension and filter feeder, DE—(sub)surface (chemosymbiotic) deposit feeder, HE—herbivores, CAR—carnivores.

	name	flow	node ID	module ID	subenvironment
Holocene taxa	**L. shore**	0,071636	74	1	L. shoreface
	Cerastoderma glaucum	0,007360	37	1	L. shoreface
	Bittium reticulatum	0,007144	60	1	L. shoreface
	Ecrobia gr ventrosa	0,006929	62	1	L. shoreface
	Dosinia lupinus	0,006912	41	1	L. shoreface
	Moerella pulchella	0,006902	56	1	L. shoreface
	Loripes orbiculatus	0,006889	45	1	L. shoreface
	Chamelea gallina	0,006836	38	1	L. shoreface
	Lucinella divaricata	0,006818	46	1	L. shoreface
	Glycymeris glycymeris	0,006757	42	1	L. shoreface
	Varicorbula gibba	0,006716	57	1	L. shoreface
	Rissoa membranacea/ventricosa	0,006702	71	1	L. shoreface
	Peronidia albicans	0,006694	54	1	L. shoreface
	Pitar rudis	0,006693	51	1	L. shoreface
	Moerella distorta	0,006687	36	1	L. shoreface
	Tritia nitida	0,006644	66	1	L. shoreface
	Lembulus pella	0,006638	48	1	L. shoreface
	Pholas dactylus	0,006634	50	1	L. shoreface
	Fustiaria rubescens	0,006610	73	1	L. shoreface
	Ostrea edulis	0,006569	49	1	L. shoreface
	Spisula subtruncata	0,006549	53	1	L. shoreface
	Abra alba	0,006545	31	1	L. shoreface
	Fabulina fabula	0,006497	55	1	L. shoreface
	Calyptraea chinensis	0,006469	61	1	L. shoreface
	Acteon tornatilis	0,006469	58	1	L. shoreface
	Nucula nitidosa	0,006438	47	1	L. shoreface
	Bela formica	0,006396	59	1	L. shoreface
	Antalis dentalis	0,006388	72	1	L. shoreface
	Acanthocardia paucicostata	0,006379	35	1	L. shoreface
	Gibbula/Steromphala spp.	0,006356	63	1	L. shoreface
	Tritia varicosa	0,006335	67	1	L. shoreface
	Tritia mutabilis	0,006255	65	1	L. shoreface
	Mangelia attenuata	0,006248	64	1	L. shoreface
	Polititapes aureus	0,006236	52	1	L. shoreface
	Abra renieri	0,006146	33	1	L. shoreface
	Acanthocardia aculeata	0,006146	34	1	L. shoreface
	U. shore	0,144200	75	2	U. shoreface
	Lentidium mediterraneum	0,008003	44	2	U. shoreface
	Donax trunculus	0,007752	40	2	U. shoreface
	Donax semistriatus	0,007700	39	2	U. shoreface
	Pyrgiscus rufus	0,007554	69	2	U. shoreface
	Abra segmentum	0,007483	32	2	U. shoreface
	Pusillina lineolata	0,007341	68	2	U. shoreface

	sample ID	flow	node ID	module ID	sub-environment
Holocene samples	251	0,0365807	1	1	L. shoreface
	253	0,0339461	3	1	L. shoreface
	255	0,019734	16	1	L. shoreface
	1658	0,018933	2	1	L. shoreface
	1112	0,011231	13	1	L. shoreface
	1179	0,0108018	28	1	L. shoreface
	806	0,0105429	20	1	L. shoreface
	1181	0,00566537	29	1	L. shoreface
	1109	0,0176364	23	1	mixed L. and U. shoreface
	1109	0,00652624	23	2	mixed L. and U. shoreface
	1101	0,0108232	11	1	mixed L. and U. shoreface
	1101	0,00652624	11	2	mixed L. and U. shoreface
	799	0,00543923	19	1	mixed L. and U. shoreface
	799	0,00652624	19	2	mixed L. and U. shoreface
	1105	0,0142309	6	2	mixed L. and U. shoreface
	1180	0,0305667	15	1	mixed L. and U. shoreface
	1115	0,0503866	9	1	mixed L. and U. shoreface
	1113	0,0355971	24	1	mixed L. and U. shoreface
	1103	0,0154902	5	2	U. shoreface
	1177	0,0140258	8	2	U. shoreface
	1102	0,0133828	30	2	U. shoreface
	1104	0,0132877	22	2	U. shoreface
	1175	0,00935892	26	2	U. shoreface
	1174	0,00901591	7	2	U. shoreface
	797	0,00886813	12	2	U. shoreface
	1098	0,00886292	4	2	U. shoreface
	1176	0,00862268	27	2	U. shoreface
	1100	0,00819406	10	2	U. shoreface
	796	0,00779488	18	2	U. shoreface
	1173	0,00786075	14	2	U. shoreface
	1099	0,00776064	21	2	U. shoreface
	795	0,00764056	17	2	U. shoreface
	1172	0,00711522	25	2	U. shoreface

Table S2. Reference solution for the network representing the mid-late Holocene succession of the Po-Adriatic System. This table contains the best partition of 500 attempts. Modules are sorted by taxa and samples. In addition, within each module, nodes are sorted by the total amount of flow they contain–their steady state population of random walkers (Rosvall and Bergstrom, 2010). Samples influencing both upper and lower nearshore at Markov time = 1 and = 2 are highlighted in light gray (see also figure 3b) and dark gray, respectively.

	name	flow	node ID	module ID	sub-environtment
Recent taxa	**U. shore**	0,0928543	100	2	U. shoreface
	Lentidium mediterraneum	0,00574005	48	2	U. shoreface
	Donax semistriatus	0,00565501	43	2	U. shoreface
	Scrobicularia plana	0,00557203	65	2	U. shoreface
	Fabulina fabula	0,00553339	69	2	U. shoreface
	Loripes orbiculatus	0,00552301	49	2	U. shoreface
	Glycymeris nummaria	0,00548071	47	2	U. shoreface
	Mangelia attenuata	0,00542155	87	2	U. shoreface
	Mytilus edulis	0,00535691	54	2	U. shoreface
	Bela formica	0,00517731	76	2	U. shoreface
	Tritia neritea	0,00512827	81	2	U. shoreface
	Macomangulus tenuis	0,00511909	71	2	U. shoreface
	Donax trunculus	0,00510886	44	2	U. shoreface
	Parvicardium scabrum	0,005067	59	2	U. shoreface
	Moerella pulchella	0,0050632	70	2	U. shoreface
	Lucinella divaricata	0,00505989	50	2	U. shoreface
	Ecrobia gr ventrosa	0,00495894	82	2	U. shoreface
	Parthenina interstincta	0,00490466	91	2	U. shoreface
	Bittium latreillii	0,00481546	78	2	U. shoreface
	Ditrupa arietina	0,00480868	98	2	U. shoreface
	Fustiaria rubescens	0,00479149	97	2	U. shoreface
	Bela fuscata	0,00478282	77	2	U. shoreface
	Gibbula.Steromphala spp.	0,00465998	86	2	U. shoreface
	Pyrgiscus rufus	0,00465998	93	2	U. shoreface
	Rissoa auriformis	0,00465998	94	2	U. shoreface
	Ruditapes philippinarum	0,00504638	64	3	U. shoreface
	Mytilus galloprovincialis	0,00497449	55	3	U. shoreface
	Cerastoderma glaucum	0,00496291	41	3	U. shoreface
	Bittium reticulatum	0,00491477	79	3	U. shoreface
	L. shore	0,0688704	99	1	L. shoreface
	Chamelea gallina	0,00598125	42	1	L. shoreface
	Abra renieri	0,00560571	33	1	L. shoreface
	Solen marginatus	0,00545109	66	1	L. shoreface
	Thracia phaseolina cf	0,00531574	72	1	L. shoreface
	Bosemprella incarnata	0,00527686	38	1	L. shoreface
	Mactra stultorum	0,00511861	51	1	L. shoreface
	Peronidia albicans	0,00511628	68	1	L. shoreface
	Polititapes aureus	0,00510107	63	1	L. shoreface
	Dosinia lupinus	0,00509211	45	1	L. shoreface
	Varicorbula gibba	0,00506865	73	1	L. shoreface
	Anadara inaequivalvis	0,00500993	37	1	L. shoreface
	Spisula subtruncata	0,00500647	67	1	L. shoreface
	Philine aperta	0,00488571	92	1	L. shoreface
	Tritia nitida	0,00485571	89	1	L. shoreface
	Pharus legumen	0,00481819	60	1	L. shoreface
	Antalis dentalis	0,00481819	95	1	L. shoreface
	Tritia mutabilis	0,00476555	88	1	L. shoreface
	Abra alba	0,00475546	31	1	L. shoreface
	Abra prismatica	0,00473518	32	1	L. shoreface
	Epitonium turtonis	0,00468811	83	1	L. shoreface
	Acanthocardia aculeata	0,00466611	34	1	L. shoreface
	Euspira nitida	0,00462046	85	1	L. shoreface
	Tritia varicosa	0,00457661	90	1	L. shoreface
	Moerella distorta	0,00456966	40	1	L. shoreface
	Acanthocardia paucicostata	0,00456902	35	1	L. shoreface
	Eulima glabra	0,00456902	84	1	L. shoreface
	Anomia ephippium	0,0045511	39	1	L. shoreface
	Aporrhais pespelecani	0,00454884	75	1	L. shoreface
	Nucula nitidosa	0,00454155	56	1	L. shoreface
	Acteon tornatilis	0,00453115	74	1	L. shoreface
	Lembulus pella	0,00452933	57	1	L. shoreface

	Aequipecten opercularis	0,00452589	36	1	L. shoreface
	Calyptraea chinensis	0,00451594	80	1	L. shoreface
	Antalis inaequicostata	0,00451399	96	1	L. shoreface
	Flexopecten glaber	0,00450849	46	1	L. shoreface
	Phaxas adriaticus	0,00450839	61	1	L. shoreface
	Mysia undata	0,00448537	53	1	L. shoreface
	Ostrea edulis	0,00448	58	1	L. shoreface
	Mimachlamys varia	0,0044715	52	1	L. shoreface
	Pitar rudis	0,00446172	62	1	L. shoreface
	name (sample ID)	flow	node ID	module ID	sub-environtment
Recent samples	251	0,0620179	1	1	L. shoreface
	253	0,0422175	2	1	L. shoreface
	255	0,039939	3	1	L. shoreface
	1658	0,0327573	7	1	L. shoreface
	259	0,0106853	5	1	L. shoreface
	257	0,00822967	4	1	L. shoreface
	1649	0,00727358	16	1	L. shoreface
	1660	0,00710615	25	1	L. shoreface
	1657	0,00668408	6	1	L. shoreface
	1661	0,00562987	17	1	L. shoreface
	1659	0,00559663	8	1	L. shoreface
	1655	0,0547118	23	2	U. shoreface
	1656	0,0224641	24	2	U. shoreface
	248	0,0207306	18	2	mixed L. and U. shoreface
	1662	0,0105595	9	1	mixed L. and U. shoreface
	1663	0,0161455	10	1	mixed L. and U. shoreface
	1648	0,0167305	15	2	U. shoreface
	1644	0,016251	13	2	U. shoreface
	1643	0,0142307	19	2	U. shoreface
	1650	0,0128266	28	2	U. shoreface
	1647	0,0119094	14	2	U. shoreface
	1664	0,00774374	27	2	U. shoreface
	1653	0,00748293	30	2	U. shoreface
	1666	0,00714578	26	2	U. shoreface
	1651	0,00695928	29	2	U. shoreface
	1652	0,0068444	22	2	U. shoreface
	1645	0,00666915	20	2	U. shoreface
	1646	0,00650212	21	2	U. shoreface
	1665	0,00548619	11	2	U. shoreface
	1654	0,0235882	12	3	U. shoreface

Table S3. Reference solution for the network representing the present-day nearshore seabed of the Po-Adriatic System. This table contains the best partition of 500 attempts. Modules are sorted by samples and taxa. In addition, within each module, nodes are sorted by the total amount of flow they contain–their steady state population of random walkers (Rosvall and Bergstrom 2010). Samples influencing both upper and lower nearshore at Markov time = 1 are highlighted in light gray (see also figure 3a).

Appendixes (datasets .csv files) and R-script files

(Appendixes and a preliminary version of the R.scripts can be downloaded at: https://)

Please download the two .csv files (i.e., Appendix-S1 and Appendix-S2), and the four R-scripts in your R-studio working directory. Open Pre-processing 2022 R-file and run it to pre-process and restrict the dataset to relevant groups of species and samples. Then open Anthropogenic impact 2022 to get the remaining figures and data for the tables of the manuscript.

Appendix S1 - Raw abundance data (i.e., taxon-n), environmental and stratigraphic information concerning investigated nearshore samples from latest Quaternary sedimentary succession and present-days seabed of the Po-Adriatic System. Abbreviations: *ID* and *#obs*: sample identification numbers; *Housed:* Institution where samples are stored, BiGeA—Department of Biological, Geological and Environmental Sciences, University of Bologna (Italy), NHM-UF—Florida Museum of Natural History University of Florida (FL-USA); *#ofsamples*: 1—no subsamples, 2—subsamples present; *Live/Dead*: L—live specimens retrieved in the sample; D—dead specimens in the sample (defined only for present-day settings); D+L—dead and live fractions not separated; *Orig_label*: assigned sample label; *Region:* EMR—Emilia-Romagna, VT—Veneto; *Province* = RA—Ravenna, FC—Forlì-Cesena, RI—Rimini, FE—Ferrara, RO—Rovigo, VE—Venezia; *Samp_method:* method of sampling; *Samp_date:* date of sampling; *S_volume*: estimate of the sample volume; *Depth_sampling_(m)*: stratigraphic depth of the sample in meters (defined only for fossil settings); *Collector:* sample collector; *Environment*: present-day environmental attribution (defined only for present-day settings). *Sheet*, *Well* and *Locality:* spatial qualifiers of the samples based on the geologic map of Italy scale 1:50000; *Systems tract*: HST—highstand systems tract; *Age*: R—last ~100 years; H—mid-late Holocene; *Substrate:* sample grain size (qualitatively estimated); *Facies association* and *Facies association_b:* integrated facies or lithofacies employed to define a sedimentary environment (info are derived by previously published literature); *Env_interpret*: attribution of samples to backshore, upper and lower nearshore sub-environments (environmental subdivision following Sistilli et al. (2015), see Methods), present-day sample attribution is based on the sample depth (i.e., site altitude) and notes of the collector (e.g., stranded assemblage); as for Holocene samples, their attribution to backshore is based on facies associations qualifiers (columns facies associations and facies association_b), whereas upper- and lower-nearshore is based on the estimated sample depth and Sistilli et al. (2015) subdivision (see Methods); *Latitude* and *Longitude:* sample geographic qualifiers*; Site altitude (m.a.s.l.):* position of a sample respect to the sea-level (if from present-day settings) or offset, respect to the sea-level, of the top-most portion of the core to which a fossil sample belongs); *Parasequences*: succession of genetically-related bedsets that is bounded by marine flooding surfaces (or their correlative surfaces) on top and at the bottom: parasequence numbers after Amorosi et al. (2017), age of parasequences boundaries are available in Amorosi et al. (2017, fig. 6); *S-depth*: sample depth, as for present-day samples it is the *Site altitude* value, for fossil samples,it has been estimated following the Wittmer et al. (2014) approach (see Methods). NA—information not available or not applicable.

Appendix S2 Ecologic and taxonomic information concerning all taxa of the Po-Adriatic dataset (i.e., 787). Please note that the study targeted nearshore samples, so only a restricted taxonomic pool of the 787 taxa shows abundance values. Abbreviation: *ID* = taxon ID, reported also in Appendix S1; *Species_depth:* species preferential depth computed by weighted averaging on data from N. Adriatic; *Ecosystem:* M—marine, B—brackish, F—freshwater, L—land; *Class, Family, Genus Species:* taxonomy categorization, as for *Class/Phylum:* P—Polyplachophora, G—Gastropoda, C—Cephalopoda, B—Bivalvia, S—Scaphopoda, Po—Polychaeta, Ma—Maxillpoda, Br—Brachiopoda, Ec—Echinoidea; *Substrate, Mobility, Fixation, Feeding:* taxon qualifiers concerning the mode of life categorization, S*ubstrate*: IN—infaunal, SI—semi-infaunal, EP—epifaunal, WB—borer/nestler, EP-IN—epifaunal and infaunal behaviour, NC—nektonic, *Mobility:* IM—immobile, SE—sedentary, AM—actively mobile, *Fixation:* UN—unattached, BA—byssaly attached, CE—cemented, *Feeding*: SU—suspension and filter feeder, DE—(sub)surface (chemosymbiotic) deposit feeder, HE—herbivores, CAR—carnivores, OM—omnivorous, PAR—parasites, SU-DE—suspension and (sub)surface (chemosymbiotic) deposit feeder, PAR-CAR—parasites and carnivores; *Family*-to-*Species*_ID: taxon ID for computational purposes; *Biogeography*: species distribution: COS—cosmopolitan, BOR—Mediterranean-to-Boreal; MED/LUS—Mediterranean-to-Lusitanian; WAF—West African; Exotic: Y = non-native species; *Edible:* Y = economically relevant species in the northeastern Adriatic.

Appendix S3. Multilayer network representation of the mid-late Holocene succession of the Po-Adriatic System. This standard file specifies nodes and links in two different sections. The first section includes the node indexes and names. The second section describes the intralayer link structure; each row includes layer index, source node index, target node index, and link weight. Interlayer links are created by Infomap from the intralayer link structure by relaxing the layer constraints on those links with probability r = 0.8.

Appendix S4. Multilayer network representation of the present-day nearshore seabed of the Po-Adriatic System. This standard file specifies nodes and links in two different sections. The first section includes the node indexes and names. The second section describes the intralayer link structure; each row includes layer index, source node index, target node index, and link weight. Interlayer links are created by Infomap from the intralayer link structure by relaxing the layer constraints on those links with probability r = 0.8.

References

Amorosi, A., Bruno, L., Campo, B., Morelli, A., Rossi, V., Scarponi, D., Hong, W., Bohacs, K.M. and Drexler, T.M. (2017) Global sea-level control on local parasequence architecture from the Holocene record of the Po Plain, Italy. Mar. Petrol. Geol., 87, 99–111.

Rosvall M., Bergstrom C.T. (2010). Mapping change in large networks. PloS one, 5(1), e8694.

Sistilli F., Scarelli F., Stecchi F., Fabbri S., Cantelli L., Gabbianelli G. (2015). Spatial and temporal evolution and morphodynamic zonation fo the Ravenna shoreface. Coastal and Marittime Mediterranean Conference, 89-92.

Wittmer J.M., Dexter T.A., Scarponi D., Amorosi A., Kowalewski M. (2014). Quantitative bathymetric models for late quaternary transgressive-regressive cycles of the po plain, Italy. Journal of Geology, 122(6), 649-670.

Chapter 5. Multi-scale characterization of shell mechanical and compositional features in *Mytilus galloprovincialis* across life stages *(manuscript in preparation)*

Multi-scale characterization of shell mechanical and compositional features in *Mytilus galloprovincialis* across life stages

Alessandro Cheli[1,2], Nicola Di Simone[3], Rajapaksha Haddokara Gedara Rasika Wathsala[3], Devis Montroni[1], Arianna Mancuso[2,7], Fiorella Prada[2,4], Claudio Marzadori[5], Jaap Kaandorp[6], Stefano Goffredo[2,7], Giuseppe Falini[1,8] and Silvia Franzellitti[2,3]

[1] *Department of Chemistry "Giacomo Ciamician", Alma Mater Studiorum – Università di Bologna, via Selmi 2, 40126 Bologna, Italy.*

[2] *Fano Marine Center, The Inter-Institute Center for Research on Marine Biodiversity, Resources and Biotechnologies, viale Adriatico 1/N 61032 Fano, Italy.*

[3] *Animal and Environmental Physiology Laboratory, Department of Biological, Geological and Environmental Sciences, University of Bologna, Via S. Alberto 163, Ravenna, Italy.*

[4] *Environmental Biophysics and Molecular Ecology Program, Department of Marine and Coastal Sciences, Rutgers, The State University of New Jersey, New Brunswick, New Jersey, USA*

[5] *Department of Science and Technology of Agriculture and Environment (DISTAL), Alma Mater Studiorum - Università di Bologna, via Fanin 40, 40127 Bologna, Italy.*

[6] *Computational Science Lab, University of Amsterdam, Science Park 904, 1098XH, Amsterdam, the Netherlands.*

[7] *Marine Science Group, Department of Biological, Geological and Environmental Sciences, University of Bologna, Via Selmi 3, Bologna, Italy*

[8] CNR, *Institute of nanostructured materials (ISMN), via Gobetti 101, 40129 Bologna, Italy.*

Abstract

Mytilus galloprovincialis is a sessile bivalve mollusk with high ecological and economical relevance. The shell has a vital protective and supportive role for the animal and its known that composition and structure change with the organism age, while less documented is their effect on mechanical properties. Here we conducted a characterization of shell features in *Mytilus galloprovincialis* of different sizes at three different life stages: sexually immature organisms, individuals in maturation and fully sexually developed individuals. The results obtained with a multiscale analysis by biometric, thermogravimetric, infrared spectroscopy, X-ray diffraction and ICP-OES measurements, associated with mechanical tests, show that the skeletal macrostructure and resistance to fracture change in shells from immature to mature organisms. With increasing shell size, a decrease in porosity, shell calcite content and intra-shell organic matrix is observed, while an increase in bulk density, thickness, maximum load to breakage and elasticity occurred. These data highlight how shell multiscale properties are strictly related to size, making this parameter a key factor to consider in biological studies addressing the effect of environmental stressors on mussels. This information has also a crucial relevance in aquaculture, being the mechanical properties of shells a key parameter in the harvesting and packaging of mussels.

Keywords: Mussel shells, shell size, mechanical properties, structural properties, composition.

Introduction

The wide distribution of marine mussels in coastal environments, along with their ecological and economical importance, have made them model organisms for physiological, ecological, and biomechanical studies (Bajt et al., 2019a; Denny & Gaylord, 2010). Along with other organisms that dominate the coastal environment, these animals are currently threatened by several anthropogenic stressors like climate change, eutrophication, pollution, or alien species input (Bajt et al., 2019b; Coll et al., 2010). These sessile animals play a key role as filter feeders, making them important bioaccumulators and are considered valuable environmental sentinels (Beyer et al., 2017; Bråte et al., 2018; Goldberg, 1975; Pavicic et al., 1993). They also represent an important source of nutrients and bioactive molecules for medical and pharmacological applications (Grienke et al., 2014).

According to statistics from the United Nation's Food and Agriculture Organization (FAO), the production of mussels for edible purposes has increased annually since 2018 in the world and was up to more than 200 million tons in 2018 (FAO, 2020). Nearly all current farm mussel production is sold as an in-shell product, either live or frozen, after primary processing. Thus, shell strength is a critical properties for a successful farm affecting the susceptibility to shell breakage during the processing stages (Penney et al., 2007).

Mussel shell comprises two calcium carbonate polymorphs: calcite and aragonite. The outer layer of the shell, referred as calcite prismatic layer, is made of long, slender fibers of calcite (some 1–2 µm wide and hundreds of µm long), which reach the internal surface of the shell (Marin et al., 2012b). This microstructure has been named anvil-type fibrous calcite. Below that, the myostracum layer is present. This is usually a very thin layer, made of aragonite, located in the attachment of the adductor muscle to the umbo of each valve. This layer is in direct contact with the inner layer formed by the nacre. The nacreous layer has a well-defined type of micro-structure characterized by small flat tablets (200-500 nm thick) of aragonite tightly packed together, glued by thin organic matrix layers, and connected by mineral bridges (Huang et al., 2019; Montroni, 2020; Nudelman et al., 2008).

Mussel shells plays an essential role for the organism ensuring structural integrity and the protection of soft vital tissues against aggressive (abiotic and biotic) environments. The process of shells formation is influenced by the environment, which can affect the energy allocation patterns in the organism (Bergström & Lindegarth, 2016b; Kroeker et al., 2016b; Telesca et al., 2018b). Environmental changes, including increasing temperature due to global warming, has direct effects on skeletal features of bivalves by affecting their morphometric characteristics and growth rates (Mackenzie et al., 2014b; Mancuso et al., 2019c). It has been observed that bivalve shells face the ongoing increasing temperature by a reduction of thickness with a consequent increase in shell fragility (Gizzi, Caccia, Simoncini, Mancuso, Reggi, Fermani, Brizi, Fantazzini, Stagioni, & Falini, 2016; Olson et al., 2012). Thus, any possible reduction in thickness and mechanical strength could have a profound effect on survival, by reducing protection of the soft tissues from predators and anthropogenic activity (Gizzi, Caccia, Simoncini, Mancuso, Reggi, Fermani, Brizi, Fantazzini, Stagioni, & Falini, 2016; Mackenzie et al., 2014b). The variation in bivalve shell thickness may be a plastic or adaptive trait (Nagarajan et al., 2006; Parsons, 1997; Proćków et al., 2018). On a local scale an increase of shell thickness can be relevant in diverse contexts like (Seed & Richardson, 1999): reduction of successful predation (Lemasson & Knights, 2021); (Leonard et al., 1999); protection of individuals from intense wave action destructive effects (Steffani & Branch, 2003); mechanical support to protect mussels from the effects of density, layering and aggregation in mussel beds (Bertness & Grosholz, 1985).

In order to provide an efficient protection, the shell must be both stiff and strong. Previous mechanical tests conducted on about 20 different species of seashells revealed an elastic modulus ranging between 40 GPa and 70 GPa, and a strength in the 20–120 MPa range (Currey & Taylor, 1974). Inside mussel shell, the nacreous layer has been observed to be the strongest one (Sun & Bhushan, 2012; Tushtev et al., 2008). Usually, the breakage pattern in the *Mytilus* genus consists of one fracture only, which does not extend from the point of loading but whose path is highly unpredictable (Zuschin & Stanton, 2001). In a recent study on *Mytilus californianus*, the shell was loaded for 15 cycles at ∼55% of its predicted breaking force (Crane & Denny, 2022). In this study repaired shells of experimentally stressed mussels were as strong as the control mussels that had not been experimentally loaded; however, stressed mussels had higher mortality and less soft tissue than the control group (Crane & Denny, 2022).

Structural, physical and mechanical properties of mussel shells change during the ontogenesis and thus is crucial to evaluate the effect of environmental and anthropogenic stresses on the organism at different life stages. Mechanical analyses of the nacreous mussel *Perumytilus purpuratus* shells of different sizes performed on cubic specimens cut from shell, have shown that stress and strain strength and elastic modulus degraded during ontogeny, showing an orthotropic behavior under compression (Muñoz-Moya et al., 2022).

This study aims to evaluate the biometric, mechanical and compositional features of *M. galloprovincialis* shell from the north-western coasts of the Adriatic Sea. Since the development of gonads and the storage of gametes for reproduction brings a variation of physiological parameters and different allocation pattern of energies, analyses were conducted on shells of different size ranges, corresponding to different stages of organism sexual maturation. This allowed to investigate shells properties variation during mussel growth.

Materials and methods

Samplings

Specimen of *M. galloprovincialis* were collected by fishermen of the “Cooperativa Pro.mo.ittica” in Cesenatico (Emilia-Romagna, Italy) in 2019. After sampling, mussels were immediately stored in coolers (+4 °C) and transferred to the laboratory to be cleaned, washed and then stored at -20 °C.

All analysis was performed on shells of three different sizes: sexually immature organism, with a maximum shell length of 3 cm (which we will refer to as "small" shells); individuals in maturation, with a shell size between 3 and 5 cm (which we will refer to as "medium" shells); fully sexually developed individuals, with a shell size greater than 5 cm, the minimum commercial size (which we will refer to as "large” shells). Although differences in the growth rate may occur due to specific local environmental parameters, mussels of above 5 cm of length can generally be considered sexually mature (Gosling, 2015).

Shell biometric parameters

The two valves from each mussel were separated so that one could be used for destructive analysis while the other one was saved for the conservative analysis. When only one valve of the organism was available for the tests and not damaged, it was assigned to the destructive analysis, being those that better help to understand the inner structure of the shell. A scalpel was used to eliminate residual calcifying epibionts. Shells were cleaned through a 24-h incubation in sodium hypochlorite solution (10 vol.%) to remove oxidable impurities such as encrustations and algae and air dried.

The dry weight was measured with an Ohaus Pioneer analytical balance precision scale (± 0.1mg), Ohaus Europe GmbH, Switzerland. Length and width of the shells were obtained through image analysis by using the software ImageJ (Rasband, n.d.; Schneider et al., 2012) (Figure 1A). Height was measured using a calliper (± 0.05 mm) (Figure 1A). For thickness measurements, shells were sectioned longitudinally with a circular saw and were measured in three points, near the umbo, at the centre and at the ventral margin (Figure 1B), using a digital micro-meter (0-25 mm range, 0.001 mm digital step). The mean thickness value from three measured points were considered.

Skeletal parameters (micro-density, porosity and bulk density) were determined with the buoyant weight technique as described in previous studies (Cheli et al., 2021b; Mancuso et al., 2019d). Briefly, using an Ohaus Pioneer Analytical kit, Ohaus Europe GmbH, Switzerland (± 0.1 mg) for hydrostatic weight added to the precision scale, it was possible to measure the weight of the shells in water (H_2O weight) and in air (air weight), both different from the dry weight since they also considered the weight of pores filled with water. Once these measurements were obtained, it was then possible to calculate the derived skeletal parameters: micro-density (mass per unit volume of the material which composes the shell, excluding the volume of pores), porosity (the volume of pores connected to the external surface), and bulk density (the density of the shell, including the volume of pores).

Shell mechanical properties

The shells were prepared to the test using a universal polishing machine (Universal Polisher LS1, Remet, Bologna, Italy) which was able to smooth the edges of each valve giving it a more uniform standing base. This procedure removed only the small bumps and ridges that often occur along mussel apertures. No additional treatments were performed on the samples, in order to maintain them as pristine as possible and shells were stored in saltwater during the different steps of the measurements.

Compression tests were performed by using an Instron universal testing machine (Illinois Tool Works Inc., Norwood – MA, USA) equipped with a force transducer of 1 kN. The compression plate moved with a downward vertical movement speed of 0.5 $\mathrm{mm \cdot min^{-1}}$. From each loading curve, the breaking force was identified as the force at which catastrophic failure occurred, we will refer to it as ‘Maximum load (kN; Supplementary Figure 1). In a rigorous data treatment, the strength should be used as the stress at failure, a force per area. However, quantifying stress distributions across the mussel shell and relevant cross-sectional areas was beyond the scope of this study. For this reason, the slope of the strain/stress curve in the typical elastic region, here reported as elasticity, is used to estimate the material’s stiffness (Supplementary Figure 1).

The fragments obtained from the mechanical tests, together with the remaining shells not used for the biometric analysis, were cleaned from superficial organic residues by soaking them in a sodium hypochlorite solution 10 wt.% for 24 hours, rinsed with distilled water, air dried and then individually pulverized using a ceramic mortar first and then an agate mortar to reach a fine granulometry (less than 100 μm). The obtained shell powders were used for further analyses.

Evaluation of organic matrix content

Thermogravimetric analyses (TGA) was performed to evaluate the content of intraskeletal material removed by the heating process, which is made of organic matrix (OM) and water. A SDT Q600 instrument (Thermal Analysis Instrument, New Castle, DE) was used to perform the measurements. About 20 mg of each sample powder were individually placed in a ceramic crucible. The measurements were carried out using a heating ramp of 10 °C·min^{-1} from 30 °C to 850 °C, prior equilibration at 30 °C and a nitrogen flux of 100 mL·min^{-1}. The content of OM was measured as the weight loss percentage between 250 °C and 450 °C.

Spectroscopic measurements

Fourier Transform Infrared spectroscopy (FTIR) analyses were carried out using a Nicolet IS10 Spectrometer (Thermo Electron Corporation). The spectra were obtained in the 400 – 4,000 cm^{-1} range at a resolution of 2 cm^{-1} and 64 scans. The samples were analysed as KBr pellets using a sample concentration of about 1 wt.%. Omnic software (Thermo Electron Corp., Woburn, MA) was used for spectra processing and baseline correction.

Diffractometric measurements

X-ray diffractometric (XRD) analyses were conducted for each sample using a X'celerator detector fitted on a PANalytical X'Pert Pro diffractometer, using a Cu-Kα radiation generated at 40 kV and 40 mA. The data were collected within the 2θ range from 20° to 60° with a step size (Δ2θ) of 0.016° and a counting time of 60 s. Fixed anti-scatter and divergence slits of 1/2° were used with 10 mm beam mask. All measurements were carried out in a continuous mode. The XRD patterns were analysed for determine polymorphic distribution using the Profex 4.3.1 software (Döbelin and Kleeberg, 2015).

Elemental analysis

Inductively coupled plasma optical emission spectroscopy (ICP-OES) measurements were performed on sodium hypochlorite treated shell powders. Samples were dissolved in a 1 M HNO_3 solution and were measured three times, 12 s each, with 60 s of pre-running, using an ICP-OES, Spectro Arcos-Ametek, Inductive Coupled Plasma Optical Emission Spectroscopy with an axial torch and high salinity kit. The calibrating curve was made using certified standards in water. Four small, five medium and five big samples were measured. The concentration of the elements was normalized over the Ca one.

Statistical analyses

Data were checked for normality using the Shapiro-Wilk test ($N < 50$) and for homogeneity using Levene's Test. ANOVA was used to compare intra-skeletal organic matrix content, max load, elasticity, skeletal mineralogy (i.e., aragonite and calcite content), and the concentration of trace elements among size classes. When assumptions for parametric statistics were not fulfilled, the non-parametric Kruskal–Wallis test was used, in particular for length, mass, width, height, thickness, micro-density, porosity, bulk density, and the concentration of trace elements among size classes. Where significant, pairwise comparisons between size classes were performed via Mann-Whitney U and LSD post hoc tests.

Results

All investigated parameters differed significantly among size classes (Kruskal-Wallis: $p < 0.001$ for width, height, mass, thickness, micro-density, porosity, bulk density, and elasticity; ANOVA: $p < 0.001$ for Max load and OM, $p < 0.01$ for aragonite). They were progressively higher from small to medium, to large individuals (Figures 2-4; Supplementary Table 1), except for OM and porosity which progressively decreased from small, to medium, to large individuals (Mann-Whitney U: $p < 0.001$; Figure 3; Supplementary Table 1). Micro-density and bulk density increased by ~ 3% and ~ 9%, respectively, while porosity decreased by ~ 45% from small to large individuals (Mann-Whitney U: $p < 0.001$; Figure 3; Supplementary Table 1). The OM content decreased by ~ 30% (LSD: $p < 0.001$) while elasticity and max load increased by an order of magnitude from small to large individuals (Mann-Whitney U: $p < 0.001$ and LSD: $p < 0.001$, respectively; Figures 3 and 4; Supplementary Table 1). Aragonite content increased by ~ 34% while calcite decreased by ~ 10% from small to large individuals (LSD: $p < 0.01$; Figures 4; Supplementary Table 1). The elemental analysis showed significant differences (Supplementary Table 2) among size classes for Mg, Na, P, and Sr concentration (Kruskal-Wallis: $p < 0.05$). Mg, Na, and P decreased by ~ 60% and Sr decreased by ~ 27 % from small to large individuals.

Discussion

Despite the economic and ecological relevance of *M. galloprovincialis* mussel, the evolution of the biometric, compositional, microstructural and mechanical properties of the shells at different life stages has been scarcely investigated. Individuals of *M. galloprovincialis* can be difficult to age (Andrisoa et al., 2019; Lowenstam, 1954; Martinez et al., 2018), so we used the shells length as a proxy of the age considering specific critical sizes associated to reproduction in the life cycle (Gosling, 2015). In agreement with previous observations conducted on the commercial clam *Chamelea gallina* of different sizes (Mancuso et al. 2019), here we observed higher porosity in small compared to medium and large shells. Mancuso et al. 2019 suggested that in younger specimens *C. gallina* may promote higher linear extension rates, resulting in higher porosity. The observed increase in shell porosity found in the current study may be also a consequence of the higher extension rates, which has been observed in younger *M. galloprovincialis* individuals (Sarà et al., 2012). Low porosity in shells could limit body growth rate (Busse et al., 2016; Palmer, 1981) increasing the time spent at smaller non-reproductive sizes, while more porous ones could be the result of higher shell linear extension rates, allowing the organism to reach the size of sexual maturity faster. Age determination through sclerochronological studies are needed to obtain linear extension rates data in *M. galloprovincialis* and test this hypothesis.

Higher porosity was accompanied by a lower bulk density and a higher micro-density in small compared to large shells. Bulk density depends both on the pattern in which the material is laid down (the meso-architecture) and on the volume of enclosed skeletal voids (occluded porosity). The micro-density is the mass per unit volume of the material which composes the skeleton (Bucher et al., 1998). Mollusk shells are composed of calcium carbonate (more than 95% by mass) intimately associated with an intra-crystalline organic matrix (OM; 0.01%–5% by mass) (Lowenstam & Weiner, 1989a). The latter is believed to initiate nucleation of calcium carbonate and provide a framework for crystallographic orientation and species-specific architecture (Lowenstam and Weiner 1989). In agreement with previous findings on the skeletons of two Mediterranean scleractinian corals (Caroselli et al. 2011; Mancuso et al. 2015), shell micro-density, elasticity and maximum load were higher in larger individuals compared to smaller ones. This was related to the lower content of OM in large individuals as here observed. In mussel shells the increase of micro-density is also determined by a higher aragonite content, as aragonite is denser than calcite (aragonite: 2.94 mg mm^{-3}; calcite: 2.71 mg mm^{-3}; (Marszalek, 1982b)). An increase in aragonite vs calcite content during the growth of mussels has been already reported (Lowenstam, 1954).

It has to be noted that during the larval stages, when the organisms are free to move in the water, aragonite is the predominant mineral phase deposited in almost every molluscan shell, including mytilaceans specie (Eyster & Morse, 1984). Aragonite may offer better defence, since is more resistant and less prone to fracture than calcite (Deng & Li, 2021). Soon after metamorphosis, calcite starts to form an external layer, being more chemically stable and less vulnerable to leaching than aragonite (Stenzel, 1964). However, aragonite content in the shell increases with the size, probably due to its better mechanical performance. Temperature and the $CaCO_3$ saturation of sea water can also affect the formation of aragonite (Telesca et al., 2019).

The observed decrease in OM content in larger shells can be explained considering that older individuals may allocate less energy towards producing OM, given its relatively high cost (Palmer, 1983) and given that higher metabolic rates are needed to support carbon requirements for calcification throughout ontogeny (Lorrain et al., 2004). The elemental analyses showed a significant decrease of the shell concentration of Mg, Na, and P from small to large individuals. The decrease of magnesium/calcium ratios with the increased size can be related with the increase of aragonite, since Mg does not replace Ca in the aragonite crystalline lattice (Fermani et al., 2017). The Na content has been related to the seawater composition (Lorens & Bender, 1980) and Na is adsorbed on calcite and aragonite (Lippmann, 1973). The content of nutrients in sea water can be related to the P concentration in the skeleton, as reported for deep-sea corals (Anagnostou et al., 2011). However, it has to be considered that there is also a biological control of element incorporation into biogenic calcium carbonates together with environmental factors (Weiner & Dove, 2003c), reported also for *M. galloprovincialis* shells (Beer et al., 2011).

Conclusion

This is the first multiscale characterization that correlates shell mechanical and compositional features in the commercially important bivalve species *M. galloprovincialis* across life stages. Immature shells were more porous and characterized by reduced stiffness and hardness compared to mature shells, mainly due to the reduced content of aragonite. This latter observation strengths the importance of considering shell size in evaluating the implication of environmental stressors on shell features. Moreover, this mechanical-structural characterization has relevant implications in mussel aquaculture and in the processing of shellfish for commercial purposes, as the shells can break in the handling processes (Penney et al., 2007). It is also relevant in the potential reuse of waste mussel shells since the change in the polymorphic distribution and the composition influence the chemical-physical properties of the calcium carbonate (Magnabosco et al., 2021; Niu et al., 2022). Finally, this research on mechanical performance of mussel shells open the route for similar studies on different commercial species, and not only, also in view of the varying environmental conditions.

Acknowledgments

This study is a partial fulfillment of the requirements for a PhD thesis of A. Cheli the PhD Course of Innovative Technologies and Sustainable Use of Mediterranean Sea Fishery and Biological Resources (FishMed-PhD) (University of Bologna, Italy), and of R.H.G.R. Wathsala at the PhD Course of Earth, Life, and Environmental Science (University of Bologna, Italy),

References

Anagnostou, E., Sherrell, R.M., Gagnon, A., LaVigne, M., Field, M.P., McDonough, W.F., 2011. Seawater nutrient and carbonate ion concentrations recorded as P/Ca, Ba/Ca, and U/Ca in the deep-sea coral Desmophyllum dianthus. Geochim. Cosmochim. Acta 75, 2529–2543.

Andrisoa, A., Lartaud, F., Rodellas, V., Neveu, I., Stieglitz, T.C., 2019. Enhanced Growth Rates of the Mediterranean Mussel in a Coastal Lagoon Driven by Groundwater Inflow . Front. Mar. Sci. .

Bajt, O., Ramšak, A., Milun, V., Andral, B., Romanelli, G., Scarpato, A., Mitrić, M., Kupusović, T., Kljajić, Z., Angelidis, M., Çullaj, A., Galgani, F., 2019. Assessing chemical contamination in the coastal waters of the Adriatic Sea using active mussel biomonitoring with Mytilus galloprovincialis. Mar. Pollut. Bull. 141, 283–298. https://doi.org/10.1016/J.MARPOLBUL.2019.02.007

Beer, N.A., Wing, S.R., Hu, Y., 2011. Physical versus biological control of element incorporation into biogenic carbonate: an in situ experiment in a New Zealand fjord. Mar. Ecol. Prog. Ser. 433, 289–301.

Bergström, P., Lindegarth, M., 2016. Environmental influence on mussel (Mytilus edulis) growth - A quantile regression approach. Estuar. Coast. Shelf Sci. 171, 123–132. https://doi.org/10.1016/J.ECSS.2016.01.040

Bertness, M.D., Grosholz, E., 1985. Population dynamics of the ribbed mussel, Geukensia demissa: the costs and benefits of an aggregated distribution. Oecologia 67, 192–204.

Beyer, J., Green, N.W., Brooks, S., Allan, I.J., Ruus, A., Gomes, T., Bråte, I.L.N., Schøyen, M., 2017. Blue mussels (Mytilus edulis spp.) as sentinel organisms in coastal pollution monitoring: A review. Mar. Environ. Res. 130, 338–365. https://doi.org/https://doi.org/10.1016/j.marenvres.2017.07.024

Bråte, I.L.N., Hurley, R., Iversen, K., Beyer, J., Thomas, K. V., Steindal, C.C., Green, N.W., Olsen, M., Lusher, A., 2018. Mytilus spp. as sentinels for monitoring microplastic pollution in Norwegian coastal waters: A qualitative and quantitative study. Environ. Pollut. 243, 383–393. https://doi.org/10.1016/J.ENVPOL.2018.08.077

Busse, C., Homs, J.L., Gustafsson, D., Palmert, F., Sjödin, B., Moverare, J.J., Simonsson, K., Leidermark, D., 2016. A finite element study of the effect of crystal orientation and misalignment on the crack driving force in a single-crystal superalloy, in: Proceedings of the ASME Turbo Expo: Turbomachinery Technical Conference and Exposition. pp. 1–8. https://doi.org/10.1115/GT2016-56305

Cheli, A., Mancuso, A., Azzarone, M., Fermani, S., Kaandorp, J., Marin, F., Montroni, D., Polishchuk, I., Prada, F., Stagioni, M., Valdré, G., Pokroy, B., Falini, G., Goffredo, S., Scarponi, D., 2021. Climate variation during the Holocene influenced the skeletal properties of Chamelea gallina shells in the North Adriatic Sea (Italy). PLoS One 16, e0247590. https://doi.org/10.1371/JOURNAL.PONE.0247590

Coll, M., Piroddi, C., Steenbeek, J., Kaschner, K., Lasram, F.B.R., Aguzzi, J., Ballesteros, E., Bianchi, C.N., Corbera, J., Dailianis, T., Danovaro, R., Estrada, M., Froglia, C., Galil, B.S., Gasol, J.M., Gertwage, R., Gil, J., Guilhaumon, F., Kesner-Reyes, K., Kitsos, M.S., Koukouras, A., Lampadariou, N., Laxamana, E., de la Cuadra, C.M.L.F., Lotze, H.K., Martin, D., Mouillot, D., Oro, D., Raicevich, S., Rius-Barile, J., Saiz-Salinas, J.I., Vicente, C.S., Somot, S., Templado, J., Turon, X., Vafidis, D., Villanueva, R., Voultsiadou, E., 2010. The Biodiversity of the Mediterranean Sea: Estimates, Patterns, and Threats. PLoS One 5, e11842. https://doi.org/10.1371/JOURNAL.PONE.0011842

Crane, R.L., Denny, M.W., 2022. Bivalves maintain repair when faced with chronically repeated mechanical stress. J. Exp. Biol. 225, jeb243813. https://doi.org/10.1242/jeb.243813

Currey, J.D., Taylor, J.D., 1974. The mechanical behaviour of some molluscan hard tissues. J. Zool. 173, 395–406. https://doi.org/10.1111/j.1469-7998.1974.tb04122.x

Deng, Z., Li, L., 2021. Intrinsic Mechanical Properties of Individual Biogenic Mineral Units in Biomineralized Skeletons. ACS Biomater. Sci. Eng. https://doi.org/10.1021/acsbiomaterials.0c01587

Denny, M.W., Gaylord, B., 2010. Marine ecomechanics. Annu Rev Mar Sci 2, 89–114.

Eyster, L.S., Morse, M.P., 1984. Early shell formation during molluscan embryogenesis, with new studies on the surf clam, Spisula solidissima. Integr. Comp. Biol. 24, 871–882. https://doi.org/10.1093/icb/24.4.871

FAO, 2020. The State of World Fisheries and Aquaculture. Sustain. action. https://doi.org/10.4060/ca9229en

Fermani, S., Džakula, B.N., Reggi, M., Falini, G., Kralj, D., 2017. Effects of magnesium and temperature control on aragonite crystal aggregation and morphology. CrystEngComm 19, 2451–2455.

Gizzi, F., Caccia, M.G., Simoncini, G.A., Mancuso, A., Reggi, M., Fermani, S., Brizi, L., Fantazzini, P., Stagioni, M., Falini, G., 2016. Shell properties of commercial clam Chamelea gallina are influenced by temperature and solar radiation along a wide latitudinal gradient. Sci. Rep. 6, 1–12.

Goldberg, E., 1975. The mussel watch-a first step in global marine monitoring. Mar. Pollut. Bull. 6, 111.

Gosling, E., 2015. Marine bivalve molluscs. John Wiley & Sons.

Grienke, U., Silke, J., Tasdemir, D., 2014. Bioactive compounds from marine mussels and their effects on human health. Food Chem. 142, 48–60. https://doi.org/10.1016/J.FOODCHEM.2013.07.027

Huang, W., Restrepo, D., Jung, J.Y., Su, F.Y., Liu, Z., Ritchie, R.O., McKittrick, J., Zavattieri, P., Kisailus, D., 2019. Multiscale Toughening Mechanisms in Biological Materials and Bioinspired Designs. Adv. Mater. 31, 1901561. https://doi.org/10.1002/adma.201901561

Kroeker, K.J., Sanford, E., Rose, J.M., Blanchette, C.A., Chan, F., Chavez, F.P., Gaylord, B., Helmuth, B., Hill, T.M., Hofmann, G.E., McManus, M.A., Menge, B.A., Nielsen, K.J., Raimondi, P.T., Russell, A.D., Washburn, L., 2016. Interacting environmental mosaics drive geographic variation in mussel performance and predation vulnerability. Ecol. Lett. 19, 771–779. https://doi.org/10.1111/ELE.12613

Lemasson, A., Knights, M., 2021. Differential responses in anti-predation traits of the native oyster Ostrea edulis and invasive Magallana gigas to ocean acidification and warming. Mar. Ecol. Prog. Ser. 665, 87–102.

Leonard, G.H., Bertness, M.D., Yund, P.O., 1999. Crab predation, waterborne cues, and inducible defenses in the blue mussel, Mytilus edulis. Ecology 80, 1–14.

Lippmann, F., 1973. Sedimentary carbonate minerals. Springer Verlag, New York.

Lorens, R.B., Bender, M.L., 1980. The impact of solution chemistry on Mytilus edulis calcite and aragonite. Geochim. Cosmochim. Acta 44, 1265–1278.

Lorrain, A., Paulet, Y.-M., Chauvaud, L., Dunbar, R., Mucciarone, D., Fontugne, M., 2004. δ13C variation in scallop shells: increasing metabolic carbon contribution with body size? Geochim. Cosmochim. Acta 68, 3509–3519.

Lowenstam, H.A., 1954. Factors affecting the aragonite: calcite ratios in carbonate-secreting marine organisms. J. Geol. 62, 284–322.

Lowenstam, H.A., Weiner, S., 1989. On biomineralization. Oxford University Press on Demand.

Mackenzie, C.L., Ormondroyd, G.A., Curling, S.F., Ball, R.J., Whiteley, N.M., Malham, S.K., 2014. Ocean Warming, More than Acidification, Reduces Shell Strength in a Commercial Shellfish Species during Food Limitation. PLoS One 9, e86764.

Magnabosco, G., Giuri, D., Di Bisceglie, A.P., Scarpino, F., Fermani, S., Tomasini, C., Falini, G., 2021. New material perspective for waste seashells by covalent functionalization. ACS Sustain. Chem. Eng. 9, 6203–6208. https://doi.org/10.1021/acssuschemeng.1c01306

Mancuso, A., Stagioni, M., Prada, F., Scarponi, D., Piccinetti, C., Goffredo, S., 2019. Environmental influence on calcification of the bivalve Chamelea gallina along a latitudinal gradient in the Adriatic Sea. Sci. Rep. 9, 11198. https://doi.org/10.1038/s41598-019-47538-1

Marin, F., Le Roy, N., Marie, B., 2012. The formation and mineralization of mollusk shell. Front. Biosci. 4, 1099.

Marszalek, D.S., 1982. The role of heavy skeletons in vertical movements of non-motile zooplankton. Mar. Freshw. Behav. Phy 8, 295–303.

Martinez, M., Mangano, M.C., Maricchiolo, G., Genovese, L., Mazzola, A., Sarà, G., 2018. Measuring the effects of temperature rise on Mediterranean shellfish aquaculture. Ecol. Indic. 88, 71–78. https://doi.org/10.1016/j.ecolind.2018.01.002

Montroni, D., 2020. Hierarchically organized chitin-based matrices. University of Bologna.

Muñoz-Moya, E., García-Herrera, C.M., Lagos, N.A., Abarca-Ortega, A.F., Checa, A.G., Harper, E.M., 2022. Evaluation of remodeling and geometry on the biomechanical properties of nacreous bivalve shells. Sci. Rep. 12, 1–11.

Nagarajan, R., Lea, S.E.G., Goss-Custard, J.D., 2006. Seasonal variations in mussel, Mytilus edulis L. shell thickness and strength and their ecological implications. J. Exp. Mar. Bio. Ecol. 339, 241–250.

Niu, Y.-Q., Liu, J.-H., Aymonier, C., Fermani, S., Kralj, D., Falini, G., Zhou, C.-H., 2022. Calcium carbonate: controlled synthesis, surface functionalization, and nanostructured materials. Chem. Soc. Rev. 51, 7883–7943.

Nudelman, F., Shimoni, E., Klein, E., Rousseau, M., Bourrat, X., Lopez, E., Addadi, L., Weiner, S., 2008. Forming nacreous layer of the shells of the bivalves Atrina rigida and Pinctada margaritifera: An environmental- and cryo-scanning electron microscopy study. J. Struct. Biol. 162, 290–300. https://doi.org/10.1016/j.jsb.2008.01.008

Olson, I.C., Kozdon, R., Valley, J.W., Gilbert, P.U.P.A., 2012. Mollusk shell nacre ultrastructure correlates with environmental temperature and pressure. J. Am. Chem. Soc. 134, 7351–7358. https://doi.org/10.1021/ja210808s

Palmer, A.R., 1983. Relative cost of producing skeletal organic matrix versus calcification: evidence from marine gastropods. Mar. Biol. 75, 287–292.

Palmer, A.R., 1981. Do carbonate skeletons limit the rate of body growth? Nature 292, 150–152.

Parsons, K.E., 1997. Contrasting patterns of heritable geographic variation in shell morphology and growth potential in the marine gastropod Bembicium vittatum: evidence from field experiments. Evolution (N. Y). 51, 784–796.

Pavicic, J., Raspor, B., Martincic, D., 1993. Quantitative determination of metallothionein-like proteins in mussels. Methodological approach and field evaluation. Mar. Biol. 115, 435–444. https://doi.org/10.1038/164914a0

Penney, R.W., Hart, M.J., Templeman, N.D., 2007. Shell Strength and Appearance in Cultured Blue Mussels Mytilus edulis, M. trossulus, and M. edulis × M. trossulus Hybrids. N. Am. J. Aquac. 69, 281–295. https://doi.org/10.1577/A06-044.1

Proćków, M., Proćków, J., Błażej, P., Mackiewicz, P., 2018. The influence of habitat preferences on shell morphology in ecophenotypes of Trochulus hispidus complex. Sci. Total Environ. 630, 1036–1043. https://doi.org/https://doi.org/10.1016/j.scitotenv.2018.02.311

Rasband, W.S., n.d. ImageJ, U. S. National Institutes of Health, Bethesda, Maryland, USA, https://imagej.nih.gov/ij/, 1997-2018.

Sarà, G., Reid, G.K., Rinaldi, A., Palmeri, V., Troell, M., Kooijman, S., 2012. Growth and reproductive simulation of candidate shellfish species at fish cages in the Southern Mediterranean: Dynamic Energy Budget (DEB) modelling for integrated multi-trophic aquaculture. Aquaculture 324, 259–266.

Schneider, C.A., Rasband, W.S., Eliceiri, K.W., 2012. NIH Image to ImageJ: 25 years of image analysis. Nat. Methods 9, 671–675. https://doi.org/10.1038/nmeth.2089

Seed, R., Richardson, C.A., 1999. Evolutionary traits in Perna viridis (Linnaeus) and Septifer virgatus (Wiegmann)(Bivalvia: Mytilidae). J. Exp. Mar. Bio. Ecol. 239, 273–287.

Steffani, C.N., Branch, G.M., 2003. Growth rate, condition, and shell shape of Mytilus galloprovincialis: responses to wave exposure. Mar. Ecol. Prog. Ser. 246, 197–209.

Stenzel, H.B., 1964. Oysters: Composition of the larval shell. Science (80-.). 145, 155–156. https://doi.org/10.1126/science.145.3628.155

Sun, J., Bhushan, B., 2012. Hierarchical structure and mechanical properties of nacre: A review. RSC Adv. 2, 7617–7632. https://doi.org/10.1039/c2ra20218b

Telesca, L., Michalek, K., Sanders, T., Peck, L.S., Thyrring, J., Harper, E.M., 2018. Blue mussel shell shape plasticity and natural environments: a quantitative approach. Sci. Reports 2018 81 8, 1–15. https://doi.org/10.1038/s41598-018-20122-9

Telesca, L., Peck, L.S., Sanders, T., Thyrring, J., Sejr, M.K., Harper, E.M., 2019. Biomineralization plasticity and environmental heterogeneity predict geographical resilience patterns of foundation species to future change. Glob. Chang. Biol. 25, 4179–4193.

Tushtev, K., Murck, M., Grathwohl, G., 2008. On the nature of the stiffness of nacre. Mater. Sci. Eng. C 28, 1164–1172. https://doi.org/10.1016/j.msec.2007.10.039

Weiner, S., Dove, P.M., 2003. An overview of biomineralization processes and the problem of the vital effect. Rev. Mineral. geochemistry 54, 1–29.

Zuschin, M., Stanton, R.J., 2001. Experimental Measurement of Shell Strength and its Taphonomic Interpretation. Palaios 16, 161–170. https://doi.org/10.1669/0883-1351(2001)016<0161:EMOSSA>2.0.CO;2

Figures

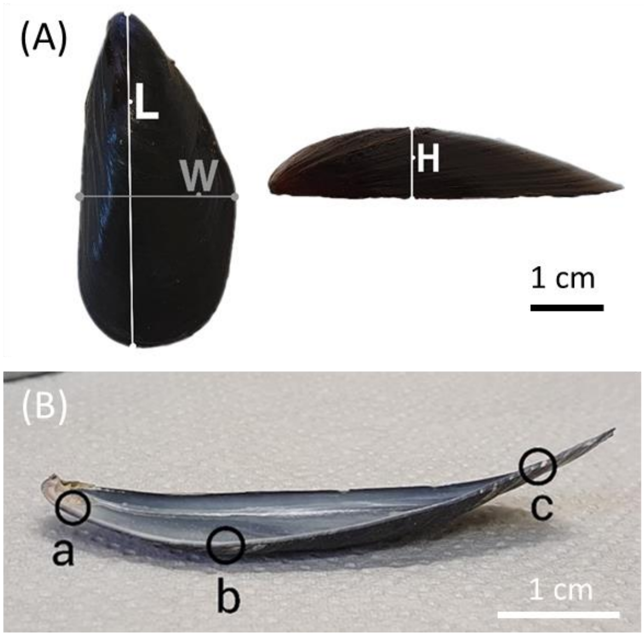

Figure 1. (A) Frontal and lateral view of a mussel shell. L: length; W: width; H: hight. (B) Longitudinal section of a shell to measure thickness. a) thickness in the umbo, b) thickness in the centre of the shell and c) thickness in the ventral side.

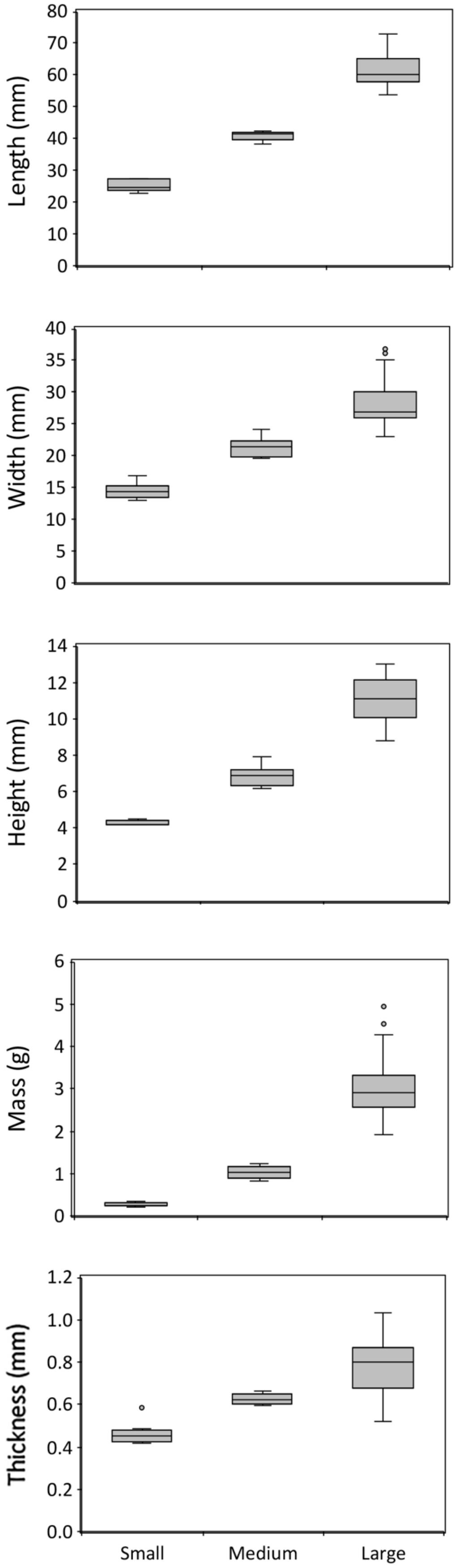

Figure 2. Shell biometric parameters. Shell length, width, height, mass and thickness for small, medium and large *M. galloprovincialis* specimens. The boxes indicate the 25th and 75th percentiles

and the line within the boxes mark the medians. Whisker length is equal to 1.5 × interquartile range (IQR). Circles represent outliers.

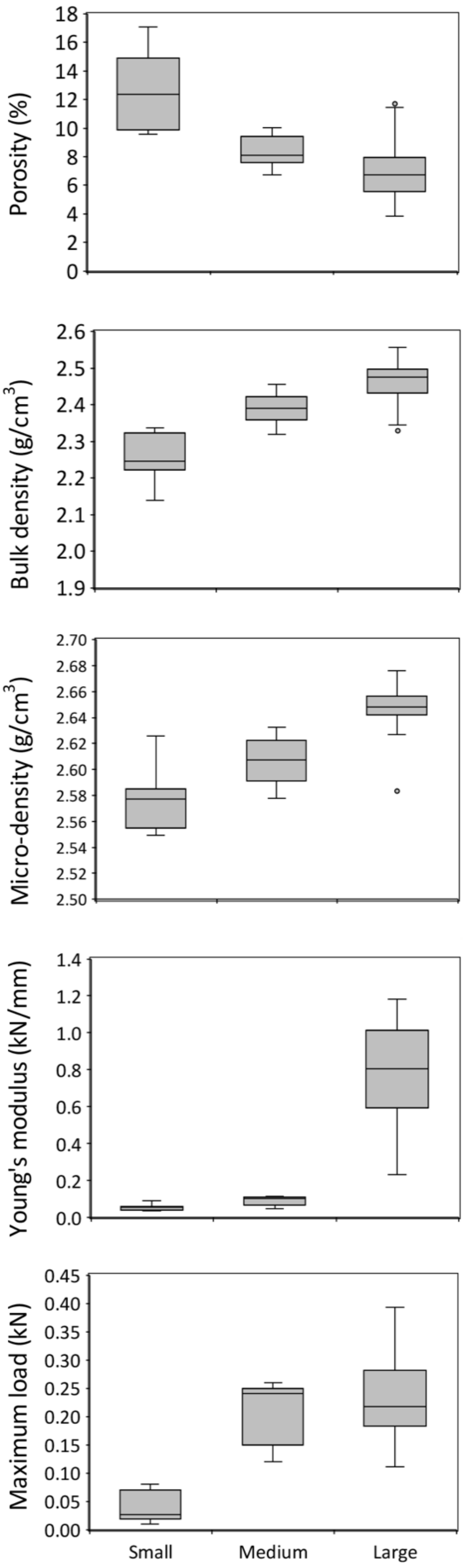

Figure 3. Shell skeletal and mechanical parameters. Shell porosity, bulk density, and micro-

density and mechanical parameters (Young's modulus and maximum load) for small, medium and large *M. galloprovincialis* specimens. The boxes indicate the 25th and 75th percentiles and the line within the boxes mark the medians. Whisker length is equal to 1.5 × interquartile range (IQR). Circles represent outliers.

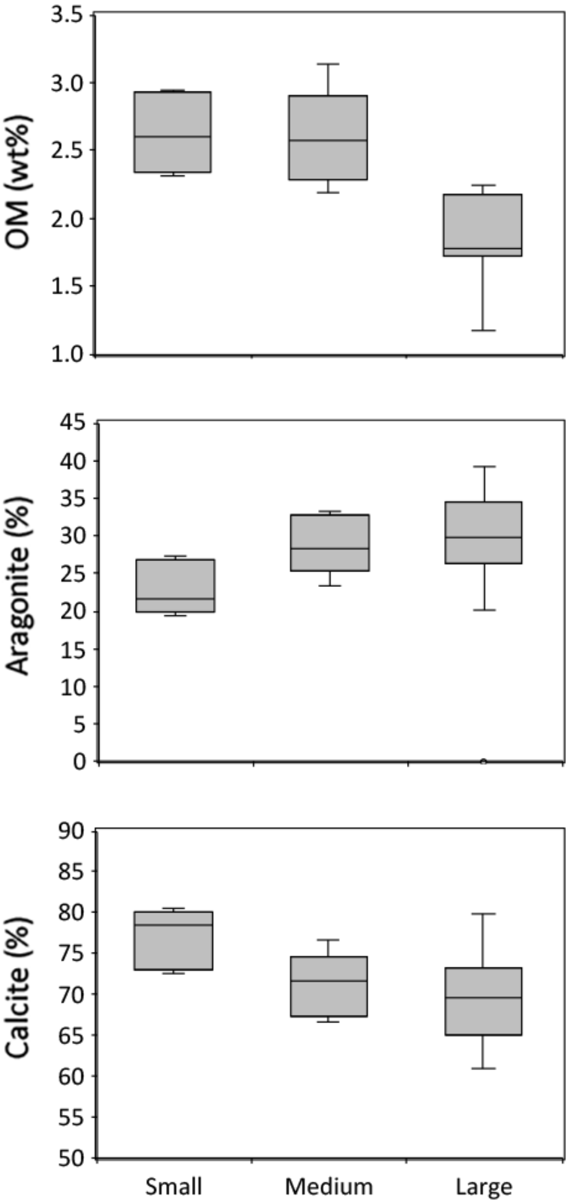

Figure 4. Shell composition. Shell organic matrix (OM), aragonite and calcite content for small, medium and large *M. galloprovincialis* specimens. The boxes indicate the 25th and 75th percentiles and the line within the boxes mark the medians. Whisker length is equal to 1.5 × interquartile range (IQR). Circles represent outliers.

Supplementary materials

Supplementary figures

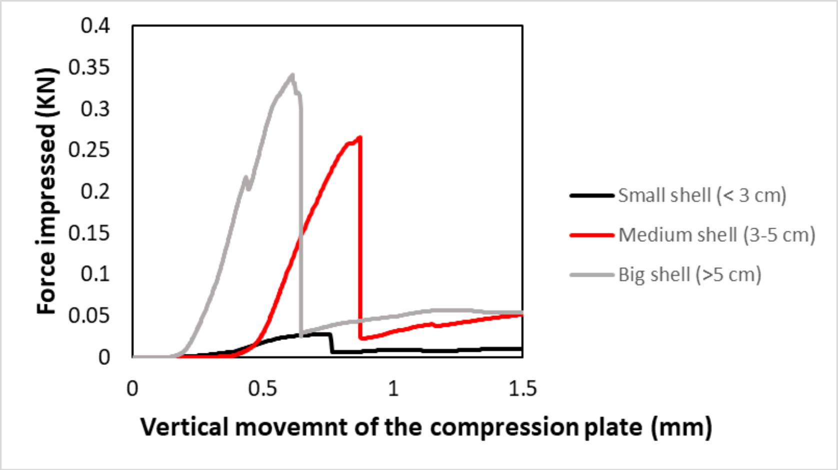

Supplementary Figure 1. Representative graphs obtained from compression test. The slope is the first upward trend of the curve and the maximum load is the highest peak, after which there is the first "crack" of the shell, represented by a sudden decrease of the resistance to the impressed force.

Supplementary Tables

Supplementary Table 1. Shell biometric, skeletal and mechanical parameters, organic matrix, aragonite, and calcite content in small, medium, and large *Mytilus galloprovincialis* specimens. Data are presented as mean ± Standard Deviation (SD). Pairwise comparisons between sizes were performed with Mann-Whitney U test or LSD test. NS = Not Significant, *p<0.05,**p<0.01,***p< 0.001.

		Length (mm)	SD	Width (mm)	SD	Heigth (mm)	SD	Mass (mm)	SD	Thikness (mm)	SD
	Large (>5 cm)	61.38	4.75	27.96	3.34	10.99	1.13	3.00	0.65	0.78	0.13
	Medium (3-5 cm	40.99	1.29	21.40	1.39	6.84	0.50	1.03	0.14	0.63	0.02
	Small (<3 cm)	25.11	1.57	14.58	1.13	4.28	0.14	0.27	0.04	0.46	0.05
Mann-Whitney U / LSD test	S vs M	***		***		**		***		**	
	S vs L	***		***		***		***		***	
	M vs L	***		***		***		***		*	

		Micro-density (g/cm3)	SD	Porosity (%)	SD	Bulk Density (g/cm3	SD	Slope (kN/mm)	SD	Max load (kN)	SD
	Large (>5 cm)	2.65	0.01	6.94	1.70	2.47	0.05	0.72	0.34	0.32	0.18
	Medium (3-5 cm	2.61	0.02	8.38	1.10	2.39	0.04	0.09	0.02	0.21	0.05
	Small (<3 cm)	2.58	0.02	12.51	2.43	2.26	0.06	0.06	0.02	0.04	0.03
Mann-Whitney U / LSD test	S vs M	**		***		***		*		***	
	S vs L	***		***		***		***		***	
	M vs L	***		**		***		**		NS	

		OM (wt%)	SD	Aragonite (%)	SD	Calcite (%)	SD
	Large (>5 cm)	1.83	0.31	29.57	7.07	67.65	12.60
	Medium (3-5 cm	2.59	0.31	28.91	3.55	71.10	3.55
	Small (<3 cm)	2.63	0.30	23.03	3.63	76.97	3.63
Mann-Whitney U / LSD test	S vs M	NS		NS		NS	
	S vs L	***		**		**	
	M vs L	***		NS		NS	

Supplementary Table 2. Shell elemental composition in small, medium, and large *Mytilus galloprovincialis* specimens. Data are presented as mean ± Standard Deviation (SD). Pairwise comparisons between sizes were performed with Mann-Whitney U test or LSD test. NS = Not Significant, *p<0.05, **p<0.01, ***p< 0.001.

		Ca	**Al**	**Fe**	**K**	**Mg**	**Na**	**P**	**Sr**	**Ti**	**Zn**
	Sample ID	ppm	ppb	ppb	ppm	ppm	ppm	ppm	ppb	ppb	ppb
Small (<3 cm)	6.1	167	0.0002	2.27E-05	0.003	0.005	0.005	0.0003	0.003	6.77E-06	3.11E-05
	6.3	233	0.0001	1.41E-05	0.002	0.004	0.004	0.0003	0.003	4.76E-06	2.74E-05
	6.5	202	0.0002	1.06E-05	0.002	0.005	0.005	0.0004	0.003	9.85E-06	3.64E-05
	6.9	208	0.0002	1.75E-05	0.002	0.005	0.005	0.0003	0.003	5.48E-06	3.26E-05
	Average	202.5	0.0002	1.62E-05	0.002	0.005	0.005	0.0003	0.003	6.72E-06	3.19E-05
Medium (3-5 cm)	6.1	237	0.0001	1.69E-05	0.002	0.005	0.005	0.0003	0.003	4.89E-06	1.82E-05
	6.8	260	0.0001	8.92E-06	0.002	0.004	0.004	0.0003	0.003	4.38E-06	1.69E-05
	6.13	255	0.0001	9.49E-06	0.002	0.003	0.003	0.0003	0.003	4.08E-06	3.41E-05
	2.1	243	0.0002	0.00014	0.010	0.002	0.002	0.0003	0.002	6.34E-06	4.81E-05
	4.8	255	0.0001	2.03E-05	0.002	0.002	0.002	0.0001	0.003	4.47E-06	1.91E-05
	Average	250	0.0002	3.9E-05	0.003	0.003	0.003	0.0003	0.003	4.83E-06	2.73E-05
Large (>5 cm)	1.1	237	0.0001	9.28E-06	0.002	0.002	0.002	0.0001	0.003	4.47E-06	1.72E-05
	1.3	247	0.0001	1.3E-05	0.002	0.002	0.002	0.0001	0.002	8.3E-06	1.64E-05
	1.4	260	0.0001	0.000013	0.002	0.002	0.002	0.0001	0.002	4.92E-06	3.71E-05
	1.6	235	0.0001	ND	0.002	0.002	0.002	0.0002	0.002	4.09E-06	3.76E-05
	2.3	243	0.0001	ND	0.002	0.001	0.001	0.0001	0.002	3.89E-06	2.23E-05
	Average	244.4	0.0001	1.18E-05	0.002	0.002	0.002	0.0001	0.002	5.14E-06	2.61E-05
Mann-Whitney U / LSD test	S vs M	**	NS	NS	NS	NS	NS	NS	NS	NS	NS
	S vs L	**	NS	NS	NS	**	**	**	*	NS	NS
	M vs L	NS	NS	NS	NS	*	*	*	NS	NS	NS

Chapter 6. General conclusion

Environmental factors, such as solar radiation, temperature, salinity and food availability, all influence energy expenditure in marine calcifying organisms, especially in temperate seas, where marine calcifiers show marked seasonal patterns in growth, reproduction and abundance.

My PhD project was primarily focused on investigating the effect of environment on biomineralization of mollusks species of great ecological importance and high economic value in the Adriatic Sea. The clam *Chamelea gallina* and the blue mussel *Mytilus galloprovincialis* have been the main subjects of my research. We used a multidisciplinary approach to investigate and characterize shell features at macro, micro and nanoscale level, with analysis on biometry, skeletal parameter, microstructure, mechanical properties and growth dynamics of shells. Thanks to this detailed examination it was possible to describe the interaction of many factors that eventually contribute to the biomineralization of the shell.

In the case of *C. gallina* we explored the recent fossil record to investigate the effect of environmental parameters on shell calcification. Well preserved fossil deposit represents biological archives of ecological responses to past environmental transition, thus offering the opportunity to investigate species long-term adaptative response to shifting climatic scenario.

Comparing fossil remains from the middle Holocene with modern specimens retrieved in the same area (Po Adriatic system) we observed that *C. gallina* shells were influenced by changes in seawater temperature. At the macroscale level, specimens from past fossil horizons, living in warmer water, presented a denser, less porous shells than modern specimens. Beside variations due to habitat conditions, differences were found in shell parameters during ontogeny and likely were the result of different biomineralization behaviour between immature and mature shells. *C. gallina* showed a marked decreasing extension rate with increasing length and clams of small size were more porous and less dense despite the bigger ones. Although these characteristics led to be more vulnerable to predators, they likely allowed to reach size at sexual maturity faster, promoting shell’s linear extension rate. At the opposite, denser shells found in bigger and older individuals could be less vulnerable to predators, but the energetic cost expended in producing skeletal material was reduced by depressing linear extension rate.

At the same time, no effects of environment were detected on shell mineral composition and on the building blocks produced by the biomineralization process of the clam shells. At the microscale level in fact, shells were all composed of pure aragonite, presenting a perfectly preserved mineral phase with no relevant diagenetic alteration and only a slight degradation of the inter-crystalline organic phase.

Interestingly the observed differences in skeletal parameters were not reflected on the growth dynamics of *C. gallina* populations from the Holocene to nowadays. Linear extension rate and net calcification rate remain constant in the analysed time gradient of ~8,000 years, showing a remarkable long-term phenotypic adaptive capacity.

The results produced by this work are partially contrasting with previous findings on biomineralization dynamics of *C. gallina* in the Mediterranean and Adriatic Seas. Notable differences can emerge depending on specific local conditions, thus using a combination of different and complementary approaches like laboratory experiments, field studies and analysis of the fossil record can ultimately help to improve our understanding of the response of this economically relevant species to a changing environment in a global change scenario.

Investigation of fossil record revealed to be a powerful tool not only to explore long-term effects of environmental variation on single marine species, but it also allowed to determine the impact of stressors on entire marine communities. This approach has been used in a project aimed to evaluate the status of north Adriatic coastal ecosystem in response to anthropogenic stresses. The Adriatic Sea is being affected by multiple anthropogenic stressors and has already been highly impacted by human activities. Holocene fossil record has been investigated to define the status of marine ecosystems prior to major phases of human impact. We compared mid-late Holocene assemblages preserved in the subsurface stratigraphic record of the Po coastal plain (Northern Italy) with surficial assemblages that accumulated along the Po Delta and Emilia Romagna coastline during the Anthropocene. Specifically, we evaluated changes in the composition of mollusc assemblages between the present-day fluvial influenced coastal shoreface and delta front settings with sustained sedimentary inputs (hereafter referred to as “nearshore”) and their mid-late Holocene counterparts representing a time interval when anthropogenic pressure were notably less significant (between ~6 and 0.5 kyr cal BP i.e., prior to the early modern period). Compared to the mid-late Holocene baseline, present-day molluscan assemblages show an increase in standardised diversity in upper nearshore settings due to increase in habitat heterogeneity and introduction of non-native species. The elevated spatial heterogeneity of mollusc assemblages is likely attributable to transformation and fragmentation of coastal habitats driven by human activities in the most recent centuries. In lower nearshore settings, on the other hand the decrease in standardised diversity and the rise of opportunistic taxa signal a strong anthropogenic transformation of these habitats related to eutrophication, increased frequency of hypoxic events and intense bottom trawling. Given the economic and socio-cultural importance of shellfish fisheries in the Mediterranean basin, it will be difficult to set the Holocene baseline for lower nearshore environments as an achievable (or desirable) restoration goal. Conservation strategies in such settings need to accept and incorporate human societies as part of the ecosystem and consider them as one of the major stakeholders that should be involved in the sustainable management of coastal ecosystems. The historical perspective provided in this study should allow us to establish better conservation strategies.

Finally, the last project described in this thesis focuses on shells growth and properties of *Mytilus galloprovincialis* from the North-western coasts of the Adriatic Sea, a bivalve mollusc with high ecological and economical relevance. The conducted analysis aimed to provide a detailed description of how shell feature changes during the growth of the organism, evaluating both the mechanical properties and the biometrical, compositional and structural features of shell along different stages of life, i.e. juvenile and adult.

The skeletal macrostructure varies between juvenile and mature organisms: young individuals (with a smaller shell) show a higher porosity than grown organisms, reflected into a lower shell density. This was a common aspect with the mineralization trends described in this Thesis for the clam *Chamelea gallina*. The content of intra-shell organic matter decreases as individuals mature, as does the calcite content of shell, one of the two calcium carbonate polymorphs that compose the shell. On the contrary, thickness, maximum load to breakage and the load/elongation ratio increased from juvenile to adult organisms. Thus, shell feature changes significantly from the early stages of life to organisms' maturity. These data highlight that juvenile shells, more porous and characterized by weaker mechanical performances, mainly due to the reduced content of aragonite, are potentially more vulnerable to the effect of environmental stresses. These data highlight how shell multiscale properties are strictly related to size, making this parameter a key factor to consider in biological studies addressing the effect of environmental stressors on mussels.

Moreover, this mechanical-structural characterization has relevant implications in mussel aquaculture and in the processing of shellfish for commercial purposes, as the shells can break in the handling processes. It is also relevant in the potential reuse of waste mussel shells since the change in the polymorphic distribution and the composition influence the chemical-physical properties of the calcium carbonate. Finally, this research on mechanical performance of mussel shells opens the route for similar studies on different commercial species, and not only, also in view of the varying environmental conditions.

An interesting implementation of this work arises from the collaboration with Professor Franzelliti, who conducted a parallel molecular analysis on the same specimens here described. The aim was to better understand the process of shell formation: how it is regulated by the organism and how the structure changes in relation to different environmental and biotic parameters. To do so, the transcriptional profiles of genes related to the shell biogenesis and neuroendocrine control of the mantle function were obtained. The analyzes are in progress, but thanks to this interdisciplinary approach we may obtain insight on how the deposition of minerals is mediated by biological processes.

Acknowledgments

First, I would like to greatly acknowledge my supervisor Prof. Jaap Kaandorp for his invaluable support and precious help throughout my PhD. It was a great misfortune for me not to have the opportunity to work together in person in Amsterdam, as originally planned. Nevertheless, you have been a precious and supportive guide even from a distance.

I’m deeply grateful to my co-supervisors Prof. Stefano Goffredo, Prof. Giuseppe Falini, and Prof. Frédéric Marin. Your passion for science, analytical eye and deep knowledge of the field were inspiring and contagious. All the suggestions and constructive critiques have always been a source of motivation in these years.

I would like to thank Prof. Daniele Scarponi for the trust he always shown me involving me in a lot of projects and for his endless patience and availability. The field samplings we did together are experiences I won't soon forget.

Special thanks go to my "senior" lab colleagues, Dr. Arianna Mancuso, Dr. Fiorella Prada and Dr. Devis Montroni. Since my master's degree and through these challenging years, you have always been my first point of reference. I am grateful to have had the opportunity to learn by working alongside brilliant researchers like you.

I will never be able to suitably thank my lab mates Carla, Silvia and Quinzia, colleagues who quickly became great and precious friends. Meeting you and sharing with you the misadventures, anxieties, but also the (rare) moments of joy and satisfaction of this journey has been a real privilege.

All the people I mentioned contributed with their support to make this journey possible, in its most difficult moments. It wouldn’t have been possible without you, literally.

I would like to thank also to the university mates met in Pisa and Bologna, for their genuine and contagious passion for nature. The world is in desperate need of crazy, brilliant and determined people like you guys. Never give up!

Thanks to all the friends met in bologna, a freak adoptive family who made this city a second home. I know the fact that I spent three years of my PhD studying clams will always make you laugh. Ah ah, how funny.

As for all my old friends in Cecina, distant but always present, I am happy that we are all reconnecting in the Granducato. See you soon in front of a glass of spuma guys.

Last but not least, I have to thank all my family, for their continuous and indiscriminate support. Mom, dad, Marta I know I can always rely on you.

A heartfelt thanks to my wife, Jessica, companion throughout this journey and invaluable help in difficult moments. Thank you for always politely pretending to be interested in my work. I love you for that too.
My last thought goes to Uncle Franco. I owe you the man I've become and what I believe in. You have been and always will be an example to imitate, I hope I can make you proud.